GROUND STATE VIBRATIONAL ANALYSIS OF FEW AROMATIC HYDROCARBONS AND AMINO ACIDS: AN AB INITIO STUDY

A Thesis Submitted

in Partial Fulfillment of the Requirements

for the Degree of

Doctor of Philosophy

by

DEBASHIS CHAKRABORTY

to the

DEPARTMENT OF CHEMISTRY
INDIAN INSTITUTE OF TECHNOLOGY, KANPUR

December, 1996

Dedicated to
my parents

HM - 1996 - D - CHA - GRO

STATEMENT

I hereby declare that the matter embodied in this thesis is the result of investigations arried out by me in the Department of Chemistry, Indian Institute of Technology, Kanpur, India under the supervision of Dr. S. Manogaran.

In keeping with the general practice of reporting scientific observations, due acknowledgement has been made wherever the work described is based on the findings of other investigators.

Debashis Chakraborty

Kanpur   Debashis Chakraborty

DEPARTMENT OF CHEMISTRY
INDIAN INSTITUTE OF TECHNOLOGY KANPUR INDIA
CERTIFICATE I

This is to certify that Mr. Debashis Chakraborty has satisfactorily completed all the courses required for the Ph.D. degree program. These courses include:

CHM 605 Principles of Organic Chemistry

CHM 621 Chemical Binding

CHM 624 Modern Physical Methods in Chemistry

CHM 625 Principles of Physical Chemistry

CHM 645 Principles of Inorganic Chemistry

CHM 679 Molecular Reaction Dynamics

CHM 800 General Seminar

CHM 801 Special Seminar

CHM 900 Ph.D. Thesis

Mr. Debashsis Chakraborty was admitted to the candidacy of the Ph.D. degree in July 1991, after he successfully completed the written and oral qualifying examinations.

(S. K. Dogra)
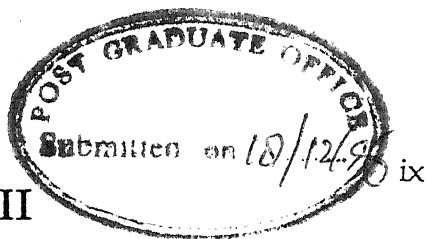
Head,

Department of Chemistry

IIT Kanpur

(T. K. Chandrashekhar)

Convenor,

Departmental Post Graduate Committee

Department of Chemistry

IIT Kanpur

CERTIFICATE II

It is certified that the work contained in this thesis entitled *Ground State Vibrational Analysis of Few Aromatic Hydrocarbons and Amino Acids: An Ab Initio Study* by *Debashis Chakraborty* has been carried out under my supervision and that this work has not been submitted elsewhere for a degree.

Dr. S. Manogaran
Associate Professor
Department of Chemistry
Indian Institute of Technology, Kanpur
Kanpur-208016 (INDIA)

December, 1996

Acknowledgments

I am grateful to my elder brother for his constant inspiration and mental support at every step of my work.

Last but not the least is the constant encouragement and love I received from Sangita, as a friend and my wife, which always kept me cheerful and enthusiastic even at the crucial stage of this work.

Debashis Chakraborty

Synopsis

An accurate knowledge of molecular force fields is essential in the prediction and interpretation of vibrational spectra and also in molecular mechanics and dynamics simulation [1]. Attempts to deduce molecular force field from spectral data alone have not been successful so far for molecules containing more than a few atoms [2]. Ab initio molecular orbital methods offer an attractive alternative to resolve this problem. Due to the recent advances in the quantum chemical methodology, an accurate description of molecular force field is possible for small molecules by extending the atomic orbital basis sets and including the electron correlation. Such a physical representation of systems of interest in chemistry and structural biology is not possible due to limited computational resources. A new approach has been introduced in this regard by using the ab initio Hartree-Fock calculations employing an optimal basis set to derive preliminary quantum mechanical force field, whose parameters are then systematically scaled by fitting the available experimental data. These scale factors are then transferred to structurally related larger systems [3]. In the present study, a new algorithm has been developed in this regard and interpretation and prediction of the vibrational spectra of few aromatic hydrocarbons [4] and amino acids have been carried out using this newly developed methodology.

In chapter 1 of the thesis, the use of ab initio calculations in the development of force field has been reviewed. Importance of the force constants for the interpretation and prediction of vibrational spectra has been discussed and the existing methodologies on scaling of ab initio force field have been reviewed along with their advantages and disadvantages. A brief outline of the thesis is also presented.

In chapter 2, the basic framework of ab initio calculations has been presented. A brief description of the basis sets employed, the Hartree-Fock model, methods of inclusion of

electron correlation and the theory behind the evaluation of force constants is given. The conversion of cartesian force constants (available from ab initio studies) to non-redundant local and symmetric force constants is also discussed. All the ab initio calculations have been carried out with Gaussian and GAMESS suit of programs.

In chapter 3, a novel method is described to obtain a scale factor for each force constant in the force constant matrix as a quantitative measure of the systematic error in the ab initio methods. These scale factors offer a simple solution to the problem of interpretation and prediction of vibrational spectra using the Scaled Quantum Mechanical (SQM) approach of Pulay et al. [3]. A detailed description of the methodology and its theoretical justification are presented. The advantages of the present methodology over the existing ones are listed. The performance of the method compared to the SQM procedure is demonstrated by using acrolein as example. A nearly unique force field of benzene is obtained by fitting the ab initio force field of five different calculations (HF/4-21G, 6-31G*, 6-311G**, 6-311++G** and MP2/6-311G**) to the harmonic frequencies of Ozkabak and Goodman [5]. Transferability of the scale factors for the prediction of vibrational spectra has been demonstrated by using pyridine and benzaldehyde as test cases.

In chapter 4, a complete set of force constants and their corresponding scale factors are obtained by fitting the experimental frequencies of naphthalene-d_0 and -d_8 to the ab initio force field obtained at HF/4-21G level using the methodology described in chapter 3. The fitting is extremely successful in producing a force field which reproduces the frequencies within an average deviation of 5.7 cm^{-1} for naphthalene-d_0 and 4.0 cm^{-1} for -d_8 from the experimentally observed fundamentals. The ab initio force constants of anthracene are obtained using the same level of theory and scaled using the scale factors of naphthalene. The earlier assignments are either confirmed or reassigned utilizing the frequencies and potential energy distributions (PED) derived from the scaled force field. The agreement between the experimental and predicted fundamentals are excellent for this molecule containing 24 atoms giving an average deviation of 8.2 cm^{-1}.

In chapter 5, the force fields of glycine hydrochloride (GH) and glycylglycine hydrochloride (GGH) are presented. A conformational study was undertaken for GGH at HF/6-31G** level of theory. By fitting the experimental vibrational frequencies of seven

isotopomers of GH to the ab initio force field for the lowest energy conformation using the methodology described in chapter 3 a complete set of force constants and their corresponding scale factors are obtained. The fitting is extremely successful in producing a force field with an average deviation of 9.7 cm^{-1} from the experimentally observed fundamentals for all the seven isotopomers. The scale factors of GH are used to obtain the scaled ab initio force field of the minimum energy conformer of GGH, which in turn was used to predict the vibrational frequencies and their PED. The very good agreement between the experimental and predicted fundamentals offer a "real" example to the concept of building a reliable force field from a smaller unit to a larger unit i.e. of a dipeptide from its parent amino acids.

In chapter 6, transferability of scale factors from smaller constituents to a larger is successfully attempted for two important amino acid hydrochlorides cysteine and serine. The scale factors of GH from chapter 5 are used to scale the ab initio force field of both the molecules. Scale factors of the side chain residues of cysteine and serine are obtained by fitting the ab initio force field of ethanethiol and ethanol to their respective experimental frequencies at the same level of theory. In both the cases the prediction of the frequencies and their normal mode descriptions are very good. This further indicates that the scale factors of structurally related small organic molecules (ethanethiol and ethanol in the present case) can be used to mimic the right features of the amino acid side chain residues.

In chapter 7, the ab initio calculation of isolated glycine zwitterion to study the vibrational spectral features is presented. Such an ab initio calculation on amino acids do not reproduce the experimental PED of the normal modes because of the strong intramolecular H-bonding which is absent in the condensed phase. Using Onsager reaction field model with a proper choice of solute radius and dielectric constant, it is shown that the ab initio method mimics the features of experimental PED very well. Several basis sets are used for identifying the right ab initio model. By fitting this ab initio force field of the solvated model to the experimental vibrational frequencies of four different isotopomers at HF/6-31++G* level a complete set of non-redundant force constants are obtained. The fitting produced a force field which produces the frequencies with an average deviation of 7.9 cm^{-1} from the experimentally observed fundamentals of all the four isotopomers.

Since most of the experimental data on amino acids are available for solution and/or solid phases, their correct interpretation requires a good theoretical model.

In chapter 8, based on our earlier glycine ab initio solvated model calculations, a complete set of scale factors are generated for alanine by fitting the ab initio solvated model force field to the experimental frequencies of five different isotopomers. Theses scale factors are then used to scale the ab initio force field of two important amino acids, cysteine and serine. Scale factors of the side chain residues of both cysteine and serine are obtained by fitting the ab initio solvated model force field of ethanethiol and ethanol to their respective experimental frequencies at the same level of theory. In both the cases the prediction of the frequencies and their normal mode descriptions are excellent compared to the size and complexity of the molecules.

In chapter 9, a summary of the findings of the present study and suggestions for future work have been forwarded.

Bibliography

[1] Derreumaux, P.; Vergoten, G. *J. Chem. Phys.*, **1995**, 102, 8586.

[2] Ozkabak, A. G.; Goodman, L. *J.Chem.Phys*, **1987**, 87,2564.

[3] a) Pulay, P.; Fogarasi, G.; Pongor, G.; Boggs, J. E.; Vargha, A. *J. Am. Chem. Soc.*, **1983**, 105, 7037. b) Fogarasi, G.; Pulay, P. *Annu. Rev. Phys. Chem.*, **1984**,35, 191; in *Vibrational Spectra and Structure*, Vol. 14, (Edited by Durig, J. R.), Elsevier, Amsterdam, 1985.

[4] Chakraborty, D.; Ambashta, R.; Manogaran, S. *J. Phys. Chem*, **1996**, 100, 13963.

[5] Goodman, L.; Ozkabak, A. G.; Thakur, S. N. *J. Phys. Chem.*, **1991**, 95, 9044.

Contents

List of Tables

List of Figures

Chapter 1

Introduction

Numerical simulations of structures and dynamics of molecules serve as an invaluable complement to experiments due to the significant developments in new generation computers, improved programs and wide accessibility to these programs. Simulation of molecular force field as an important tool in the study of structure and dynamics of molecules rest on the hypothesis that the potential energy of a molecule or assembly of molecules can be reproduced by a low order Taylor series expansion in terms of internal coordinates. At the harmonic level the prediction of good vibrational spectra greatly enhances its use as a structural tool in cases where other structural methods such as NMR or diffraction methods cannot be applied, e.g. transient species, polymers, low temperature matrices, adsorbed layers or for structural phenomena which are fast in the NMR time scale. Improved thermodynamic functions can be obtained from the vibrational spectra whose fundamentals are correctly identified. Another important application of accurate force fields is the evaluation of the vibrational averaging effects on observed molecular properties, e.g. geometries, dipole moments etc. There is a great deal of interest in the field due to the recent technical developments of molecular spectroscopy [1-9].

Attempts to deduce molecular force fields from spectral data alone have not been successful so far for molecules containing more than a few atoms [10-12]. As the number of atoms increase, the number of force constants to be determined becomes more than the experimentally available frequencies and multiple solution becomes a problem. Ab initio calculations due to their firm theoretical basis tend to be more systematic and reliable, than other methods available for the development of force fields. With the advent of

1

faster computers and widely accessible programs, rapid strides have been made in the calculation of ab initio force fields at various levels of sophistication [13-20]. As an outcome, in the last decade, there has been a tremendous growth in the ab initio quantum mechanical calculation of force constants for polyatomic molecules and the prediction of vibrational spectra [21-30].

Due to the recent advances in the quantum chemical methodology, an accurate description of molecular force field is possible for small molecules by extending the atomic orbital basis sets and including electron correlation. Such a physical representation of a typically large macro molecular system of interest in structural biology is not possible due to the limited computational resources. As a result, the simulation of macromolecules such as proteins and nucleic acids and their interactions have led to a large number of empirical force fields through refinement of parameters and their transferability from small model systems [31-50]. Most of these currently available force fields involve the electrostatic potential and the solvation free energy as the focus of attention. These force fields are perfectly adequate to the applications of molecular recognition or identification of closely related minima. However, these force fields largely ignore the accurate reproduction of the vibrational frequencies [50]. The acceptability of the force field is apparently gauged by the agreement between the calculated and experimentally observed fundamental vibrational frequencies of the parent molecule and its isotopomers. Thus it seems that an accurate description of vibrational frequencies of some model compounds using theoretically sound methodology (ab initio) can provide improved force field parameters for a better description of molecular mechanics or molecular dynamics simulation of biologically important macromolecules.

Transferability of molecular force constants between structurally related molecules and refining them with the aid of experimental vibrational frequencies using normal coordinate analysis is known for long [51]. In this method the force constants are simply guessed based on their values in related molecules and modified so as to reproduce all the isotopic frequencies closely. Ab initio methods could give better force constants because they are evaluated based on firm theoretical basis [52,53]. However at the Hartree-Fock (HF) level of ab initio theory, finite basis set and neglect of electron correlation result in

over-estimated values of force constants and frequencies. Although highly sophisticated methods like CCSD(T) and CASS are capable of yielding more accurate harmonic force constants can not be applied on a routine basis to medium sized molecules. Even when accurate harmonic force constants become available, for prediction of experimental frequencies we need anharmonic force constants which involve the evaluation of cubic and quartic force constants.

As a reasonable solution to this problem use of both the experimental data and the ab initio information had been advocated. A new approach has been introduced in this regard by using the ab initio Hartree-Fock calculations employing an optimal basis set to derive a preliminary quantum mechanical force field, whose parameters are then systematically scaled by fitting them to the available experimental data [11,54-66]. All these approaches are based on the assumption that the errors involved in the ab initio calculations are fairly systematic. Analysis of the calculated harmonic force constants of a large number of molecules using HF theory leads to the following general conclusions [10].

i) Diagonal stretching force constants are systematically overestimated by 10-15%.

ii) Diagonal bending force constants are systematically overestimated by 20-30%, slightly higher than stretching.

iii) For coupling constants the errors are less systematic, large values are reproduced within 10-30% and for small values an absolute error seems more appropriate, within 0.05-0.10 mdyne/Å.

The combination of theory and experiment in evaluating the force constants was first attempted by Pulay and Meyer through their simple scaling scheme of 10% reduction of the stretchings, 20% reduction for the bendings and the interaction terms left unchanged at their theoretical values [54]. Another procedure proposed by Botschwina et al. [55,56] and Pouchan et al. [58] involves fitting of the diagonal force constants to the experimental frequencies while the off-diagonal terms are taken from calculated results. Blom and Altona in their more detailed scaling scheme introduced separate scale factors for several types of distortions and also optimization of these scale factors by fitting them to the experimental frequencies in a least squares procedure [59]. Ha, Mayer and Günthard

proposed a relatively different scaling scheme of using both unscaled force constants and experimental frequencies as experimental data and the best compromised force constants were determined as those reproducing both sets of data as closely as possible in the least squares sense [62]. But so far, the most successful and most widely used scaling procedure was the scaled quantum mechanical (SQM) approach proposed by Pulay et al. [2,60]. In their method all the diagonal force constants are separated into different groups according to their chemical type and a scale factor is assigned to each group and the geometric mean of the diagonal scale factors are used for the off-diagonal force constants. The scale factors are optimized by minimizing the weighted mean square deviation between the calculated and observed fundamental frequencies. An arithmetic mean rather than the geometric mean of the diagonal scale factors for the off-diagonal force constants were attempted by Hipps and Poshusta in their scaling scheme [61]. More recently several other simpler scaling schemes were found in the literature where a fixed set of scale factors were used for every molecule [63,64] e.g. a scale factor of 0.9 for stretchings, 0.8 for bendings and their respective geometric mean for the coupling force constants was proposed by Durig et al. [64]. In all these scaling procedures the diagonal force constants are modified by using different scale factors while the off-diagonal force constants may be left unaltered or scaled down in some average manner. Since each force constant is physically distinct, it is more realistic to think that each force constant is associated with its own scale factor. Besides, the least squares method need not converge all the time, specially when the parameters are many and do not lead to a unique assignment, specially in less symmetric molecules. Goddard et al. for the first time proposed a different scheme of evaluating the force constants in the cartesian space from the experimental frequencies to use in their molecular mechanical studies [65]. Very recently Vijay and Sathyanarayana proposed their RECOVES (recovery in the eigenvector space) procedure. This procedure uses a computationally simple scheme where the ab initio force constants are modified in a single step by the direct use of experimental eigenvalues of vibrational secular equation in the ab initio calculated eigenvector space. This method works well if the assignments are correct. However, it does not retain the sign of the ab initio force constants.

In this thesis we propose a new way of scaling the ab initio force constants and show

its applicability in the evaluation of reliable force constants and also in the theoretical prediction of vibrational spectra. The aim of this work is to present the methodology for scaling of ab initio force constants and compare its performance with the existing methods. As a result, we have chosen few very well studied systems like acrolein, benzene, naphthalene etc. for which earlier SQM results are available.

Secondly, a set of amino acids and a small dipeptide are chosen to show how this methodology can be extended to these systems to obtain a reliable theoretical force fields for these less symmetric molecules as an aid to determination of the force field parameters for molecular mechanics or molecular dynamics simulation of large biologically important molecules. Amino acids, being the building block of biologically active compounds are of special interest in both biological and structural chemistry. Amino acids exist as zwitterions in the condensed phase, whereas isolated molecules exhibit a neutral structure. While the zwitterionic structure is accessible via X-ray methods, the structure determination of neutral form posses severe experimental problems, since amino acids usually decompose before melting. As a result, so far the gas phase vibrational frequencies of amino acids are limited to glycine only. Any fitting or scaling procedure will perform well only when the ab initio model can reasonably mimic the gross features of experimental spectra. Since the ab initio calculations are mostly performed on isolated molecules, the best compromise between the theory and experiment is possible with gas phase vibrational data. The presence of intermolecular forces in the solid and solution phase leads to shift in the frequencies from the isolated molecular spectra. Thus, a judicial choice of the level of calculation or an improvement of the ab initio isolated model itself to account for this intermolecular effects, are very often needed to reproduce the experimental solid or solution phase spectra with all the isotopic shifts for amino acids [67]. Onsager reaction field approach of using a dielectric continuum is attempted to include the intermolecular H-bonding effects. A brief outline of the thesis is discussed in the next section.

1.1 Outline of the Thesis

The thesis has been arranged in the following manner:

In chapter 2, a brief discussion of the theory underlying ab initio force field calculations

6

are presented. In chapter 3, The newly developed scaling procedure is described in detail and testing of the present methodology is discussed with the examples of benzene, pyridine, acrolein and benzaldehyde. Benzene is used to compare the reliability of the force constants generated by the present methodology with that of Ozkabak and Goodman [3]. In chapter 4, the studies of naphthalene and anthracene in the light of transferability of scale factors between structurally related molecules are discussed in detail. In chapter 5, conformational and vibrational analysis of glycine hydrochloride and glycylglycine hydrochloride along with a theoretical prediction of the latter one from the former by the transfer of scale factors are discussed. In chapter 6, results of the calculations on cysteine and serine hydrochloride and a theoretical prediction of them from glycine hydrochloride and ethanethiol and ethanol respectively are discussed. Chapter 7, deals with glycine zwitterion. We explicitly show in this chapter that the isolated ab initio model fails to mimic the experimental spectra properly and incorporation of solvent effect can only improve the model. A set of non-redundant scale factors are obtained for solvated glycine zwitterion. In chapter 8, we use the same strategy as in glycine zwitterion to model the experimental spectra of alanine followed by a theoretical prediction of the vibrational spectra of cysteine and serine zwitterions using the alanine scale factors. Conclusions and future scope of the present work is discussed in chapter 9.

Bibliography

[1] Barron, L. D. in *Vibrational Spectra and Structure*, Vol. 17B, p.343(Edited by Bist, H. D., Durig, J. R. and Sullivan, J. F.) Elsevier, Amsterdam, 1989.

[2] Nafie, L. A.; Zimba, C. G. in *Biological Applications of Raman Spectroscopy*, Vol. 1, p.307(Edited by Spiro, T. G.) Wiley, New York, 1987.

[3] Bose, P. K.; Barron, L. D.; Polavarapu, P. L. *Chem. Phys.*, **1989**, 155, 423.

[4] Bose, P. K.; Polavarapu, P. L.; Barron, L. D.; Hecht, L. *J. Phys. Chem.*, **1990**, 94, 1734.

[5] Diem. M.; Polavarapu, P. L.; Oboodi, M.; Nafie, L. A. *J. Am. Chem. Soc.*, **1982**, 104, 3329.

[6] Black, T. M.; Bose, P. K.; Polavarapu, P. L.; Barron, L. D.; Hecht, L. *J. Am. Chem. Soc.*, **1990**, 112, 1479.

[7] Barron, L. D.; Gargaro, A. R.; Wen, Z. Q. *J. Chem. Soc., Chem. Comm.*, **1990**, 1034.

[8] Barron, L. D.; Gargaro, A. R.; Hecht, L.; Polavarapu, P. L. *Spectrochim. Acta.*, **1992**, 48A, 261.

[9] Barron, L. D.; Wen, Z. Q.; Hecht, L. *J. Am. Chem. Soc.*, **1992**, 114, 784.

[10] Fogarasi, G.; Pulay, P. *Annu. Rev. Phys. Chem.*, **1984**,35, 191; in *Vibrational Spectra and Structure*, Vol. 14, (Edited by Durig, J. R.), Elsevier, Amsterdam, 1985.

[11] Pulay, P.; Fogarasi, G.; Pongor, G.; Boggs, J. E.; Vargha, A. *J. Am. Chem. Soc.*, **1983**, 105, 7037.

8

[12] Goodman, L.; Ozkabak, A. G.; Thakur, S. N. *J. Phys. Chem.*, **1991**, 95, 9044.

[13] Frisch, M. J.; Trucks, G. W.; Schlegel, H. B.; Gill, P. M. W.; Johnson, B. G.; Robb, M. A.; Cheeseman, J. R.; Keith, T.; Petersson, G. A.; Montgomery, J. A.; Raghavachari, K.; Al-Laham, M. A.; Zakrzewski, V. G.; Ortiz, J. V.; Foresman, J. B.; Cioslowski, J.; Stefanov, B. B.; Nanayakkara, A.; Challacombe, M.; Peng, C. Y.; Ayala, P. Y.; Chen, W.; Wong, M. W.; Andres, J. L.; Replogle, E. S.; Gomperts, R.; Martin, R. L.; Fox, D. J.; Binkley, J. S.; Defrees, D. J.; Baker, J.; Stewart, J. P.; Head-Gordon, M.; Gonzalez, C.; Pople, J. A.; Gaussian 94, Revision C.2, Gaussian Inc., Pittsburgh, PA, 1995.

[14] Schmidt, M. W.; Baldridge, K. K.; Boatz, J. A.; Elbert, S. T.; Gordon, M. S.; Jensen, J. J.; Koseki, S.; Matsunaga, N.; Nguyen, K. A.; Su, S.; Windus, T. L.; Dupuis, M.; Montgomery, J. A. *J.comput.Chem.*, **1993**, 14, 1347.

[15] Texas: TX 90, Pulay, P. Fayetville, AR, 1990; Pulay, P. *Theor. Chim. Acta*, **1979**, 50, 299.

[16] Hondo: Dupuis, M.; Rys, J.; King, H. F. *Quantum Chem. Program Exch. Bull.*, **1977**, 11, 336: **1977**, 11, 338: **1981**, 13, 401; *J. Chem. Phys.*, **1976**, 65, 111.

[17] Turbomole: Ahlrichs, R.; Bär, M.; Häser. M.; Horn, H.; Kölmel, C. *Chem. Phys. Lett.*, **1989**, 162, 165.

[18] Cadpac: Amos, R. D.; Rice, J. E. CADPAC : The Cambridge Analytic Derivatives Package, Issue 4.0, Cambridge, 1987.

[19] Molecule-Sweden: Almlöf, J.; Bauschlicher, C. W.; Blomberg, M. R. A.; Chong, D. P.; Heiberg, A.; Langhoff, S. R.; Malmqvist, P.-A.; Rendell, A. P.; Roos, B. A.; Siegbahn, P. E. M.; Taylor, P. R.

[20] Monstergauss: Peterson, M. R.; Poirier, R. A.; Program MONSTERGAUSS, University of Toronto, Canada, 1981.

[21] Schutte, C. J. H.; in *Structure and Bonding*, Vol. 9, p 213, Springer Verlag, Berlin, 1971.

[22] Schrader, B.; Bougeard, D.; Niggeman, W. in *Computational methods in Chemistry*, (Edited by Bargan, J.), Plenum, New York, 1980.

[23] Fredkin, D. R.; Komoronicki, A.; White, S. R.; Wilson, K. R. *J. Chem. Phys.*, **1983**, 78, 7077.

[24] a) Pulay, P.; Fogarasi, G.; Boggs, J. E. *J. Chem. Phys.*, **1981**, 74, 3999. b) Sellers, H.; Pulay, P.; Boggs, J. E. *J. Am. Chem. Soc.*, **1985**, 107, 6487.

[25] Hess, B. A., Jr.; Schaad, L. J.; Cársky, P.; Zahradník, R.; *Chem. Rev.*, **1986**, 86, 709.

[26] Dulter, R.; Rauk, A.; Shaw, R. A. *J. Phys. Chem.*, **1990**, 94, 118.

[27] Murphy, W. F.; Fernández-Sánchez. J. M.; Raghavachari, K. *J. Phys. Chem.*, **1991**, 95, 1124.

[28] a) Bérces, A. R.; Szalay, P. G.; Magdó, I.; Fogarasi, G.; Pongor, G. *J. Phys. Chem.*, **1993**, 97, 1356. b) Durig, J. R.; Wang, A. *J. Mol. Struct.*, **1993**, 294, 13.

[29] Estirin, D. A.; Paglieri, L.; Corongiu, G. *J. Phys. Chem*, **1994**, 98, 5653.

[30] Rauhut, G.; Pulay, P. *J. Phys. Chem.*, **1995**, 99. 3093.

[31] Momany, F. A.; McGuire, R. F.; Burgess, A. W.; Scheraga, H. A. *J. Phys. Chem.*, **1975**, 79, 2361.

[32] Nemethy, G.; Pottle, M. S.; Scheraga, H. A. *J. Phys. Chem.*, **1983**, 87, 1883.

[33] Sippl, M. J.; Nemethy, G.; Scheraga, H. A. *J. Phys. Chem.*, **1984**, 88, 6231.

[34] a) Weiner, P.; Kollman, P. *J. Comput. Chem.*, **1981**, 2, 287. b) Weiner, S. J.; Kollman, P. A.; Nguyen, D. T.; Case, D. A. *J. Comput. Chem.*, **1986**, 7, 230.

[35] Weiner, S. J.; Kollman, P. A.; Case, D. A.; Singh, U. C.; Ghio,C.; Alagona, C.; Profeta, S.; Weiner, P. *J. Am. Chem. Soc.*, **1984**, 106, 765.

[36] Cornell, W. D.; Cieplak, P.; Bayly, C. I.; Gould, I. R.; Merz, K. M. Jr.; Ferguson, D. M.; Spellmeyer, D. C.; Fox, T.; Caldwell, J. W.; Kollman, P. A. *J. Am. Chem. Soc.*, **1995**, 117, 5179.

10

[37] Brooks, B. R.; Bruccoleri, R. E.; Olafson, B. D.; States, D. J.; Swaminathan, S.; Karplus, M. *J. Comput. Chem.*, **1983**, 4, 187.

[38] Momany, F. A.; Klimkowsky, V. J.; Schäfer, L. *J. Comput. Chem.*, **1990**, 11, 654.

[39] Allinger, N. L.; Burkert, U. *Molecular Mechanics*, ACS Monograph 177, American Chemical Society, Washington DC, 1982.

[40] Allinger, N. L. *J. Am. Chem. Soc.*, **1977**, 99, 8127.

[41] a) Allinger, N. L.; Yuh, Y. H.; Lii, H. J. *J. Am. Chem. Soc.*, **1989**, 111, 8551. b) Lii, H. J.; Allinger, N. J. *J. Am. Chem. Soc.*, **1989**, 111, 8566.

[42] Lii, H. J.; Allinger, N. J. *J. Comput. Chem.*, **1991**, 12, 186.

[43] Allinger, N. L. *J. Am. Chem. Soc.*, **1992**, 114, 1.

[44] Hermans, J.; Berendsen, H. J. C.; van Günsteren, W. F.; Postma, J. P. M. *Biopolymers*, **1984**, 33, 1513.

[45] a) Jorgensen, W. L.; Swenson, C. J. *J. Am. Chem. Soc.*, **1985**, 107, 569. b) Jorgensen, W. L.; Swenson, C. J. *J. Am. Chem. Soc.*, **1985**, 107, 1489.

[46] a) Hagler, A. T.; Lifson, S.; Huler, E. *J. Am. Chem. Soc.*, **1974**, 96, 5319. b) Lifson, S.; Hagler, A. T.; Dauber, P. J. *J. Am. Chem. Soc.*, **1979**, 101, 5111. c) Hagler, A. T.; Stern, P. S.; Sharon, R.; Becker, J. M.; Naider, F. *J. Am. Chem. Soc.*, **1979**, 101, 6842. d) Lifson, S.; Stern, P. S. *J. Chem. Phys.*, **1982**, 77, 4542.

[47] Dauber-Osguthorpe, P.; Roberts, V. A.; Osguthorpe, D. J.; Wolff, J.; Genest, M.; Hagler, A. T. *Proteins: Struct. Funct. Genetics*, **1988**, 4, 31.

[48] Mayo, S. L.; Olafson, B. D.; Goddard III, W. A. *J. Phys. Chem.*, **1990**, 94, 8897.

[49] Amodeo, P.; Barone, V. *J. Am. Chem. Soc.*, **1992**, 114, 9085.

[50] Derreumaux, P.; Vergoten, G. *J. Chem. Phys.*, **1995**, 102, 8586.

[51] a) Wilson, E. B.; Decius, J. C.; Cross, P, C. *Molecular Vibrations*, Mc Graw Hill, New York, 1955. b) Schachtschneider, J. H.; Synder, R. G. *Spectrochim. Acta*, **1963**, 19, 117.

[52] Pulay, P.; in *Modern Theoretical Chemistry*, Vol. 4, p.153, (Edited by Schaefer, H. F. III), Plenum, New York, 1977.

[53] Flanigan, M. C.; Komornicki, A.; McIver, J. W.; in *Modern Theoretical Chemistry*, Vol. 8, p.1, (edited by Segal G. A.), Plenum, New York, 1977.

[54] Pulay, P.; Meyer, W. *Mol. Phys.*, **1974**, 27, 473.

[55] Bleicher, W.; Botschwina, P. *Mol. Phys.*, **1975**, 30, 1029.

[56] Botschwina, P.; Meyer, W.; Semkow, A. M. *Chem. Phys.*, **1976**, 15, 25.

[57] Fogarasi, G.; Pulay, P.; Molt, K.; Sawodny, W. *Mol. Phys.*. **1977**, 33, 1565.

[58] Pouchan. C.; Liotard, D.; Dargelos, A.; Chaillet, M. *J. Chim. Phys.*, **1976**, 73, 1046.

[59] Blom, C. E.; Altona, C. *Mol. Phys.*, **1976**, 31, 1377.

[60] a) Fogarasi, G.; Pulay, P.; *J. Mol. Struct.*, **1977**, 39, 275. b) Török, F.; Hegedüs, A.; Kosa, K.; Pulay, P. *J. Mol. Struct.*, **1976**, 32, 93.

[61] Hipps, K. W.; Poshusta, R. D. *J. Phys. Chem.*, **1982**, 86, 4112.

[62] Ha, T. -K.; Meyer, R.; Günthard, Hs. H. *Chem. Phys. Lett.*, **1978**, 59, 17.

[63] Nobes, R. H.; Radom, L. *Org. Mass Spectrom.*, **1982**, 17, 340.

[64] Durig, J. R.; Wang, A. Y.; Little, J. S.; Brletic, P. A. *J. Chem. Phys.*, **1990**, 93, 905.

[65] a) Goddard, W. A. III.; Wendel, J. A. *J. Chem. Phys.*, **1992**, 97, 5048. b) Dasgupta, S.; Goddard, W. A. III. *J. Chem. phys.*, **1989**, 90, 7207.

[66] Sathyanarayana, D. N.; Vijay, A. *J. Mol. Struct.*, **1994**, 328, 269.

[67] Yu, G.; Freedman, T. B.; Nafie, L. A.; Deng, Z.; Polavarapu, P. L. *J. Phys. Chem.*, **1995**, 99, 835.

Chapter 2

Methodology

The literature on ab initio calculations and normal coordinate analysis is vast and extensive. Hence this chapter does not purport to be a review of these methods. A flavour of the various theories and nuances underlying these methods are however presented in this chapter. Detailed description of these methods is given in references [1-19].

2.1 Ab Initio Methods

The Hamiltonian of a molecule consisting of N electrons and M nuclei in atomic units is -

$$\hat{H} = -\sum_{\alpha=1}^{M} \frac{1}{2m_\alpha} \nabla_\alpha^2 - \sum_{i=1}^{N} \frac{1}{2} \nabla_i^2 - \sum_{i=1}^{N} \sum_{\alpha=1}^{M} \frac{Z_\alpha}{r_{i\alpha}} + \sum_{\beta>\alpha} \sum_{\alpha} \frac{Z_\alpha Z_\beta}{r_{\alpha\beta}} + \sum_{j>i} \sum_{i} \frac{1}{r_{ij}} \qquad (2.1)$$

where m_α is the ratio of the mass of nucleus α to the mass of an electron, Z_α is the atomic number of nucleus α, $r_{i\alpha}$ is the distance between electron i and nucleus α, r_{ij} is the distance between electron i and electron j and $r_{\alpha\beta}$ is the distance between the nucleus α and nucleus β respectively.

Within Born-Oppenheimer (B.O) approximation [20] one can consider that electrons in a molecule to be moving in the field of fixed nuclei and hence the kinetic energy of the nuclei can be neglected and the nuclear-nuclear repulsion can be considered to be a constant. Hence the Schrödinger equation for the electronic motion is -

$$\hat{H}_{el} \psi_{el} = E_{el} \psi_{el} \qquad (2.2)$$

where,

$$\hat{H}_{el} = -\sum_{i=1}^{N}\frac{1}{2}\nabla i^2 - \sum_{i=1}^{N}\sum_{\alpha=1}^{M}\frac{Z_{\alpha}}{r_{i\alpha}} + \sum_{j>i}\sum_{i}\frac{1}{r_{ij}} \qquad (2.3)$$

The solution to Schrödinger equation involving the electronic Hamiltonian, is the electronic wave function,

$$\psi_{el} = \psi_{el}(r_i; r_{\alpha}) \qquad (2.4)$$

which describes the motion of the electrons and explicitly depends on the electronic coordinates but depends parametrically on the nuclear coordinates, as does the electronic energy,

$$E_{el} = E_{el}(r_{\alpha}) \qquad (2.5)$$

Thus the electronic energy including nuclear-nuclear repulsion for a fixed nuclei system must be

$$U = E_{el} + \sum_{j>\alpha}\sum_{\alpha}\frac{Z_{\alpha}Z_{j}}{r_{\alpha j}} \qquad (2.6)$$

The vibration, rotation or translation of a molecule needs the solution to a nuclear Schrödinger equation

$$\hat{H}_{nuc}\phi_{nuc} = E_{tot}\phi_{nuc} \qquad (2.7)$$

where E_{tot} is the total energy. The nuclear Hamiltonian for the motion of the nuclei in the average field of the electrons can be written as

$$\hat{H}_{nucl} = -\sum_{\alpha=1}^{M}\frac{1}{2m_{\alpha}}\nabla\alpha^2 + U(r_{\alpha}) \qquad (2.8)$$

Thus the total electronic energy including nuclear-nuclear repulsion constitutes a potential energy surface for the nuclear motion obtained by solving the electronic problem.

2.1.1 Hartree Fock Theory

The electronic problem is solved by considering a single Slater determinant as the ground state antisymmetric wave function in terms of molecular orbital Ψ_i,

$$\Psi_i = \sum_{\mu=1}^{N}C_{\mu_i}\Phi_{\mu} \qquad (2.9)$$

where each molecular orbital is approximated as linear combination of finite set of basis functions and $C_{\mu i}$ are the molecular orbital expansion coefficients.

The coefficients $C_{\mu i}$ are chosen in such a way that the calculated total energy is minimum. This leads to the well known Roothan equations [21,22];

$$\sum_{\nu=1}^{N} (F_{\mu\nu} - \epsilon_i S_{\mu\nu}) C_{\nu i} = 0, \qquad \mu = 1, 2, \ldots, N; \qquad i = 1, 2, \ldots, N \qquad (2.10)$$

where N is the total number of basis functions, ϵ_i is the orbital energy of the ith molecular orbital Ψ_i, $S_{\mu\nu} = \langle \Phi_\mu \mid \Phi_\nu \rangle$ are the overlap integrals and $F_{\mu\nu}$ are the elements of the Fock matrix given by

$$F_{\mu\nu} = H_{\mu\nu}^{core} + \sum_{\lambda=1}^{N} \sum_{\sigma=1}^{N} P_{\lambda\sigma} \left[(\mu\nu \mid \lambda\sigma) - \frac{1}{2} (\mu\lambda \mid \nu\sigma) \right] \qquad (2.11)$$

where

$$H_{\mu\nu}^{core} = \left\langle \Phi_\mu \mid -\frac{1}{2}\nabla^2 - \sum_\alpha V_\alpha \mid \Phi_\nu \right\rangle$$

is the one electron integral and

$$P_{\lambda\sigma} = 2 \sum_{i=1}^{OCC} C_{\lambda i}^* C_{\sigma i} \qquad (2.12)$$

is the density matrix. The summation in equation (2.12) is over the occupied molecular orbitals only. Here $P_{\lambda\sigma}$ represents the total electron population existing in the overlap region of the basis functions Φ_μ and Φ_ν. The factor 2 indicates that two electrons occupy each molecular orbital and the asterisk denotes complex conjugation. The electronic energy E_{el} can be expressed as

$$E_{el} = \frac{1}{2} \sum_{\mu=1}^{N} \sum_{\nu=1}^{N} P_{\mu\nu}(F_{\mu\nu} + H_{\mu\nu}^{core}) \qquad (2.13)$$

The Roothan-Hall equation 2.10 is nonlinear, since the Fock matrix $F_{\mu\nu}$ itself depends on the molecular orbital coefficients, $C_{\mu i}$, through the density matrix expression 2.12. Solution of it necessarily involves an iterative procedure. Since the resulting molecular orbitals are derived from their own effective potential, the technique is frequently called Self Consistent Field (SCF) theory. SCF calculations are known to give a good account of

the energy hypersurface only in the region close to the equilibrium molecular geometry. At larger deviations from the minima, the SCF potential curve starts to depart considerably from the "experimental" curve because of the neglect of electron correlation.

2.1.2 Electron Correlation

The inability of the Hartree Fock (HF) procedure to adequately account for the correlation of electron motion can be corrected by using more elaborate models comprising a multi-determinant wave function. Two techniques are widely used to incorporate the effect of electron correlation, one the configuration interaction [23] and the other the Moller Plesset perturbation theory [24]. The first method is variational but not size consistent but the second is size consistent but not variational. Variational implies that the calculated electronic energy should correspond to an upper bound to the energy that would result from the exact solution of the Schrödinger equation. Size consistency means that the method must give additive results when applied to an assembly of isolated molecules.

Thus the non-relativistic exact energy would be

$$E_{(exact)} = E_{(HF)} + E_{(correlation)} \tag{2.14}$$

Configuration Interaction (CI)

CI methods begin by noting that the exact wave function Ψ cannot be expressed as a single determinant, as HF theory assumes. CI proceeds by constructing other determinants by replacing one or more occupied orbitals within the HF determinant with virtual orbitals. A detailed account of CI and its applications are given in reference [25]. The size consistency of these methods can also be improved by coupled cluster methods [25]. Full CI is the most complete non-relativistic treatment of the molecular system possible, within the limitations imposed by the chosen basis set, though generally not computationally feasible. The rapid advancement of computer technology made it possible to consider yet upto one billion determinants full CI energy calculation of Be_2 molecule so far [26].

Moller-Plesset Perturbation Theory (MP)

Since we have only employed the second order MP theory in our calculations, we briefly discuss the features of the second order Moller Plesset (MP2) calculations [27].

Perturbation theory is based upon dividing the Hamiltonian into two parts

$$H = H_0 + \lambda V \tag{2.15}$$

such that H_0 is soluble exactly. λV is a perturbation applied to H_0, a correction which is assumed to be small in comparison to it. The assumption that V is a small perturbation to H_0 suggests that the perturbed wave function and the energy can be expressed in a power series in terms of λ according to the Rayleigh-Schrödinger perturbation theory [27].

In the MP theory H_0 is defined as the sum of the one electron Fock operators.

$$H_0 = \sum_i F^i \tag{2.16}$$

The HF determinant and all other substituted determinants are eigenfunctions of H_0 and we get

$$H_0 \Psi_s = E_s \Psi_s \tag{2.17}$$

where Ψ_s are the unperturbed functions representing all possible Slater determinants formed from n different spin orbitals.

When $\Psi^{(0)}$ denotes the ground state, its energy is simply the sum of the orbital energies

$$E^{(0)} = \left\langle \Psi^{(0)} \mid \sum_i F^i \mid \Psi^{(0)} \right\rangle = \sum_i \epsilon_i \tag{2.18}$$

The first order correction to the energy is given by

$$E^{(1)} = \left\langle \Psi^{(0)} \mid V \mid \Psi^{(0)} \right\rangle \tag{2.19}$$

Adding $E^{(0)}$ and $E^{(1)}$ yields the HF energy (since H_0+V is the full HF Hamiltonian).

$$E^{(0)} + E^{(1)} = \left\langle \Psi^{(0)} \mid (H_0 + V) \mid \Psi^{(0)} \right\rangle = E^{(HF)} \tag{2.20}$$

Thus the first order term does not incorporate any correction to the HF approximation.

The second order correction to the energy is given by

$$E^{(2)} = \left\langle \Psi^{(0)} \mid V \mid \Psi^{(1)} \right\rangle \tag{2.21}$$

where $\Psi^{(1)}$ is a linear combination of substituted determinantal wave functions

$$\Psi^{(1)} = \sum_s a_s \Psi_s \tag{2.22}$$

Perturbation theory gives the following expression for $\Psi^{(1)}$

$$\Psi^{(1)} = \sum_s \left[\frac{\left\langle \Psi_s \mid V \mid \Psi^{(0)} \right\rangle}{E^{(0)} - E_s} \right] \Psi_t \tag{2.23}$$

The second order energy correction can be written as [27]

$$E^{(2)} = - \sum_s \frac{\left| \left\langle \Psi^{(0)} \mid V \mid \Psi_s \right\rangle \right|^2}{E_s - E^{(0)}} \tag{2.24}$$

Thus, the value $E^{(2)}$, the first correction to the HF energy, will always be negative. The numerator will be nonzero only for double substitutions. Single substitutions are known to make this expression zero by Brillouin's theorem.

2.1.3 Basis Sets

Basis sets play an important role in the evaluation of the energies. A limiting HF treatment would involve an infinite number of basis functions. This is clearly impractical since the computational expense of HF molecular orbital calculation is formally proportional to the fourth power of the total number of basis functions. Therefore the ultimate choice of basis set size depends on a compromise between accuracy and cost. For computational utilities it is desirable to use gaussian basis functions $g(r)$,[28] where r is the position vector (x, y, z). Excellent reviews exist on basis sets [19,29-32] and their limitations. Methods to construct new basis sets are described in reference [19]. We discuss here briefly the salient features of different basis sets.

Minimal Basis Set

The STO-3G minimal basis set was developed by Pople and co workers for first row elements [33]. It was later extended to the second row [34], third row [35] and fourth row [36] elements. It has also been applied to first and second row transition metals [37]. It is characterized by its small size and effectiveness in predicting geometries [38]. The remarkable agreement of the STO-3G geometries to the experimental geometries is due to the large basis set superposition error which helps cancel other defects to produce

reasonable bond parameters. It can be expressed as

$$\Phi_{nl}(\zeta = 1, r) = \sum_{k=1}^{3} d_{nl,k}\ g_l(\alpha_n, k, r) \qquad (2.25)$$

where the subscripts n and l define the specific principal and angular quantum numbers, g_ls are the normalized gaussian functions, α_ns are the gaussian exponents and $d_{nl,k}$s are the linear expansion coefficients. The values of α are determined by minimizing the error in the fit of the gaussian expansion to the exact Slater orbitals. The STO-3G basis description of conjugated systems and polar molecules is far from satisfactory. This is due to the fact that all the elements of a single row of the periodic table have the same description.

Split Valence Basis Set

A basis set formed by doubling or tripling all functions of the minimal representation is usually termed a double-zeta or triple-zeta basis set. An even simpler extension of the minimal basis set is to double or triple only the number of basis functions representing the valence region and is known as split valence basis set. These split valence basis sets are a compromise between the speed obtained using a minimal basis and the accuracy of the larger ones. The 4-21G [38] basis is extremely suitable for geometry optimizations utilizing the analytic gradients. A reduced version of the 4-21G basis set, the 3-21G basis set [39,40] is also used in routine calculations. The characteristics of both the basis sets are similar. The 4-31G and 6-31G bases are generated by increasing the number of primitives devoted to the core and first valence electron functions. The 4-31G [41] and 6-31G [42] bases improve upon 3-21G energetics at the expense of increased computer time.

Polarization Basis Set

Polarization functions are needed for the description of the highly polar molecules and of systems incorporating small strained rings. These systems require that some allowance be made for the possibility of non-uniform displacement of charges away from the atomic centers. Adding all the five components of a cartesian d function to the first row elements of 6-31G basis set gives the 6-31G* basis set. Further addition of p functions to the hydrogen atoms results in the 6-31G** basis set. These basis sets are first proposed by Hariharan and Pople [43] for the first row elements and later extended to the second

row elements [44]. A larger polarization basis set, 6-311G** has been formulated for the first row elements [45]. It comprises an inner core of six s type gaussians and an outer (valence) region, which has been split into three parts, represented by three, one and one primitives, respectively. This basis set is supplemented by a single set of five /six d-type gaussian functions for first row atoms and a single set of uncontracted p-type gaussians for hydrogen.

Diffused Basis Set

This set of functions are needed for species with significant electron density far removed from the nuclear center. Such species involve anions for which the extra electron is only weakly bound and hence is needed to include in the basis representation one or more sets of highly diffuse functions [46]. The 3-21+G and 6-31+G* basis sets for the first row elements and 3-21+G, 3-21+G* and 6-31+G* basis sets for second row elements [47] are constructed from the underlying 3-21G, 3-21G* and 6-31G* representations by the addition of a single set of diffuse gaussian s and p-type functions. The higher 6-31++G* and 6-31++G** basis sets include an extra diffuse function to the hydrogen of the corresponding 6-31+G* and 6-31++G* basis sets.

2.1.4 Reaction Field Model of Solvation

In the vibrational analysis of amino acid zwitterions the Onsager reaction field model is used in this thesis. A brief outline of this method is presented here.

Onsager Reaction Field Model

In this model [48] the solute is placed in a cavity (usually spherical) immersed in a continuum medium with a dielectric constant ϵ [49]. A dipole in the molecule will induce a dipole in the medium and the electric field applied to the solute by the solvent (reaction) dipole will in turn interact with the molecular dipole leading to a net stabilization. In the MO theory, the electrostatic solvent effect may be taken as an additional term H_1 in the Hamiltonian of the isolated molecule H_0 giving,

$$H_{rf} = H_0 + H_1 \qquad (2.26)$$

The perturbation term (H_1) describes the coupling between the molecular dipole operator ($\hat{\mu}$) and the reaction field, $\vec{R}$

$$H_1 = -\hat{\mu}\vec{R} \qquad (2.27)$$

The reaction (electric) field, $\vec{R}$, is proportional to the molecular dipole moment, $\vec{\mu}$

$$\vec{R} = g\vec{\mu} \qquad (2.28)$$

The proportionality constant g, which gives the strength of the reaction field depends on the dielectric constant of the medium ϵ [50], and on the radius of the spherical cavity a_0. The value of g is given by the equation

$$g = \frac{2(\epsilon - 1)}{(2\epsilon - 1)a_0^3} \qquad (2.29)$$

For the case of a self-consistent field wave function the effects of the reaction field can be incorporated as an additional term in the Fock matrix as

$$F_{\lambda\sigma} = F_{\lambda\sigma}^0 - g\vec{\mu}\langle\phi_\lambda \mid \hat{\mu} \mid o_\sigma\rangle \qquad (2.30)$$

where ϕ_λ and o_σ are basis functions. When the solvent polarization is included, the energy of the system is given by

$$E = \langle\Psi \mid H_0 \mid \Psi\rangle - \frac{1}{2}\vec{\mu}\vec{R} \qquad (2.31)$$

where Ψ is the full wave function of the molecule.

2.1.5   Force Constants

The evaluation of force fields is one of the foci of this thesis. The starting point of all force field evaluations is the harmonic approximation.

Harmonic Approximation

Within the harmonic approximation, the nuclear potential $V(R_1....R_M)$ is expressed as the quadratic terms in a power series expansion of the total energy $E(R_1...R_M)$ about the equilibrium position,

$$E = E(X_1^o,....X_{3M}^o) + \sum_{i=1}^{3M} \frac{\partial E}{\partial X_i}\Big|_o \Delta X_i + \frac{1}{2}\sum_{y=1}^{3M} \frac{\partial^2 E}{\partial X_i \partial X_j}\Big|_o \Delta X_i \Delta X_j + \cdots \qquad (2.32)$$

where $X_1, X_2, \ldots X_{3M}$ are the cartesian coordinates of the M nuclei. The first term in the R. H. S of equation (2.32) is constant for all E_{nucl} and hence can be ignored. Since E is a minimum at the equilibrium geometry

$$\frac{\partial E}{\partial X_i} \Big|_o = 0 \tag{2.33}$$

Hence the second term in equation (2.32) vanishes. If all terms of order higher than two are neglected, the potential is a quadratic function of the nuclear displacements ΔX_i

$$E(X_1, \ldots X_{3M}) \equiv \frac{1}{2} \sum_{j=1}^{3M} F_{ij} \Delta X_i \Delta X_j \tag{2.34}$$

where the force constants F_{ij} are given by

$$F_{ij} = \frac{\partial^2 E}{\partial X_i \partial X_j} \Big|_o \tag{2.35}$$

Equation (2.34) represents the harmonic approximation. For small displacements about the equilibrium position, equation (2.34) is valid, but it is not accurate for large distortions.

A transformation to mass weighted cartesian coordinates $\rho_i = (m_i)^{\frac{1}{2}} \Delta X_i$ followed by rotation of the coordinates to coincide with the principal axes of the quadratic form in equation (2.34) gives an expression for V containing only squared terms.

$$V = \frac{1}{2} \sum_{i=1}^{3M} \lambda_i Q_i^2 \tag{2.36}$$

where Q_i are coordinates relative to the principal axes and hence called "normal coordinates". As a result of these transformations equation (2.34) which depends on 3M variables separates into 3M equations, each depending upon a single Q_i. Further each of these is a harmonic oscillator equation with eigen value λ_i.

For non linear molecules six of the λ_is corresponding to three translational and three rotational motions of the entire molecule are zero. These six λ_is can be removed by working in a coordinate system having the origin at the center of mass and rotating with the molecule. The remaining 3M-6 degrees of freedom are usually specified by internal coordinates such as bond lengths, bond angles and dihedral angles. As a result, fewer force constants need to be evaluated and those that are evaluated have physical interpretation.

22

Though the harmonic approximation is good enough for most vibrational calculations, recent studies indicate that the inclusion of anharmonicity leads to a better agreement with the experimental frequencies. But these are limited to small molecules [51] and extension of the anharmonic treatment to a relatively large system of chemists' interest is yet in its infancy.

Anharmonicity

Most of the vibrational calculations to date have used the harmonic approximation of equation (2.34) but with the progress in ab initio calculations, cubic and quartic force constants can now be evaluated. These are the third and fourth order terms dropped from equation (2.34). The inclusion of them in equation (2.34) allows the possibility of including anharmonicity in ab initio treatments. Perturbation theory yields the following formula for anharmonicity [17].

$$\chi_{rr} = \frac{1}{16}\Phi_{rrrr} - \frac{1}{16}\sum_s \Phi_{rrs}^2 \frac{[8\omega_r^2 - 3\omega_s^2]}{\omega_s(4\omega_r^2 - \omega_s^2)} \qquad (2.37)$$

Equation (2.37) contains the quadratic, diagonal quartic and semi diagonal cubic force constants. The ω_k are the harmonic frequencies. The evaluation of the quartic force constant Φ_{rrrr} is given in reference [52]. A detailed treatment of anharmonicity and its inclusion in force field calculations is given in references [53-55].

2.2 Transformation of Force Constants

The quantum mechanically calculated ab initio force constants are generally derived with respect to the cartesian coordinates. Transformation of these cartesian force constants to internal coordinates helps to interpret the results within the GF matrix formalism of the vibrational problem by Wilson [11].

In cartesian coordinates the diagonal force constants are not necessarily dominant and the useful concept of partitioning the potential into dominant diagonal versus less important coupling terms is lost. The force constants in internal coordinates are physically meaningful and are easy to compare and transfer between structurally related molecules.

The basic types of internal coordinates bond stretching, valence angle bending, out of plane bending and torsions proposed by Wilson, Decius and Cross [11] are generally accepted, although there are variations in handling of redundancy and symmetry. A set of non-redundant internal coordinates were recommended by Pulay et al. as an alternative [18]. These coordinates are local, i.e., use of local coordinates which extend over a few neighbouring atoms only, based on local symmetry. These non-redundant local coordinate facilitate the transfer of force constants from one molecule to the other.

The main bottleneck in the conversion of the cartesian force constants to internal force constants is that the force field matrix in cartesian coordinates spans a 3N dimensional space, N being the number of atoms, while the number of non-redundant internal coordinates is only 3N-6 (or 3N-5 for linear molecules). The transformation from cartesian to internal coordinates can be described as follows [56]. The potential energy surface of a given state can be described both in cartesian coordinates and in internal coordinates as

$$E(x) = E_o(x) + g.x + 0.5.x^\dagger.H.x \cdots \qquad (2.38)$$

$$E(q) = E_o(q) + f.q + 0.5.q^\dagger.F.q \cdots \qquad (2.39)$$

where q is the internal coordinate vector, x is the cartesian vector, g and f are the gradients, H and F are the second derivative matrices in the two frameworks. Wilson's B matrix transforms cartesian into internal coordinates, as q=Bx [11] and from 2.38 and 2.39 we get

$$F = B^{-1\dagger}.H.B^{-1} \qquad (2.40)$$

Since B is a rectangular matrix, to invert it, it is necessary to use the notion of a generalized inverse matrix.

$$B^{-1\dagger} = (BB^\dagger)^{-1}.B \qquad (2.41)$$

However $BB^\dagger$ could be singular so that the conversion is always not possible. The symmetric G is non-singular [57] and can be inverted. If A is the inverse of B and M is the atomic mass diagonal matrix of order 3Nx3N then we have

$$AB = E$$

$$ABM^{-1}B^\dagger = EM^{-1}B^\dagger$$

$$AG = M^{-1}B^\dagger$$

$$A = M^{-1}B^\dagger G^{-1}$$

as given in [58]. Translating to local symmetry,

$$A_{loc}B_{loc} = E \qquad where B_{loc} = U_{loc}B$$

Postmultiplying $M^{-1}B^\dagger_{loc}$ on both sides we have

$$A_{loc}B_{loc}M^{-1}B^\dagger_{loc} = M^{-1}B^\dagger_{loc}$$

$$A_{loc}G_{loc} = M^{-1}B^\dagger_{loc}$$

$$A_{loc} = M^{-1}B^\dagger_{loc}G^{-1}_{loc}$$

From equation 2.40, $\qquad F_{loc} = A^\dagger_{loc}F_{cart}A_{loc}$

Here A_{loc}, G_{loc}, F_{loc} are the local symmetric A, G and F matrices respectively. U_{loc} is the transformation matrix which contains the description of the local symmetry coordinates in terms of internal coordinates.

The local symmetric force constants could be transformed to the symmetric force constants easily using

$$F_{sym} = U_{ortho}F_{loc}U^\dagger_{ortho} \tag{2.42}$$

where U_{ortho} is the orthogonal transformation matrix. .

2.3 Computational Details

All ab initio calculations were done using Gaussian 90-94 [59] and GAMESS [60] suit of programs installed on Convex-C220, HP-9000/735 and Dec-Alpha computer systems. The normal coordinate analyses were done based on the modified version of the programs of Schachtschneider [61]. The conversion of cartesian force constants to local symmetric force constants were done using a modified version of the program VECEIG kindly provided by Dr. Amarendra Vijay and Professor D. N. Satyanarayana.

Bibliography

[1] Richards, N. G.; Cooper, D. L. *Ab Initio Molecular Orbital Calculations for Chemists*, second edn., Clarendon Press, Oxford, 1983.

[2] Wilson, S. *Electron Correlation in Molecules*, Clarendon Press, Oxford, 1984.

[3] Hehre, W. J.; Radom, L.; Schleyer, P. v. R.; Pople, J. A. *Ab Initio Molecular Orbital Theory*, Wiley, New York, 1986.

[4] Advances in Chemical Physics, *Ab Initio Methods in Quantum Chemistry*, Vols. 67 and 69, Wiley, New York, 1987.

[5] Naray-Szabo, G.; Surjan, P.; Angyan, J. A. *Applied Quantum Chemistry*, Akademiai Kiado, Budapest, 1987.

[6] Hirst, D. M. *A Computational approach to Chemistry*, Blackwell Scientific, London, 1990.

[7] Szabo, A.; Ostlund, N. S.; *Modern Quantum Chemistry*, Mc Graw Hill, New York, 1989.

[8] Dykstra, C. E. *Quantum Chemistry and Molecular Spectroscopy*, Prentice Hall, Englewood Cliffs., N. J., 1992.

[9] Schatz, G. C.; Ratner, M. A. *Quantum Mechanics in Chemistry*, Prentice Hall, Englewood Cliffs., N. J., 1993.

[10] Pople, J. A. in *Modern Theoretical Chemistry*, Ed. Schaefer III, H. F., Vol. 4, Plenum, New York, 1977.

[11] Wilson, E. B.; Decius, J. C.; Cross, P, C. *Molecular Vibrations*, Mc Graw Hill, New York, 1955.

26

[12] Herzberg, G. *Infrared and Raman Spectra of Polyatomic Molecules*, D. van Nostrand, New York, 1945.

[13] Shimanouchi, T. in *Physical Chemistry an Advanced Treatise*, Vol. IV, Molecular Properties, Ed. Henderson, D., Ch. 6, Academic Press, New York, 1970

[14] Sverdlov, L. M.; Kovner, M. A.; Krainiv, E. P. *Vibrational Spectra of Polyatomic Molecules*, Halsted Press, Wiley, New York, 1974.

[15] Bauschewitz, P. *Spectroscopic Infrarouge*, Vols. 1 and 2, Gauthier Villars, Paris, 1961, 1967.

[16] Cyvin, S. J. *Molecular Vibrations and Mean Square Amplitudes*, Elsevier, Amsterdam, 1968.

[17] Mills, I. M.; in *Molecular Spectroscopy*, Eds. Rao, K. N. and Mathews, C. W., Academic Press, New York, 1972.

[18] Fogarasi, G.; Pulay, P. in *Vibrational Spectra and Structure*, A series of Advances, Ed. Durig, J. R. Vol. 14, Elsevier, Amsterdam, 1985.

[19] Poirier, R.; Kari, R.; Csizamadia, I. G. *Handbook of Gaussian Basis sets*, Elsevier Science, New York, 1985.

[20] Born, M.; Oppenheimer, R. *Ann. Phys. (Leipzig)*, **1927**, 84, 457.

[21] Roothan, C. C. J. *Rev. Mod. Phys.*, **1951**, 23, 69.

[22] Hall, G. *Proc. Roy. Soc. (London)*, **1951**, A205, 541.

[23] a) Salem. L.; Rowland, C. *Angew. Chem. Int. Edn. Engl.*, **1972**, 11, 92. b) Hehre, W. J.; Salem, L.; Wilcott, M. R. *J. Am. Chem. Soc.*, **1974**, 96, 4328. c) Townshend, R. E.; Ramuni, G.; Segal, G.; Hehre, W. J.; Salem, L. *J. Am. Chem. Soc.*, **1976**, 98, 2190. d) Langhoff, S. R.; Davidson, E. R. *Int. J. Quant. Chem.*, **1974**, 8, 61. e) Pople, J. A.; Seeger, R.; Krishnan, R. *Int. J. Quant. Chem. Symp.*, **1977**, 11, 149.

[24] a) Moller, C.; Plesset, M. S. *Phys. Rev.*, **1934**, 46, 618. b) Pople, J. A.; Binkley, J. S.; Seeger, R. *Int. J. Quant. Chem. Symp.*, **1976**, 10, 1.

[25] Bauschlicher, C. W.; Lanhoff, S. R.; Taylor, P. R. *Adv. Chem. Phys.*, **1990**, 77, 103.

[26] Evangelisti. S.; Bendazzoli, G. L.; Ansaloni, R.; Duri, F.; Rossi, E. *Chem. Phys. Lett.*, **1996**, 252, 437.

[27] a) Levine, I. N. *Quantum Chemistry*, p.222, Fourth edn., Prentice Hall, Englewood Cliffs., N. J., 1991. b) Foresman, J. B.; Frisch, A. in *Exploring Chemistry with Electronic Structure Methods*, Second Edition, Gaussian, Inc., Pittsburgh, PA.

[28] Boys, S. F. *Proc. Roy. Soc. (London)*, **1950**, A200, 542.

[29] Davidson, E. R.; Feller, D. *Chem. Rev.*, **1986**, 86, 681.

[30] Setters, H.; Almlöf, J. *J. Phys. Chem.*, **1989**, 93, 5136.

[31] Dunning, T. H.; Hay, P. J. in *Modern Theoretical Chemistry*, Ed. Schaefer III, H. F., Vol. 3, p.1, Plenum Press, New York, 1977.

[32] Gaussian Basis Sets for Molecular Calculations, Ed. Huzinaga, S., Elsevier, Amsterdam, 1984.

[33] Hehre, W. J.; Stewart, R. F.; Pople, J. A. *J. Chem. Phys.*, **1969**, 51, 2657.

[34] Hehre, W. J.; Ditchfield, R.; Stewart, R. F.; Pople, J. A. *J. Chem. Phys.*, **1970**, 52, 2769.

[35] Pietro, W. J.; Levi, B. A.; Hehre, W. J.; Stewart, R. F. *Inorg. Chem.*, **1980**, 19, 2225.

[36] Pietro, W. J.; Blurock, F. S.; Hout, R. S.; Hehre, W. J.; Defrees, D. J.; Stewart, R. F. *Inorg. Chem.*, **1981**, 20, 3650.

[37] Pietro, W. J.; Hehre, W. J. *J. Comput. Chem.*, **1983**, 4, 241.

[38] Pulay, P.; Fogarasi, G.; Pang, F.; Boggs, J. E. *J. Am. Chem. Soc.*, **1979**, 101, 2550.

[39] Binkley, J. S.; Pople, J. A.; Hehre, W. J. *J. Am. Chem. Soc.*, **1980**, 102, 939.

[40] Gordon, M. S.; Binkley, J. S.; Pople, J. A.; Pietro, W. J.; Hehre, W. J. *J. Am. Chem. Soc.,* **1982,** 104, 2797.

[41] a) Ditchfield, R.; Hehre, W. J.; Pople, J. A. *J. Chem. Phys.,* **1971,** 54, 724. b) Hehre, W. J.; Pople, J. A. *ibid,* **1972,** 56, 4233. c) Dill, J. D.; Pople, J. A. *ibid,* **1975,** 62, 2921. d) Hehre, W. J.; Lathan, W. A. *ibid,* **1972,** 56, 5255.

[42] a) Hehre, W. J.; Ditchfield, R.; Pople, J. A. *J. Chem. Phys.,* **1972,** 56, 2257. b) Binkley, J. S.; Pople, J. A. *ibid,* **1977,** 66, 879

[43] Hariharan, P. C.; Pople, J. A. *Chem. Phys. Lett.,* **1972,** 66, 217.

[44] Francl, M. M.; Pietro, W. J.; Hehre, W. J.; Binkley, J. S.; Gordon, M. S.; Defrees, D. J.; Pople, J. A. *J. Chem. Phys.,* **1982,** 77, 3654.

[45] Krishnan, R.; Frisch, M. J.; Pople, J. A. *J. Chem. Phys.,* **1980,** 72, 4244.

[46] a) Dykstra, C. E.; Hereld, M.; Lucchese, R. R.; Scaefer, H. F. III; Meyer, W. *J. Chem. Phys.,* **1977,** 67, 4071. b) Dykstra, C. E.; Arduengo, A. J.; Fukunga, T. *J. Am. Chem. Soc.,* **1978,** 100, 6007. c) Jordon, K. D. *Acc. Chem. Res.,* **1979,** 12, 36. d) Carsky, P.; Urban, M. *Lectures Note in Chemistry,* 16, *Ab Initio Calculations. Methods and Applications in Chemistry,* Springer-Verlag, Berlin 1980 and refernces cited there in.

[47] Clark, T.; Chandrasekhar, J.; Spitznagel, G. W.; Schleyer, P. v. R. *J. Comput. Chem.,* **1983,** 4, 294. b) Frisch, M. J.; Pople, J. A.; Binkley, J. S. *J. Chem. Phys.,* **1984,** 80, 3265.

[48] Wong, M. W.; Frisch, M. J.; Wiberg, K. B. *J. Am. Chem. Soc.,* **1991,** 113, 4776.

[49] Onsager, L. *J. Am. Chem. Soc.,* **1936,** 58, 1486.

[50] a) *A Handbook of Chemistry and Physics,* 70th. ed., Weast, R. C. Ed.; CRC Press, Boca Raton, Fl, 1989. b) *Lange's Handbook of Chemistry,* Dean, J. A. Ed., McGraw-Hill, New York, 1985.

[51] East, A. L. L.; Allen, W. D.; Klippenstein, S. J.; *J. Chem. Phys.,* **1995,** 102, 8506.

[52] Pulay, P.; Fogarasi, G.; Pang, F.; Boggs, J. E. *J. Am. Chem. Soc.,* **1979,** 101, 256.

[53] a) Botschwina, P. *Chem. Phys. Lett.*, **1974**, 29, 98. b) Botschwina, P. *Chem. Phys.*, **1979**, 40, 33. c) Botschwina, P.; Härtner, H.; Sawodny, W. *Chem. Phys. Lett.*, **1980**, 74, 156. d) Botschwina, P.; *Chem. Phys.*, **1982**, 68, 41. (e) Botschwina, P. *Mol. Phys.*, **1982**, 47, 241.

[54] a) Pulay, P.; Ruoff, A.; Sawodny, W. *Mol. Phys.*, **1975**, 30, 1123. b) Pulay, P.; Meyer, W.; Boggs, J. E.; *J. Chem. Phys.*, **1978**, 68, 5077. c) Pulay, P.; Lee, J. G.; Boggs, J. E. *J. Chem. Phys.*, **1983**, 79, 3382. (d) see reference 17, p.198.

[55] a) Schlegel, H. B.; Wolfe, S.; Bernardi, F. *J. Chem. Phys.*, **1977**, 67, 4181, 4194, **1975**, 63, 3632. b) Bock, C. W.; Trachtman, M.; George, P. *J. Mol. Spectrosc.*, **1980**, 84, 256. c) Bock, C. W.; Trachtman, M.; George, P. *J. Mol. Str.*, **1981**, 89, 76. d) Steel, D.; Person, W. B.; Brown, K. G. *J. Phys. Chem.*, **1981**, 85, 2007.

[56] Pulay, P. *Mol. Phys.*, **1969**, 17, 197.

[57] Papoušek, D.; Plíva, J. *Czech. Chem. Commun.*, **1963**, 28, 755.

[58] Crawford, B. L.; Fletcher, W. H. *J. Chem. Phys.*, **1951**, 19, 141.

[59] Frisch, M. J.; Trucks, G. W.; Schlegel, H. B.; Gill, P. M. W.; Johnson, B. G.; Robb, M. A.; Cheeseman, J. R.; Keith, T.; Petersson, G. A.; Montgomery, J. A.; Raghavachari, K.; Al-Laham, M. A.; Zakrzewski, V. G.; Ortiz, J. V.; Foresman, J. B.; Cioslowski, J.; Stefanov, B. B.; Nanayakkara, A.; Challacombe, M.; Peng, C. Y.; Ayala, P. Y.; Chen, W.; Wong, M. W.; Andres, J. L.; Replogle, E. S.; Gomperts, R.; Martin, R. L.; Fox, D. J.; Binkley, J. S.; Defrees, D. J.; Baker, J.; Stewart, J. P.; Head-Gordon, M.; Gonzalez, C.; Pople, J. A. Gaussian 94, Revision C.2, Gaussian Inc., Pittsburgh, PA, 1995.

[60] Schmidt, M. W.; Baldridge, K. K.; Boatz, J. A.; Elbert, S. T.; Gordon, M. S.; Jensen, J. J.; Koseki, S.; Matsunaga, N.; Nguyen, K. A.; Su, S.; Windus, T. L.; Dupuis, M.; Montgomery, J. A. *J.comput.Chem.*, **1993**, 14, 1347.

[61] Schachtschneider, J. H. *Vibrational Analysis of Polyatomic Molecules*, Part-V, Technical Report No. 23164, Shell Development Company, Emeryville CA, 1964.

Chapter 3

Interpretation and Accurate Prediction of Vibrational Spectra - A Modification to Scaled Quantum Mechanical Approach

An accurate knowledge of molecular force fields is essential in the prediction and interpretation of vibrational spectra and also in molecular mechanics and dynamics calculations [1-4]. Attempts to deduce molecular force fields from spectral data alone have not been successful so far for molecules containing more than a few atoms [1,2]. As the number of atoms increases, the number of force constants to be determined becomes more than the experimentally available frequencies and multiple solutions become a problem. Ab initio molecular orbital methods offer an attractive alternative to resolve these problems. However, finite basis set and neglect of electron correlation in the HF procedure overestimates most of the harmonic force constants by 10-30% [1]. Although recent methods like CCSD(T) and CASS are capable of yielding more accurate harmonic force constants compared to Hartree-Fock theory, still produce errors compared to the experimental values [5]. These methods can not be applied on a routine basis to medium sized molecules of 5-30 atoms which are of chemists' interest. Even when accurate harmonic force constants become available, for prediction of experimental frequencies we need anharmonic force constants which involve the evaluation of cubic and quartic force constants. So it appears that, as pointed out by Pulay, the realistic solution is to stay at the Hartree Fock level of theory and make a correction for the systematic errors by means of some scaling procedure [6]. Of the different scaling procedures, the scaled quantum mechanical(SQM)

approach of Pulay appears to be the most successful one [1]. However, SQM approach uses least squares procedure to optimize a small number of scale factors as a measure of the systematic errors in the ab initio calculation. Since each force constant is physically distinct, it is more realistic to think that each force constant is associated with its own scale factor. Besides, the least-squares method need not converge all the time, specially when the parameters are many and do not lead to a unique assignment [7]. In this chapter we give a novel numerical procedure which overcomes these difficulties.

In the first part of the chapter a detailed description of the methodology and its theoretical justification is presented. The advantages of the present methodology over the existing ones are listed. In the second part the performance of the method is demonstrated by using acrolein, benzene, pyridine and benzaldehyde as examples.

3.1 Methodology

Evaluation of force constants of a molecule involves the solution of the inverse eigenvalue equation $GFL=L\Lambda$ where F is the force constant matrix, Λ the frequency matrix($\Lambda_i=4\pi^2\nu_i^2$), G the Wilson's G matrix and L the eigenvector matrix describing the normal modes [8]. Usually F is varied and Λ is calculated until Λ matches with the experimental frequencies. As long as we are modifying the force constants to obtain the frequencies of the molecule, the method would involve intuition and an element of arbitrariness depending on how we modify the F matrix elements. To get around this difficulty we modify the frequencies in the proposed method, so that the force constants automatically get refined in the right direction to reproduce the experimental frequencies.

The method involves the following steps:

(1)   Diagonalize G matrix: $G=D\Gamma D^t$

(2)   Form $W_1=D\Gamma^{1/2}$ and $W_2=D\Gamma^{-1/2}$

           iter=0

(3)   Start F_1; iter=iter+1

(4)   Form $W_1{}^t F_1 W_1 = H_1$

(5)   Diagonalize H_1 matrix: $H_1 = C\Lambda_1 C^t$

(6)   Form $L = W_1 C$ and normalize C such that $LL' = G$

(7)   Modify Λ_1 with a small correction $\Delta\Lambda$ given by $\Delta\Lambda = (\Lambda_{exp} - \Lambda_1)(\text{iter}-1)/\text{Niter}$

where Niter is the total number of iterations (we used Niter=1000);

$$\Lambda_2 = \Lambda_1 + \Delta\Lambda$$

(8)   Form $H_2 = C\Lambda_2 C^t$

(9) $F_2 = W_2 H_2 W_2{}^t$

The F_2 elements are averaged to retain the symmetry. This means that the force constants which are equal in the unscaled F matrix will be made equal. For example, benzene in-plane F matrix contains only 26 different numbers as described in references 2 and 8.

(10)   Replace F_1 by F_2 and go to step 3.

After going through the cycle Niter times Λ_{calc} will be equal to Λ_{exp} and we will have the refined F which will reproduce the experimental frequencies. The frequencies of many isotopically substituted molecules could be fitted , using the fact that the F matrix is the same for the different isotopomers. In each cycle F_2 is calculated for each isotopic species and an average F_2 is used as F_1 in the next cycle.

To get the scale factors in the desired range we can define values for the lowest and the highest permitted scale factor. After step 9, the F_2 elements are compared with the unscaled ab initio force constants. If the scale factors are between the allowed values they are updated; otherwise the value from the last cycle is retained. The flowchart of the algorithm is given in Figure 3.1.

Theoretical Justification

The theoretical justification for the above procedure could be given based on perturbation theory. Each step in the iteration is a small perturbation. The Wilson's GF matrix

equation can be written in terms of time independent Schrödinger equation [8] -

$$H_0 \Psi_0 = E_0 \Psi_0 \qquad (3.1)$$

where, $GF_1 = H_0$, $L_1 = \Psi_0$ and $\Lambda_1 = E_0$

When a small perturbation (ΔF) is applied (since each step is a small perturbation), $H' = G \Delta F$ and the first order correction is given by

$$E_1 = \left\langle \Psi_0 \mid H' \mid \Psi_0 \right\rangle = \Delta \Lambda = (L_1)^{-1} G \Delta F (L_1) \qquad (3.2)$$

Since $G = L_1 L_1^t$,

$$\Delta \Lambda = (L_1)^{-1} L_1 L_1^t \Delta F (L_1) = L_1^t \Delta F L_1 \qquad (3.3)$$

As long as the perturbation ΔF is small compared to F, the perturbation theory is expected to give valid results. Our goal is to retain the characteristics of the ab initio force field *as far as possible* when making the correction for the systematic over-estimation of the force constants. So we choose ΔF in such a way that $\Delta \Lambda$ is diagonal. This means L_1 is an eigenfunction of H' also and so the ab initio characteristics are retained. Since we do not calculate $\Delta \Lambda$ from ΔF but calculate only ΔF from $\Delta \Lambda$ choosing ΔF such that $\Delta \Lambda$ is diagonal is not a problem.

From $GF_1 L_1 = L_1 \Lambda_1$ and $G = L_1 L_1^t$, it can be easily shown that

$$\Lambda_1 = L_1^t F_1 L_1 \qquad (3.4)$$

In each iteration $\Delta \Lambda$ ($\lambda_{exp} - \lambda_1$ is negative for overestimated ab initio frequencies) is added to the previous calculated frequency to get the modified frequency. Since, $\Lambda_2 = \Lambda_1 + \Delta \Lambda$, combining 3.3 and 3.4 we get

$$\Lambda_2 = L_1^t (F_1 + \Delta F) L_1 \cdot \qquad (3.5)$$

or,

$$\Lambda_2 = L_1^t F_2 L_1 \qquad (3.6)$$

which leads to

$$F_2 = (L_1^t)^{-1} \Lambda_2 (L_1)^{-1} \qquad (3.7)$$

Since, $L_1 = W_1 C$, we get

$$F_2 = [(W_1 C)^t]^{-1} \Lambda_2 [W_1 C]^{-1} = (D\Gamma^{-1/2})(C \Lambda_2 C^t)(D\Gamma^{-1/2})^t = (D\Gamma^{-1/2}) H_2 (D\Gamma^{-1/2})^t \qquad (3.8)$$

from which we get,

$$F_2 = W_2 H_2 W_2'$$

(3.9)

The justification for averaging the F_2 elements according to symmetry comes from the fact that the F matrix always should reflect the symmetry of the molecule. For example in C_6H_6, all C-C stretching force constants should be equal. Because of the numerical procedure of calculating F_2 ($F_2=W_2H_2W_2'$), the C-C force constants will not agree in all decimal places, although they are all close. To impose the symmetry constraint, we average all the C-C stretching force constants so that they are equal in all decimal places.

Since F_2 elements are averaged to retain the symmetry and only those elements which give the right scale factors are updated, in the next cycle many of the new F_1 elements will be different from the corresponding F_2 elements obtained using equation 3.9. If the perturbation is small, this difference will be very small reproducing the same calculated λ_2. However, since the ΔF is different from that of F_2 obtained from equation 3.9, $\Delta\lambda=L_1'\Delta FL_1$ is not diagonal. As a result the eigenvectors of the last cycle will get mixed up in the present cycle.

Using first order perturbation theory

$$\Psi_n^{(1)} = \sum_{k\neq n} \frac{\left\langle \Psi_k^0 \mid H' \mid \Psi_n^0 \right\rangle}{E_n^0 - E_k^0} \Psi_k^0$$

(3.10)

where, $< \Psi_k^0 \mid H' \mid \Psi_n^0 >$ is very small in each step as explained above. Hence only when $\lambda_n-\lambda_k$ is small, the eigenvectors will get mixed. This means that when two frequencies are close, their potential energy distributions will get mixed up and in the worst case, the assignments will get interchanged. Since the ab initio calculation is for a non-interacting isolated molecule whereas the real experimental frequencies are from 'interacting environment', when the frequencies are close, a certain amount of mixing or interchange of assignments could be justified. This happens most of the time among the CH_3 stretching frequencies, where a certain amount of mixing or exchange between the assignments are permitted. It is to be noted that the mixing among degenerate modes does not create any problem.

To investigate the performance of the present methodology to obtain corrections for the over-estimation of the force constants we used benzene as the test case. The experimentally determined force constants of Ozkabak and Goodman from reference [2] are used to

obtain the harmonic frequencies of benzene. These calculated frequencies are used as 'simulated experimental frequencies' and the force constants are randomly over-estimated by multiplying with a scale factor between $1/0.6$ and 1.0. These over-estimated force constants are fitted to the simulated frequencies and the results are given in Table-3.1. As indicated in the Table, with one decimal accuracy in the harmonic frequencies the 2x2 blocks of force constants are reproduced. When the accuracy is $=1cm^{-1}$, the A_{1g} block off-diagonal element is off by 8%. In 3x3 block even one decimal accuracy in frequencies does not reproduce OG values for $F_{18,20}$ and $F_{19,20}$. This clearly proves that the true force constants could not be obtained from frequency data alone for 3x3 blocks and higher. However, with an error limit of $=1cm^{-1}$ which is the accuracy for the experimental frequencies, the numbers are very close to the real ones and represents a reliable force field. It appears that if the ab initio force field is the right one except for the over-estimation, the present methodology produces a satisfactory set of force constants when sufficient number of frequencies are available.

The choice of the number of iterations only requires that $\Delta\Lambda$ is small compared to Λ so that the perturbation $G\Delta F$ is small. We tested with Niter=100 to Niter=1500 in steps of 100. It appears that after Niter=500, the results do not change significantly, at least for the molecules we have tested. If there are sufficient number of experimental frequencies as long as $\Delta\Lambda$ is small, the results are expected to be largely independent of Niter. When there are not enough experimental frequencies, for example, when only one isotopomer experimental frequencies are available, the final force constants are good approximations to the true values and different Niter values may not produce force constants which agree in all decimals although they will be close to each other (see the pyridine results described latter). However, since the present method offers a systematic procedure, the force constants from two structurally related molecules fitted with same Niter could be compared or scale factors could be transferred among them to obtain good results. Similar considerations apply to the lower and upper limit of the scale factors, which is based on the assumption that the errors are systematic.

If ab initio theory is a good model for the real system then the assignments are reasonable if the final potential energy distributions (PED)s are close to that of the original

unscaled PEDs. If the assignment is incorrect, the fitted frequency will be very much off form the experimental frequency and the PEDs will be unacceptable.

The Advantages of the Current Procedure are:

(1) We get a set of scale factors which could be used to study the trends related to structural variations and for predicting the frequencies of the structurally related molecules.

(2) There is an in-built check to detect the mathematical inconsistencies arising from a wrong assignment by giving fitted frequencies which are very different from the experimental numbers.

(3) The effort needed to fit the frequencies of one isotopomer is almost the same as fitting the frequencies of any number of isotopically substituted molecules and very much less than that of the least squares method.

This method could be used for other inverse eigenvalue problems, for example in NMR spectroscopy [9]. Another interesting application could be in obtaining a good estimate for electron correlation by scaling the Fock matrix of the Hartree-Fock theory.

The normal coordinate analyses are done with a modified version of the UMAT program [10].

3.2   Results

3.2.1   Interpretation of Vibrational Spectra

Acrolein

To see how this method performs compared to the known SQM cases, we calculated the fitted force constants, frequencies and potential energy distributions of all the molecules described in reference 1. The results for a representative case, acrolein-d_0 and d_1 are shown in Table-3.2. We used the same scale factor limits of 0.7 and 1.0. The agreement with the experimental frequencies are almost quantitative. The average deviations of all the frequencies of acrolein-h_4 and acrolein-d_1 is only 2.3 cm^{-1}. Since, the gas phase

experimental numbers are used, the agreement is so excellent and the final fitted PEDs exactly reproduce the ab initio unscaled PEDs, as expected. In almost all the bands, our calculated numbers show an improvement over the earlier SQM results [1].

Benzene

The first demonstration of benzene potential surface was due to the pioneering work of Wilson as early as 1934, using only six force constants [11]. After that several papers appeared on the generation of the force field and reliable vibrational frequency assignments for benzene [12-17]. But the real improvement in the frequency data came in the last decade with the introduction of new experimental techniques [18-20]. Accurate measurement of the inactive fundamentals in IR and Raman spectra and unambiguous identification of A_{2g} and B_{1u} modes in lower symmetry isotopically labelled benzenes had become possible due to the invention of the two-photon spectroscopy [19,20]. So far the most reliable and detailed analysis of benzene ground state vibrational force field available was that of OG [2]. On the other hand, there was a good deal of advancement in the theoretical force field of benzene through the analytic derivatives of the electronic energy at the HF and correlated level using the gradient algorithm of Pulay [21]. A reliable theoretical force field was first proposed by Pulay et al. by scaling the ab initio force constants using their SQM methodology [22]. HF and higher correlated level ab initio calculations were carried out by Guo and Karplus to obtain the benzene force constants for planar vibrations [23]. These theoretical force fields differ in some values especially in the off-diagonal force constants compared to the OG force field.

Since we start with the assumption that the ab initio force field is the right one except for the systematic errors, the multiple solution problem in the usual sense i.e. entirely different sets of force constants giving identical frequencies [24] does not arise although the different ways of scaling could produce different approximations to the *same* theoretical force field which are very similar to each other. After correcting the systematic errors by means of scaling what we get is the scaled ab initio force field.

All the 34 different scaled ab initio force constants of benzene obtained by fitting

the harmonic frequencies of the four D_6h isotopomers using five different basis sets (4-21G, 6-31G*, 6-311G**, 6-31++G** at HF level and 6-311G** at MP2 level) are shown in Table-3.3 along with the OG force field [2] and that of Pulay et al. [22]. Table-3.4 contains the corresponding scaled frequencies of benzene-d_0 along with the calculated harmonic frequencies of OG. Since, the calculated frequencies are almost same in all the different levels of calculation, the harmonic frequencies for all the three (C_6D_6, $^{13}C_6H_6$ and $^{13}C_6D_6$, C_6H_6 frequencies appear in Table-3.4) isotopes are shown in Table-3.5 only at HF/4-21G level. The force field is obtained by fitting the respective ab initio force constants to the most accurate OG experimental frequencies at the experimental geometry of benzene. The fitted force constants presented in Table-3.3 are nearly unique with respect to different levels of calculations and obviously appear as an improvement over the earlier theoretical force fields. The agreement with the experimental OG force field is very good in the diagonal force constants and in many of the off-diagonal force constants. But the discrepancy arises (mainly in the off-diagonal constants) at those places, where the ab initio model itself predict entirely different values including the sign. The scaling procedure retains the sign of the ab initio force constants. Such a difficulty cannot be resolved by merely scaling the force constants.

It is tempting to explain the scaled force constants of benzene given in Table-3.3 in the following way. In the one dimensional cases (A_{2g}, A_{2u}, E_{1g}) only one frequency is needed and it gives a unique force constant. In 2x2 ($A_{1g}, B_{1u}, B_{2u}, B_{2g}, E_{2u}$) we require at least three observed frequencies to get a unique set of force constants (3 equations and 3 unknowns). In 3x3 (E_{1u}) we need 6 frequencies to make 6 equations with 6 unknown force constants. In 4x4 (E_{2g}) we require 10 frequencies to solve for 10 force constants. The scaled force field is nearly identical in all blocks except for E_{2g} because sufficient number of frequencies are not available for exact solution in E_{2g}. Only 9 distinct frequencies are available when 10 are required for exact solution [24]. As a result the force field varies marginally for E_{2g} based on the starting F matrix. But unfortunately, 'uniqueness' does not imply 'accuracy' as shown in the methodology section. Some of the force constants are *very sensitive* to frequencies to the extent that their correct values could not be determined from *frequency data alone*. For example, in the 2x2 solutions, A_{1g} and B_{1u} off-diagonal

elements are different from that of OG although the OG numbers are reproduced when calculated frequencies from OG force constants are used as simulated experimental data with 3 decimal accuracy! Probably the 'uniqueness' is an 'accidental coincidence' due to the selection of range of scale factors for the different basis sets (see Table-3.3).

The question whether ab initio methods can produce the true force constants, however, cannot be answered at this point. Extended basis set calculations including correlation appears to disagree in some values with the experimental force field of OG. However, in *many* of the force constants the agreement with experimental force field is *quantitative* after scaling with the *present methodology*. Since experimental force field is available only for few small symmetric molecules, the scaled ab initio values appear to offer an attractive alternative.

3.2.2   Prediction of Vibrational Frequencies

Pyridine

Experimental vibrational spectra of pyridine in crystalline as well as matrix isolated form along with several deuterium substituted species are widely available in the literature [25-32]. Transferability of benzene force constants/scale factors to predict pyridine fundamentals had been attempted by several authors [6,33,34]. But so far the most successful study of this kind was done by Pulay et al. where they transferred the ab initio 4-21G scale factors of benzene to predict the pyridine spectra [6]. We obtained a set of scale factors of benzene-d_0 and d_6 individually and collectively at HF/4-21G level and used them to predict the frequencies of pyridine-d_0 and d_5 from ab initio force constants. No experimental numbers are used in prediction. For comparison we list the predicted values by the SQM method in Table-3.6. Table-3.6 clearly shows that the overall fitted frequencies are in better agreement compared to the individual ones, except for the C-H and C-D stretching frequencies. Since the associated anharmonicity is more in these modes, the individual fitted scale factors when transferred can produce better correction to the calculated frequencies compared to the overall fitted scale factors. Our predicted frequencies are in good agreement with the earlier predicted SQM frequencies which included

40

the cubic force constants also in the analysis.

Benzaldehyde

As an additional test the same set of scale factors, as obtained by fitting benzene-d_0 individually to the experimental spectra, combined with scale factors of acetaldehyde-d_0 at 4-21G level are used to predict the frequencies of benzaldehyde-d_0 using ab initio force constants obtained at the same level of theory. The results are in excellent agreement with the experimental numbers [35] as shown in Table-3.7. The average error of the predicted frequencies is less than 5.9 cm^{-1}. Larger deviations are found mainly in the 3000 cm^{-1} (C-H stretching) region, which are highly anharmonic.

Internal coordinates of acetaldehyde and benzaldehyde, force constants of acrolein, benzaldehyde and scale factors of benzene and acetaldehyde are presented in Tables-3.8 to 3.15.

3.3 Conclusions

All the results presented in this study indicate that the present methodology of fitting the experimental frequencies to the ab initio force constants and transferring the scale factors from structurally related molecules to predict the fundamental frequencies offer an attractive solution to the vibrational spectral interpretation and prediction.

Step 1: Convert cartesian force constants obtained from the ab initio program to force constants in local symmetry coordinates. We refer to this F matrix as F_{ab}

Step 2: Input: No. of isotopic species (nmol), masses (M), Wilson's B matrix (B), local U (U_{loc}). We used Niter = 1000 and a scale factor range of 0.7 to 1.0.

Step 3:
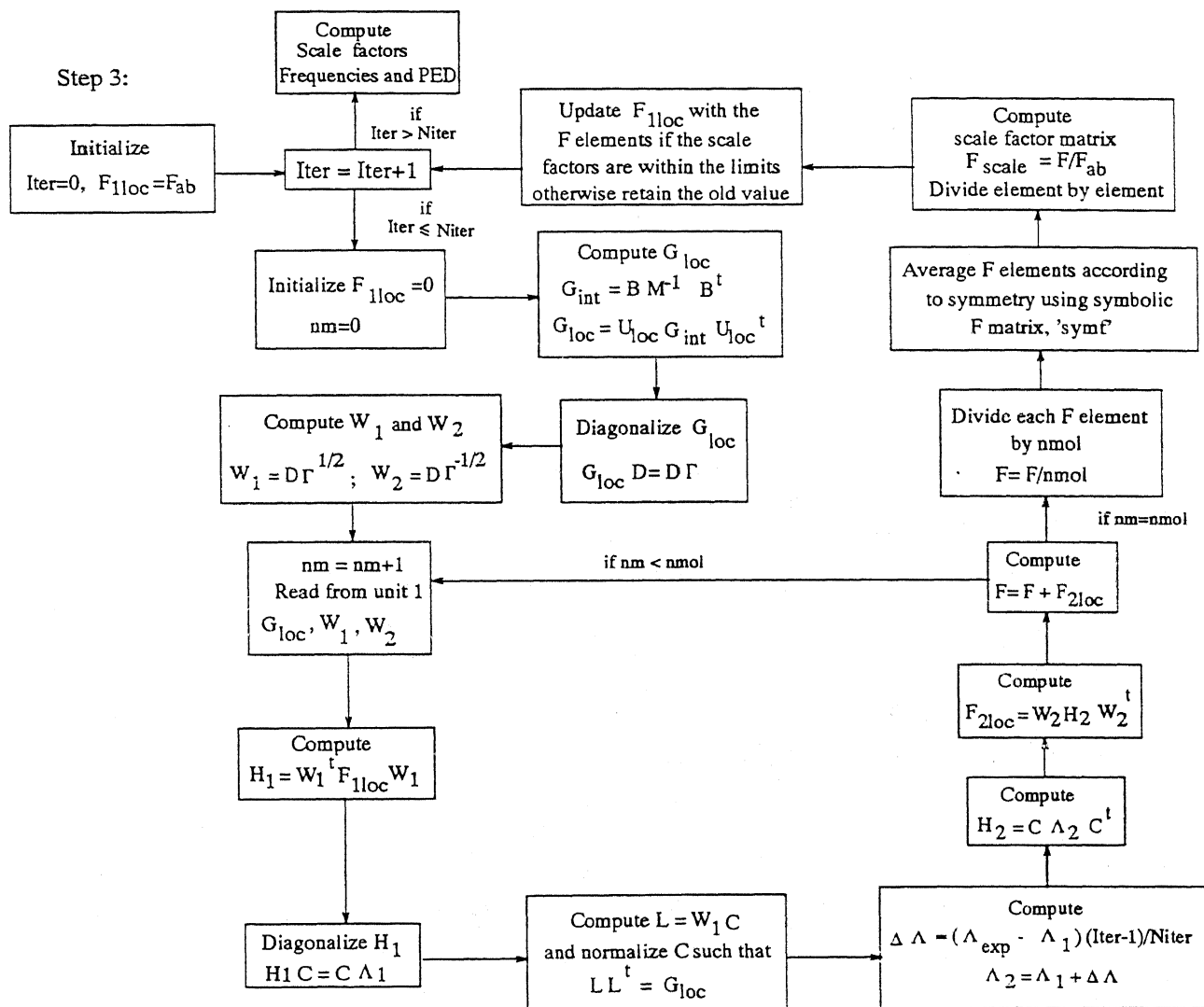
Figure 3.1: Flowchart of the fitting algorithm
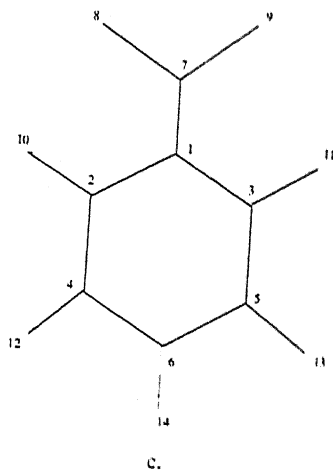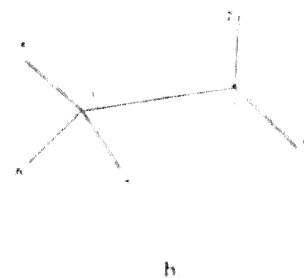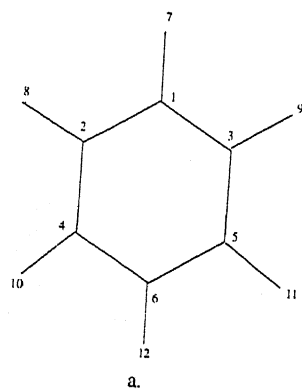
Figure 3.2: Atom numberings of a. benzene b. acetaldehyde c. benzaldehyde

Table 3.1: Force constants obtained after fitting to 'simulated frequencies' of different accuracies of four isotopomers of C_6H_6

| Symmetry blocks | F-matrix elements | Random scaling with factors between 1/0.6 and 1.0 | | | | |
		A	B	C	D	Ozkabak-Goodman[e]
A_{1g}	$F_{1,1}$	7.631	7.599	7.615	7.616	7.616
	$F_{1,2}$	0.167	0.169	0.168	0.157	0.157
	$F_{2,2}$	5.559	5.553	5.556	5.554	5.554
A_{2g}	$F_{3,3}$	0.879	0.876	0.877	0.877	0.877
B_{1u}	$F_{12,12}$	0.659	0.656	0.657	0.658	0.658
	$F_{12,13}$	-0.234	-0.235	-0.234	-0.239	-0.237
	$F_{13,13}$	5.573	5.566	5.570	5.572	5.571
B_{2u}	$F_{14,14}$	3.944	3.934	3.939	3.939	3.939
	$F_{14,15}$	0.299	0.298	0.298	0.298	0.298
	$F_{15,15}$	0.830	0.826	0.828	0.828	0.828
E_{1u}	$F_{18,18}$	0.929	0.925	0.927	0.927	0.926
	$F_{18,19}$	0.211	0.208	0.209	0.209	0.209
	$F_{18,20}$	0.161	0.161	0.161	0.160	0.151
	$F_{19,19}$	7.387	7.364	7.376	7.381	7.380
	$F_{19,20}$	0.579	0.573	0.576	0.584	0.572
	$F_{20,20}$	5.571	5.563	5.567	5.568	5.568

A. Frequencies rounded to nearest integer +1.0
B. A-2.0 C. A-1.0 D. rounded to one decimal
e. Ref. 2.

Table 3.2: Calculated(4-21G) and Experimental frequencies[a] of acrolein and acrolein-d_1

| acrolein-h_4 | | | | acrolein-d_1 | | |
This method	SQM	Expt.	PED[b]	This method	SQM	Expt.
In-Plane						
3102	3115	3102	νCH_2	3102	3115	3101
2994	3082	(3000)	$\nu CH''+\nu CH_2$	2994	3082	(2988)
2994	3024	3000	$\nu CH''+\nu CH_2$	2994	3024	2988
2780	2768	2777	νCH^f	2058	2049	2060
1725	1732	1723	νCO	1707	1713	1709
1624	1623	1625	$\nu C=C+\delta CH_2$	1622	1622	1621
1423	1434	1422	$\delta CH_2+\rho CH^f$	1402	1419	1403
1363	1383	1361	$\rho CH^f+\delta CH_2$	1059	1057	1060
1276	1266	1276	$\rho CH''+\rho CH_2+\nu C=C$	1276	1266	1275
1160	1149	1159	$\nu C\text{-}C+\rho CH''+\rho CH_2$	1152	1145	1153
914	910	913	$\rho CH_2+\nu C\text{-}C$	876	877	877
564	559	564	$\delta CCO+\nu C\text{-}C+\delta CCC$	561	557	561
323	314	324	$\delta CCC+\delta CCO$	314	306	313
Out-of-Plane						
998	1003	993	$\omega CH_2+\omega CH''+t CH_2$	997	1003	993
976	1002	(980)	$t CH_2+\omega CH^f+\omega' CH_2$	970	975	959
961	969	959	$\omega CH^f+\omega CH_2$	848	869	846
588	580	589	$\omega CH''+t CH_2$	551	546	556
158	(158)	158	τCC	151	(151)	151

a. Frequencies are taken from ref 1. b. All coordinates are according to ref 1.

Table 3.3: Fitted ab initio harmonic force field of benzene in different basis sets in terms of symmetry coordinates[a,b]

Symm. blocks	F-elem ents	A	B	C	D[c]	E[c]	OG[d]	4-21G this[e]	SQM[f]
A_{1g}	$F_{1,1}$	7.610	7.610	7.610	7.610	7.610	7.616	7.604	7.609
	$F_{1,2}$	0.137	0.137	0.137	0.137	0.136	0.157	0.100	0.110
	$F_{2,2}$	5.526	5.526	5.526	5.526	5.526	5.554	5.185	5.218
A_{2g}	$F_{3,3}$	0.877	0.877	0.877	0.877	0.877	0.877	0.864	0.855
$B_{1}u$	$F_{12,12}$	0.652	0.652	0.652	0.652	0.652	0.658	0.653	0.650
	$F_{12,13}$	-0.160	-0.161	-0.162	-0.162	-0.164	-0.237	-0.156	-0.184
	$F_{13,13}$	5.565	5.566	5.566	5.566	5.568	5.571	5.219	5.154
$B_{2}u$	$F_{14,14}$	3.936	3.936	3.936	3.936	3.936	3.939	3.952	3.917
	$F_{14,15}$	0.297	0.297	0.297	0.297	0.297	0.298	0.308	0.290
	$F_{15,15}$	0.828	0.828	0.828	0.828	0.828	0.828	0.817	0.811
$E_{2}g$	$F_{6,6}$	0.644	0.641	0.642	0.643	0.641	0.644	0.647	0.639
	$F_{6,7}$	-0.137	-0.134	-0.136	-0.137	-0.136	-0.136	-0.144	-0.123
	$F_{6,8}$	0.296	0.308	0.305	0.302	0.320	0.308	0.306	0.280
	$F_{6,9}$	-0.153	-0.146	-0.160	-0.159	-0.189	-0.140	-0.107	-0.125
	$F_{7,7}$	5.539	5.538	5.547	5.546	5.568	5.510	5.164	5.156
	$f_{7,8}$	0.087	0.101	0.099	0.097	0.096	0.054	0.061	0.061
	$F_{7,9}$	0.036	0.040	0.042	0.040	0.056	-0.066	0.025	0.028
	$F_{8,8}$	6.615	6.636	6.626	6.621	6.648	6.690	6.622	6.700
	$F_{8,9}$	-0.392	-0.386	-0.389	-0.389	-0.386	-0.398	-0.411	-0.421
	$F_{9,9}$	0.902	0.903	0.902	0.902	0.902	0.895	0.898	0.881
$E_{1}u$	$F_{18,18}$	0.926	0.926	0.926	0.926	0.926	0.926	0.916	0.910
	$F_{18,19}$	0.212	0.212	0.212	0.212	0.212	0.209	0.221	0.221
	$F_{18,20}$	0.002	0.003	0.004	0.004	0.002	0.151	0.003	0.006
	$F_{19,19}$	7.362	7.362	7.364	7.364	7.361	7.380	7.352	7.270
	$F_{19,20}$	0.226	0.230	0.225	0.222	0.232	0.572	0.159	0.175
	$F_{20,20}$	5.524	5.524	5.523	5.522	5.525	5.568	5.165	5.185
$A_{2}u$	$F_{11,11}$	0.250	0.250	0.250	0.250	0.250	0.249	0.249	0.241
$B_{2}g$	$F_{4,4}$	0.202	0.202	0.202	0.202	0.202	0.202	0.201	0.193
	$F_{4,5}$	0.249	0.249	0.249	0.249	0.250	0.249	0.248	0.236
	$F_{5,5}$	0.520	0.520	0.520	0.520	0.520	0.519	0.520	0.505
$E_{1}g$	$F_{10,10}$	0.337	0.337	0.337	0.337	0.337	0.337	0.337	0.330
$E_{2}u$	$F_{16,16}$	0.160	0.160	0.160	0.160	0.160	0.160	0.159	0.162
	$F_{16,17}$	-0.168	-0.168	-0.168	-0.168	-0.168	-0.168	-0.166	-0.168
	$F_{17,17}$	0.419	0.419	0.419	0.419	0.419	0.420	0.419	0.418
g		0.6-1.0	0.7-1.1	0.7-1.2	0.7-1.2	0.6-1.55			

A. HF/4-21G; B. HF/6-31G* C. HF/6-311G** D. HF/6-311++G** E. MP2/6-311G**
a. Non-redundant symmetry coordinates are as defined in ref 2. b.Symmetry coordinates for ring deformation and CH rock and wagg are multiplied by the respective bond lenths. c. Ab initio force constants are taken from ref 2. d. Ref 2. e. Experimental frequencies and reference geometry of Pulay et al.(ref.22) is used for comparison f. Ref 22. g. Scale factors range used for each basis set.

Table 3.4: Fitted ab initio harmonic frequencies of benzene in different basis sets

Symmetry blocks	HF/ 4-21G	HF/ 6-31G*	HF/ 6-311G**	HF/ 6-311++G**	MP2/ 6-311G**	Ozkabak-Goodman[a]	expt[a]
A_{1g}	3184.0	3184.1	3184.1	3184.1	3184.0	3191.0	3191.0
	993.8	993.8	993.8	993.8	993.8	994.4	994.4
A_2g	1366.7	1366.7	1366.7	1366.7	1366.7	1367.0	1367.0
B_1u	3176.1	3176.2	3176.2	3176.2	3176.4	3166.3	3174.0
	1010.7	1010.6	1010.6	1010.6	1010.6	1014.4	1010.0
B_2u	1309.5	1309.5	1309.5	1309.5	1309.5	1309.4	1309.4
	1149.7	1149.7	1149.7	1149.7	1149.7	1149.7	1149.7
E_2g	3169.3	3169.4	3170.3	3170.1	3172.5	3167.5	3174.0
	1609.7	1609.7	1609.5	1609.6	1609.1	1609.9	1607.0
	1179.8	1179.8	1179.7	1179.7	1179.3	1178.2	1177.8
	607.4	607.4	607.4	607.4	607.4	607.2	607.8
E_1u	3177.2	3177.3	3177.2	3177.1	3177.4	3181.9	3181.0
	1494.9	1494.8	1494.9	1494.9	1494.8	1494.4	1494.0
	1039.2	1039.2	1039.3	1039.3	1039.2	1038.3	1038.3
A_2u	674.9	674.9	674.9	674.9	674.9	674.0	674.0
B_2g	990.7	990.7	990.7	990.7	990.7	990.0	990.0
	707.5	707.5	707.5	707.5	707.5	707.0	707.0
E_1g	847.8	847.8	847.8	847.8	847.8	847.1	847.1
E_2u	966.4	966.4	966.4	966.4	966.4	967.0	967.0
	397.7	397.7	397.7	397.7	397.7	398.0	398.0

a. Ref 2.

Table 3.5: Fitted ab initio harmonic frequencies of C_6D_6, $C^{13}_6H_6$ and $C^{13}_6D_6$

Symmetry blocks	C_6D_6			$^{13}C_6H_6$			$^{13}C_6D_6$	
	calc	O.G.[a]	expt[a]	calc	O.G.	expt	calc	expt
A_{1g}	2361.8	2366.1	2362.0	3172.9	3179.8	3167.0	2344.0	2343.0
	947.7	948.6	947.0	958.0	958.8	957.4	917.3	918.0
A_2g	1063.1	1063.3	0.0	1355.6	1354.1	0.0	1048.3	0.0
B_1u	2342.5	2326.7	2344.0	3166.5	3157.6	0.0	2326.8	0.0
	969.4	976.5	970.0	973.8	977.1	0.0	936.5	0.0
B_2u	1286.0	1286.3	1286.3	1270.3	1269.6	1270.1	1236.1	1236.3
	828.1	827.9	827.9	1138.6	1138.8	1138.4	827.7	828.0
E_2g	2335.7	2340.7	2332.0	3159.9	3157.6	0.0	2320.2	0.0
	1561.3	1559.8	1564.0	1556.1	1556.0	0.0	1504.3	0.0
	865.5	863.5	867.0	1172.1	1170.8	0.0	862.0	0.0
	579.7	579.1	580.5	585.5	585.3	584.2	561.2	561.3
E_1u	2350.4	2346.7	2345.9	3166.8	3172.2	3180.0	2333.6	2325.0
	1340.2	1342.5	1341.0	1464.7	1464.0	1463.0	1299.4	1301.0
	813.9	813.9	814.3	1019.2	1018.1	1018.4	807.7	808.6
A_2u	495.5	494.9	496.2	672.9			492.8	
B_2g	828.4	827.8	829.0	982.8			804.4	
	598.6	598.1	599.0	685.1			592.1	
E_1g	659.4	658.9	660.0	840.9			650.6	
E_2u	787.5	788.0	787.0	955.5			771.3	
	345.2	345.5	345.0	386.4			338.6	

a. Ref 2.

Table 3.6: Predicted frequencies of pyridine[a] using 4-21G basis set

	C_5H_5N				C_5D_5N		
expt.	calc.		SQM	expt.	calc.		SQM
	indiv.[b]	overall[b]			indiv.	overall	
3079	3093	3108	3093	2294	2295	2309	2305
3077	3085	3098	3102	2281	2284	2295	2292
3065	3073	3086	3078	2271	2274	2285	2280
3042	3066	3080	3065	2252	2262	2273	2267
3034	3062	3074	3071	2248	2261	2270	2262
1581	1584	1585	1585	1550	1547	1542	1544
1574	1580	1578	1582	1537	1545	1538	1546
1483	1476	1480	1475	1339	1335	1335	1330
1437	1435	1436	1436	1298	1300	1298	1290
1355	1339	1345	1353	1228	1245	1236	1231
1227	1256	1246	1240	1041	1027	1032	1036
1217	1205	1207	1214	1009	993	994	1005
1146	1151	1153	1156	963	968	969	954
1069	1057	1058	1073	888	882	888	885
1052	1057	1058	1053	835	837	843	840
1030	1028	1029	1025	824	819	822	822
991	1005	1005	980	824	819	821	819
654	652	655	654	624	623	625	627
603	596	596	604	581	575	574	583

a. all coordinates and experimental frequencies are taken from ref 6
b. indiv.- refers to fitting one molecule C_6H_6 or C_6D_6, overall- refers to fitting two isotopic molecules simultaneously.

Table 3.7: Predicted frequencies of benzaldehyde using 4-21G basis set

Expt.[a]	Calc.	% Error	Expt.	Calc.	% Error
3099	3088	0.3	–	1035	–
3081	3078	0.1	1026	1030	-0.5
3065	3068	0.4	1026	1028	-0.2
3043	3058	-0.5	1003	1003	0.0
3034	3045	-0.4	996	987	0.9
2806	2834	-1.0	918	939	-2.2
1728	1728	0.0	(852)	844	1.0
1614	1609	0.3	825	827	-0.2
1603	1595	0.5	740	738	0.2
(1492)	1495	-0.2	688	681	1.0
1460	1461	0.0	649	652	-0.4
1387	1388	-0.1	617	616	0.1
1314	1326	-0.9	450	443	1.5
1292	1309	-1.4	437	441	-0.9
1202	1197	0.4	(400)	399	0.2
1168	1171	-0.3	224	232	-3.5
(1158)	1161	-0.2	217	215	1.0
1074	1080	-0.6	(126)	122	2.9

a. experimental frequencies are taken from ref 35 and numbers within paranthesis are taken from liquid phase spectra

Table 3.8: Fitted force field of acrolein*

In-Plane

	C-C st	C=C st	C=O st	CH^{v}st	CH^{f}st	CH^{c}st	CH^{t}st	CCC de	CCO de	CH^{v}ro	CH^{f}ro	CH$_2$de	CH$_2$ro
C-C st	4.355												
C=C st	0.335	8.740											
C=O st	0.697	-0.108	12.136										
CH^{v}st	0.009	0.093	0.046	4.914									
CH^{f}st	0.097	0.053	0.467	0.004	4.267								
CH^{c}st	-0.012	0.062	0.010	0.009	0.002	5.240							
CH^{t}st	-0.008	0.117	0.007	-0.003	0.015	0.044	4.970						
CCC de	0.227	0.283	0.051	-0.114	-0.023	0.047	-0.042	1.132					
CCO de	0.174	0.092	0.274	-0.122	-0.147	0.012	-0.003	0.246	1.282				
CH^{v}ro	0.168	-0.166	-0.009	-0.116	0.026	0.010	-0.018	0.036	-0.091	0.483			
CH^{f}ro	0.182	-0.009	-0.390	0.026	0.030	-0.003	0.015	-0.038	0.068	0.012	0.627		
CH$_2$de	-0.006	-0.186	-0.003	-0.006	-0.008	0.061	0.050	-0.022	-0.022	0.013	-0.003	0.440	
CH$_2$ro	0.028	0.007	0.029	-0.014	-0.003	0.092	-0.128	0.072	0.016	0.031	-0.002	0.011	0.561

Out-of-Plane

	C-C to	CH^{v}wa	C-H^{f}wa	CH$_2$wa	CH$_2$wa
C-C to	0.0251				
CH^{v}wa	-0.007	0.247			
C-H^{f}wa	-0.003	-0.021	0.419		
CH$_2$wa	-0.003	0.024	-0.008	0.272	
CH$_2$wa	0.011	0.003	0.022	0.001	0.122

*All coordinates are as given in ref 1.

Table 3.9: In plane scale factors of benzene*

1																				
2	1																			
3	2	1																		
4	3	2	1																	
3	4	3	2	1																
3	3	4	3	2	1															
6	7	7	7	6	5	8														
5	6	7	7	6	5	9	8													
5	5	6	7	6	5	10	9	8												
6	7	5	7	7	6	11	10	9	8											
7	7	5	7	7	6	10	11	10	9	8										
6	6	6	6	6	5	15	10	11	10	9	8									
13	13	12	11	13	12	0	15	16	15	0	-15	17								
12	12	12	13	12	11	-15	0	15	0	16	-16	18	17							
-12	-12	-13	-14	-13	-12	-16	-15	0	16	0	16	19	18	17						
-13	-13	-12	-14	-11	-13	0	-16	-15	0	15	15	20	19	18	17					
14	14	13	14	14	13	16	0	-15	-16	0	0	19	20	19	18	17				
13	13	12	13	13	12	15	16	-16	0	-21	-21	18	19	20	19	18	17			
-14	-12	-12	-12	0	0	21	0	-21	21	21	26	0	0	0	0	0	0	17		
14	-13	-13	0	0	0	25	21	26	26	26	-30	27	27	27	27	27	27	0	22	
23	23	24	23	23	24	26	25	26	30	30		32	32	32	32	32	32	-27	0	28
29	-29	0	29	29	-29	0	30	-30	0	-30	-30	31	31	31	31	31	31	32	0	28·

1=(0.877,0.869,0.873), 2=(0.701,0.715,0.720), 3=(0.729,0.720,0.719), 4=(0.700,0.700,0.702), 5=(1.000,1.000,0.730), 6=(0.704,0.700,0.726), 7=(0.700,0.907,0.998), 8=(0.828,0.844,0.834), 9=(0.700,0.715,0.707), 10=(1.000,0.999,0.999), 11=(0.711,0.997,0.999), 12=(0.786,0.832,0.789), 13=(1.000,1.000,1.000), 14=(0.781,1.000,0.783), 15=(0.999,0.998,0.700), 16=(0.701,0.700,1.000), 17=(0.770,0.782,0.778), 18=(0.894,1.000,0.893), 19=(0.957,1.000,1.000), 20=(1.000,1.000,0.736), 21=(0.700,0.700,0.701), 22=(0.774,0.778,0.776), 23=24=29=(0.948,0.888,1.000), 25=26=30=(0.700,0.872,0.700), 27=31=32=(0.700,0.771,0.845), 28=((0.700,0.750,0.753)

*All coordinates are according to ref 2.
numbers within paranthesis are the fitted scale factors for C_6H_6, C_6D_6 and their combined fit.

Table 3.11: Internal coordinates of acetaldehyde

C=O	$=r_1$
C-C	$=r_2$
C-H$_{ald}$	$=r_3$
θ_1	$=2\alpha_1-\alpha_2-\alpha_2$
θ_2	$=\alpha_2-\alpha_2$
C-H$_{wag}$	$=\gamma$
C-C$_{tor}$	$=\tau$

Table 3.12: Scale factors of acetaldehyde taken for prediction

	r_1	r_2	r_3	θ_1	θ_2	γ	τ
r_1	0.831						
r_2	1.000	0.883					
r_3	0.833	0.808	0.798				
θ_1	0.977	1.000	0.836	0.872			
θ_2	0.706	0.890	1.000	0.753	0.797		
γ						0.761	
τ							0.771

r,θ etc. are internal coordinates as defined in Table-3.11

Table 3.13: Internal coordinates of benzaldehyde

$r_1=$	1-3	a_{15}-$a_{20}=$	$\beta_{1-6}(\beta$=217-317)
$r_2=$	3-5	a_{21}-$a_{26}=$	$\alpha_{1-6}(\alpha$=213)
$r_3=$	5-6	$a_{27}=$	178
$r_4=$	6-4	$a_{28}=$	179
$r_5=$	4-2	$a_{29}=$	879
$r_6=$	2-1	$a_{30}=$	γC_7
$r_7=$	1-7	$a_{31}=$	γH_{11}
$r_8=$	3-11	$a_{32}=$	γH_{13}
$r_9=$	5-13	$a_{33}=$	γH_{14}
$r_{10}=$	6-14	$a_{34}=$	γH_{12}
$r_{11}=$	4-12	$a_{35}=$	γH_{10}
$r_{12}=$	2-10	$a_{36}=$	γH_9
$r_{13}=$	7-8	a_{37}-$a_{42}=$	τ_{1-6}
$r_{14}=$	7-9	$a_{43}=$	τ_7

Table 3.14: Symmetry coordinates of benzaldehyde

1	1	1.000											
2	2	1.000											
3	3	1.000											
4	4	1.000											
5	5	1.000											
6	6	1.000											
7	7	1.000											
8	11	1.000											
9	13	1.000											
10	14	1.000											
11	12	1.000											
12	10	1.000											
13	8	1.000											
14	9	1.000											
15	15	1.000											
16	16	1.000											
17	17	1.000											
18	18	1.000											
19	19	1.000											
20	20	1.000											
21	21	0.408	22	-0.408	23	0.408	24	-0.408	25	0.408	26	-0.408	
22	21	0.577	22	-0.289	23	-0.289	24	0.577	25	-0.289	26	-0.289	
23	22	0.500	23	-0.500	25	0.500	26	-0.500					
24	27	0.816	28	-0.408	29	-0.408							
25	28	0.707	29	-0.707									
26	30	1.000											
27	31	1.000											
28	32	1.000											
29	33	1.000											
30	34	1.000											
31	35	1.000											
32	36	1.000											
33	37	0.408	38	-0.408	39	0.408	40	-0.408	41	0.408	42	-0.408	
34	37	0.577	38	-0.289	39	-0.289	40	0.577	41	-0.289	42	-0.289	
35	38	0.500	39	-0.500	41	0.500	42	-0.500					
36	43	1.000											

Table 3.15: Non-redundant scaled 4-21G force constants of benzaldehyde*

```
 1    1   6.753
 2    1    .624   2   6.773
 3    1   -.459   2    .662   3   6.747
 4    1    .435   2   -.449   3    .657   4   6.640
 5    1   -.427   2    .456   3   -.449   4    .665   5   6.908
 6    1    .612   2   -.425   3    .419   4   -.458   5    .621   6   6.694
 7    1    .331   2   -.037   3   -.079   4   -.042   5   -.057   6    .421   7   4.607
 8    1   -.019   2   -.020   3   -.003   4    .101   5    .105   6   -.004   7   -.001
      8   5.169
 9    1   -.102   2    .048   3   -.034   4   -.013   5    .034   6   -.069   7    .820
      8    .009   9  11.930
10    1    .042   2    .013   3   -.009   4   -.001   5    .005   6    .008   7    .077
      8    .003   9    .394  10   4.433
11    1   -.007   2   -.017   3   -.017   4    .001   5    .080   6    .105   7   -.053
      8    .009   9    .027  10    .001  11   5.218
12    1   -.019   2   -.002   3    .099   4    .099   5   -.002   6   -.020   7    .002
      8    .010   9    .003  10    .001  11    .002  12   5.155
13    1    .119   2    .099   3   -.002   4   -.020   5   -.019   6   -.001   7   -.005
      8    .001   9    .009  10    .015  11    .001  12    .004  13   5.095
14    1   -.004   2    .101   3    .101   4   -.004   5   -.020   6   -.018   7   -.001
      8    .003   9    .009  10    .003  11    .001  12    .010  13    .010  14   5.168
15    1    .464   2    .056   3   -.052   4    .098   5   -.054   6   -.624   7   -.270
      8   -.016   9    .040  10   -.105  11    .151  13   -.066  14    .016  15   5.511
16    1   -.413   2    .414   3    .036   4   -.040   5    .049   6   -.024   7    .034
      9    .034  10   -.033  11   -.014  12    .015  14   -.019  15    .004  16   3.608
17    1   -.029   2   -.439   3    .432   4    .027   5   -.048   6    .052   7   -.018
      8    .015   9   -.023  10   -.003  12   -.019  13    .022  15   -.101  16    .059
     17   3.583
18    1    .054   2   -.039   3   -.423   4    .416   5    .040   6   -.050   7    .005
      8   -.018   9   -.006  10    .002  11    .012  13   -.016  14    .019  15   -.020
     16   -.086  17    .056  18   3.589
19    1   -.052   2    .050   3   -.026   4   -.430   5    .432   6    .023   7    .011
      9    .013  10    .009  11   -.020  12    .019  14   -.015  15   -.073  16   -.007
     17   -.085  18    .057  19   3.576
20    1    .023   2   -.054   3    .049   4   -.025   5   -.401   6    .419   7   -.044
      8    .020   9    .083  10   -.009  12   -.014  13    .019  15    .065  16   -.092
     17   -.004  18   -.082  19    .054  20   3.499
21    7   -.458   8   -.161   9   -.048  10   -.038  11    .166  12    .163  13    .171
     14   -.162  21   4.505
22    1    .231   2   -.619   3    .338   4    .305   5   -.601   6    .180   7   -.497
      8    .080   9   -.087  10   -.044  11    .099  12   -.160  13    .087  14    .081
     16   -.288  17    .296  19   -.290  20    .328  22   4.390
```

Table 3.15 (Continued): Non-redundant scaled 4-21G force constants
of benzaldehyde

```
23    1    .569  3  -.508  4   .503  6  -.541  7   .034  8  - .26  9    .0: ;
     10  -.009 11   .129 13  -.144 14   .136 15   .321 16  - .70 17  - .1
     18   .350 19  -.170 20  -.156 23  4.240
24    1   .143  2   .051  3  -.085  4   .021  5  -.008  6  - 077  7    59
      8  -.002  9   .453 10  -.263 11  -.090 12   .006 13   010 14    01
     15   .381 16  -.021 17  -.032 18   .011 19  - 026 20  - 041 21   - 05
     22  -.165 23   .227 24  3.645
25    1  -.015  2   .003  3  -.007  4  -.012  5   .008  6   078  7    40
      8   .005  9  -.528 10   .071 11   .003 12   .000 13   022 14    00
     15  -.289 16  -.025 17  -.001 18   .003 19   .021 20   003 21   - 09
     22  -.088 23  -.046 24   .204 25  2.207
26   26  1.198
27   26   .045 27  1.160
28   26  -.072 27   .042 28  1.117
29   26  -.118 27  -.081 28   .051 29  1.183
30   26  -.088 27  -.103 28  -.076 29   .051 30  1.127
31   26   .020 27  -.076 28  -.103 29  -.079 30   .049 31  1.221
32   26  -.142 27  -.030 28   .022 29   .016 30  -.001 31  - .060 32  1.633
33   26   .098 27  -.110 28   .089 29  -.101 30   .096 31  - .085 32   .086
     33  1.305
34   27  -.098 28   .004 30  -.085 31   .016 32   .083 34  1.059
35   26   .045 27   .062 28  -.111 29   .049 30   .056 31  - .092 32    020
     35  1.086
36   26  -.066 27  -.018 28   .031 29   .010 30  -.019 31  - .013 32   .063
     33   .007 34   .042 35  -.082 36   .418
```

* Non-redundant local coordinates are according to Table-3.14.

Bibliography

[1] Pulay, P.; Fogarasi. G.; Pongor, G.; Boggs, J. E.; Vargha, A. *J. Am. Chem. Soc.*, **1983**, 105, 7037.

[2] Goodman, L.; Ozkabak, A. G.; Thakur, S. N. *J. Phys. Chem.*, **1991**, 95, 9044 and references there in.

[3] Palmo, K.; Pietila. L. O.; Krimm, S. *J. Comput. Chem.*, **1991**, 12, 385.

[4] Nakamura, R.; Machida, K.; .Oobatake, M.; Hayashi, S. *Mol. Phys.*, **1988**, 64, 215.

[5] Francisco, J. S.; Sander, S. P. *J. Chem. Phys.*, **1995**, 102, 9615.

[6] Pongor, G.; Pulay, P.; Fogarasi, G.; Boggs, J. E. *J. Am. Chem. Soc.*, **1984**, 106, 2765.

[7] Williams, R. W.; Kalasinsky, V. F.; Lowrey, A. H. *J. Mol. Struct.(Theochem)*, **1993**, 281, 157.

[8] Wilson, Jr., E. B.; Decius, J. C.; Cross, P. C. *Molecular Vibrations, The Theory of Infrared and Raman Vibrational Spectra* McGraw-Hill Book Company, New York, 1955. For perturbation results see page 231.

[9] Toman, S.; Pliva, J. *J. Mol. Spectrosc.*, **1966**,21, 362.

[10] McIntosh, D. F.; Peterson, M. R. *General Vibrational Analysis System*, QCPE 576, Indiana University, Bloomington, Indiana,47405.

[11] Wilson, Jr., E. B. *Phys. Rev.*, **1934**, 45, 706.

[12] a) Miller, F. A.; Crawford, Jr., B. L. *J. Chem. Phys.*, **1946**, 14, 282. b) Crawford, Jr., B. L.; Miller, F. A. *J. Chem. Phys.*, **1949**, 17, 249.

58

[13] a) Ingold, C. K.; Angus, W. R.; Bailey, C. R.; Hale, J. B.; Leckie, A. H.; Raisin, L. (; Thompson, J. W. *J. Chem. Soc. London,* **1936**, p.912. b) Ingold, C. K.; Bailey, C. R.; Be, ; A. P.; Carson, S. C.; Gordon, R. R.; Hale, J. B.; Harzfeld, N; Hodden, J. W.; Poole,] . G.; Weldon, I. H. P.; Wilson, C. L. *J. Chem. Soc. London,* **1946**, p.222.

[14] a) Whiffen, D. H. *Philos. Trans. R. Soc. London,* **1955**, 248A, 131. b) Albrecht, A. C. *Mol. Spectrosc.,* **1960**, 5, 236.

[15] Duinker, J. C.; Mills, I. M. *Spectrochim. Acta,* **1968**, 24A, 417.

[16] Brodersen, S.; Langseth, A. *Mat. Fys. Skr. Dan. Vid. Selsk.,* **1956**, 1, 1. **1959**, 1, 7.

[17] Colloman, J. H.; Dunn, T. M.; Mills, I. M. *Philos. Trans. R. Soc. London* , **1966**, 259, 49(

[18] a) Pliva, J.; Pine, A. S. *J. Mol. Spectrosc.,* **1982**, 93, 209; *J. Mol. Spectrosc.,* **1987**, 107, 318 b) Pliva, J.; Johns, J. W. C. *Can. J. Phys.,* **1983**, 61, 269; *J. Mol. Spectrosc.,* **1984**, 107, 318 c) Pliva, J.; Valentin, A.; Chazelas, J.; Henry, L. *J. Mol. Spectrosc.,* **1989**, 134, 220. d Pliva, J.; Johns, J. W. C.; Goodman, L. *J. Mol. Spectrosc.,* **1989**, 134, 227; **1990**, 140, 214.

[19] a) Hochstrasser, R. M.; Sung, H. N.; Wessel, J. E. *J. Am. Chem. Soc.,* **1973**, 95, 8179. b) Hochstrasser, R. M.; Wessel, J. E.; Sung, H. N. *J. Chem. Phys.,* **1974**, 60, 317. c) Wunsch, L.; Metz, F.; Neusser, H. J.; Schlag, E. W. *J. Chem. Phys.,* **1977**, 66, 386.

[20] Berman, J. M.; Goodman, L. *J. Chem. Phys.* **1987**, 87, 1479.

[21] Pulay, P.; Fogarasi, G.; Pang, F.; Boggs, J. E. *J. Am. Chem. Soc.,* **1979**, 101, 2550.

[22] Pulay, P.; Fogarasi, G.; Boggs, J. E. *J. Chem. Phys.,* **1981**, 74, 3999.

[23] Guo, H.; Karplus, M. *J. Chem. Phys.,* **1988**, 89, 4235.

[24] Ozkabak, A. G.; Goodman, L. *J.Chem.Phys,* **1987**, 87, 2564.

[25] Innes, K. K.; Byrne, J. P.; Ross, I, G. *J. Mol. Spectrosc.,* **1967**, 22, 125.

[26] Loisel, J.; Lorenzelli, V. *J. Mol. Struct.,* **1967**, 1, 157.

[27] Castellucci, E.; Sbrana, G.; Verderame, E. D. *J. Chem. Phys.,* **1969**, 51, 3762.

[28] Kakiuti, Y.; Akiyama, M.; Saito, N.; Saito, H. *J. Mol. Spectrosc.*, **1976**, 61, 164.

[29] Stidham, H. D.; DiLella, D. P. *J. Raman. Spectrosc.*, **1979**, 8, 180.

[30] DiLella, D. P.; Stidham. H. D. *J. Raman. Spectrosc.*, **1980**, 9, 90.

[31] DiLella, D. P. *J. Raman. Spectrosc.*, **1980**, 9, 239.

[32] Stidham, H. D.; DiLella, D. P. *J. Raman. Spectrosc.*, **1980**, 9, 247.

[33] a) Long, D. A.; Murfin, F. S.; Thomas, E. L. *Trans. Faraday. Soc.*, **1963**, 59, 12. b) Long, D. A.; Thomas, E. L. *Ibid.*, **1963**, 59, 783.

[34] Harsanyi, L.; Kilar, F. *J. Mol. Struct.*, **1980**, 61, 141.

[35] a) Green, J. H. S.; Harrison, D. J. *Spectrochim. Acta*, **1976**, 32A, 1265. b)Pietila, L. O.; Mannfors, B.; Palmo, K. *Spectrochim. Acta*, **1988**, 44A, 141.

Chapter 4

Force Field and Assignment of the Vibrational Spectra of Naphthalene and Anthracene

The vibrational spectra of polyaromatic hydrocarbons and their cations received mu h attention recently due to their importance as the origin of infrared emission bands in t e intersteller radiation from many gallactic sources [1]. Naphthalene is the smallest memb r in the family and was studied by several authors [2-18]. Pulay et al. reported for the fil t time a complete theoretical force field of naphthalene obtained by using the scale facto s from their benzene work [3]. However benzene and naphthalene are not really structural related (naphthalene is a coupled ring system) and the direct transfer of scale factors fro i benzene leads to poor predicted numbers. A geometry refinement which includes th approximate cubic force constants was needed to obtain a good fit between experiment and predicted frequencies of naphthalene. Also, the number of force constants liste for naphthalene(208) is more than the number of symmetric force constants(189). Mor recently the vibrational spectra of naphthalene and its radical cation were studied usin matrix isolation spectroscopy by Szczepanski et al. [2]. The second simplest membei anthracene, is also studied by several theoretical and experimental methods [19-28]. Th early work of Bruhn and Mecke [21] and Califano [22] identified many of the fundamenta frequencies of anthracene and anthracene-d_{10} based on their polarization measurements The IR spectra of anthracene and anthracene-d_{10} crystals were analyzed by Bree and Kydd [23]. Bekke et al. using a five parameter approximation analyzed all the in-plane fun·

60

damentals of anthracene and proposed their probable assignments [20]. More recently, Szczepanski et al. analyzed the vibrational spectra of anthracene and its radical cation using matrix isolation spectroscopy [19]. On the theoretical side, a detailed calculation of the normal modes of anthracene and anthracene-d_{10} was reported by Krainov using the complete system of induction coefficients from naphthalene [25]. A simplified valence force field calculation for benzene,naphthalene and anthracene was reported by Neto et al. [9]. Evans and Scully [26] reported a theoretical calculation for the out of plane vibrations of anthracene, anthracene-d_2 and anthracene-d_{10} by transferring the benzene force constants. Although a number of vibrational spectral studies have been reported for anthracene, some of the assignments still remain uncertain and the complete force field is not yet available. In this chapter we report the ab initio force field of naphthalene and anthracene at the HF/4-21G level. We explicitly show that the benzene molecule is not structurally related to anthracene whereas naphthalene and anthracene are structurally related. Using the newly developed methodology described in chapter 3 we report a set of 189 non-redundant local force constants which reproduces the naphthalene fundamental frequencies with an average error of 5.7 cm^{-1}. The scale factors obtained from naphthalene force constants were used to obtain the complete anthracene force field which simulates the vibrational spectra of anthracene with remarkable accuracy. It is to be noted that *no experimental data* is used in the *prediction* of anthracene frequencies.

4.1   Calculations

The ab initio force constants and frequencies of naphthalene and anthracene were calculated using 4-21G basis set. The cartesian force constant matrices were then transformed to the non-redundant local coordinate space. The non-redundant local coordinates of naphthalene and anthracene are shown in Table-4.1 and Table-4.2 and in Figure 4.1 and Figure 4.2. The number of force constants getting adjusted due to the change in frequencies is smaller when the fitting is done in symmetry blocks compared to local coordinates. Also mixing between degenerate modes is avoided by fitting the frequencies in symmetry

coordinates. Hence the fitting is done in symmetry coordinates adjusting the scale factors in local coordinates. A flow chart of the modified algorithm is given in Figure 4.3.

4.2 Results

As pointed out by Pulay et al. [3] in their SQM study of naphthalene, the naphthalene force field is quite different from that of benzene and hence simple transfer of benzene force field would poorly reproduce the naphthalene fundamental vibrational frequencies. So, our present method also fails to achieve a better fit for naphthalene by simple transfer of benzene scale factors largely because of the absence of inter-ring $CC-CC$ couplings in benzene. However, it is possible to predict the vibrational frequencies of anthracene from naphthalene as naphthalene and anthracene resemble each other even in $CC-CC$ couplings. Because the prediction requires a complete set of scale factors, we fitted the experimental frequencies of naphthalene-d_0 and -d_8 to the theoretically calculated ab initio HF/4-21G force field. The fitting produced an excellent agreement between the experimental and the calculated frequencies. The average deviation is $5.7 cm^{-1}$ ($4.0 cm^{-1}$ in $C_{10}D_8$) including C-H frequencies and $3.6 cm^{-1}$ ($2.4 cm^{-1}$ in $C_{10}D_8$) excluding C-H frequencies.

4.2.1 Force Field of Naphthalene and Anthracene

The force constant values obtained for benzene are 6.715 for C-C stretch, 5.181 for C-H stretch, 0.510 for C-H deformation, 1.274 and 1.239 for ring deformation and 0.319 and 0.388, 0.307 are for out of plane C-H wag and ring bending respectively. These when compared to naphthalene force constants indicate clearly that the benzene force field is very different from that of naphthalene. For naphthalene our fitted force field shows a good agreement with the earlier SQM predicted force field in both in-plane and out of plane diagonal force constants. Obviously such a good agreement is not expected in the case of the coupling constants because of the oversimplification involved in the evaluation of the coupling force constants in the SQM procedure. The fitted force field produced frequencies for both naphthalene and naphthalene-d_8 better than the earlier SQM prediction so

can be considered as an improvement over the earlier force field. A representative set of force constants of naphthalene and anthracene is listed in Table-4.3 and the complete force field is given in Tables-4.9 to 4.12 from which we can draw the following conclusions.

(1) C-H diagonal force constants of naphthalene and anthracene are almost identical except for a minor deviation of the anthracene central ring. Interactions involving C-H bonds(σ bond) are small and only the first neighbours contribute significantly.

(2) C-C force constants exhibit similar trends although the absolute values are different because of π-π interaction. The trend and the accuracy of the predicted C-C frequencies indicate the transferability of the scale factors. The diagonal force constants are in accordance with the Huckel π bond order [29]. Interactions involving C-C bonds(σ and π bonds) are much stronger and extend over the entire ring in both systems confirming the earlier preliminary conclusion based on only naphthalene [30].

(3) Diagonal f_{β_i}s are almost the same for the naphthalene and anthracene. $CH_i - \beta_i$ interactions are less than 0.01 and negligible in most cases. $CC_i - \beta_i$ interactions are substantial only for the connecting bonds. For outer rings of naphthalene and anthracene they are almost the same while central ring has slightly higher values.

(4) Diagonal ring deformation force constants are similar for naphthalene and the outer rings of anthracene and somewhat higher for the central ring.

These conclusions clearly indicate that the force field of the outer rings of anthracene is almost identical with that of naphthalene and the central ring differ to some extent. As a result the prediction is excellent for the outer ring modes of anthracene and the deviation is slightly more from the experimental frequencies for the central ring.

4.2.2 Vibrational Spectra of Naphthalene

The 48 normal modes of naphthalene in D_{2h} symmetry factorize in 8 symmetry blocks as $9A_g, 8B_{3g}, 8B_{1u}, 8B_{2u}, 4A_u, 4B_{3u}, 3B_{1g}$ and $4B_{2g}$. The calculated fundamentals from the fitting procedure of naphthalene -d_0 and -d_8 are given in Table-4.4 along with their assignments. The assignments agree well with that of Pulay et al. in almost all the modes. However there is a controversy regarding one of the B_{2u} fundamentals. It could be at 1144 or 1163

cm^{-1}. In the SQM method, the predicted number 1158 cm^{-1} was closer to 1163 cm^{-1}. We tried fitting both the frequencies separately. 1163 cm^{-1} gave the C-C force constant in agreement with the expected bond orders. As a result we assigned it at 1163 cm^{-1}. In 3_{1u}, the band at 810 [9,11-12] and 748 cm^{-1} [6] were suggested as possible alternatives for the $\delta_1 + \delta_3$ mode. The fitting using 810 cm^{-1} produced 805 cm^{-1} as the calculated fundamental while the 748 cm^{-1} produced 765 cm^{-1} as the calculated frequency. This clearly indicates that 810 cm^{-1} band is more likely to be the correct one and this is in agreement with the earlier SQM assignment.

C-H stretching vibrations:

Due to anharmonicity and the perturbations because of Fermi resonance the C-H fundamentals are *difficult to assign*. However, we used the following strategy to address the effect of anharmonicity on the naphthalene frequencies. We started with the assumption that the anharmonicity of the C-H and C-D bonds are the same for benzene and naphthalene because the C-H force constants are nearly same(5.181-C_6H_6, 5.113-α-$C_{10}H_8$ and 5.153-β-$C_{10}H_8$) and the C-H and C-D stretching frequencies appear in the same narrow range of frequencies. The harmonic frequencies could be estimated from the equation

$$\omega_i = \nu_i + \Delta_i \qquad (.1)$$

where Δ_i represents the total anharmonic corrections to the fundamental frequency. Following Goodman et al. [31] we adopted a 117 cm^{-1} anharmonic correction for C-H fundamentals and 59 cm^{-1} for C-D ones. The second assumption we made is that the deuterated fundamentals are not perturbed by Fermi resonance because there is no frequency in the 1100-1150 cm^{-1} range whose overtone can interact with the C-D fundamentals(2200-2300 cm^{-1}). (However, it is possible to have a combination band of the right frequency. We neglect such a possibility because without further experimental data this problem could not be addressed). The best fitted C-D fundamentals are converted to harmonic frequencies based on equation(2) and fitted to get the harmonic force constants. During the fitting all $C_{10}H_8$ and $C_{10}D_8$ frequencies other than C-H stretching ones are used. The computed harmonic force constants are in good agreement with the benzene value obtained by Goodman et al. [31] (5.567-C_6H_6, 5.459-α-$C_{10}H_8$ and 5.486-β-$C_{10}H_8$). These harmonic

force constants are used to predict the harmonic C-H frequencies which in turn used to calculate the corresponding anharmonic frequencies using equation 4.1. The predicted anharmonic frequencies agree well with the observed fundamentals except for one of the B_{3g} modes (3031 cm^{-1}) as shown in Table-4.5 indicating that this particular frequency is a likely candidate for Fermi resonance. The computed mean amplitudes of vibration (Figure 4.4) are in good agreement with the reported values [32,33] indicating that the final force field is reliable.

4.2.3   Vibrational Spectra of Anthracene

Anthracene is planar with D_2h symmetry and is characterized by 66 vibrational degrees of freedom. The 45 in-plane and 21 out of plane normal vibrations span the irreducible representations as $12A_g+ 11B_{3g}+ 11B_{1u}+ 11B_{2u}+ 4b_{1g}+ 6b_{2g}+ 5a_{1u}+ 6b_{3u}$. The fundamental frequencies of anthracene are predicted separately by transferring scale factors of benzene and naphthalene respectively. Table-4.6 shows the predicted frequencies obtained from the scale factors of benzene and naphthalene along with their assignments. The table clearly indicates that transferring the diagonal force constants and taking their geometric mean for the off-diagonal elements give poor agreement compared to transferring all the scale factors. When the molecules are structurally related the assumption that each force constant is associated with its own scale factor, works well rather than the geometric mean of diagonal force constants for the off-diagonal elements because the characteristics of each force constant is retained. The average deviations for the 66 frequencies are 15.0, 13.5 and 9.2 cm^{-1} (13.6,13.2 and 8.2 cm^{-1} excluding CH stretch) for the different predictions as shown in Table-4.6. As expected the predicted anthracene frequencies from naphthalene scale factors are better than those predicted from benzene even in geometric mean approximation. In the prediction, corrections for basis set error, correlation and anharmonicity were transferred through scale factors from naphthalene to anthracene.

4.2.4 In-plane frequencies

C-H stretching vibrations:

The νC-H frequencies appear as independent modes and all the C-H stretching fundamentals appear in the region $\nu > 3000$ cm^{-1}. To address the problem of anharmonicity, the harmonic scale factors are transferred from naphthalene to anthracene to predict the harmonic frequencies. The harmonic frequencies are then corrected for anharmonicity as in the case of naphthalene. The final values are given in Table-4.5 along with the experimental numbers. The agreement is good for six frequencies indicating the other four are possibly perturbed by Fermi resonance.

A_g modes:

The frequencies in this block is only Raman active, and the earlier assignments proposed by several authors are quite consistent and agree within the experimental error. One of the R_{CC} band in the earlier assignment was doubtful, either at 1412 or 1400 cm^{-1} [20], which was resolved later assigning 1412 cm^{-1} to A_{1g} mode and 1400 cm^{-1} to B_{2u} fundamental [19]. The predicted numbers 1408 cm^{-1} and 1404 cm^{-1} agree very well with the later assignment. The prediction is poor only in the case of 1264 cm^{-1} band with a deviation of 21 cm^{-1}. This is clearly due to the differences between the naphthalene and anthracene force constants for the diagonal R_1, R_7 and their interactions.

B_{3g} modes:

In this block a weak Raman band observed by Bakke et al. [20] at 1574 cm^{-1} was assigned at 1596 cm^{-1} by Neto et al. [9] and Colombo [24]. Our predicted number 1596 cm^{-1} exactly matches with the latter assignment. So we confirm this mode at 1596 cm^{-1}. With this modification all predicted frequencies match well with the earlier assignments except the one at 1433 cm^{-1}. This band shows a deviation of 55 cm^{-1}, the predicted one being at 1388 cm^{-1}. It is unlikely that the force fields of naphthalene and anthracene are very different to cause this much error. It is likely that either this assignment is incorrect or something like Fermi interaction occurs for this mode. Bakke et al. observed a Raman band at 1384 cm^{-1} [20] which agrees well the predicted value of 1388 cm^{-1}. It is interesting to note that the earlier calculated values based on NCA also occur at 1389 cm^{-1} [9] and 1396 cm^{-1} [25].

B$_{1u}$ modes:

These IR and Raman active bands are available from the more recent work [19]. The agreement with the earlier experimental numbers are within few cm^{-1}, except for the one at 1346 cm^{-1}. The earlier workers assigned this band at around 1317 cm^{-1} [9,20-24,28]. The predicted frequency at 1340 cm^{-1} agrees well with the recent assignment. All the other predicted numbers in this block agree very well with the experimental numbers.

B$_{2u}$ modes:

This is probably the most controversial block in the anthracene spectra. Deviations of 100-150 cm^{-1} could be found in the existing assignments. The R_{CC} band is assigned at different frequencies by different authors. 1695 [23], 1720 [24], 1690 [20], 1533 [9,22] and 1524 [28] cm^{-1} are some of the available assignments. The most recent work [19] assigned it at 1542 cm^{-1}. The predicted number 1560 cm^{-1} confirms this assignment. The other controversial bands were assigned at 1460,1400,and 1318 cm^{-1} in the latest work [19]. For the 1460 cm^{-1} fundamental earlier assignments were made at 1534 [20], 1533 [23], 1680 [24] and 1462 [9,22]. The predicted number appear at 1445 cm^{-1} is in agreement with 1460 cm^{-1}. The 1400 cm^{-1} band was assigned at 1494 [20], 1398 [9,22], 1495 [23], 1537 [24] and 1350 [28] cm^{-1}. Our predicted frequency 1404 cm^{-1} confirms the assignment at 1400 cm^{-1}. The predicted frequency corresponding to the experimental 1318 cm^{-1} band [19] occurs at 1283 cm^{-1}, off by 33 cm^{-1}. This band corresponds to $(R_7+\beta_5)$ which represent the central ring and there is no exact counterpart of this in naphthalene. Hence, the deviation is higher than the expected one.

4.2.5 Out of plane frequencies

A$_{1u}$ modes:

This class is inactive in both Raman and IR spectra of the free molecule and hence comparison is made with the IR active crystal bands. Only three out of five fundamentals were reported [20,21,27]. The highest frequency mode was assigned at 988 cm^{-1} [20] and 979 cm^{-1} [27]. The predicted value 984 cm^{-1} is closer to the first one. The other two bands agree between the different authors as well as with the predicted ones. For the two lower

frequencies the predictions are at 491 and 126 cm^{-1}. Early work of Chantry et al. [27] gives the experimental frequency at 126 cm^{-1}.

B$_{3u}$ modes:

The highest frequency in this symmetry is assigned at around 956 [2,20-24,27] and at 920 cm^{-1} [28]. The predicted frequency 970 cm^{-1} supports the higher number in agreement with most of the literature. The next higher band is assigned at 883 cm^{-1} [20] and 879 cm^{-1} [19]. These are within experimental error and we took the most recent value of 879 cm^{-1} for the predicted value 895 cm^{-1}. The other three numbers are in excellent agreement with the most recent paper [19]. It is of interest to note that the torsional numbers > 300 cm^{-1} were predicted very well compared to the out of plane wag fundamentals. Again this is a reflection of the differences in force fields between naphthalene and anthracene. It is known that the ab initio method gives very low value for the torsions below 300 cm^{-1}.

B$_{1g}$ and B$_{2g}$ modes:

The earlier work of Evans and Scully [26] do not agree with that of bakke et al. [20]. It appears that the only reliable values are that of Bakke et al. [20] for these modes. Although there is overall agreement between the predicted and the experimental frequencies, deviations are quite large in three of the fundamentals assigned at 896,773 and 580 cm^{-1}. The 896 cm^{-1} band if assigned at 852 cm^{-1} [26] gives better agreement with the predicted 831 cm^{-1}. An experimental reinvestigation of these frequencies may give a better agreement with the prediction.

The symbolic force constant matrices in terms of symmetry unique local force constants and the orthogonal transformation matrices from local to symmetric coordinates for naphthalene and anthracene and the complete mean amplitudes of vibration of naphthalene are given in Tables-4.7 to 4.13.

4.3 Conclusions

The fitting procedure to obtain the scale factors and frequencies from the ab initio force field has shown to be remarkably successful for naphthalene producing an average devi-

ation of 5.7 cm^{-1} between the predicted and experimental frequencies. These scale factors when used to predict the frequencies of anthracene, the results are in excellent agreement with the experimental ones with an average average deviation of 8.2 cm^{-1} for a molecule of 24 atoms. From the accuracies of the computed frequencies it is clear that the methodology could be used successfully for the prediction of frequencies of unknown molecules. The earlier assignments of naphthalene were confirmed and the anthracene assignments were either confirmed or reassigned. A complete set of non-redundant force constants are obtained for both naphthalene and anthracene.
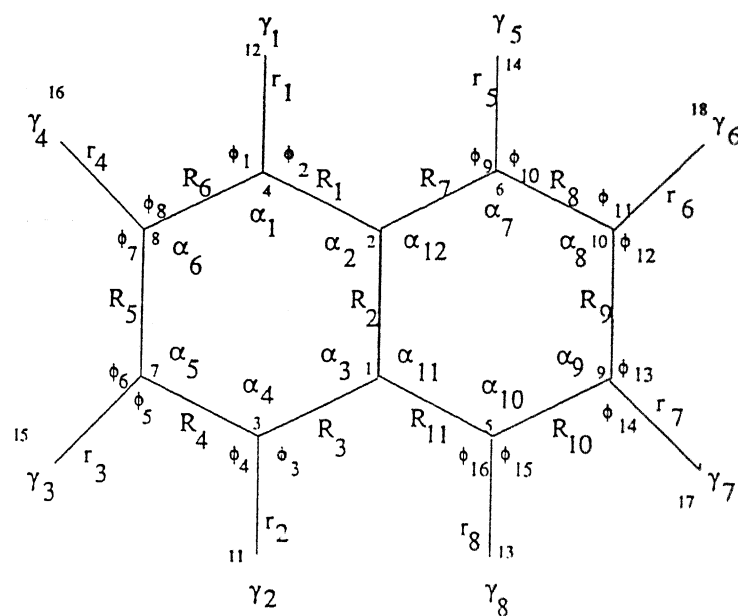
τ numberings are same as defined in R

Figure 4.1: Internal coordinates of naphthalene
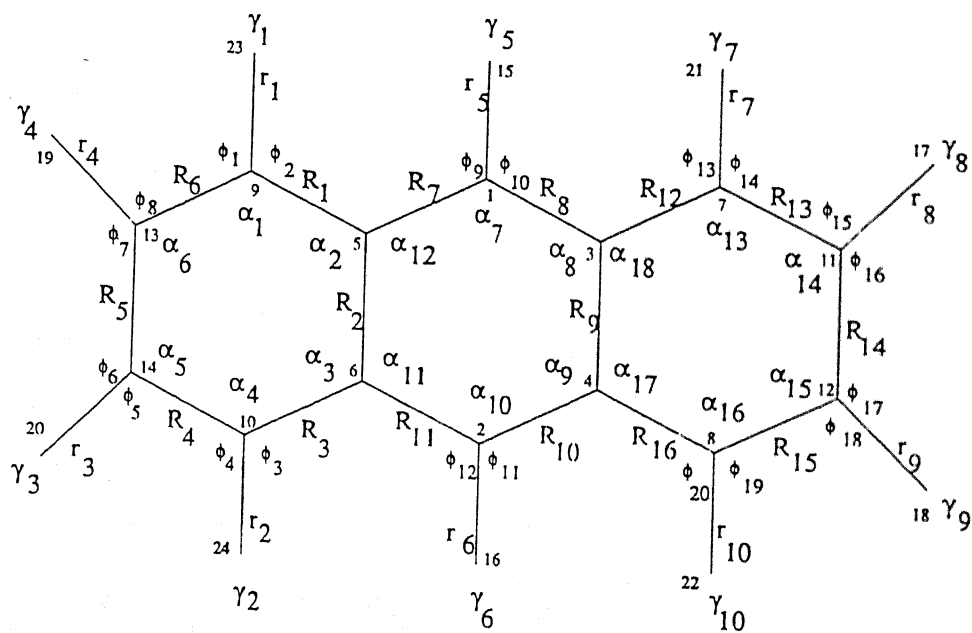
τ numberings are same as defined in R

Figure 4.2: Internal coordinates of anthracene

Step 1: Convert cartesian force constants obtained from the ab initio program to force constants in local symmetry coordinates as recommended by Pulay et al. We refer to this F matrix as F_{ab}

Step 2: Input: No. of isotopic species(nmol), masses(M), Wilson's B matrix(B), local U (U_{loc}), orthogonal U (U_{ortho}) - transformation matrix from local U to symmetric U. We used Niter= 1000.

Step 3:
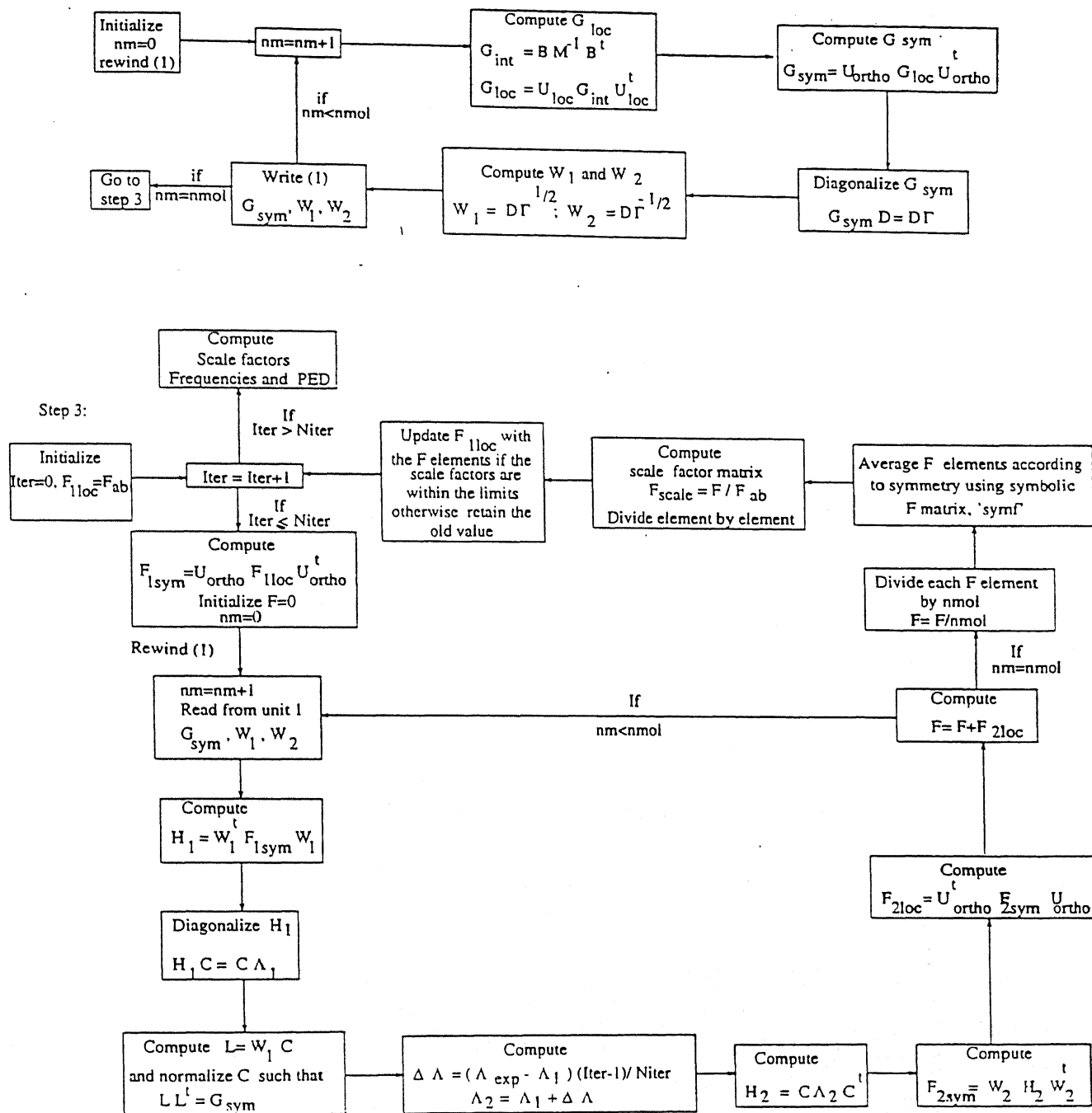
Figure 4.3: Flowchart of the modified algorithm
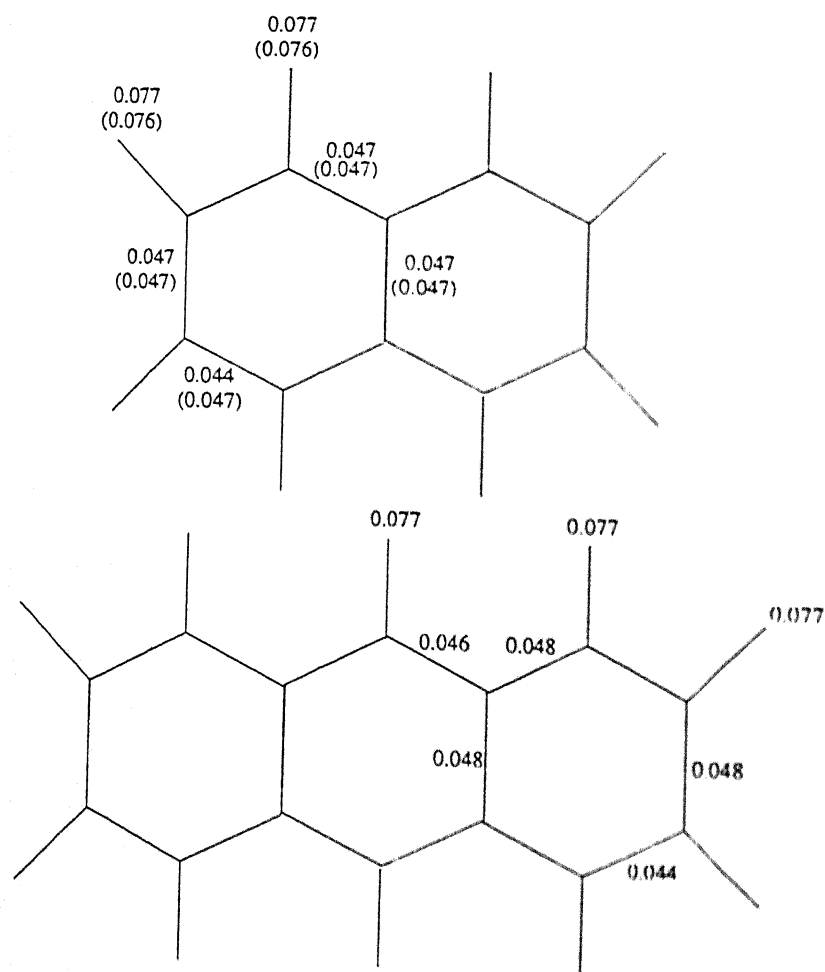
Figure 4.4: Mean amplitudes of vibration of naphthalene and anthracene (Å)

Numbers are obtained from our predicted force field. Numbers in the parentheses re observed values taken from ref. 33.

Table 4.1: Non-redundant local coordinates of naphthalene

In plane

S_{1-11}	$= R(\text{CC-stretch})(R_i)$
S_{12-19}	$= r(\text{CH-stretch})(r_i)$
S_{20-27}	$= 2^{-1/2}(\phi_1-\phi_2); 2^{-1/2}(\phi_3-\phi_4); \dots$ etc. (CH-deform.)(β_i)
$S_{28,31}$	$= 6^{-1/2}(\alpha_1-\alpha_2+\alpha_3-\alpha_4+\alpha_5-\alpha_6)(\text{ring deform.})(\delta_1,\delta_4,)$
$S_{29,32}$	$= 12^{-1/2}(2\alpha_1-\alpha_2-\alpha_3+2\alpha_4-\alpha_5-\alpha_6)(\text{ring deform.})(\delta_2,\delta_5)$
$S_{30,33}$	$= 2^{-1/2}(\alpha_2-\alpha_3+\alpha_5-\alpha_6)(\text{ring deform.})(\delta_3,\delta_6)$

Out of plane

S_{1-8}	$= \gamma(\text{CH-wagg})(\gamma_i)$
$S_{9,12}$	$= 6^{-1/2}(\tau_1-\tau_2+\tau_3-\tau_4+\tau_5-\tau_6)(\text{ring torsion})(\tau_1,\tau_4)$
$S_{10,13}$	$= 12^{-1/2}(\tau_1-2\tau_2+\tau_3+\tau_4-2\tau_5+\tau_6)(\text{ring torsion})(\tau_2,\tau_5)$
$S_{11,14}$	$= 2^{-1/2}(\tau_1-\tau_3+\tau_4-\tau_6)(\text{ring torsion})(\tau_3,\tau_6)$
S_{15}	$= \tau_{3126}-\tau_{4215}(\tau)$

*All internal coordinates are according to figure-4.1.

Table 4.2: Non-redundant local coordinates* of anthracene

In plane

S_{1-16}	$= R(\text{CC-stretch})(R_i)$
S_{17-26}	$= r(\text{CH-stretch})(r_i)$
S_{27-36}	$= 2^{-1/2}(\phi_1-\phi_2); 2^{-1/2}(\phi_3-\phi_4); \dots$ etc. (CH-deform.)(β_i)
$S_{37,40,43}$	$= 6^{-1/2}(\alpha_1-\alpha_2+\alpha_3-\alpha_4+\alpha_5-\alpha_6)(\text{ring deform.})(\delta_1,\delta_4,\delta_7)$
$S_{38,41,44}$	$= 12^{-1/2}(2\alpha_1-\alpha_2-\alpha_3+2\alpha_4-\alpha_5-\alpha_6)(\text{ring deform.})(\delta_2,\delta_5,\delta_8)$
$S_{39,42,45}$	$= 2^{-1/2}(\alpha_2-\alpha_3+\alpha_5-\alpha_6)(\text{ring deform.})(\delta_3,\delta_6,\delta_9)$

Out of plane

S_{1-10}	$= \gamma(\text{CH-wagg})(\gamma_i)$
$S_{11,14,17}$	$= 6^{-1/2}(\tau_1-\tau_2+\tau_3-\tau_4+\tau_5-\tau_6)(\text{ring torsion})(\tau_1,\tau_4,\tau_7)$
$S_{12,15,18}$	$= 12^{-1/2}(\tau_1-2\tau_2+\tau_3+\tau_4-2\tau_5+\tau_6)(\text{ring torsion})(\tau_2,\tau_5,\tau_8)$
$S_{13,16,19}$	$= 2^{-1/2}(\tau_1-\tau_3+\tau_4-\tau_6)(\text{ring torsion})(\tau_3,\tau_6,\tau_9)$
S_{20}	$= \tau_{7342}-\tau_{1348}(\tau')$
S_{21}	$= \tau_{15610}-\tau_{9562}(\tau'')$

*All internal coordinates are according to figure-4.2.

Table 4.3: Selected scaled force constants of naphthalene and anthracene*

Naphthalene			Anthracene		
local coordinates	force constants	πbond order	local coordinates	force constants	πbond order
(R_1,R_3,R_7,R_{11})	6.076	0.554	(R_1,R_3,R_{12},R_{16})	5.695	0.53
(R_4,R_6,R_8,R_{10})	7.513	0.725	(R_4,R_6,R_{13},R_{15})	7.988	0.73
(R_5,R_9)	6.112	0.603	(R_5,R_{14})	5.703	0.58
(R_2)	5.607	0.518	(R_2,R_9)	5.242	0.48
(R_1,r_1)	0.060		(R_1,r_1)	0.057	
(R_6,r_1)	0.076		(R_6,r_1)	0.077	
(r_1,r_1)	5.113		(r_1,r_1)	5.115	
(R_4,r_3)	0.075		(R_4,r_3)	0.076	
(R_5,r_3)	0.096		(R_5,r_3)	0.093	
(r_3,r_3)	5.153		(r_3,r_3)	5.155	
			(R_7,r_5)	0.092	
			(R_8,r_5)	0.092	
			(r_5,r_5)	5.085	

C-C coupling

	R_1	R_2	R_3	R_4	R_5	R_6	R_7	R_8
R_1(nap)	6.076	0.586	-0.332	0.301	-0.438	0.608	0.705	-0.169
R_1(anth)	5.695	0.442	-0.241	0.217	-0.363	0.529	0.769	-0.253
r_1(nap)	0.060	-0.015	-0.020	-0.016	0.002	0.076	0.003	0.004
r_1(anth)	0.057	-0.015	-0.019	-0.016	0.001	0.077	0.004	0.007
β_1(nap)	-0.183	0.001	0.017	-0.019	0.005	0.164	0.018	0.001
β_1(anth)	-0.183	0.005	0.016	-0.017	0.003	0.167	0.018	0.000

	R_9	R_{10}	R_{11}	R_{12}	R_{13}	R_{14}	R_{15}	R_{16}
R_1(nap)	0.073	-0.251	0.135					
R_1(anth)	0.025	-0.193	0.141	0.103	-0.047	0.053	-0.051	0.042
r_1(nap)	0.005	0.013	-0.001					
r_1(anth)	0.005	0.008	-0.002	0.000	0.002	-0.002	0.001	-0.001
β_1(nap)	-0.006	0.000	-0.004					
β_1(anth)	-0.006	0.000	-0.003	-0.001	0.000	0.000	0.000	0.000

C-H coupling

	r_1	r_2	r_3	r_4	r_5	r_6	r_7	r_8
r_1(nap)	5.113	0.002	0.004	0.011	0.013	0.001	0.000	0.02
r_1(anth)	5.115	0.002	0.004	0.011	0.011	0.002	0.000	0.00

	r_9	r_{10}
r_1(anth)	0.000	0.000

*stretch,bend and stretch-bend constants are in mdyn/Å,mdynÅ/rad and mdyn/rad respectively.

Table 4.4: Fitted ab initio(4-21G) frequencies of naphthalene

Symmetry blocks	present work		SQM[a]		HF/6-31G[*b]	Experiment[a]		PED
	d_0	d_8	d_0	d_8	scaled(d_0)	d_0	d_8	
A_{1g}	3079	2285	3085	2289	3085	3060	2291	r_3+r_1
	3053	2253	3056	2257	3056	3031	2257	r_1+r_3
	1579	1554	1590	1563	1645	1578	1553	$R_4+R_5+\delta_2$
	1461	1292	1458	1287	1453	1460	1298	$\beta_1+\beta_2+R_5$
	1384	1381	1385	1385	1355	1380	1386	$R_2+R_1+R_4$
	1166	837	1170	838	1134	1163	835	$\beta_2+\beta_1$
	1023	861	1023	860	1043	1020	863	$R_5+\beta_1+R_4$
	762	691	757	689	780	761	692	$R_1+R_2+\delta_2$
	513	494	505	486	517	514	493	δ_2+R_1
B_{3g}	3063	2270	3067	2273	3069	3055	2276	r_3+r_1
	3046	2249	3047	2246	3046	$(3055)^c$	2257	r_1+r_3
	1632	1602	1644	1617	1673	1624	1605	$R_4+R_1+\beta_1$
	1455	1355	1458	1359	1461	1458	1353	$\beta_2+R_1+R_4$
	1245	828	1255	833	1219	1240	828	$\beta_1+R_1+\delta_1$
	1153	1024	1156	1030	1149	1158	1027	$\beta_2+\beta_1+R_4$
	940	882	940	879	917	939	883	δ_1
	508	491	512	495	491	508	491	δ_3
B_{1u}	3066	2274	3070	2275	3071	3056	2295	r_3+r_1
	3050	2252	3049	2249	3047	3029	2278	r_1+r_3
	1594	1546	1595	1546	1654	1595	1545	$R_4+\beta_2$
	1395	1254	1391	1248	1364	1389	1260	$\beta_2+\beta_1+R_1$
	1271	1044	1272	1049	1261	1265	1045	$\beta_1+R_1+\delta_1$
	1129	887	1137	882	1130	1125	885	$\delta_1+\beta_2+R_4+\beta_1$
	805	740	792	737	781	810	734	$\delta_1+\delta_3+R_1$
	358	327	354	323	364	359	326	δ_3+R_1
B_{2u}	3077	2284	3083	2288	3083	3056	2295	r_3+r_1
	3048	2250	3052	2253	3052	3029	2258	r_1+r_3
	1509	1446	1515	1446	1539	1509	1445	$R_5+\beta_2+R_1+\beta_1$
	1354	1294	1341	1288	1321	1361	1290	$R_4+\beta_1$
	1208	1090	1204	1081	1165	1209	1089	$R_1+\beta_2$
	1154	839	1158	840	1091	1163	840	$\beta_1+R_1+\beta_2+R_4$
	1008	827	1002	826	988	1008	828	$R_5+R_4+\beta_1$
	620	593	626	600	596	619	594	δ_2
A_{1u}	975	816	981	815	970	970	−	$\gamma_3+\gamma_1$
	837	657	825	647	824	841	−	$\gamma_1+\gamma_3$
	591	501	622	531	606	581	−	$\tau_1+\gamma_1$
	190	171	188	169	184	195	−	$\tau_2+\tau_1$

Table 4.4: (Continued): Fitted frequencies of naphthalene

Symmetry blocks	present work		SQM[a]		HF/6-31G*[b] scaled(d_0)	Experiment[c]		PED
	d_0	d_8	d_0	d_8		d_0	d_8	
B_{3u}	962	790	969	797	977	958	791	$\gamma_1+\tau_1+\gamma_3$
	781	629	777	627	791	780	629	$\gamma_3+\gamma_1$
	476	401	480	404	485	476	401	$\tau_1+\tau+\gamma_3$
	166	153	172	159	172	166	153	$\tau+\tau_3$
B_{1g}	954	762	952	761	968	951	766	$\gamma_1+\gamma_3$
	712	538	705	532	708	717	541	$\gamma_3+\gamma_1$
	392	345	387	341	397	386	350	$\tau_3+\gamma_3$
B_{2g}	992	871	987	857	985	983	875	$\gamma_3+\gamma_1+\tau_1+\tau$
	887	758	879	766	880	876	761	$\gamma_1+\gamma_3$
	772	635	773	634	785	772	646	$\tau_1+\tau_2$
	472	417	471	413	478	470	413	$\tau_2+\gamma_1+\gamma_3$
Ave. error	[5.7]	[4.0]	incl.	C-H				
Ave. error	[3.6]	[2.4]	excl.	C-H				

a. Ref 3.

b. Ref 2.

c. Number in the parenthesis is not used in fitting.

Table 4.5: Anharmonic and harmonic frequencies and force constants of C-H and C-D vibrations of naphthalene and anthracene

Naphthalene

Symmetry blocks	Anharmonic $C_{10}D_8$	$C_{10}H_8$	Expt [3]	Harmonic $C_{10}D_8$	$C_{10}H_8$
A_{1g}	2291	3060	3060	2350	3177
	2257	3034	3031	2315	3150
B_{3g}	2276	3046	3055	2334	3162
	2257	3031	(3055)	2315	3146
B_{1u}	2295	3048	3056	2354	3164
	2278	3034	3029	2336	3150
B_{2u}	2295	3058	3056	2354	3175
	2258	3030	3029	2316	3145
f_{C-H_α}	5.113	—	—	5.459	—
f_{C-H_β}	5.153	—	—	5.486	—

Anthracene

Symmetry blocks	Harmonic $C_{14}H_{10}$	Anharmonic $C_{14}H_{10}$	Expt [19]
A_{1g}	3177	3079	3072
	3150	3052	3048
	3141	3040	3027
B_{3g}	3164	·3066	3054
	3149	3049	3017
B_{1u}	3165	3066	3084
	3150	3050	3052
	3150	3050	3052
	3143	3042	3022
B_{2u}	3176	3079	3067
	3148	3051	3021
f_{C-H_α}	5.461	5.115	
f_{C-H_β}	5.489	5.155	
f_{C-H}	5.429	5.085	

Table 4.6: Predicted vibrational frequencies of anthracene

Symmetry blocks	Benzene G.M[a]	Naphthalene G.M[a]	All[b]	Expt[c]		PED
A_{1g}	-19	-8	-7	3072		r_3+r_1
	-15	-4	-4	3048		r_1+r_3
	-28	-17	-13	3027		r_5
	-28	-9	-3	1561		$R_4+R_2+R_5+R_7$
	3	-10	-4	1480		$R_5+\beta_3+\beta_1+R_7$
	-9	6	4	1412		$R_2+R_4+R_1+R_7$
	4	-11	-21	1264		$R_1+R_7+\beta_1$
	-15	-11	-8	1164		$\beta_2+\beta_1$
	13	1	8	1007		$R_5+R_4+\beta_1$
	1	9	5	754		$R_2+\delta_2+R_7+R_1$
	3	0	-1	625		δ_2
	8	3	0	397		$\delta_2+R_7+R_1$
B_{3g}	-22	-11	-12	3054		r_3+r_1
	-39	-28	-32	3017		r_1+r_3
	-37	-46	-2	1632		$R_4+R_7+R_1$
	-24	-22	0	1596		R_7+R_4
	-2	-4	-4	1384[d]	,1433	$\beta_3+\beta_1+R_1$
	-13	-13	-20	1273		$\beta_5+\beta_1$
	-11	-8	0	1187		$\beta_1+\beta_5+R_1$
	-1	-6	-1	1098		$R_1+\beta_3+R_4$
	-13	-20	-13	903		δ_1
	1	-2	-2	522		δ_3
	10	7	9	397		δ_2
B_{1u}	7	18	18	3084		r_3+r_1
	-5	6	2	3052		$r_1+r_3+r_5$
	-30	-20	-20	3022		r_5+r_1
	-44	-30	-9	1627		R_4+R_1
	-7	-18	-7	1450		$\beta_3+R_1+R_7$
	24	13	6	1346		$R_7+\delta_1+\beta_3$
	5	0	1	1272		$\beta_1+\delta_2+R_1$
	-12	-7	-4	1151		$\beta_3+\beta_1+R_4$
	1	-5	-4	908		δ_1
	7	0	7	652		$\delta_3+\delta_1+R_1$
	5	3	2	234		δ_3+R_7
B_{2u}	-24	-12	-12	3067		r_3+r_1
	-40	-29	-30	3021		r_1+r_3
	-28	-23	-18	1542		$R_4+R_5+R_7$
	10	8	15	1460		$\beta_1+\beta_3+R_5+R_1$
	-7	13	-4	1400		$R_2+\beta_5+R_1+R_4$

Table 4.6: (Continued): Predicted frequencies of anthracene

Symmetry blocks	Benzene G.M[a]	Naphthalene G.M[a]	All[b]	Expt[c]	PED
	35	38	33	1318	$R_7+\beta_5+\beta_1$
	-2	1	0	1167	$\beta_3+R_1+\beta_5$
	38	31	-13	1124	$R_7+\beta_1+R_4$
	19	5	5	998	$R_5+\beta_1$
	16	18	13	809	R_1+R_2
	6	4	1	603	δ_2
A_{1u}	-11	-6	4	988	$\gamma_3+\gamma_1$
	17	18	3	858	$\gamma_1+\gamma_3$
	-6	5	4	743	$\tau_1+\tau_2$
	7	-9	0	$(491)^f$	$\tau_2+\gamma_1+\tau_1$
	9	3	0	126	$\tau_2+\tau_1$
B_{3u}	-18	-26	-12	958	$\gamma_1+\gamma_3+\tau_3$
	-17	-20	-16	879	$\gamma_5+\tau_3+\gamma_3$
	12	14	5	726	$\gamma_1+\gamma_3+\gamma_5$
	7	8	4	469	$\tau''+\tau'+\tau_3$
	14	4	-1	380	τ_3
	19	19	19	106	$\tau'+\tau''+\tau_3$
B_{1g}	-14	-22	-8	956	$\gamma_1+\gamma_3+\tau_3$
	16	20	9	760	$\gamma_1+\gamma_3$
	11	12	8	479	$\tau'+\tau''+\tau_3$
	22	20	21	244	$\tau_3+\tau''+\tau'$
B_{2g}	-23	-19	-9	977	$\gamma_3+\gamma_1$
	1	7	0	916	$\gamma_5+\gamma_3$
	29	36	21	$852^e,896$	$\gamma_1+\gamma_3+\gamma_5$
	-9	24	16	773	τ_1
	6	21	29	580	$\tau_1+\gamma_1+\tau_2$
	29	22	24	287	$\tau_2+\tau_1$
Ave.error	[15.0]	[13.5]	[9.2]	including CH	
Ave.error	[13.6]	[13.2]	[8.2]	excluding CH	

a. Geometric mean of the respective diagonal scale factors are taken for the off-diagonal scale factors.
b. All(diagonal and off-diagonal) scale factors are taken.
c. Ref. 19.
d. Ref. 23.
e. Ref. 26.
f. Number in the parenthesis is our predicted frequency.

Table 4.7: Orthogonal transformation matrix of naphthalene

```
In-plane
 1    1   0.5000   3   0.5000   7   0.5000  11   0.5000
 2    2   1.0000
 3    4   0.5000   6   0.5000   8   0.5000  10   0.5000
 4    5   0.7071   9   0.7071
 5   12   0.5000  13   0.5000  16   0.5000  19   0.5000
 6   14   0.5000  15   0.5000  17   0.5000  18   0.5000
 7   20   0.5000  21  -0.5000  24  -0.5000  27   0.5000
 8   22   0.5000  23  -0.5000  25   0.5000  26  -0.5000
 9   29   0.7071  32   0.7071
10    1   0.5000   3  -0.5000   7  -0.5000  11   0.5000
11    4   0.5000   6  -0.5000   8   0.5000  10  -0.5000
12   12   0.5000  13  -0.5000  16  -0.5000  19   0.5000
13   14   0.5000  15  -0.5000  17   0.5000  18  -0.5000
14   20   0.5000  21   0.5000  24   0.5000  27   0.5000
15   22   0.5000  23   0.5000  25   0.5000  26   0.5000
16   28   0.7071  31  -0.7071
17   30   0.7071  33   0.7071
18    1   0.5000   3   0.5000   7  -0.5000  11  -0.5000
19    4   0.5000   6   0.5000   8  -0.5000  10  -0.5000
20    5   0.7071   9  -0.7071
21   12   0.5000  13   0.5000  16  -0.5000  19  -0.5000
22   14   0.5000  15   0.5000  17  -0.5000  18  -0.5000
23   20   0.5000  21  -0.5000  24   0.5000  27  -0.5000
24   22   0.5000  23  -0.5000  25  -0.5000  26   0.5000
25   29   0.7071  32  -0.7071
26    1   0.5000   3  -0.5000   7   0.5000  11  -0.5000
27    4   0.5000   6  -0.5000   8  -0.5000  10   0.5000
28   12   0.5000  13  -0.5000  16   0.5000  19  -0.5000
29   14   0.5000  15  -0.5000  17  -0.5000  18   0.5000
30   20   0.5000  21   0.5000  24  -0.5000  27  -0.5000
31   22   0.5000  23   0.5000  25  -0.5000  26  -0.5000
32   28   0.7071  31   0.7071
33   30   0.7071  33  -0.7071

Out-of-plane
 1    1   0.5000   2  -0.5000   5   0.5000   8  -0.5000
 2    3   0.5000   4  -0.5000   6  -0.5000   7   0.5000
 3    9   0.7071  12  -0.7071
 4   10   0.7071  13  -0.7071
 5    1   0.5000   2   0.5000   5  -0.5000   8  -0.5000
```

Table 4.7: (Continued): Orthogonal matrix of naphthalene

```
 6     3   0.5000   4   0.5000   6  -0.5000   7  -0.5000
 7    11   0.7071  14  -0.7071
 8     1   0.5000   2  -0.5000   5  -0.5000   8   0.5000
 9     3   0.5000   4  -0.5000   6   0.5000   7  -0.5000
10     9   0.7071  12   0.7071
11    10   0.7071  13   0.7071
12     1   0.5000   2   0.5000   5   0.5000   8   0.5000
13     3   0.5000   4   0.5000   6   0.5000   7   0.5000
14    11   0.7071  14   0.7071
15    15   1.0000
```

Table 4.8: Orthogonal transformation matrix of anthracene

In-plane
```
 1     1   0.5000   3   0.5000  12   0.5000  16   0.5000
 2     2   0.7071   9   0.7071
 3     4   0.5000   6   0.5000  13   0.5000  15   0.5000
 4     5   0.7071  14   0.7071
 5     7   0.5000   8   0.5000  10   0.5000  11   0.5000
 6    17   0.5000  18   0.5000  23   0.5000  26   0.5000
 7    19   0.5000  20   0.5000  24   0.5000  25   0.5000
 8    21   0.7071  22   0.7071
 9    27   0.5000  28  -0.5000  33  -0.5000  36   0.5000
10    29   0.5000  30  -0.5000  34   0.5000  35  -0.5000
11    38   0.7071  44   0.7071
12    41   1.0000
13     1   0.5000   3  -0.5000  12  -0.5000  16   0.5000
14     4   0.5000   6  -0.5000  13   0.5000  15  -0.5000
15     7   0.5000   8  -0.5000  10   0.5000  11  -0.5000
16    17   0.5000  18  -0.5000  23  -0.5000  26   0.5000
17    19   0.5000  20  -0.5000  24   0.5000  25  -0.5000
18    27   0.5000  28   0.5000  33   0.5000  36   0.5000
19    29   0.5000  30   0.5000  34   0.5000  35   0.5000
20    31   0.7071  32   0.7071
21    37   0.7071  43  -0.7071
22    39   0.7071  45   0.7071
23    42   1.0000
24     1   0.5000   3   0.5000  12  -0.5000  16  -0.5000
25     2   0.7071   9  -0.7071
26     4   0.5000   6   0.5000  13  -0.5000  15  -0.5000
```

Table 4.8: (Continued): Orthogonal matrix of anthracene

```
27     5   0.7071 14 -0.7071
28     7   0.5000  8 -0.5000 10 -0.5000 11  0.5000
29    17   0.5000 18  0.5000 23 -0.5000 26 -0.5000
30    19   0.5000 20  0.5000 24 -0.5000 25 -0.5000
31    27   0.5000 28 -0.5000 33  0.5000 36 -0.5000
32    29   0.5000 30 -0.5000 34 -0.5000 35  0.5000
33    31   0.7071 32 -0.7071
34    38   0.7071 44 -0.7071
35     1   0.5000  3 -0.5000 12  0.5000 16 -0.5000
36     4   0.5000  6 -0.5000 13 -0.5000 15  0.5000
37     7   0.5000  8  0.5000 10 -0.5000 11 -0.5000
38    17   0.5000 18 -0.5000 23  0.5000 26 -0.5000
39    19   0.5000 20 -0.5000 24 -0.5000 25  0.5000
40    21   0.7071 22 -0.7071
41    27   0.5000 28  0.5000 33 -0.5000 36 -0.5000
42    29   0.5000 30  0.5000 34 -0.5000 35 -0.5000
43    37   0.7071 43  0.7071
44    39   0.7071 45 -0.7071
45    40   1.0000
```

```
Out-of-plane
 1     1   0.5000  2 -0.5000  7  0.5000 10 -0.5000
 2     3   0.5000  4 -0.5000  8 -0.5000  9  0.5000
 3     5   0.7071  6 -0.7071
 4    11   0.7071 17 -0.7071
 5    12   0.7071 18 -0.7071
 6    14   1.0000
 7     1   0.5000  2  0.5000  7 -0.5000 10 -0.5000
 8     3   0.5000  4  0.5000  8 -0.5000  9 -0.5000
 9    13   0.7071 19 -0.7071
10    20   0.7071 21 -0.7071
11     1   0.5000  2 -0.5000  7 -0.5000 10  0.5000
12     3   0.5000  4 -0.5000  8  0.5000  9 -0.5000
13    11   0.7071 17  0.7071
14    12   0.7071 18  0.7071
15    15   1.0000
16     1   0.5000  2  0.5000  7  0.5000 10  0.5000
17     3   0.5000  4  0.5000  8  0.5000  9  0.5000
18     5   0.7071  6  0.7071
19    13   0.7071 19  0.7071
20    16   1.0000
21    20   0.7071 21  0.7071
```

Table 4.9: Naphthalene in plane symbolic F matrix in non-redundant
local coordinates

```
1
2   3
4   2   1
5   6   7   8
9  10   9  11  12
7   6   5  13  11   8
14   2  15  16  17  18   1
18   6  16  19  20  21   7   8
17  10  17  20  22  20   9  11  12
16   6  18  21  20  19   5  13  11   8
15   2  14  18  17  16   4   5   9   7   1
23  24  25  26  27  28  29  30  31  32  33  34
25  24  23  28  27  26  33  32  31  30  29  35  34
36  37  38  39  40  41  42  43  44  45  46  47  48  49
38  37  36  41  40  39  46  45  44  43  42  48  47  50  49
29  24  33  32  31  30  23  28  27  26  25  51  52  53  54  34
46  37  42  43  44  45  38  39  40  41  36  54  53  55  56  48  49
42  37  46  45  44  43  36  41  40  39  38  53  54  56  55  47  50  49
33  24  29  30  31  32  25  26  27  28  23  52  51  54  53  35  47  48  34
57  58  59  60  61  62  63  64  65  66  67  68  69  70  71  72  73  74  75  76
-59 -58 -57 -62 -61 -60 -67 -66 -65 -64 -63 -69 -68 -71 -70 -75 -74 -73 -72  77
76
78  79  80  81  82  83  84  85  86  87  88  89  90  91  92  93  94  95  96  97
98  99
-80 -79 -78 -83 -82 -81 -88 -87 -86 -85 -84 -90 -89 -92 -91 -96 -95 -94 -93  98
97 100  99
-63 -58 -67 -66 -65 -64 -57 -62 -61 -60 -59 -72 -75 -74 -73 -68 -71 -70 -69 101
102 103 104  76
88  79  84  85  86  87  80  81  82  83  78  96  93  94  95  90  91  92  89 104
103 105 106  98  99
-84 -79 -88 -87 -86 -85 -78 -83 -82 -81 -80 -93 -96 -95 -94 -89 -92 -91 -90 103
104 106 105  97 100  99
67  58  63  64  65  66  59  60  61  62  57  75  72  73  74  69  70  71  68 102
101 104 103  77  97  98  76
107   0-107 108   0-108 109 110   0-110-109 111-111 112-112 113 114-114-113 115
115 116 116 117 118 118 117 119
120 121 120 122 123 122 124 125 126 125 124 127 127 128 128 129 130 130 129 131
-131 132-132 133 134-134-133   0 135
```

Table 4.9: (Continued): Naphthalene in plane symbolic F matrix in loc l
coordinates

```
136    0-136 137    0-137 138 139    0-139-138 140-140 141-141 142 143-143-: l2 144
144 145 145 146 147 147 146 148    0 149
109    0-109-110    0 110 107-108    0 108-107 113-113-114 114 11:-112 112-1 1-117
-117-118-118-115-116-116-115 150    0 151 119
124 121 124 125 126 125 120 122 123 122 120 129 129 130 130 127 128 128 1 7-133
133 134-134-131 132-132 131    0 152    0    0 135
-138    0 138 139    0-139-136 137    0-137 136-142 142 143-143-140 141-141 1 0 146
146 147 147 144 145 145 144-151    0 153-148    0 149
```

Fitted in plane force constants of naphthalene

6.076	0.586	5.607	-0.332	0.301	-0.226	0.608	7.513	-0.438	0 .75
0.647	6.112	-0.362	0.705	0.135	-0.251	0.073	-0.169	0.139	-0. 08
0.150	0.242	0.060	-0.015	-0.020	-0.016	0.002	0.076	0.003	0. 04
0.005	0.013	-0.001	5.113	0.002	-0.027	-0.024	-0.006	0.075	0. 96
-0.003	0.000	0.000	-0.003	0.001	0.005	0.004	0.011	5.153	0. 11
0.013	0.002	0.000	0.001	0.000	0.001	-0.183	0.001	0.017	-0. 19
0.005	0.164	0.018	0.001	-0.006	0.000	-0.004	0.003	0.000	0. 06
-0.006	-0.010	0.000	0.000	-0.002	0.503	-0.001	0.021	-0.011	0. 08
0.178	-0.159	-0.008	-0.001	-0.001	-0.004	0.003	0.005	-0.006	-0. 08
0.005	0.004	0.001	0.000	0.001	0.000	-0.009	0.008	0.506	0. 07
-0.003	0.003	0.001	0.000	0.000	-0.001	0.124	-0.035	0.286	0. 2
-0.094	-0.088	-0.006	0.005	-0.001	-0.002	0.008	0.011	1.426	0. 7
-0.112	0.071	-0.426	0.147	-0.032	-0.154	-0.094	0.044	-0.014	0. 7
0.003	0.061	-0.009	0.005	1.332	0.080	0.308	-0.221	-0.055	0. 5
-0.072	0.008	-0.005	-0.071	0.052	-0.008	-0.010	-0.188	1.358	0. 7
-0.291	0.247	-0.303							

* The non-redundant local coordinates are as given in Table-4.1.

Table 4.10: Naphthalene out of plane symbolic F matrix in non-redundant
local coordinates

```
  1
  2   1
  3   4   5
  4   3   6   5
  7   8   9  10   1
 10   9  11  12   4   5
  9  10  12  11   3   6   5
  8   7  10   9   2   3   4   1
 13 -13  14 -14  15  16 -16 -15  17
 18 -18  19 -19  20  21 -21 -20  22  23
 24  24  25  25  26  27  27  26   0   0  28
-15  15  16 -16 -13  14 -14  13  29  30   0  17
-20  20  21 -21 -18  19 -19  18  30  31   0  22  23
 26  26  27  27  24  25  25  24   0   0  32   0   0  28
 33  33  34  34  33  34  34  33   0   0  35   0   0  35  36
```

Fitted out of plane force constants of naphthalene.

```
 0.315  -0.025  -0.023   0.030   0.320   0.010   0.006  -0.011  -0.004   0.007
-0.001   0.005  -0.022  -0.032  -0.014  -0.012   0.328   0.029  -0.039   0.020
 0.013   0.010   0.310  -0.039  -0.014   0.008   0.001   0.312  -0.043   0.048
-0.056  -0.018   0.012   0.034  -0.062   0.347
```

* The non-redundant local coordinates are as given in Table-4.1.

Table 4.11: Anthracene in plane symbolic F matrix in non-redundant local coordinates

```
 1
 2   3
 4   2   1
 5   6   7   8
 9  10   9  11  12
 7   6   5  13  11   8
14  15  16  17  18  19  20
21  22  23  24  25  26  27  20
28  29  28  30  31  30  22  15   3
23  22  21  26  25  24  32  33  15  20
16  15  14  19  18  17  33  32  22  27  20
34  28  35  36  37  38  21  14   2  16  23   1
38  30  36  39  40  41  26  19   6  17  24   7   8
37  31  37  40  42  40  25  18  10  18  25   9  11  12
36  30  38  41  40  39  24  17   6  19  26   5  13  11   8
35  28  34  38  37  36  23  16   2  14  21   4   5   9   7   1
43  44  45  46  47  48  49  50  51  52  53  54  55  56  57  58  59
45  44  43  48  47  46  53  52  51  50  49  58  57  56  55  54  60  59
61  62  63  64  65  66  67  68  69  70  71  72  73  74  75  76  77  78  79
63  62  61  66  65  64  71  70  69  68  67  76  75  74  73  72  78  77  80  79
81  82  83  84  85  86  87  87  82  88  88  81  86  85  84  83  89  90  91  92
93
83  82  81  86  85  84  88  88  82  87  87  83  84  85  86  81  90  89  92  91
94  93
54  51  58  57  56  55  50  49  44  53  52  43  48  47  46  45  95  96  97  98
89  90  59
76  69  72  73  74  75  70  71  62  67  68  63  64  65  66  61  98  97  99 100
92  91  78  79
72  69  76  75  74  73  68  67  62  71  70  61  66  65  64  63  97  98 100  99
91  92  77  80  79
58  51  54  55  56  57  52  53  44  49  50  45  46  47  48  43  96  95  98  97
90  89  60  77  78  59
101 102 103 104 105 106 107 108 109 110 111 112 113 114 115 116 117 118 119 120
121 122 123 124 125 126 127
-103-102-101-106-105-104-111-110-109-108-107-116-115-114-113-112-118-117-119-119
-122-121-126-125-124-123 128 127
129 130 131 132 133 134 135 136 137 138 139 140 141 142 143 144 145 146 147 148
149 150 151 152 153 154 155 156 157
-131-130-129-134-133-132-139-138-137-136-135-144-143-142-141-140-146-145-147 -147
-150-149-154-153-152-151 156 155 158 157
```

Table 4.11: (Continued): Anthracene in plane symbolic F matrix in local
coordinates

```
 159  160  161  162  163  164  165-165-160  166-166-159-164-163-162-161  167  168  169  170
   0    0-167-170-169-168  171  172  173  174  175
-161-160-159-164-163-162  166-166  160  165-165  161  162  163  164  159-168-167-170-169
   0    0  168  169  170  167  172  171  174  173  176  175
-112-109-116-115-114-113-108-107-102-111-110-101-106-105-104-103-123-126-125-124
-121-122-117-120-119-118  177  178  179  180  171  172  127
 144  137  140  141  142  143  138  139  130  135  136  131  132  133  134  129  154  151  152  153
 150  149  146  147  148  145  180  179  181  182  174  173  156  157
-140-137-144-143-142-141-136-135-130-139-138-129-134-133-132-131-151-154-153-152
-149-150-145-148-147-146  179  180  182  181  173  174  155  158  157
 116  109  112  113  114  115  110  111  102  107  108  103  104  105  106  101  126  123  124  125
 122  121  118  119  120  117  178  177  180  179  172  171  128  155  156  127
 183    0-183  184    0-184  185  186    0-186-185  187  188    0-188-187  189-189  190-190
 191-191  192  193-193-192  194  194  195  195  196  196  197  198  198  197  199
 200  201  200  202  203  202  204  205  206  205  204  207  208  209  208  207  210  210  211  211
 212  212  213  214  214  213  215-215  216-216  217-217  218  219-219-218    0  220
 221    0-221  222    0-222  223  224    0-224-223  225  226    0-226-225  227-227  228-228
 229-229  230  231-231-230  232  232  233  233  234  234  235  236  236  235  237    0  238
 239    0-239  240    0-240  241  241    0-241-241  239-240    0  240-239  242-242  243-243
 244-244  242-243  243-242  245  245  246  246    0    0-245-246-246-245  247    0  248  249
 250  251  250  252  253  252  254  254  251  254  254  250  252  253  252  250  255  255  256  256
 257  257  255  256  256  255  258-258  259-259    0    0-258  259-259  258    0  260    0    0
 261
 262    0-262  263    0-263  264-264    0  264-264-262  263    0-263  262  265-265  266-266
   0    0-265  266-266  265  267  267  268  268  269  269  267  268  268  267  270    0  271    0
   0  272
 187    0-187-188    0  188  186  185    0-185-186  183-184    0  184-183  192-192-193  193
 191-191  189-190  190-189-197-197-198-198-196-196-194-195-195-194  273    0  274  247
   0-270  199
 207  206  207  208  209  208  205  204  201  204  205  200  202  203  202  200  213  213  214  214
 212  212  210  211  211  210-218  218  219-219-217  217-215  216-216  215    0  275    0    0
 260    0    0  220
-225    0  225  226    0-226-224-223    0  223  224-221  222    0-222  221-230  230  231-231
-229  229-227  228-228  227  235  235  236  236  234  234  232  233  233  232-274    0  276-248
   0  271-237    0  238
```

Table 4.11: (Continued): Anthracene in plane symbolic F matrix in lo al
coordinates

Scaled in plane force constants of anthracene

```
 5.695   0.442   5.242  -0.241   0.217  -0.126   0.529   7.988  -0.363   0.067
 0.579   5.703  -0.291   0.769   0.728   0.141  -0.263   0.098  -0.194   7.019
-0.253  -0.432  -0.193   0.144  -0.125   0.157   0.785   0.025   0.105   0.062
 0.167   0.279  -0.394   0.103   0.042  -0.051   0.053  -0.047   0.046   0.048
 0.039   0.069   0.057  -0.015  -0.019  -0.016   0.001   0.077   0.004   0.007
 0.005   0.008  -0.002   0.000   0.002  -0.002   0.001  -0.001   5.115   0.002
-0.026  -0.024  -0.007   0.076   0.093  -0.002   0.000   0.000  -0.003   0.001
 0.005   0.000   0.001  -0.001   0.001   0.000   0.004   0.011   5.155   0.011
 0.000  -0.011  -0.001   0.009   0.007   0.004   0.092  -0.017   0.011   0.002
 0.000   0.001   5.085   0.003   0.000   0.000   0.000   0.000   0.000   0.000
-0.183   0.005   0.016  -0.017   0.003   0.167   0.018   0.000  -0.006   0.000
-0.003  -0.001   0.000   0.000   0.000   0.000   0.005   0.000   0.006   0.000
-0.010  -0.003   0.000   0.000   0.000   0.000   0.502  -0.001   0.006  -.006
 0.007   0.181  -0.159  -0.008  -0.002   0.000  -0.003   0.004   0.019  -.010
 0.001  -0.001   0.001   0.000  -0.006  -0.009   0.008   0.004   0.005  -.001
 0.000   0.000   0.000   0.000  -0.009   0.008   0.506   0.007   0.001   .001
 0.004  -0.001   0.004  -0.001   0.209   0.016   0.010   0.003  -0.014  -.001
-0.004   0.004   0.001   0.000   0.511  -0.001   0.000   0.000   0.000   .000
 0.000   0.000   0.132  -0.035   0.294   0.096   0.008   0.004   0.000   .000
-0.006   0.000   0.001   0.000  -0.002   0.009  -0.001   0.001  -0.093  -( 087
-0.090   0.066  -0.422   0.148  -0.031  -0.176   0.004   0.003   1.429  ( 287
 0.045  -0.011   0.002   0.002   0.003   0.061  -0.006   0.001  -0.009  -( 093
 0.058   0.285  -0.223  -0.057  -0.005   0.002   0.004   0.001   0.001   1 316
 0.000  -0.070   0.051  -0.008  -0.001  -0.001   0.004  -0.072   0.008  -0 001
 0.147  -0.005  -0.005  -0.101  -0.008  -0.001  -0.192   1.327   0.290  -0 069
-0.235  -0.036  -0.154   0.231  -0.013   0.007   0.324  -0.282   1.583   0 154
 1.468   0.222  -0.056  -0.109  -0.009  -0.004  -0.148   0.010   0.006   0 250
-0.308   1.527   0.016  -0.012   0.011   0.005  -0.008  -0.010  -0.077   0 294
```

* Non-redundant local coordinates are as given in Table-4.2.

Table 4:12: Anthracene out of plane symbolic F matrix in non-redundant
local coordinates

```
 1
 2   1
 3   4   5
 4   3   6   5
 7   8   9  10  11
 8   7  10   9  12  11
13  14  15  16   7   8   1
16  15  17  18  10   9   4   5
15  16  18  17   9  10   3   6   5
14  13  16  15   8   7   2   3   4   1
19 -19  20 -20  21 -21  22  23 -23 -22  24
25 -25  26 -26  27 -27  28  29 -29 -28  30  31
32  32  33  33  34  34  35  36  36  35   0   0  37
38 -38  39 -39  40 -40  38 -39  39 -38  41  42   0  43
44 -44  45 -45   0   0 -44  45 -45  44  46  47   0   0  48
49  49  50  50  51  51  49  50  50  49   0   0  52   0   0  53
-22  22  23 -23 -21  21 -19  20 -20  19  54  55   0 -41  46   0  24
-28  28  29 -29 -27  27 -25  26 -26  25  55  56   0 -42  47   0  30  31
35  35  36  36  34  34  32  33  33  32   0   0  57   0   0  52   0   0  37
58  58  59  59  60  60  61  62  62  61   0   0  63   0   0  64   0   0  65  66
61  61  62  62  60  60  58  59  59  58   0   0  65   0   0  64   0   0  63  67
66
```

Scaled out of plane force constants of anthracene

```
 0.307  -0.024  -0.020   0.036   0.315   0.008   0.007  -0.011  -0.004   0.006
 0.310  -0.030   0.000   0.001   0.001  -0.001   0.000   0.000  -0.016  -0.030
-0.018   0.001   0.001   0.315   0.040  -0.039   0.025  -0.002  -0.001   0.014
 0.283  -0.033  -0.031   0.009  -0.001   0.000   0.301   0.009  -0.010   0.020
-0.031   0.037   0.305  -0.029   0.014   0.059  -0.068   0.341   0.014   0.005
-0.030  -0.017   0.294   0.003  -0.004   0.004   0.003  -0.015  -0.035  -0.005
 0.004   0.003   0.080   0.017  -0.002   0.342  -0.048
```

* The non-redundant local coordinates are as given in Table-4.2.

Table 4.13: Mean amplitudes of vibration(Å) of naphthalene

parameter*	calc.	[ref.32]	[ref.33]	parameter*	calc.	[ref.32]	[ref.33]
14-18	0.160	0.159	0.159	10-12	0.132	0.133	0.133
14-17	0.131	0.134	0.134	2-15	0.094	0.095	0.095
12-18	0.168	0.159	0.159	6-11	0.106	0.108	0.108
14-12	0.188	0.188	0.188	10-11	0.124	0.123	0.123
14-16	0.168	0.171	0.171	6-15	0.097	0.099	0.099
14-13	0.119	0.119	0.119	10-16	0.102	0.107	0.107
14-11	0.130	0.133	0.133	10-15	0.099	0.101	0.101
14-15	0.145	0.145	0.145	6-10	0.044	0.047	0.047
18-16	0.135	0.141	0.141	1-2	0.047	0.047	0.047
18-15	0.123	0.125	0.125	2-6	0.047	0.048	0.047
6-14	0.077	0.077	0.076	10-9	0.047	0.048	0.047
10-14	0.101	0.100	0.097	2-10	0.054	0.056	0.058
6-18	0.098	0.100	0.097	6-9	0.056	0.056	0.058
2-14	0.099	0.101	0.098	2-5	0.056	0.057	0.060
10-17	0.099	0.101	0.098	3-5	0.060	0.065	0.068
6-12	0.132	0.132	0.132	2-9	0.062	0.061	0.070
6-17	0.094	0.097	0.098	6-5	0.063	0.060	0.070
2-18	0.095	0.097	0.097	6-8	0.062	0.068	0.072
10-13	0.096	0.098	0.098	6-3	0.060	0.064	0.068
2-13	0.096	0.098	0.098	6-7	0.066	0.067	0.077
2-17	0.094	0.095	0.098	8-10	0.063	0.068	0.078
6-13	0.095	0.095	0.095	7-10	0.066	0.068	0.078

*Atom numberings are according to Figure 4.1.

Bibliography

[1] Szczepanski, J.; Vala, M. *Nature*, **1993**, 363, 699.

[2] a) Szczepanski, J.; Roser, D.; Personette, W.; Eyring, M.; Pellow, R.; Vala, M. *J. Phys. Chem.*, **1992**, 96, 7876. b) Pauzat, F.; Talbi, D.; Miller, M. D.; Defrees, D. J.; Ellinger, Y. *J. Phys. Chem.*, **1992**, 96, 7882.

[3] Sellers, H.; Pulay, P.; Boggs, J. E. *J. Am. Chem. Soc.*, **1985**, 107, 6487.

[4] a) Hanson, D. M.; Gee, A. R. *J. Chem. Phys.*, **1969**, 51, 5052. b) Hanson, D. M. *ibid.*, **1969**, 51, 5063.

[5] Behlen, F. M.; Mcdonald, D. B.; Sethuraman, V.; Rice, S. A. *J. Chem. Phys.*, **1981**, 75, 5685.

[6] Krainov, E. P. *Opt. Spektrosk.*, **1964**, 16, 415 and 763.

[7] Freeman, S. D. E.; Ross, I. G.; *Spectrochim. Acta*, **1960**, 16, 1393.

[8] Mitra, S. S.; Bernstein, H. J. *Can. J. Chem.*, **1959**, 37, 553.

[9] Neto, N.; Scorocco, M.; Califano, S. *Spectrochim. Acta*, **1966**, 22, 1981.

[10] Bree, A.; Kydd, R. A.; *Spectrochim. Acta*, **1970**, 26A, 1791.

[11] Scully, D. B.; Whiffen, D. H. *Spectrochim. Acta*, **1960**, 16, 1409.

[12] Ohno, K. *J. Mol. Spectrosc.*, **1978**, 72, 238.

[13] a) Luther, H.; Feldmann, K.; Hampel, B. *Z. Electrochem.*, **1955**, 59, 1008. b) Luther, H.; Brandes, G.; Guenzler, H.; Hampel, B. *ibid.*, **1955**, 59, 1012.

[14] Stenman, F.; *J. Chem. Phys.*, **1971**, 54, 4217.

[15] Lippincot, E. R.; O'Reilly, E. J. *J. Chem. Phys.*, **1955**, 23, 238.

[16] Hollas, J. M. *J. Mol. Spectrosc.*, **1962**, 9, 138.

[17] Rich, N.; Dows, D. *Mol. Cryst. Liq. Cryst.*, **1968**, 5, 111.

[18] Pietila, L. O.; Stenmann, F. *Commentat. Phys-Math. Soc. Sci. Fenn.*, **1978**, 48, 145.

[19] Szczepanski, J.; Vala, M.; Talbi, D.; Parisel, O.; Ellinger, Y. *J. Chem. Phys.*, **1993**, 9 , 4494.

[20] Bakke, A.; Cyvin, V. N.; Whitmer, J. C.; Cyvin, S. J.; Gustavsen, J. E.; Klaeboe, P. *Naturforsch. Teil. A.*, **1979**, 43, 579.

[21] Bruhn, W.; Mecke, R.; *Z. Elektrochemie.*, **1961**, 65, 543.

[22] Califano, S.; *J. Chem. Phys.*, **1962**, 36, 903.

[23] a) Bree, A.; Kydd, R. A. *J. Chem. Phys.*, **1968**, 48, 5319. b) Bree, A.; Kydd, R. A. *ibid* **1969**, 51, 989.

[24] Colombo, L. *Spectrochim. Acta*, **1964**, 20, 547.

[25] Krainov, E. P. *Opt. Spektrosk.*, **1964**, 16, 984.

[26] Evans, D. J.; Scully, D. B. *Spectrochim. Acta*, **1964**, 20, 891.

[27] Chantry, G. W.; Anderson, A.; Browning, D. J.; Gebbie, H. A. *Spectrochim. Acta*, **196!** 21, 217.

[28] Mecke, R.; Bruhn, W.; Chafik, A. Z. *Naturforsch*, **1964**, 19a, 41.

[29] Streitweiser, A. jr., *Molecular Orbital Theory for Organic Chemists*, John Wiley, Nev York, 1961, p-170.

[30] Fogarasi, G.; Pulay, P. in *Vibrational Spectra and Structure*, Ed.J.R.Durig, **1985**, vol.14 p-193.

[31] Goodman, L.; Ozkabak, A. G.; Thakur, S. N. *J. Phys. Chem.*, **1991**, 95, 9044.

[32] Cyvin, S. J.; Cyvin, B. N.; Brunvoll, J. Z. *Naturforsch. Teil.A.*, **1979**, 34, 887.

[33] Kethkar, S. N.; Fink, M. *J. Mol. Struct.*, **1981**, 77, 139.

Chapter 5

Theoretical Prediction of Vibrational Spectrum of N-Glycylglycine Hydrochloride

In this chapter, theoretical prediction of the vibrational spectrum of the smallest dipeptide hydrochloride from its parent amino acid frequencies is presented by transferring the complete set of scale factors obtained by using the fitting procedure described in chapter 3.

The scaled quantum mechanical (SQM) approach proved to be very successful for a large number of symmetric organic molecules [1,2]. However the success is limited when the SQM procedure is applied to amino acids. Since there is no symmetry in the amino acids (point group C_1), each force constant is different from the other and many set of scale factors give equally good fit and hence becomes difficult to obtain a unique solution [3]. Also, equally difficult problem is that the ab initio PEDs are different from the experimentally obtained PEDs implying that the ab initio result of isloted molecule is a poor model for amino acids in condensed phase [4]. This is because the ab initio calculation of isolated zwitterion either goes to neutral gas phase spectrum [5] or even when it retains the geometry exhibits intramolecular H-bonding which is absent in the solution or solid state [4,6]. Attempts are being made to improve the model by explicitly including water molecules in the calculation (supermolecular calculation) or implicitly by introducing a dielectric medium (Onsager reaction field) [3,7-15]. SQM force field calculation on glycine cation supermolecule is available for cis and trans conformations

at HF/4-31G* level [3]. Such supermolecular calculations although aimed at building a generalized scale factors for peptides, are difficult to extend to higher systems because of the increase in the number of atoms included as water molecules. Also the PEDs of water molecules get mixed up with amino acid vibrations and difficult to separate. Alanine zwitterion is studied by the reaction field approach in water environment [14]. This improves the ab initio model of isolated molecule although the agreement is not very good with the experimental PEDs.

An alternative solution to this problem could be the transfer of scale factors from smaller amino acids to the larger dipeptides for which the ab initio model correctly describes the gross features of experimental vibrational spectra. Ab initio calculations of isolated amino acids in their cationic or anionic forms (in acidic or basic solution) grossly resemble the experimental features because the intramolecular H-bonding is less pronounced in these molecules compared to their zwitterions. It appears that if the basis set is chosen carefully the intramolecular H-bonding problem could be reduced further. Hence, the present study involves a complete conformational and vibrational analysis of glycine hydrochloride (GH) and glycylglycine hydrochloride (GGH) and transfer of scale factors between them to obtain a reliable theoretical force field for the smallest dipeptide hydrochloride.

Many ab initio conformational and vibrational analyses of neutral amino acids are found in the literature [4,16-17]. To the best of our knowledge a complete ab initio vibrational analysis of any peptide is limited to our study of GGH [18]. An experimental Raman study of glycylglycine zwitterion (GG) and its normal mode analysis was reported by Lagant et al. [19].

5.1   Calculations

The geometry optimizations and frequency calculations for both GH and GGH were done using 4-21G and 6-31G** basis sets. The ab initio force constants and frequencies of GH were calculated analytically and that of GGH numerically. The cartesian force constants of both GH and GGH were then transformed to the non-redundant local coordinates. The

non-redundant local coordinates of GH and GGH are shown in Table-5.1, Table-5.2 and Figure 5.1 and 5.2. The fitting procedure described in chapter 3 was used to get the scale factors for GH by fitting the frequencies of seven different isotopomers simultaneosly. The fitting is extremely successful in producing an average deviation of 9.7 cm^{-1} from the available experimental data. The ab initio force constants of GGH are scaled using the scale factors of GH. Durig's scaling procedure [20] was applied when there is no equivalent local symmetry coordinates between the two compounds. Durig's scaling involves using a scale factor of 0.9 for stretching, 0.8 for bending and their geometric mean for the off-diagonal ones. The experimental IR spectra of GGH was taken from our reported spectra [18]. Glycylglycine methyl ester hydrochloride (GGMH) was prepared by reacting SOCl$_2$ with N-glycylglycine in methanol. The solution was dried under high vacuum. The IR spectrum was recorded using a Perkin-Elmer spectrophotometer.

5.2   Results

Amino acid hydrochlorides in solution dissociates into amino acid cation and Cl$^-$ and hence, to a good approximation the spectral features could be accounted by the cation. Similar treatments were given successful results for other systems, for example, acetlcholine [21]. In solid state, each Cl$^-$ is ionically bonded to the planar H-atom of the N$^+$H$_3$ group with a bond distance of 2.59 Å in GH. The room temperature spectra of NH$_4$Cl and NH$_4$Br are essentially identical, indicating that the anion has very small effect on the spectra [22]. The difference between the solid and solution phase spectra can be accounted in most cases to the phase change (mainly the strong intermolecular H-bonded network in the crystal structure vs. intermolecular H-bonding in a dielectric medium). Thus, as a reasonable approximation, the cations can be considered as a good theoretical model for the vibrational spectra of amino acid hydrochlorides and hence in the present study optimization and frequency calculations were performed with the respective cations of GH and GGH. Furthermore, the fully optimized structure of GH at HF/6-31G** level of calculation by including Cl$^-$ explicitly results in the dissociation of GH into neutral amino acid and HCl.

5.2.1 Conformations of GH

The conformational space of GH has been studied by several authors using ab initio theory. These studies clearly indicate that the lowest energy conformation is basis set dependent [23,24]. Since we are looking for a conformation in which the intramolecular H-bonding will be minimum so that it will mimic the solution or solid state spectra, we used 4-21G, a low level and 6-31G**, a high level basis sets. For the present work we took only the two lowest energy conformations of GH from the earlier study [24]. At 4-21G level C1 is the lowest energy form whereas at 6-31G**, C2 is the most stable one (Figure 5.3). Inclusion of correlation at the MP2 level does not improve 4-21G results while C2 changes to a structure closer to C1 at 6-31G** level indicating that the HF/4-21G calculation reproduces the structure close to the global minima, though C2 is closer to the crystal structure [25]. In all the cases the frequency calculations on the optimized structure were done to make sure that they are real minima. Since the minimum energy conformation at HF/6-31G** does not have the intramolecular H-bonding and also replicate the crystal structure, this basis set is used for the vibrational spectral study.

5.2.2 Conformations of GGH

Eight possible different conformations were selected by rotating the N-terminal and C-terminal groups of GGH. Each conformation is fully optimized at 6-31G** basis set. The optimized structures are given in Figure 5.4 and the final results of different calculations are listed in Table-5.3. C1 is the minimum energy structure. Further MP2/6-31G** single point calculations were performed to see the effect of correlation on the relative energies of these eight conformations. Frequency calculation was done only on the minimum energy conformation.

5.2.3 Vibrational Frequencies of GH

The solution phase IR and Raman spectra of several isotopomers of GH were reported by Williams et al. [3]. However, the supermolecular calculation with water molecules introduces strong coupling between the vibrational modes of GH and water. As a result regions below 600 cm^{-1} are not very well described in their work. Also since the least

squares method does not lead to unique assignment, they constrained the scale factor in their SQM approach to yield PEDs that were in agreement with their empirical assignment. In the present work the fitting of the experimental frequencies of seven isotopomers produced a better fit than that of Wiliiams et al. except for the peak at 568 cm^{-1} in GH-d_0. For this mode the absolute deviation from the fitted one is 30 cm^{-1}. It is possible that this frequency might have been misassigned. For all fundamentals the assignments are very close to that of unscaled ab initio normal modes. The PEDs of scaled force field are in good agreement with that of Williams et al. [3] and hence the assignment for GH will not be discussed further. The force field cannot be compared, as our results are based on isolated molecule. The fitted frequencies and their PEDs for GH-d_0 are given in Table 5.4 and the corresponding fitted frequencies for the isotopomers are given in Table-5.5.

5.2.4 Vibrational Frequencies of GGH

The frequencies obtained from the scaled force field and the corresponding PEDs of GGH are shown in Table-5.6. The predicted frequencies are in excellent agreement with the available experimental data with an average deviation of 7.6 cm^{-1}. For a comparative study, the experimental frequencies of GG and GGMH are also given in the table.

The νC=O acid and νC=O amide bands are predicted at 1738 and 1676 cm^{-1} and are observed at 1746 and 1677 cm^{-1}. This is in agreement with the 1724 and 1678 cm^{-1} bands of the corresponding GGMH. The C=O in acetic acid [3] is observed at 1712 cm^{-1} and at 1682 cm^{-1} in GG [19].

Both the δ_aN$^+$H$_3$ modes are predicted at 1641 and 1602 cm^{-1} and are not observed in our IR spectra. However the 1629 and 1611 cm^{-1} Raman bands of GG [19] are in very good agreement with our predicted numbers. These modes appear as degenerate bands at 1607 cm^{-1} in GH in accordance with the prediction. The 1648 cm^{-1} band and the weak shoulder at 1622 cm^{-1} in the corresponding GGMH spectra compare well with these assignments. The asymmetric NH(amide) bend is predicted at 1593 cm^{-1} along with νCN, νC=O(amide) and νNC' is assigned to 1584 cm^{-1}. This amide II mode is observed at a lower frequency (1531 cm^{-1}) in the zwitterion. The 1535 cm^{-1} band observed in the GGMH spectrum is in agreement with this assignment. The symmetric N$^+$H$_3$ deformation is predicted at

1472 cm^{-1} agrees very well with the 1480 cm^{-1} in the zwitterionic spectra. This mode is assigned to the 1452 cm^{-1} peak in the corresponding GGMH. Both the ρN$^+$H$_3$ modes are predicted at 1155 and 1126 cm^{-1} and are observed at 1135 and 1117 cm^{-1} in the GGH spectra, 1158 and 1100 cm^{-1} in the zwitterion and 1130 and 1090 cm^{-1} in the GGMH. In many amino acids these ρN$^+$H$_3$ modes appear as two closely spaced bands around 1100 to 1150 cm^{-1} [26-28].

The observed band at 1487 cm^{-1} is predicted very well at 1486 cm^{-1} and is assigned to the mixed mode of ωC$'$H$_2$, νC$'$C, νC-O and ωCH$_2$. The various CH$_2$ bending modes (δCH$_2$, ωCH$_2$ and tCH$_2$) are predicted at 1443, 1433, 1408, 1329 and 1242 cm^{-1} and are assigned to the observed bands at 1434, 1434, 1410, 1308 and 1219 cm^{-1} respectively. The 1447 cm^{-1} Raman band assigned to δCH$_2$ by Lagant et al. in the zwitterion spectra agrees very well with our predicted 1443 cm^{-1} band. This mode is assigned to the observed band at 1437 cm^{-1} in the GGMH. The ωCH$_2$ mode at 1408 cm^{-1} is assigned to 1399 and 1402 cm^{-1} in the corresponding GG and GGMH. The CH$_2$ rocking modes are predicted at 1002 and 925 cm^{-1}. Higher one is assigned to the observed band at 1013 cm^{-1} and is consistent with the earlier assignment of Lagant et al. at 1007 cm^{-1} in the zwitterionic spectra for this mode. Although there is no band corresponding to the lower one in our hydrochloride spectra this agrees well with the 918 cm^{-1} band assignment of the zwitterionic spectra [19].

The predicted band at 1362 cm^{-1} is assigned to δCOH and ωC$'$H$_2$ is in agreement with the observed band at 1350 cm^{-1}. This band is observed at 1378 cm^{-1} in GH and is consistent with this assignment. There is no corresponding mode in the zwitterion spectra but appear at 1362 cm^{-1} in the spectrum of GGMH. The νN$^+$C and one of the νCC$'$+νCC modes are predicted at 1050 and 907 cm^{-1} are in excellent agreement with the observed bands of all the three compounds and also consistent with the 1044 and 873 cm^{-1} bands of GH.

Bands predicted at 700 and 661 cm^{-1} agree very well with the observed bands at 708 and 661 cm^{-1} in the hydrochloride spectra, 708 and 665 cm^{-1} in the zwitterion and 708 and 644 cm^{-1} in the GGMH. Bands below 600 cm^{-1} are not available for GGH and hence the predicted numbers below 600 cm^{-1} are compared with the zwitterionic spectra of Lagant

et al. [19].

The optimized cartesian coordinates obtained by using 6-31G** basis set for the minimum energy conformation of GH and GGH and their non-redundant scaled force constants are given in Table-5.7 to Table-5.10.

5.3 Conclusions

The fitting procedure to obtain the scale factors from the ab initio force field of GH has shown to be very successful giving an average deviation of $9.7 cm^{-1}$ between the predicted and the experimental frequencies for seven isotopomers. These scale factors when used to predict the frequencies of GGH the results were shown to be in good agreement with the experimental ones with an average deviation of $7.6 cm^{-1}$ for the smallest dipeptide hydrochloride. A complete set of non-redundant force constants were obtained for both GH and GGH. From the accuracy of the predicted frequencies it is clear that the methodology could, in principle, be used successfully for the prediction of vibrational frequencies and their force fields of larger polypeptides from their parent amino acids.
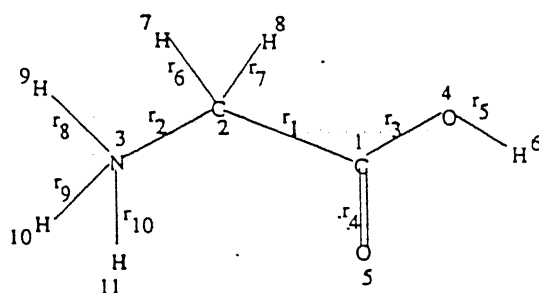
$a_1 = C_2\, C_1\, O_4$, $b_1 = C_2\, C_1\, O_5$, $b_2 = O_4\, C_1\, O_5$, $a_2 = C_1\, O_4\, H_6$

$a_3 = H_7\, C_2\, H_8$, $a_4 = N_3\, C_2\, H_7$, $a_5 = N_3\, C_2\, H_8$, $b_3 = N_3\, C_2\, C_1$

$b_4 = C_1\, C_2\, H_7$, $b_5 = C_1\, C_2\, H_8$, $a_6 = H_{10}\, N_3\, H_{11}$, $a_7 = H_9\, N_3\, H_{10}$

$a_8 = H_9\, N_3\, H_{11}$, $b_6 = C_2\, N_3\, H_9$, $b_7 = C_2\, N_3\, H_{10}$, $b_8 = C_2\, N_3\, H_{11}$

Figure 5.1: Internal coordinates of GH.
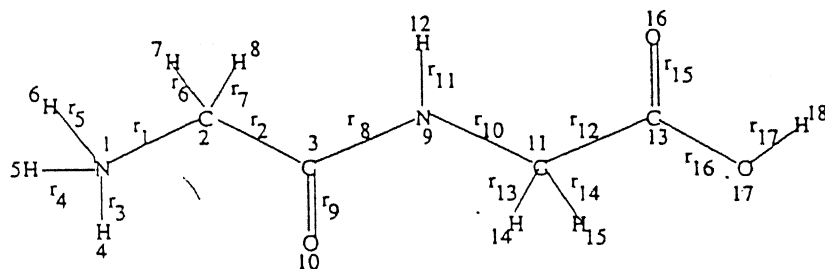
$a_1 = H_5\, N_1\, H_6$, $a_2 = H_4\, N_1\, H_5$, $a_3 = H_4\, N_1\, H_6$, $b_1 = C_2\, N_1\, H_4$, $b_2 = C_2\, N_1\, H_5$, $b_3 = C_2\, N_1\, H_6$

$a_4 = H_7\, C_2\, H_8$, $a_5 = N_1\, C_2\, H_7$, $a_5 = N_1\, C_2\, H_8$, $b_4 = N_1\, C_2\, C_3$, $b_5 = C_3\, C_2\, H_7$, $b_6 = C_3\, C_2\, H_8$

$a_7 = C_2\, C_3\, N_9$, $a_8 = C_3\, N_9\, H_{12}$, $a_9 = C_{11}\, N_9\, H_{12}$, $b_7 = C_2\, C_3\, O_{10}$, $b_8 = N_9\, C_3\, O_{10}$, $b_9 = C_3\, N_9\, C_{11}$

$a_{10} = N_9\, C_{11}\, C_{13}$, $a_{11} = N_9\, C_{11}\, H_{14}$, $a_{12} = N_9\, C_{11}\, H_{15}$, $b_{10} = H_{14}\, C_{11}\, H_{15}$, $b_{11} = C_{13}\, C_{11}\, H_{14}$, $b_{12} = C_{13}\, C_{11}\, H_{15}$

$a_{13} = C_{11}\, C_{13}\, O_{16}$, $a_{14} = O_{17}\, C_{13}\, O_{16}$, $b_{13} = C_{11}\, C_{13}\, O_7$, $b_{14} = C_{13}\, O_{17}\, H_{18}$

Figure 5.2: Internal coordinates of GGH.
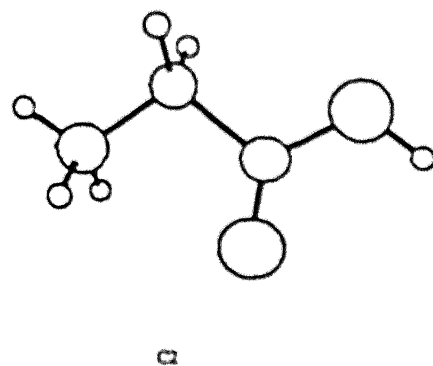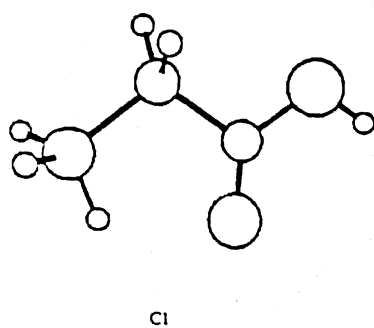
Figure 5.3: HF/6-31G** optimized structures of the two conformers of GH.
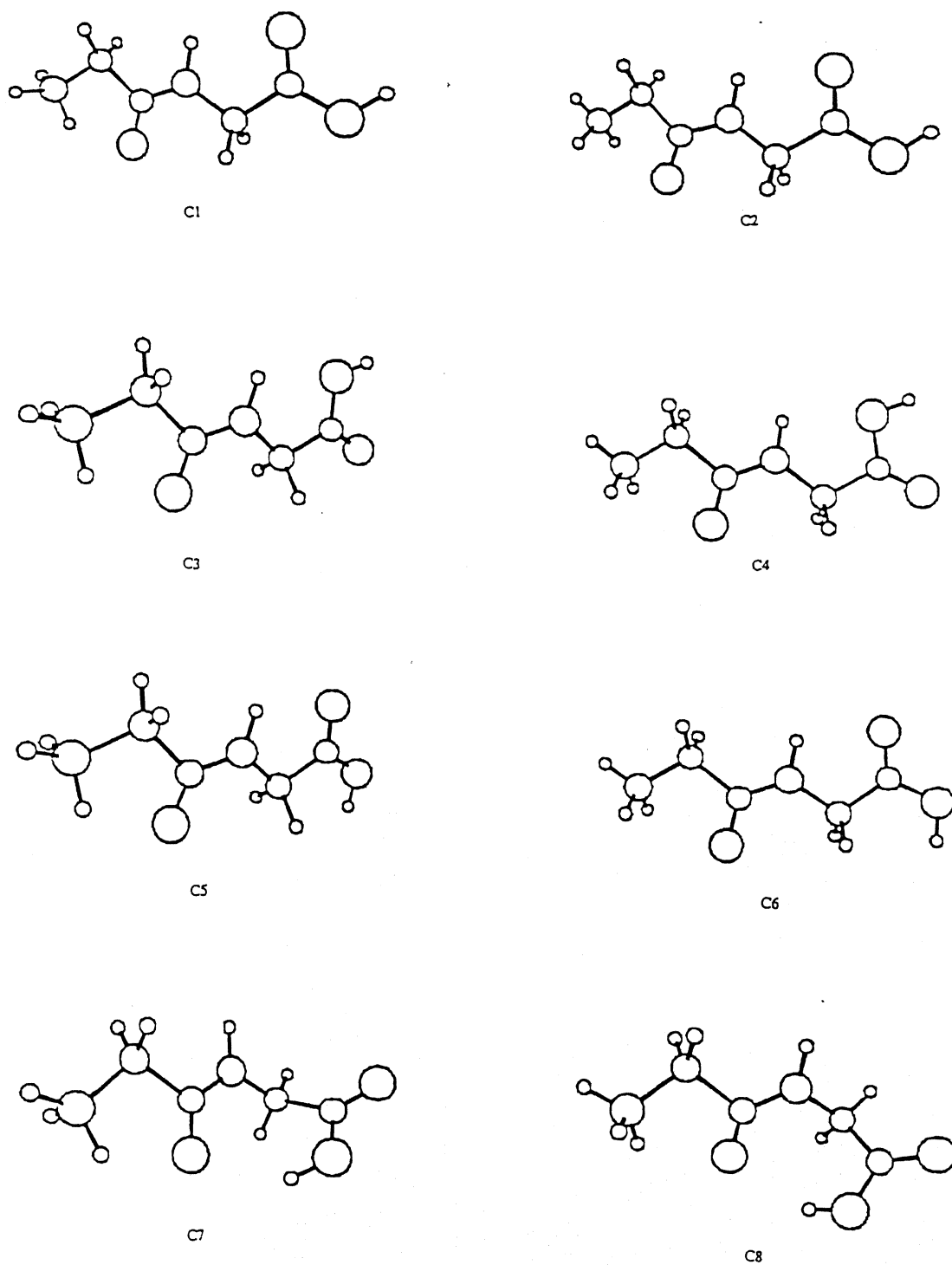
Figure 5.4: HF/6-31G** optimized structures of the eight conformers of GGH.

Table 5.1: Non-redundant local coordinates* of GH

S_{1-10}	$=r_{1-10}$(all stretch)	S_{19}	$=2a_6-a_7-a_8(\delta_a N^+H_3)$
S_{11}	$=2a_1-b_1-b_2(\delta_s CO)$	S_{20}	$=a_7-a_8(\delta_a N^+H_3)$
S_{12}	$=b_1-b_2(\delta_a CO)$	S_{21}	$=2b_6-b_7-b_8(\rho N^+H_3)$
S_{13}	$=4a_3-a_4-a_5-b_4-b_5(\delta CH_2)$	S_{22}	$=b_7-b_8(\rho N^+H_3)$
S_{14}	$=a_4+a_5-b_4-b_5(\omega CH_2)$	S_{23}	$=a_2(\delta COH)$
S_{15}	$=a_4-a_5+b_4-b_5(\rho CH_2)$	S_{24}	$=\gamma C_1O_5(\gamma CO)$
S_{16}	$=a_4-a_5-b_4+b_5(tCH_2)$	S_{25}	$=\tau_{12}(\tau CC)$
S_{17}	$=5b_3-a_3-a_4-a_5-b_4-b_5(\delta N^+CC)$	S_{26}	$=\tau_{14}(\tau CO)$
S_{18}	$=a_6+a_7+a_8-b_6-b_7-b_8(\delta_s N^+H_3)$	S_{27}	$=\tau_{23}(\tau CN^+)$

* All internal coordinates are according to Figure 5.1.

Table 5.2: Non-redundant local coordinates* of GGH

S_{1-17}	$=r_{1-17}$(all stretch)	S_{33}	$=a_{11}+a_{12}-b_{11}-b_{12}(\omega C'H_2)$
S_{18}	$=a_1+a_2+a_3-b_1-b_2-b_3(\delta_s N^+H_3)$	S_{34}	$=a_{11}-a_{12}+b_{11}-b_{12}(\rho C'H_2)$
S_{19}	$=2a_1-a_2-a_3(\delta_a N^+H_3)$	S_{35}	$=a_{11}-a_{12}-b_{11}+b_{12}(tC'H_2)$
S_{20}	$=a_2-a_3(\delta_a N^+H_3)$	S_{36}	$=5a_{10}-b_{10}-a_{11}-a_{12}-b_{11}-b_{12}(\delta NC'C)$
S_{21}	$=2b_1-b_2-b_3(\rho N^+H_3)$	S_{37}	$=2b_{13}-a_{13}-a_{14}(\delta_s CO_{acid})$
S_{22}	$=b_2-b_3(\rho N^+H_3)$	S_{38}	$=a_{13}-a_{14}(\delta_a CO_{acid})$
S_{23}	$=4a_4-a_5-a_6-b_5-b_6(\delta CH_2)$	S_{39}	$=b_{14}(\delta COH)$
S_{24}	$=a_5+a_6-b_5-b_6(\omega CH_2)$	S_{40}	$=\gamma C_3O_{10}(\gamma CO_{amide})$
S_{25}	$=a_5-a_6+b_5-b_6(\rho CH_2)$	S_{41}	$=\gamma N_9H_{12}(\gamma NH)$
S_{26}	$=a_5-a_6-b_5+b_6(tCH_2)$	S_{42}	$=\gamma C_{13}O_{16}(\gamma CO_{acid})$
S_{27}	$=5b_4-a_4-a_5-a_6-b_5-b_6(\delta N^+CC)$	S_{43}	$=\tau_{12}(\tau N^+C)$
S_{28}	$=2a_7-b_7-b_8(\delta_s CO_{amide})$	S_{44}	$=\tau_{23}(\tau CC)$
S_{29}	$=b_7-b_8(\delta_a CO_{amide})$	S_{45}	$=\tau_{39}(\tau CN)$
S_{30}	$=2b_9-a_8-a_9(\delta_s NH)$	S_{46}	$=\tau_{911}(\tau NC')$
S_{31}	$=a_8-a_9(\delta_a NH)$	S_{47}	$=\tau_{1113}(\tau C'C)$
S_{32}	$=4b_{10}-a_{11}-a_{12}-b_{11}-b_{12}(\delta C'H_2)$	S_{48}	$=\tau_{1317}(\tau CO)$

* All internal coordinates are according to Figure 5.2.

Table 5.3: Relative energies (in kJ/mol) of GH and GGH

Structure	HF/6-31G**	MP2/6-31G**
GH		
C1	15.30	0.03
	(0.00)	
C2	0.00	0.00
	(5.07)	
GGH		
C1	0.0	0.0
C2	2.2	7.1
C3	21.2	18.5
C4	23.3	25.4
C5	36.2	33.5
C6	38.2	40.2
C7	61.6	54.8
C8	60.7	53.9

The numbers in the parenthesis are the 4-21G energies.

Table 5.4: Fitted vibrational frequencies of GH (cm^{-1})

Sym. species	6-31G** scaled	Assignments	Expt.[a]	SQM
1	3412	νOH	(3200)	—
2	3179	νN^+H	3182	—
3	3124	νN^+H	3152	—
4	3060	νN^+H	3058	—
5	3019	νCH	3012	3022
6	2961	νCH	2973	2961
7	1746	νC=O	1740	1750
8	1616	$\delta_a N^+H_3$	1607	1618
9	1610	$\delta_a N^+H_3$	1607	1594
10	1512	$\delta_s N^+H_3+\omega CH_2$	1512	1518
11	1489	$\delta_s N^+H_3+\omega CH_2+\nu CC+\nu$C-O	(1484)	1476
12	1427	δCH_2	1435	1434
13	1378	δCOH$+\omega CH_2+\nu$C-O	1378	1384
14	1328	$tCH_2+\rho N^+H_3$	1320	1324
15	1252	νC-O$+\delta$COH	1263	1284
16	1148	$\rho N^+H_3+\omega CH_2+\nu CN^+$	1135	1153
17	1121	$tCH_2+\rho N^+H_3$	1125	1137
18	1042	νCN^+	1044	1058
19	923	$\rho CH_2+\rho N^+H_3+\gamma$CO	917	923
20	884	$\nu CC+\rho N^+H_3$	873	880
21	657	τCO$+\gamma$CO	657	669
22	598	δ_aCO$+\delta N^+CC$	568	563
23	521	γCO$+\tau$CO$+\rho CH_2$	504	453
24	498	δ_sCO	(483)	—
25	297	$\delta N^+CC+\delta_s CO+\delta_a CO$	301	250
26	174	$\tau CN^++\tau CC$	(175)	—
27	34	$\tau CC+\tau CN^+$	(35)	—

a.Experimental frequencies are taken from ref. 3.

Since the fitting algorithm requires all the experimental frequencies at least for one isotopic species, the numbers in parenthesis are introduced as a good guess for GH-d_0 and do not have any other significance.

Table 5.5: Fitted vibrational frequencies of all the seven isotopomers of GH (cm^{-1})

N⁺H₃CH₂COOH		N⁺H₃¹³CH₂COOH		N⁺H₃CH₂¹³COOH		N⁺H₃CD₂COOH		N⁺D₃CH₂COOD		N⁺D₃¹³CH₂COOD		N⁺D₃CH₂¹³COOD	
Expt.	Calc.	Expt.	Calc.	Expt.	Calc.	Expt.	Calc.	Expt.	Calc.	Expt.	Calc.	Expt.	Calc.
—	3412	—	3412	—	3412	—	3412	—	2184	—	2184	—	2484
3182	3179	—	3179	—	3179	3182	3179	2341	2347	—	2347	—	2347
3152	3124	—	3124	—	3124	3152	3124	2263	2306	—	2306	—	2306
3058	3060	—	3060	—	3060	3058	3060	2203	2199	—	2199	—	2199
3012	3019	—	3007	—	3019	2232	2249	3015	3019	—	3007	—	3019
2973	2961	—	2955	—	2961	2166	2161	2975	2961	—	2955	—	2961
1740	1746	1741	1745	1700	1703	1741	1744	1733	1732	1732	1731	1688	1687
1607	1616	1608	1616	1614	1614	1608	1614	—	1160	1166	1159	1168	1160
1607	1610	1608	1609	1614	1610	1608	1607	—	1153	—	1152	—	1153
1512	1512	1510	1507	1520	1507	1518	1503	—	1186	1166	1182	1168	1186
—	1489	—	1481	—	1475	1443	1455	—	1480	1435	1464	1438	1464
1435	1427	1431	1424	1437	1427	1044	1037	1429	1427	1411	1423	1406	1427
1378	1378	1360	1374	1370	1367	1317	1302	1340	1313	1336	1311	1321	1290
1320	1328	1316	1325	1320	1328	1201	1217	1278	1272	1277	1270	1271	1271
1263	1252	1263	1252	1246	1243	1210	1227	1073	1078	1060	1076	1066	1078
1135	1148	1133	1140	1139	1147	926	921	780	768	775	764	776	766
1125	1121	1113	1118	1119	1117	918	917	815	793	805	793	808	789
1044	1042	1027	1024	1044	1042	1112	1109	1008	1003	989	986	1007	1003
917	923	915	919	910	916	804	802	1043	1042	1032	1032	1025	1034
873	884	864	873	869	881	842	837	951	956	941	915	949	956
657	657	648	657	656	653	644	632	618	598	608	597	614	589
568	598	566	595	559	596	—	592	561	552	558	550	555	550
504	521	501	521	502	514	—	463	—	419	—	419	—	417
—	498	—	496	—	497	480	487	485	470	483	468	483	468
301	297	301	296	301	296	301	295	287	275	290	275	287	274
—	174	—	172	—	174	—	166	—	148	—	146	—	148
—	34	—	34	—	34	—	33	—	27	—	27	—	27

Table 5.6: Predicted Vibrational Frequencies of GGH (cm^{-1})

Sym. species	6-31G** scaled	Assignments	GGH expt.	GG expt.^{a}	GGMH expt.
1	3436	νOH	—	—	—
2	3265	νNH	—	3285	—
3	3161	νN$^+$H	—	—	—
4	3109	νN$^+$H	—	—	3080
5	3017	νCH	—	3013	—
6	2977	νC$'$H	—	2960	2960
7	2964	νN$^+$H+νCH	—	—	—
8	2957	νCH+νN$^+$H	—	—	—
9	2938	νC$'$H	—	2927	—
10	1738	νC=O$_{acid}$	1746	—	1724
11	1676	νC=O$_{amide}$+νCN	1677	1682	1678
12	1641	δ_aN$^-$H$_3$	—	1629	1648
13	1602	δ_aN$^-$H$_3$	—	1611	1622
14	1593	δ_aNH+νCN+νC=O$_{amide}$+νNC$'$	1584	1531	1535
15	1486	ωC$'$H$_2$+νC$'$C+νC-O+ωCH$_2$	1487	—	—
16	1472	δ_sN$^+$H$_3$+ωC$'$H$_2$	—	1480	1452
17	1443	δC$'$H$_2$	1434	1447	1437
18	1433	δCH$_2$+δ_sN$^+$H$_3$	1434	—	1420
19	1408	ωCH$_2$+δCH$_2$	1410	1399	1402
20	1362	δCOH+ωC$'$H$_2$	1350	—	1362
21	1329	tCH$_2$+ρN$^+$H$_3$	1308	1315	1307
22	1266	δ_sNH+νC-O	1265	1249	1249
23	1247	νC-O+ωC$'$H$_2$+δCOH	—	—	—
24	1242	tC$'$H$_2$	1219	1242	1219
25	1188	νCN	—	—	—
26	1155	ρN$^+$H$_3$+ωCH$_2$+tCH$_2$	1135	1158	1130
27	1126	tCH$_2$+ρN$^+$H$_3$	1117	1100	1090
28	1050	νN$^+$C	1040	1046	1032
29	1002	ρC$'$H$_2$+γCO$_{acid}$	1013	1007	—
30	985	νCC+νC$'$C	—	968	980
31	925	ρCH$_2$+γCO$_{amide}$+ρN$^+$H$_3$	—	918	946
32	907	νCC$'$+νCC	903	910	—
33	700	δ_aCO$_{amide}$+δNCC	708	708	708
34	661	τCO$_{acid}$+γCO$_{acid}$+ρC$'$H$_2$	661	665	644
35	618	τCN+γCO$_{amide}$+γNH+ρCH$_2$	—	—	—
36	594	δ_aCO$_{acid}$+δNC$'$C	—	598	—
37	568	δ_sCO$_{acid}$+δ_aCO$_{amide}$	—	588	—
38	537	γCO$_{amide}$+γNH	—	535	—
39	508	γCO$_{acid}$+τC-O	—	—	—

Table 5.6: (Continued): Predicted vibrational frequencies of GGH

40	405	$\delta N^+CC + \delta_s CO_{acid}$	—	396	—
41	331	$\delta_s CO_{amide} + \delta_s CO_{acid} + \delta_a CO_{amide}$	—	317	—
42	269	$\delta NC'C + \delta_a CO_{acid}$	—	298	—
43	196	$\tau C'C + \tau CC + \gamma NH + \tau N^+C$	—	—	—
44	179	$\tau N^+C + \tau C'C$	—	—	—
45	111	$\delta_s NH_{amide} + \delta_s CO_{amide} + tCH_2$	—	—	—
46	89	$\tau CC + \tau N^+C$	—	—	—
47	79	$\tau C'C + \tau CN$	—	—	—
48	40	$\tau NC' + \gamma NH + \tau CC$	—	—	—

a.Taken from ref. 12.

110

Table 5.7: Optimized cartesian coordinates of the minimum energy conformation of GH*
at 6-31G** basis set

1	6	0.000000	0.000000	0.000000
2	6	0.000000	0.000000	1.516600
3	7	1.430186	0.000000	1.949957
4	8	-1.209458	0.000000	-0.475575
5	8	1.017835	0.000000	-0.606826
6	1	-1.211000	0.000000	-1.427873
7	1	-0.486890	-0.881658	1.909255
8	1	-0.486890	0.881658	1.909255
9	1	1.521335	0.000000	2.955535
10	1	1.916723	-0.805370	1.579298
11	1	1.916723	0.805370	1.579298

* Atom numberings are according to Figure 5.1.

Table 5.8: Optimized cartesian coordinates of the minimum energy conformation of GGH*
at 6-31G** basis set

1	7	0.000000	0.000000	0.000000
2	6	0.000000	0.000000	1.494700
3	6	1.477563	0.000000	1.909195
4	1	0.925435	0.336112	-0.279188
5	1	-0.105207	-0.928158	-0.380962
6	1	-0.718988	0.583323	-0.398060
7	1	-0.485599	0.902803	1.838720
8	1	-0.544079	-0.859478	1.857572
9	7	1.724873	-0.202930	3.188811
10	8	2.296971	0.202016	1.048108
11	6	3.069443	-0.181293	3.731447
12	1	0.994800	-0.372897	3.849195
13	6	2.966343	-0.442684	5.215785
14	1	3.690395	-0.941255	3.273683
15	1	3.545475	0.777382	3.566448
16	8	1.932781	-0.625710	5.772838
17	8	4.144177	-0.439886	5.788509
18	1	4.058569	-0.605608	6.720221

* Atom numberings are according to Figure 5.2.

Table 5.9: Non-redundant fitted force constants of GH*

```
 1  1  5.176
 2  1   .161  2  4.935
 3  1   .271  2   .011  3  7.435
 4  1   .524  2   .043  3  1.147  4 11.593
 5  1  -.017  2  -.002  3   .143  4  -.090  5  6.517
 6  1   .041  2   .059  3   .001  4  -.007  5   .005  6  4.908
 7  1   .041  2   .059  3   .001  4  -.007  5   .005  6   .029  7  4.908
 8  1  -.003  2   .031  3  -.012  4  -.008  5   .001  6   .005  7   .005
    8  5.550
 9  1  -.021  2   .044  3  -.010  4  -.019  5   .002  6   .004  7  -.019
    8   .013  9  5.341
10  1  -.021  2   .044  3  -.010  4  -.019  5   .002  6  -.019  7   .004
    8   .013  9   .020 10  5.341
11  1   .089  2   .187  3   .374  4  -.649  5   .061  6  -.017  7  -.017
    8  -.004  9   .004 10   .004 11  1.136
12  1   .449  2  -.062  3  -.264  4   .100  5   .056  6   .011  7   .011
    8  -.005  9  -.035 10  -.035 11   .050 12  1.008
13  1  -.119  2  -.197  3   .005  4  -.023  5  -.001  6   .062  7   .062
    8   .002  9   .001 10   .001 11   .025 12  -.025 13   .527
14  1  -.131  2   .477  3  -.024  4  -.068  5   .004  6  -.007  7  -.007
    8  -.020  9  -.004 10  -.004 11   .049 12  -.050 13  -.043 14   .742
15  6   .072  7  -.072  9  -.016 10   .016 15   .689
16  6  -.028  7   .028  9  -.014 10   .014 15   .134 16   .662
17  1   .530  2   .398  3   .019  4   .063  5   .007  6  -.031  7  -.031
    8   .025  9  -.062 10  -.062 11   .085 12   .115 13   .008 14  -.014
   17  1.634
18  1   .004  2  -.295  3   .006  4  -.019  5  -.004  6  -.008  7  -.008
    8   .056  9   .056 10   .056 11  -.031 12   .014 13   .016 14  -.039
   17  -.021 18   .562
19  1  -.019  2  -.021  3  -.030  4   .046  5   .003  6   .000  7   .000
    8  -.071  9   .069 10   .069 11   .020 12  -.016 13   .005 14  -.002
   17  -.021 18   .015 19   .575
20  6   .001  7  -.001  9   .064 10  -.064 15   .020 16   .000 20   .583
21  1   .021  2  -.034  3   .055  4  -.037  5  -.004  6  -.001  7  -.001
    8   .030  9  -.014 10  -.014 11   .028 12  -.010 13   .022 14  -.057
   17   .069 18   .023 19   .001 21   .735
22  6  -.004  7   .004  9   .025 10  -.025 15  -.062 16  -.070 20   .032
23  1   .053  2   .018  3   .255  4   .018  5   .139  6   .003  7   .003
    8   .001  9  -.001 10  -.001 11   .102 12   .116 13   .000 14   .003
   17   .028 18  -.004 19   .005 21   .002 23   .801
24  6   .015  7  -.015  9  -.004 10   .004 15   .070 16  -.064 20  -.007
   22   .018 24   .433
```

Table 5.9: (Continued): Non-redundant fitted force constants of GH*

```
25  6  -.009  7   .009  9  -.013 10   .013 15   .071 16  -.003 20  -.019
    22  .031 24  -.009 25   .102
26  6   .006  7  -.006  9   .002 10  -.002 15   .001 16  -.016 20  -.001
    22 -.001 24   .018 25  -.029 26   .156
27  6  -.001  7   .001  9  -.021 10   .021 15  -.004 16  -.009 20  -.025
    22  .037 24  -.006 25  -.038 26   .000 27   .027
```

* Local symmetry coordinates are as given in Table 5.1.

Table 5.10: Non-redundant scaled force constants of GGH*

```
 1  1   5.023
 2  1    .195  2  4.991
 3  1    .225  2  -.008  3  4.893
 4  1    .016  2  -.001  3   .031  4  5.423
 5  1    .010  2  -.002  3   .019  4   .010  5  5.460
 6  1    .055  2   .046  3  -.002  4  -.015  5   .014  6  4.880
 7  1    .048  2   .029  3  -.007  4   .012  5  -.003  6   .032  7  4.920
 8  1   -.073  2   .262  3   .071  4  -.016  5  -.012  6   .002  7   .012
    8   8.623
 9  1    .054  2   .626  3  -.148  4   .004  5  -.007  6  -.001  7   .002
    8   1.436  9 10.177
10  1    .008  2  -.009  3  -.009  4   .003  5   .002  6   .004  7   .004
    8    .160  9  -.060 10  6.068
11  1   -.002  2   .012  3  -.004  4   .003  5   .003  6   .002  7   .006
    8    .048  9  -.067 10   .067 11  5.896
12  1    .002  2  -.001  3   .000  4  -.001  5  -.001  6   .000  7   .000
    8    .001  9   .021 10   .180 11  -.040 12  5.323
13  1    .002  2   .000  3   .000  4   .000  5   .000  6   .000  7  -.001
    8   -.033  9   .025 10   .154 11  -.005 12   .039 13  4.814
14  1    .002  2   .000  3   .000  4   .000  5   .000  6  -.001  7  -.001
    8   -.033  9   .026 10   .154 11  -.005 12   .039 13   .054 14  4.811
15  1   -.003  2   .005  3   .005  4  -.002  5  -.001  6   .000  7   .000
    8    .019  9  -.020 10   .051 11  -.049 12   .455 13  -.009 14  -.009
    15 11.351
16  1    .000  2   .000  3   .003  4  -.003  5  -.003  6  -.001  7  -.002
    8   -.053  9   .050 10  -.005 11   .026 12   .259 13   .004 14   .004
    15  1.203 16  7.027
17  1    .001  2   .001  3  -.001  4   .001  5   .001  6   .000  7   .000
    8    .010  9  -.006 10  -.003 11  -.002 12  -.022 13   .005 14   .005
    15  -.085 16   .132 17  6.610
```

Table 5.10: (Continued): Non-redundant scaled force constants of GGH*

```
18  1  -.325  2   .033  3  -.066  4   .068  5   .063  6  -.007  7  -.006
    8   .031  9  -.044 10  -.009 11  -.002 12   .000 13   .000 14   .000
   15   .002 16   .005 17  -.001 18   .562
19  1  -.003  2  -.031  3  -.040  4   .037  5   .049  6   .001  7   .001
    8  -.001  9  -.002 10   .000 11  -.001 12   .000 14   .000 15   .001
   16   .000 17   .000 18   .007 19   .568
20  1  -.031  2  -.020  3   .088  4   .098  5  -.083  6  -.003  7   .002
    8  -.021  9   .040 10   .004 11   .002 12   .000 13   .000 14   .000
   15  -.002 16  -.002 17   .001 18   .026 19  -.004 20   .602
21  1   .032  2  -.061  3   .270  4  -.011  5  -.016  6   .002  7   .003
    8  -.077  9   .079 10   .011 11   .009 12  -.001 13   .000 14   .000
   15  -.006 16  -.009 17   .001 18  -.022 19  -.024 20  -.027 21   .806
22  1   .007  2  -.007  3   .025  4   .011  5  -.009  6   .010  7  -.008
    8  -.014  9   .012 10   .002 11   .003 12   .000 13   .000 14   .000
   15  -.001 16  -.002 17   .000 18  -.006 19   .007 20   .015 21  -.010
   22   .754
23  1  -.211  2  -.106  3  -.007  4   .009  5   .007  6   .066  7   .071
    8   .001  9  -.022 10  -.003 11  -.005 12   .000 13   .000 14   .000
   15   .001 16   .000 17   .000 18   .020 19   .004 20   .004 21  -.014
   22  -.013 23   .527
24  1   .528  2  -.135  3  -.020  4  -.011  5  -.016  6  -.007  7   .005
    8  -.044  9  -.055 10  -.001 11   .004 12   .001 13   .001 14   .001
   15  -.004 16  -.001 17   .000 18  -.055 19   .007 20   .000 21   .036
   22   .021 23  -.060 24   .766
25  1  -.005  2   .038  3   .028  4   .021  5  -.018  6   .070  7  -.061
    8  -.018  9   .017 10   .003 11   .000 12   .000 13   .000 14   .000
   15  -.002 16   .000 17   .000 18   .009 19  -.009 20  -.012 21  -.045
   22   .038 23   .005 24   .010 25   .702
26  1   .008  2   .001  3  -.029  4   .018  5  -.016  6  -.023  7   .016
    8   .006  9   .011 10  -.003 11  -.001 12   .000 13   .000 14   .000
   16   .000 17   .000 18  -.008 19   .001 20  -.056 21  -.027 22   .040
   23   .001 24   .010 25   .146 26   .685
27  1   .390  2   .865  3   .132  4  -.016  5   .010  6  -.031  7  -.035
    8  -.105  9   .218 10   .026 11   .009 12   .001 13   .001 14   .000
   15  -.012 16  -.005 17   .002 18   .016 19  -.052 20  -.043 21  -.049
   22  -.044 23  -.001 24   .010 25   .044 26  -.006 27  2.084
28  1   .188  2   .002  3  -.049  4   .005  5   .002  6  -.004  7  -.017
    8   .186  9  -.712 10   .047 11  -.033 12  -.006 13   .005 14   .005
   15   .020 16  -.006 17   .002 18  -.063 19   .010 20   .016 21   .032
   22  -.014 23   .026 24   .016 25   .001 26  -.018 27  -.021 28  1.188
29  1  -.092  2   .695  3  -.001  4  -.019  5  -.011  6   .007  7   .015
    8  -.379  9   .161 10   .074 11   .005 12  -.014 13   .004 14   .003
   15  -.026 16  -.016 17   .004 18   .045 19  -.019 20  -.015 21  -.052
   22   .007 23  -.025 24  -.039 25   .014 26   .022 27   .376 28  -.085
   29  1.181
```

Table 5.10: (Continued): Non-redundant scaled force constants of GGH*

```
30   1  .028   2  .037   3 -.015   4  .000   5  .000   6  .001   7  .000
     8  .114   9 -.033  10  .118  11 -.069  12  .003  13 -.016  14 -.016
    15 -.006  16  .049  17 -.003  18 -.006  19 -.001  20  .003  21  .005
    22 -.001  23  .001  24  .003  25  .003  26 -.003  27  .042  28  .077
    29  .062  30  .658
31   1 -.018   2  .014   3  .008   4  .001   5  .001   6  .003   7  .005
     8  .182   9  .029  10 -.151  11 -.102  12  .029  13 -.009  14 -.009
    15 -.065  16  .039  17 -.005  18  .003  19  .000  20 -.001  21 -.004
    22  .000  23  .001  24 -.009  25 -.001  26  .004  27 -.015  28 -.004
    29 -.052  30  .011  31  .522
32   1  .000   2 -.001   3 -.001   4  .001   5  .001   6  .001   7  .001
     8  .006   9 -.004  10 -.201  11 -.009  12 -.127  13  .078  14  .078
    15 -.022  16  .006  17 -.001  18 -.001  19  .000  20  .000  21  .001
    22  .000  23  .000  24  .000  25  .001  26  .000  27  .002  28  .004
    29  .009  30  .004  31  .017  32  .542
33   1  .004   2  .003   3 -.001   4 -.001   5 -.001   6 -.001   7 -.002
     8 -.094   9  .052  10  .490  11  .001  12 -.171  13 -.013  14 -.013
    15 -.065  16 -.025  17  .005  18  .000  19  .000  20  .000  21 -.001
    22  .000  23  .000  24 -.001  25  .001  26 -.001  27  .001  28  .012
    29  .010  30 -.025  31 -.041  32 -.017  33  .732
34   1  .001   2 -.002   3  .000   4  .000   5  .000   6 -.001   7  .002
     8  .002   9  .000  10 -.001  11  .001  12  .000  13  .082  14 -.082
    15  .001  16 -.001  17  .000  18  .000  19  .000  20  .000  21  .000
    22  .001  24  .001  25 -.002  26  .003  27  .002  28 -.001  29  .000
    30  .000  31  .000  32  .000  33  .000  34  .707
35   1  .001   2 -.002   3  .000   4  .000   5  .000   6 -.002   7  .002
     8  .002   9  .000  10  .000  11  .001  13 -.037  14  .037  15 -.001
    16  .000  17  .000  18  .000  19  .000  20  .000  21  .000  22  .001
    23  .000  24  .001  25 -.004  26  .004  27  .002  28 -.001  29  .000
    30  .000  31  .000  32  .000  33 -.001  34  .114  35  .674
36   1  .005   2  .005   3  .002   4 -.004   5 -.003   6 -.001   7 -.001
     8  .019   9  .067  10  .353  11 -.024  12  .612  13 -.035  14 -.035
    15  .074  16  .015  17  .010  18  .002  19  .000  20 -.002  21 -.005
    22 -.002  23 -.001  24  .000  25 -.001  26 -.001  27  .001  28  .001
    29 -.024  30  .032  31  .036  32  .011  33 -.042  34  .000  35  .000
    36 1.683
37   1  .003   2  .006   3  .000   4 -.001   5  .000   6  .000   7  .000
     8  .004   9 -.009  10  .166  11 -.003  12  .078  13 -.020  14 -.020
    15 -.623  16  .339  17  .068  18  .000  19  .000  20  .000  21 -.002
    22 -.001  23  .000  24 -.001  25  .000  26  .000  27  .003  28  .025
    29  .009  30  .029  31 -.028  32  .026  33  .042  34  .000  35  .000
    36  .054  37 1.198
```

Table 5.10: (Continued): Non-redundant scaled force constants of GGH*

```
38   1 -.003  2 -.005  3  .004  4 -.004  5 -.004  6 -.001  7 -.001
     8 -.040  9  .060 10 -.053 11 -.022 12  .450 13  .013 14  .013
    15 -.014 16 -.286 17  .060 18  .004 19  .000 20 -.002 21 -.009
    22 -.002 23  .000 24 -.001 25 -.001 26  .000 27 -.015 28 -.014
    29 -.031 30 -.005 31  .025 32 -.025 33 -.049 34  .000 35  .000
    36  .176 37  .054 38 1.049
39   1  .001  2  .002  3  .000  4  .000  5  .000  6  .000  7  .000
     8  .008  9 -.006 10  .017 11 -.004 12  .042 13  .004 14  .004
    15  .019 16  .241 17  .147 18 -.001 19  .000 20  .000 21  .001
    22  .000 23  .000 24  .000 27  .001 28  .003 29  .004 30  .000
    31 -.004 32  .001 33  .003 34  .000 36  .031 37  .106 38  .119
    39  .816
40   1 -.004  2  .019  3 -.015  4 -.002  5  .000  6  .018  7 -.014
     8 -.001  9  .002 10  .001 11 -.002 12  .000 13  .002 14 -.002
    15  .001 16 -.001 17  .000 18 -.004 19  .004 20 -.023 21  .014
    22 -.013 23 -.005 24 -.010 25  .064 26 -.048 27 -.002 28  .002
    29  .018 30  .002 31  .000 32  .000 33  .001 34 -.008 35 -.010
    36  .000 37  .000 38  .000 39  .000 40  .453
41   1  .000  2 -.004  3 -.001  4  .001  5 -.001  6  .001  7  .001
     8  .006  9 -.002 10  .003 11  .004 12  .000 13 -.011 14  .011
    15 -.001 16  .001 17  .000 18  .000 19  .000 20 -.002 21  .001
    22 -.002 23  .002 24  .002 25  .003 26  .002 27  .002 28 -.001
    29  .001 30  .001 31 -.001 32  .000 33  .000 34 -.014 35 -.020
    36  .001 37  .000 38  .000 39  .000 40 -.037 41  .102
42   1  .000  2  .000  3  .000  4  .000  5  .000  6  .000  7  .000
     8  .000  9  .000 10  .000 11  .000 12  .000 13  .019 14 -.018
    15 -.001 16  .000 17  .000 18  .000 19  .000 20  .000 21  .000
    22  .000 23  .000 24  .000 25  .000 26  .000 27  .000 28  .000
    29  .000 30  .000 31  .000 33  .000 34  .062 35 -.062 37  .000
    38  .000 39  .000 40  .004 41 -.014 42  .478
43   1 -.031  2 -.024  3 -.110  4  .006  5  .011  6  .007  7  .005
     8  .025  9 -.028 10 -.003 11 -.002 12  .000 13  .000 14  .000
    15  .001 16  .002 17  .000 18 -.015 19  .015 20 -.073 21  .055
    22 -.032 23  .007 24 -.023 25 -.009 26  .013 27  .001 28  .000
    29 -.008 30 -.003 31  .002 32 -.001 33  .000 34  .000 35  .000
    36  .001 38  .002 39  .000 40  .013 41  .001 42  .000 43  .065
44   1  .013  2  .033  3 -.038  4 -.004  5  .001  6  .003  7  .003
     8  .002  9  .010 10  .002 11  .004 12  .000 13  .000 14  .000
    15 -.002 16  .002 17  .000 18 -.013 19  .006 20 -.087 21  .030
    22 -.018 23 -.005 24  .004 25  .075 26  .006 27  .047 28 -.025
    29  .034 30  .000 31  .000 32  .000 33  .001 34  .003 35  .002
    36  .000 37  .000 38  .001 39  .000 40  .013 41  .016 42 -.001
    43  .068 44  .169
```

Table 5.10: (Continued): Non-redundant scaled force constants of GGH*

```
45   1  -.006   2   .014   3   .001   4  -.002   5   .001   6   .011   7  -.011
     8  -.007   9   .005  10  -.001  11   .002  12   .000  13   .002  14  -.002
    15  -.001  16   .001  17  -.001  18   .000  19   .000  20   .000  21   .002
    22  -.003  23   .002  24  -.004  25   .006  26  -.024  27  -.008  28   .007
    29   .000  30  -.001  31   .001  32   .000  33   .000  34  -.017  35  -.016
    36   .000  38   .000  39   .000  40  -.034  41  -.050  42   .002  43   .001
    44  -.029  45   .294
46   1   .001   2   .000   3   .000   4   .000   5   .000   6   .000   7  -.001
     8  -.001   9   .000  10   .000  11   .000  12   .000  13   .016  14  -.016
    15  -.003  16   .001  18   .000  19   .000  20   .001  21  -.001  22   .001
    23  -.001  24   .000  25  -.001  26   .001  27   .000  28   .001  29   .000
    30   .000  31   .001  32   .000  33   .000  34   .014  35   .044  36   .000
    37   .000  38   .000  39   .000  40   .008  41  -.034  42   .017  43  -.001
    44  -.004  45   .004  46   .066
47   1   .001   2   .000   3   .000   4   .000   5   .000   6   .000   7   .000
     8   .000   9   .000  10   .000  11   .000  12   .000  13  -.015  14   .015
    15  -.001  16   .000  17  -.001  18   .000  19   .000  20   .000  21   .000
    22   .001  23  -.001  24   .000  25  -.002  26   .001  27   .001  28   .000
    29   .000  30   .000  31   .000  32   .000  33   .000  34   .058  35   .014
    36   .000  37   .000  39   .000  40   .004  41  -.036  42  -.008  43   .000
    44  -.003  45  -.003  46   .047  47   .144
48   1   .000   2   .000   3   .000   4   .000   5   .000   6   .000   7   .000
     8   .000  10   .000  12   .000  13   .007  14  -.007  15   .000  16   .000
    17   .000  19   .000  20   .000  21   .000  22   .000  23   .000  24   .000
    25   .001  26   .000  27   .000  28   .000  29   .000  30   .000  31   .000
    33   .000  34   .001  35  -.015  36   .000  37   .000  39   .000  40   .000
    41   .003  42   .012  43   .000  44   .001  45  -.001  46   .001  47  -.029
    48   .157
```

* Local symmetry coordinates are as given in Table 5.2.

Bibliography

[1] Kozlowski, P. M.; Jarzecki, A. A.; Pulay, P.; Li, X. Y.; Zgierski, M. Z. *J. Phys. Chem.*, **1996**, 100, 13985.

[2] Pongor, G.; Pulay, P.; Fogarasi, G.; Boggs, J. E. *J. Am. Chem. Soc.*, **1984**, 106, 2765.

[3] Williams, R. W.; Kalasinsky, V. H.; Lowrey, A. H. *J. Mol. Struct. (Theochem)*, **1993**, 281, 157.

[4] Barron, L. D.; Gargaro, A. R.; Hecht, L.; Polavarapu, P. L. *Spectrochim. Acta.*, **1991**, 47A, 1001.

[5] Alper, J. S.; Dothe, H.; Lowe, M. A. *Chem. Phys.*, **1992**, 161, 199.

[6] Tarakeshwar, P.; Manogaran, S. *Spectrochim. Acta*, **1995**, 51A, 925.

[7] Lowrey, A. H.; Williams, R. W. *Struct. Chem.*, **1993**, 4, 289.

[8] Williams, R. W. *Biopolymers*, **1992**, 32, 829.

[9] Lowrey, A. H.; Williams, R. W. *J. Mol. Struct. (Theochem)*, **1992**, 253, 57.

[10] Lowrey, A. H.; Williams, R. W. *J. Mol. Struct. (Theochem)*, **1992**, 253, 35.

[11] Williams, R. W.; Lowrey, A. H. *J. Comput. Chem.*, **1991**, 12, 761.

[12] Mirkin, N. G.; Krimm, S. *J. Am. Chem. Soc.*, **1991**, 113, 9742.

[13] Guo, H.; Karplus, M. *J. Phys. Chem.*, **1992**, 96, 7273.

[14] Yu, G.; Freedman, T. B.; Nafie, L. A.; Deng, Z.; Polavarapu, P. L. *J. Phys. Chem.*, **1995**, 99, 835.

118

[15] Ding, Y.; Krogh-Jespersen, K. *J. Comput. Chem.*, **1996**, 17, 338.

[16] Vijay, A.; Sathyanarayana, D. N. *J. Phys. Chem.*, **1992**, 96, 10735.

[17] Tarakeshwar, P.; Manogaran, S. *J. Mol. Struct. (Theochem)*, **1994**,

[18] Chakraborty, D.; Manogaran, S. *J. Mol. Struct. (Theochem)*, *1994*, 303, 265.

[19] Lagant, P.; Vergoten, G.; Loucheuxlefebvre, M. H.; Fleury, G. *Biopolymers*, **1983**, 22, 1267.

[20] Durig, J. R.; Wang, A. Y.; Little, J. S.; Breltic, P. A. *J. Chem. Phys.*, **1990**, 93, 905.

[21] Aslanian, D. in *Molecules in Physics, Chemistry and Biology*, Ed. Maruani, J., Kluwer Academic Press, 1989, vol.IV, p.233-280.

[22] Wagner, E. L.; Hornig, D. F. *J. Chem. Phys.*, **1950**, 18, 296 and 305.

[23] Jensen, F. *J. Am. Chem. Soc.*, **1992**, 114, 9533.

[24] Yu, D.; Rauk, A.; Armstrong, D. A. *J. Am. Chem. Soc.*, **1995**, 117, 1789.

[25] Al-Karaghouli, A. R.; Cole, F. E.; Lehmann, M. S.; Miskell, C. F.; Verbist, J. J.; Koetzle, T. F. *J. Chem. Phys.*, **1975**, 63, 1360.

[26] Ghazanfar, S. A. S.; Myers, D. V.; Edsall, J. T. *J. Am. Chem. Soc.*, **1964**, 86, 3439.

[27] Kakihana, M.; Akiyama, M.; Nagumo, T.; Okamoto, M. *Z. Naturforsch.*, **1988**, 43A, 774.

[28] Diem, M.; Polavarapu, P. L.; Oboodi, M.; Nafie, L. A. *J. Am. Chem. Soc.*, **1982**, 104, 3329.

Chapter 6

Theoretical prediction of vibrational spectra of cysteine and serine Hydrochloride

In continuation with our earlier investigation of the vibrational spectra of hydrochlorides of amino acids glycine (GH) and glycylglycine (GGH) (chapter 5), in this chapter we address this problem, using cysteine and serine hydrochloride (CYSH and SERH).

Cysteine (CYS) owing to the presence of thiol group SH is one of the most important amino acids. It is responsible for the stabilization of secondary structures of proteins through the formation of H-bonds and more importantly disulfide bridges. Thus the CYS residue side chain, -CH$_2$SH was the subject of a number of spectroscopic studies for characterization of its conformers [1-23]. The theoretical modelling of thiol group in CYS is very important because the earlier force field developers have shown that an inaccurately described SH group does not tend to form H-bonds [24]. The H-bonding effect on νSH frequency has been studied in different proteins [1-8]. Effect of the C$_\alpha$-C$_\beta$-S-H dihedral angles on the νSH mode has been sought through experimental [9-11] and normal mode analyses [12,13] of some model alkanethiols. Information on rotational barriers from the low frequency torsional modes have also been reported in the literature [14-16]. The conformational assignment of ν CS frequency with respect to C-C$_\alpha$-C$_\beta$-S dihedral angle in several thiols, [17,18] dialkyl disulfide [19,20] or alkyl sulfides [21], and the normal coordinate analyses [22,23] are found in the literature. Serine (SER) due to the presence of two hydroxyl groups readily forms H-bonds and hence is found in turns of

119

protein secondary structures. A study of the effect of the torsional angle C-C_α-C_3-O on the $\nu C_3 O$ frequency in SER was reported. [25]. There is a large number of experimental vibrational spectral study (IR and Raman) on CYS and SER zwitterions [26-31]. The most recent one being the ROA spectra of Gargaro et al. [31] based on their alanine results [32]. But a detailed theoretical vibrational analysis of both CYS and SER in their gaseous and zwitterionic forms is limited to the recent study from our laboratory based on their isolated ab initio model [25].

In this chapter our endeavour is to generate a reliable force field for CYSH and SERH. The scale factors of glycine hydrochloride from previous chapter is used to scale the ab initio force field of both the compounds at the same level of theory (HF/6-31G**). The side chain residues of CYSH and SERH are scaled by using the scale factors of ethanethiol (EtSH) and ethanol (EtOH) respectively, obtained by fitting their ab initio force field to the respective experimental vibrational spectra [13,33]. A complete set of nonredundant force constants were obtained for CYSH and SERH.

6.1   Calculations

The ab initio force constants and frequencies of CYSH, SERH, EtSH and EtOH were calculated analytically for the optimized geometry at 6-31G** level. The cartesian force constant matrices were transformed to the non-redundant local coordinate space. The nonredundant local coordinates of both EtSH and EtOH are given in Table-6.1 and Figure 6.1 and that of CYSH and SERH are given in Table-6.2 and Figure 6.2. The optimized geometries of CYSH and SERH are given in Table-6.3. The ab initio force fields of EtSH and EtOH were then fitted to their corresponding experimental spectra to obtain a non-redundant set of force constants and scale factors using the methodology described in chapter 3. The fitting is very successful for both the compounds. The scale factors of EtSH and EtOH along with glycine hydrochloride when used to scale the ab initio force field of CYSH and SERH, a very good agreement is obtained with experimental frequencies for both the molecules.

6.2 Results

6.2.1 EtSH

Of the different possible conformers, the gauche form (H(4)-S(2)-C(1)-C(3) ~ 60°) of EtSH is most stable in the ground state, as shown by Qian and Krimm, based on their ab initio (3-21G and 4-31G*) calculations [34]. We did not do any conformational analysis further at our required level of theory (6-31G**) in the present study. The fully optimized geometry of EtSH at this level generates the gauche form as the most stable one. Since the intermolecular H-bonding is less pronounced in EtSH, the isolated molecule ab initio calculation serves as a good model for the condensed phase vibrational spectra. Several experimental vibrational spectra of EtSH were found in the literature [9,13,16]. We used the condensed phase spectra [13] for the analysis. Fitted frequencies of all the fundamentals are shown in Table-6.4. Such a force field obtained from a single isotopomer frequencies might be considered as a good approximation but the reliability of this force field should be judged by its ability to predict the vibrational frequencies of CYSH. The fitted force field retains the ab initio PEDs in all the frequencies. The 2571 cm^{-1} band is assigned to νSH, the νCC mode appears at 1052 cm^{-1} and 970 cm^{-1} and νCS is assigned to the band at 657 cm^{-1}. These are in good agreement with the earlier assignments of EtSH and Propane thiol (PrSH) [34].

6.2.2 EtOH

In EtOH the most staggered conformation is the most stable one at 6-31G** level of calculation [35]. The trans-gauche rotational barrier is known to be 4.89 kJ/mol [36]. The earlier microwave study also indicates the trans form as the more stable one over the gauche form [37]. So we calculated the ab initio force field for the fully optimized staggered(trans) conformer of EtOH only at the required 6-31G** level of theory. In condensed phase there exists intermolecular H-bonding in EtOH and the corresponding vibrational spectra will be different from the isolated molecular spectra. However the isolated molecule-ab initio model can serve as a reasonable approximation to the condensed phase vibrational spectra

when *fitted* to the *experimental numbers*. Several experimental vibrational spectra of EtOH in liquid, crystal and/or vapour phase are available in the literature [33,38,39]. For the present study we used the liquid and crystal frequencies of EtOH and EtOD of Mikawa et al. [33]. The fitted numbers are in good agreement for all the fundamentals, except the νOH, which is highly overestimated in the isolated model calculation compared to the condensed phase experimentally observed frequency. So this frequency is not included in the error estimation. The average error is 4.0 cm^{-1} for the observed fundamentals. The normal modes obtained after fitting the experimental frequencies to the calculated ones agree well with the earlier reported assignments with few exceptions. The δCOH appear as a mixed mode in the ab initio PED with ωCH$_2$ at 1430 cm^{-1}, while the earlier experimental assignment was at 1328 cm^{-1}, which we assign to tCH$_2$ mode. The assignment of the corresponding δCOD (954 cm^{-1}) matches well with the earlier assignment. We assigned the δCCO(γOH) mode at 439 cm^{-1}, which was earlier assigned at 657 cm^{-1} in IR and 660 cm^{-1} in polarized Raman [33]. The usefulness of the calculated force field could be tested by its ability to predict the vibrational spectra of the side chain residue of SERH successfully.

6.2.3 Vibrational Frequencies of CYSH

The predicted frequencies of CYSH are given in Table-6.5 along with their PEDs. The prediction is in good agreement with the experimental frequencies producing an average error of 11.9 cm^{-1} for CYSH spectra. Since glycine does not have any chiral carbon atom, the scale factors for the methylene group is difficult to transfer to the higher amino acids. But these bending modes generally appear around 1000-1400 cm^{-1} and a simple Durig's scaling produces reasonable agreement with the observed bands in this region. The side chain -CH$_2$SH residue is successfully represented by using the scale factors from EtSH. There is no detailed assignment of IR/Raman spectra of CYSH in the literature except the earlier report from our laboratory [25]. We re-recorded the spectra of CYSH (commercial sample of L-cysteine hydrochloride from S. D. Fine Chemicals, India) as a mull in Nujol in the spectral range of 600-4000 cm^{-1}. The CYS-OMe spectra [25] and the L-CYS zwitterionic spectra [30] are also included in the Table-6.5 for a comparison.

The observed band at 3377 cm^{-1} in CYSH is assigned to νOH and is calculated at 3407 cm^{-1}. All the three νN$^+$H bands are predicted above the νCH bands at 3166, 3115 and 3019 cm^{-1}. These bands are not observed in our spectra of CYSH and CYS-OMe. However in L-CYS zwitterion, these bands appear at 3167 and 3055 cm^{-1}. The νSH band is predicted at 2590 cm^{-1} and is observed at 2567 cm^{-1} in the CYSH spectra. This assignment is in accordance with the observed bands at 2571 cm^{-1} in EtSH, 2564 cm^{-1} in PrSH and around 2590 cm^{-1} in the model protein for cysteine residue [34] and also 2582 cm^{-1} in zwitterion. The νC$_\beta$S is predicted at 680 cm^{-1} and is also comparable to EtSH (660 cm^{-1}) and PtSH (655 cm^{-1}) but appear at 696 cm^{-1} in the zwitterion. This band is not observed in our CYSH and CYS-OMe spectra. The νC=O band is slightly overestimated in the predicted spectra (1776 cm^{-1}) and this mode is assigned to the observed band at 1743 cm^{-1} in CYSH and 1735 cm^{-1} in CYS-OMe. This band is observed at 1750 cm^{-1} in glycine hydrochloride. Both the δ_aN$^+$H$_3$ appear very close in our predicted spectra followed by δ_sN$^+$H$_3$ band. Both the δ_aN$^+$H$_3$ are predicted at 1634 and 1614 cm^{-1} and are assigned to the observed bands at 1633 and 1613 cm^{-1} in our CYSH spectra and the lower one corresponds to the 1593 cm^{-1} CYS-OMe spectra. These two bands are observed at 1616 cm^{-1} in the zwitterion. The δ_sN$^+$H$_3$ band is predicted at 1481 cm^{-1} and is assigned to the observed band at 1490 cm^{-1} in CYSH. In our predicted spectra the νCC+νCO mode appear above δCH$_2$ in accordance with glycine hydrochloride. But in zwitterion they appear in the reverse order. The predicted bands at 1444 and 1410 cm^{-1} are assigned to νCC+νCO and δC$_\beta$H$_2$ and are observed at 1428 and 1399 cm^{-1} in CYSH and 1437 and 1408 cm^{-1} in CYS-OMe and 1427 and 1400 cm^{-1} in the zwitterion. The δCOH mode is predicted at 1348 cm^{-1}, and is observed at 1348 cm^{-1} in CYSH spectra and obviously absent in the CYS-OMe and zwitterionic spectra. Both the ωC$_\beta$H$_2$ and tC$_\beta$H$_2$ modes are attributed to the predicted bands at 1292 and 1196 cm^{-1} and are observed at 1309, 1203 cm^{-1} in CYSH and 1313, 1205 cm^{-1} in CYS-OMe spectra. These bands appear at 1300 and 1201 cm^{-1} in CYS zwitterion. Both the ρN$^+$H$_3$ modes are predicted at 1161 and 1102 cm^{-1} as expected and only one of them appear in our observed spectra. The 1069 cm^{-1} predicted band is assigned to νC$_\alpha$N$^+$ and is attributed to the observed band at 1059 cm^{-1} in CYSH and 1068 cm^{-1} in zwitterion. The observed band at 736 cm^{-1} in both the spectra is assigned to

$\gamma CO + \nu CC + \nu CN^+$ mode and is predicted at 732 cm^{-1}. The lower frequency modes below 400 cm^{-1} are not available and hence our predicted numbers cannot be compared.

6.2.4 Vibrational Frequencies of SERH

The predicted frequencies of SERH along with the PED is given in Table-6.6. Same strategy of transferring the scale factors of glycine hydrochloride and EtOH, as in CYSH was used. There is no report on the IR or Raman spectra of SERH in the literature except that reported from our laboratory earlier [25]. We have used the same reported spectra for SERH and SER-OMe for the present study. Since only few bands are observed in these two spectra it is difficult to judge the accuracy of our prediction. As a result, vibrational frequencies from both L-serine and D,L-serine [29] are included in Table-6.6. The average error is difficult to estimate in such cases. In case of SERH and SER-OMe spectra the average is quite high (13.1 and 12.2 cm^{-1}) for 11 and 17 observed frequencies respectively out of the expected 39 fundamentals. The $\nu OH_{(alc)}$ is predicted above $\nu OH_{(acid)}$ as expected. The ν C=O band is predicted at 1744 cm^{-1} and matches very well with the observed numbers at 1734 in SERH ans 1735 in SER-OMe spectra. Both the $\delta_s N^+H_3$ bands appear at the same region in our predicted spectra, as in case of CYSH. Both the $\delta C_\beta H_2$ and $\delta_s N^+H_3$ modes are predicted very close to each other, though $\delta_s N^+H_3$ appear below $\delta C_\beta H_2$. Many of the other modes ρCC_3H (1365), δCOH (1340), $\nu CO + \delta COH$ (1249), ρN^+H_3 (1174,1144), νCN^+ (1094) and γCO (728) in our predicted SERH spectra appear very similar to their corresponding observed frequencies. The tCH$_2$ (1297) appear above the ωCH_2 (1225) in the predicted SERH spectra, reverse to that of CYSH. The $\delta C_\beta OH$ mode is expected to appear at much higher frequency compared to the $\delta C_\beta SH$ mode in CYSH. As a result the 1437 cm^{-1} band in SERH correspond to $\delta C_\beta OH$, whereas the $\delta C_\beta SH$ band in CYSH appear at 991 cm^{-1} in our prediction. A comparison of the amino acid backbone and side chain frequencies of all related molecules used in the present study appear in Tables-6.7 and 6.8.

The predicted non redundant force constants of both CYSH and SERH are given in Table-6.9 and 6.10 respectively.

6.3 Conclusions

The theoretical prediction of amino acid hydrochloride vibrational spectra based on isolated ab initio calculation is found to be very successful. The choice of right basis set is considered to be an important factor for mimicking the experimental spectra through isolated molecule ab initio model. The scale factors of smallest amino acid, glycine is found to be very useful in predicting the higher chiral amino acids. The earlier prediction of glycylglycine hydrochloride and the present study, led us to infer that this nonredundant set of scale factors of glycine hydrochloride could be used to predict successfully the vibrational spectra of other amino acids and structurally related dipeptides in acidic pH. However further study of other amino acids is needed to verify this conclusion. This further implies that the structurally related small organic compounds can be used to mimic the amino acid side chain residues.
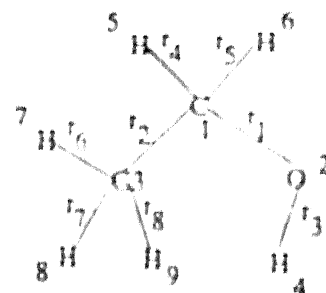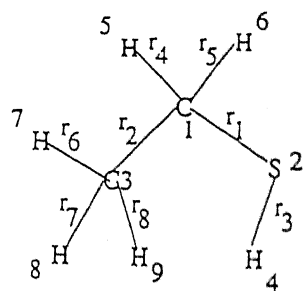
a= C(1)-O(2)/S(2)-H(4), a1= H(5)-C(1)-H(6), a2= C(3)-C(1)-H(5)

a 3= C(3)-C(1)-H(6), b1= C(3)-C(1)-O(2)/S(2), b2= O(2)/S(2)-C(1)-H(5)

b3= O(2)/S(2)-C(1)-H(6), a 4= H(8)-C(3)-H(9), a5= H(7)-C(3)-H(8)

a 6= H(7)-C(3)-H(9), b4= C(1)-C(3)-H(7), b5= C(1)-C(3)-H(8), b6= C(1)-C(3)-H(9)

Figure 6.1: Internal coordinates of EtSH and EtOH.
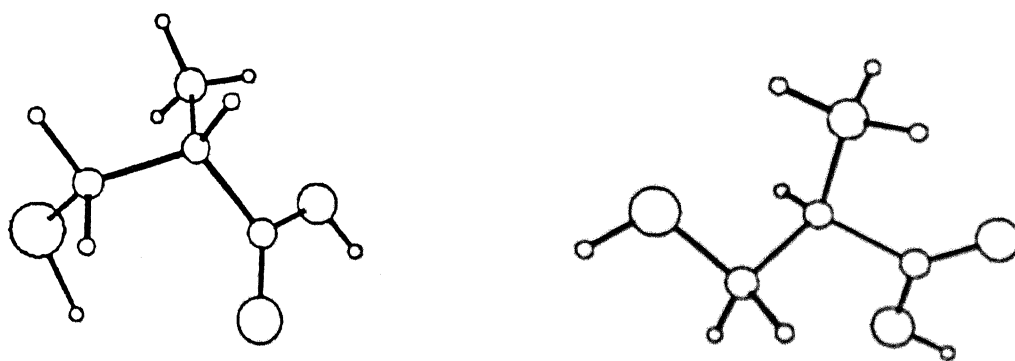
Figure 6.3: Optimized structure of a) CYSH and b) SERH at HF/6-31G** level.

Table 6.1: Local symmetry coordinates of EtSH and EtOH *

$S_{1-8}=$	r_{1-8}(all stretch)	$S_{15}=$	$a_4+a_5+a_6-b_4-b_5-b_6$ $(\delta_s CH_3)$
$S_9=$	$4a_1-a_2-a_3-b_2-b_3(\delta CH_2)$	$S_{16}=$	$2a_4-a_5-a_6(\delta_a CH_3)$
$S_{10}=$	$a_2+a_3-b_2-b_3(\omega CH_2)$	$S_{17}=$	$a_5-a_6(\delta_a CH_3)$
$S_{11}=$	$a_2-a_3+b_2-b_3$ (ρCH_2)	$S_{18}=$	$2b_4-b_5-b_6(\rho CH_3)$
$S_{12}=$	$a_2-a_3-b_2+b_3$ (tCH_2)	$S_{19}=$	$b_5-b_6(\rho CH_3)$
$S_{13}=$	$5b_1-a_1-a_2-a_3-b_2-b_3$ $(\delta CCS/\delta CCO)$	$S_{20}=$	$\tau_{1-2}(\tau CS/\tau CO)$
$S_{14}=$	a $(\delta CSH/\delta COH)$	$S_{21}=$	$\tau_{1-3}(\tau CC)$

* Internal coordinate numberings are according to Figure 6.1.

Table 6.2: Local symmetry coordinates of CYSH and SERH *

$S_{1-14}=$	r_{1-14}(all stretch)	$S_{27}=$	$b_7-b_8(\rho COO)$
$S_{15}=$	$a_1+a_2+a_3-b_1-b_2-b_3$ $(\delta N^+C_\alpha C)$	$S_{28}=$	a_8 (δCOH)
$S_{16}=$	$2a_1-a_2-a_3(\delta C_\beta C_\alpha C)$	$S_{29}=$	$4a_9-a_{10}-a_{11}-b_{10}-b_{11}(\delta C_\beta H_2)$
$S_{17}=$	a_2-a_3 $(\rho C_\beta C_\alpha C)$	$S_{30}=$	$a_{10}+a_{11}-b_{10}-b_{11}$ $(\omega C_\beta H_2)$
$S_{18}=$	$2b_1-b_2-b_3$ $(\delta C_\beta C_\alpha H)$	$S_{31}=$	$a_{10}-a_{11}+b_{10}-b_{11}$ $(\rho C_\beta H_2)$
$S_{19}=$	b_2-b_3 $(\rho C_\beta C_\alpha H)$	$S_{32}=$	$a_{10}-a_{11}-b_{10}+b_{11}$ $(tC_\beta H_2)$
$S_{20}=$	a $(\delta C_\beta SH/\delta C_\beta OH)$	$S_{33}=$	$5b_9-a_9-a_{10}-a_{11}-b_{10}-b_{11}$ $(\delta C_\alpha C_\beta S/\delta C_\alpha C_\beta O)$
$S_{21}=$	$a_4+a_5+a_6-b_4-b_5-b_6$ $(\delta_s N^+H_3)$	$S_{34}=$	τ_{710}/τ_{26} $(\gamma C=O)$
$S_{22}=$	$2a_4-a_5-a_6$ $(\delta_a N^+H_3)$	$S_{35}=$	τ_{15}/τ_{48} $(\tau C_\beta S/\tau C_\beta O)$
$S_{23}=$	a_5-a_6 $(\delta_a N^+H_3)$	$S_{36}=$	τ_{26}/τ_{13} $(\tau C_\alpha N^+)$
$S_{24}=$	$2b_4-b_5-b_6$ (ρN^+H_3)	$S_{37}=$	τ_{12}/τ_{14} $(\tau C_\alpha C_\beta)$
$S_{25}=$	b_5-b_6 (ρN^+H_3)	$S_{38}=$	τ_{27}/τ_{12} $(\tau C_\alpha C)$
$S_{26}=$	$2a_7-b_7-b_8$ (δCOO)	$S_{39}=$	τ_{711}/τ_{27} (τCO)

*. Internal coordinate numberings are according to Figure 6.2.

Table 6.3: Optimized geometrical parameters of CYSH and SERH (6-31G**)

param	CYSH	SERH	param	CYSH	SERH	param	CYSH	SERH
r_1	1.530	1.531	a_3	112.8	113.6	b_9	114.0	104.6
r_2	1.083	1.088	b_1	110.2	109.4	b_{10}	106.6	111.6
r_3	1.079	1.083	b_2	106.4	107.3	b_{11}	110.5	112.9
r_4	1.818	1.395	b_3	107.0	110.7	τ_{2159}/τ_{14815}	79.7	173.5
r_5	1.505	1.497	a_4	107.7	109.4	τ_{6213}/τ_{31412}	-65.3	-72.2
r_6	1.527	1.518	a_5	108.2	106.4	τ_{6215}/τ_{3148}	54.2	48.0
r_7	1.085	1.082	a_6	108.6	110.0	τ_{7213}/τ_{21412}	171.6	46.7
r_8	1.326	0.946	b_4	111.3	110.4	τ_{7215}/τ_{2148}	-68.8	166.1
r_9	1.176	1.185	b_5	109.5	111.9	τ_{12612}/τ_{4139}	-169.7	81.1
r_{10}	1.321	1.304	b_6	111.5	108.8	τ_{82612}/τ_{5139}	70.6	-160.7
r_{11}	1.011	1.012	a_7	111.5	111.5	τ_{72612}/τ_{2139}	-44.8	-41.9
r_{12}	1.015	1.013	a_8	111.0	111.3	τ_{12710}/τ_{4126}	-31.0	-114.1
r_{13}	1.010	1.009	b_7	122.4	121.5	τ_{62710}/τ_{3126}	-154.7	5.6
r_{14}	0.953	0.952	b_8	126.0	127.0	τ_{82710}/τ_{5126}	90.3	122.3
a	97.8	112.2	a_9	107.5	108.7	$\tau_{271115}/\tau_{12714}$	176.8	-179.4
a_1	109.4	107.0	a_{10}	109.8	110.6	$\tau_{1071115}/\tau_{62714}$	-1.2	-0.4
a_2	110.7	108.5	a_{11}	108.1	108.3			

* All internal coordinates are according to Figure 6.2.

Table 6.4: Fitted frequencies of EtSH and EtOH

no.	EtSH			EtOH			EtOD		
	expt[a]	calc	PED	expt[b]	calc	PED	expt[b]	calc	PED
1	2988	2988	$\nu C(H_3)+\nu C(H_2)$	3336	3511	νOH	—	2557	νOD
2	2967	2967	$\nu C(H_2)+\nu C(H_3)$	2975	2975	$\nu C(H_3)$	—	2975	$\nu C(H_3)$
3	2932	2932	$\nu C(H_2)$	2940	2940	$\nu C(H_3)$	—	2940	$\nu C(H_3)$
4	2902	2902	$\nu C(H_2)$	2920	2920	$\nu C(H_2)$	—	2920	$\nu C(H_2)$
5	2875	2875	$\nu C(H_3)$	2890	2890	$\nu C(H_3)$	—	2890	$\nu C(H_3)$
6	2571	2571	νSH	2877	2877	$\nu C(H_2)$	—	2877	$\nu C(H_2)$
7	1460	1460	$\delta_a CH_3$	1498	1494	δCH_2	1490	1490	$\delta CH_2+\delta_a CH_3$
8	1450	1450	$\delta_a CH_3$	1480	1478	$\delta_a CH_3$	1474	1475	$\delta_a CH_3+\delta CH_2$
9	1434	1434	δCH_2	1450	1449	$\delta_a CH_3+\rho CH_3$	1447	1449	$\delta_a CH_3+\rho CH_3$
10	1376	1376	$\delta_s CH_3$	1430	1446	$\delta COH+\omega CH_2+\delta CH_2+\delta_a CH_3$	1404	1401	$\delta_s CH_3+\omega CH_2+\nu CC$
11	1273	1273	ωCH_2	1381	1385	$\delta_s CH_3$	1365	1357	$\omega CH_2+\delta_s CH_3$
12	1251	1251	$tCH_2+\rho CH_3$	1328	1318	$tCH_2+\rho CH_3$	1309	1318	$tCH_2+\rho CH_3$
13	1091	1091	$\rho CH_3+\delta CSH+tCH_2+\rho CH_2$	1273	1277	$\omega CH_2+\delta COH$	1170	1170	$\rho CH_3+\delta COD+\delta CCO+\nu CC$
14	1052	1052	$\nu CC+\rho CH_3+tCH_2$	1149	1153	$\rho CH_2+\rho CH_3+tCH_2$	1158	1153	$\rho CH_2+\rho CH_3+tCH_2$
15	970	970	$\nu CC+\rho CH_3$	1089	1091	ρCH_3	1055	1054	$\nu CO+\nu CC$
16	869	869	$\delta CSH+tCH_2+\rho CH_3$	1050	1051	$\nu CC+\nu CO$	954	946	$\delta COD+\rho CH_3+\omega CH_2$
17	737	737	$\rho CH_2+\rho CH_3+\delta CSH$	880	887	$\nu CO+\nu CC+\rho CH_3$	877	870	$\nu CO+\nu CC+\rho CH_3$
18	657	657	νCS	802	799	$\rho CH_2+\rho CH_3+tCH_2$	797	799	$\rho CH_2+\rho CH_3+tCH_2$
19	319	319	δCCS	433	439	$\delta CCO+\rho CH_3$	435	429	$\delta CCO+\rho CH_3$
20	247	247	τCC	264	264	$\tau CO+\tau CC$	—	236	τCC
21	191	191	τCS	200	219	$\tau CC+\tau CO$	—	183	$\tau CO+\tau CC$

a. ref. [14] b. ref. [34]

Table 6.5: Predicted frequencies and PED of CYSH

no.	calc	PED	expt CYSH[a]	CYS-OMe[a]	CYS-zwitt.[b]
1	3407	νOH	3377	—	—
2	3166	νN$^+$H	—	—	—
3	3115	νN$^+$H	—	—	3167
4	3019	νN$^+$H	—	—	—
5	3003	νC$_\beta$H	—	3000	3055
6	2950	νC$_\beta$H	2943	2953	2998
7	2934	νC$_\alpha$H	2943	—	2960
8	2590	νSH	2567	—	2918
9	1776	νC=O	1743	1735	2582
10	1634	δ_aN$^+$H$_3$	1633	—	—
11	1614	δ_aN$^+$H$_3$	1613	1593	1616
12	1481	δ_sN$^+$H$_3$	1490	—	1616
13	1444	νCC+νCO+ρC$_\beta$C$_\alpha$H	1428	1437	—
14	1410	δC$_\beta$H$_2$	1399	1408	1427
15	1357	ρC$_\beta$C$_\alpha$H+δC$_\beta$C$_\alpha$H	1371	1377	1400
16	1348	δCOH+δC$_\beta$C$_\alpha$H+ρN$^+$H$_3$	1348	—	1351
17	1292	ωC$_\beta$H$_2$	1309	1313	—
18	1221	νCO+δCOH+ρC$_\beta$C$_\alpha$H	1222	—	1300
19	1196	tC$_\beta$H$_2$+δC$_\beta$C$_\alpha$H	1203	1205	—
20	1161	ρN$^+$H$_3$+ρC$_\beta$C$_\alpha$H	1141	1176	1201
21	1102	ρN$^+$H$_3$+tC$_\beta$H$_2$+δC$_\beta$C$_\alpha$H	1141	1176	—
22	1069	νC$_\alpha$N$^+$+δC$_\beta$SH	1059	—	—
23	991	δC$_\beta$SH+νC$_\alpha$C$_\beta$+ρN$^+$H$_3$+ρC$_\beta$H$_2$	988	1009	1068
24	943	νC$_\alpha$N$^+$+νC$_\alpha$C$_\beta$+δC$_\beta$SH+νC$_\alpha$C	931	942	1004
25	852	δN$^+$C$_\alpha$C+γCO+νC$_\alpha$C	863	882	943
26	779	ρC$_\beta$H$_2$+δC$_\beta$SH	777	781	870
27	732	γCO+νC$_\alpha$C+νC$_\alpha$N$^+$	736	736	773
28	680	νC$_\beta$S	—	—	696
29	621	τCO+νC$_\beta$S	644	637	642
30	549	δCOO+δC$_\beta$C$_\alpha$C	—	—	—
31	513	ρCOO	524	—	—
32	444	δN$^+$C$_\alpha$C+γCO+δC$_\alpha$C$_\beta$S	458	—	—
33	327	ρC$_\beta$C$_\alpha$C+δC$_\beta$C$_\alpha$C+τC$_\beta$S	—	—	—
34	315	τC$_\beta$S	—	—	—
35	270	ρC$_\beta$C$_\alpha$C+τC$_\alpha$N$^+$+δCOO+δC$_\beta$C$_\alpha$C+τC$_\beta$S	—	—	—
36	242	τC$_\alpha$N$^+$+τC$_\beta$S	—	—	—
37	193	δC$_\alpha$C$_\beta$S+δN$^+$C$_\alpha$C+τCC$_\beta$	—	—	—
38	94	τC$_\alpha$C$_\beta$	—	—	—
39	59	τC$_\alpha$C	—	—	—

a. Ref. [26] and present study
b. Ref. [31]

Table 6.6: Predicted frequencies and PED of SERH

no.	calc	PED	expt		
			SERH[a]	SER-OMe[a]	SER-zwitt.[b]
1	3490	νOH_{alc}	—	—	—
2	3412	νOH_{acid}	3385	—	—
3	3155	νN^+H	—	—	—
4	3132	νN^+H	—	—	—
5	3045	νN^+H	—	—	—
6	3000	$\nu C_\beta H_2$	—	—	—
7	2970	$\nu C_\alpha H$	—	2956	2975
8	2937	$\nu C_\beta H_2$	—	—	2945
9	1744	$\nu C=O$	1734	1735	—
10	1628	$\delta_a N^+H_3$	—	—	(1637)
11	1612	$\delta_a N^+H_3$	—	1596	(1626)
12	1484	$\delta C_\beta H_2$	—	—	—
13	1481	$\delta_s N^+H_3$	—	—	—
14	1471	$\delta_s N^+H_3 + \nu C\text{-}O + \nu C_\alpha C$	—	1450	1450
15	1437	$\delta C_\beta OH + \omega C_\beta H_2 + \nu C_\alpha C_\beta$	1408	—	1435
16	1365	$\rho C_\beta C_\alpha H + \delta C_\beta C_\alpha H + \delta COH$	—	1378	1364
17	1340	$\delta COH + \delta C_\beta C_\alpha H + \delta C_\beta OH$	1344	1346	—
18	1297	$tC_\beta H_2$	—	1309	1312
19	1249	$\nu C\text{-}O + \delta COH$	1242	—	1248
20	1225	$\omega C_\beta H_2 + \delta C_\beta OH$	—	1227	—
21	1174	$\delta C_\beta C_\alpha H + \rho N^+H_3 + tC_\beta H_2 + \rho C_\beta H_2$	—	1177	1180
22	1144	$\rho N^+H_3 + \rho C_\beta C_\alpha H + \nu C_\alpha N^+$	1132	1131	1162
23	1094	$\nu C_\alpha N^+ + \nu C_\alpha C_\beta$	1077	1064	1095
24	1030	$\nu C_\beta O$	1025	1044	1030
25	980	$\rho C_\beta H_2 + \nu C_\alpha C_\beta + \rho N^+H_3$	970	—	983
26	947	$\rho C_\beta H_2 + \nu CC_\alpha$	—	945	—
27	852	$\nu C_\alpha N^+ + \rho C_\beta H_2 + \nu C_\alpha C_\beta$	829	857	849
28	728	$\gamma CO + \tau CO$	—	—	—
29	620	$\rho COO + \tau CO$	—	635	(619)
30	583	$\tau CO + \delta C_\alpha C_\beta O + \rho COO + \gamma CO$	—	562	566
31	539	$\delta COO + \delta N^- C_\alpha C$	538	514	525
32	425	$\delta C_\alpha C_\beta O + \delta COO + \nu CC_\alpha$	—	—	—
33	340	$\delta N^+ C_\alpha C + \delta CC_\alpha C_\beta + \delta C_\alpha C_\beta O$	—	—	—
34	300	$\delta CC_\alpha C_\beta + \delta COO + \delta N^+ C_\alpha C + \rho COO$	—	—	—
35	265	$\tau C_\beta O$	—	—	—
36	201	$\tau C_\alpha N^+ + \rho CC_\alpha C_\beta$	—	—	—
37	177	$\tau C_\alpha N^+ + \rho CC_\alpha C_\beta$	—	—	—
38	114	$\tau C_\alpha C_\beta$	—	—	—
39	65	$\tau CC_\alpha + \tau CO$	—	—	—

a. Ref. [26]   b. Ref. [30]

* Numbers in the parentheses are from

D,L-serine[33]

Table 6.7: Comparative calculated frequencies of
the amino acid hydrochloride backbone

CYSH	SERH	GH[a]	GGH[a]	PED
3407	3412	3412	3436	νOH
3166	3155	3179	3161	νN⁺H
3115	3132	3124	3109	νN⁺H
3019	3045	3060	2964	νN⁺H
1776	1744	1746	1738	νC=O
1634	1628	1616	1641	δ_aN⁺H₃
1614	1612	1610	1602	δ_aN⁺H₃
1481	1481	1512	1472	δ_sN⁺H₃
1348	1340	1378	1362	δCOH+ωCH₂
1221	1249	1252	1247	νCO+δCOH
1161	1174	1148	1155	ρN⁺H₃
1102	1144	1121	1126	ρN⁺H₃
1069	1094	1042	1050	νCN⁺
732	728	657	661	τC=O
549	539	598	594	δCOO+δN⁺CC

a. Ref.[1]

Table 6.8: Comparative calculated frequencies of
the amino acid hydrochloride sidechain

EtSH	CYSH	EtOH	SERH	PED
—	—	3336	3490	νOH
2932	3003	2920	3000	νCH₂
2902	2950	2877	2937	νCH₂
2571	2590	—	—	νSH
1434	1410	1494	1484	δCH₂
1273	1292	1277/ 1446	1225/ 1437	ωCH₂
1251	1196	1318	1297	tCH₂
—	—	1051	1030	νC-O
737	779	799/ 1153	947/ 980	ρCH₂
657	680	—	—	νCS

Table 6.9: Non-redundant scaled force constants of CYSH

```
 1  4.321
 1   .067  2  4.872
 1   .036  2   .024  3  4.866
 1   .222  2   .063  3   .038  4  3.145
 1   .204  2   .021  3  -.018  4  -.009  5  4.533
 1   .193  2  -.009  3  -.038  4  -.009  5   .187  6  5.042
 1   .064  2   .006  3   .006  4  -.004  5   .068  6   .073  7  4.737
 1  -.006  2  -.015  3   .008  4  -.012  5   .002  6  -.004  7   .000
 8  3.862
 1  -.007  2  -.005  3   .009  4   .032  5   .039  6   .420  7  -.003
 8  -.003  9 12.134
 1  -.025  2   .007  3  -.005  4  -.009  5   .053  6   .321  7   .003
 8   .002  9  1.177 10  6.588
 1  -.008  2   .002  3  -.003  4  -.005  5   .051  6  -.039  7   .001
 8   .000  9  -.003 10  -.062 11  5.506
 1   .005  2   .003  3   .000  4   .004  5   .111  6  -.001  7  -.011
 8  -.001  9  -.035 10   .005 11   .023 12  5.124
 1   .009  2   .002  3   .000  4   .001  5   .033  6  -.014  7   .007
 8   .000  9  -.009 10  -.001 11   .013 12   .013 13  5.396
 1   .003  2  -.002  3   .002  4   .002  5   .004  6  -.011  7   .004
 8   .000  9  -.087 10   .153 11  -.002 12   .004 13   .001 14  6.499
 1   .318  2   .014  3   .000  4   .012  5   .186  6   .256  7  -.120
 8  -.009  9   .050 10   .030 11  -.016 12   .016 13   .013 14   .003
15  1.084
 1  -.295  2  -.018  3   .026  4  -.006  5   .266  6   .286  7   .014
 8   .006  9   .056 10   .127 11  -.070 12  -.030 13   .014 14   .006
15   .061 16  1.322
 1   .066  2  -.018  3   .058  4   .033  5   .310  6  -.238  7   .004
 8   .011  9  -.013 10  -.049 11   .008 12   .002 13  -.016 14  -.002
15   .115 16  -.007 17  1.112
 1   .137  2  -.001  3   .001  4   .044  5  -.179  6  -.088  7  -.030
 8  -.002  9  -.005 10  -.027 11   .008 12   .000 13   .006 14  -.001
15  -.004 16  -.044 17  -.017 18   .609
 1  -.013  2  -.002  3   .008  4  -.004  5   .304  6  -.099  7  -.025
 8  -.006  9  -.036 10  -.021 11  -.012 12  -.002 13  -.019 14   .000
15  -.093 16   .008 17   .020 18  -.051 19   .711
 1   .011  2   .017  3  -.017  4   .227  5  -.007  6   .004  7  -.001
 8  -.004  9   .022 10  -.009 11   .000 12  -.006 13   .000 14   .002
15   .014 16  -.008 17   .003 18  -.001 19   .002 20   .846
```

Table 6.9: (Continued): Non-redundant scaled force constants of CYSH

```
21   1    .002  2  -.005  3    .000  4    .002  5  -.276  6  -.002  7  -.008
     8   -.002  9  -.002 10   -.023 11    .041 12   .015 13   .065 14  -.006
    15   -.004 16  -.022 17   -.019 18    .011 19  -.028 20   .001 21   .553
22   1    .014  2   .006  3   -.001  4    .003  5  -.011  6  -.013  7  -.001
     8   -.001  9   .004 10   -.010 11   -.060 12   .053 13   .047 14  -.001
    15    .004 16  -.041 17    .011 18   -.009 19   .005 20   .004 21   .009
    22    .593
23   1    .011  2   .002  3    .000  4    .003  5   .001  6  -.005  7  -.002
     8    .001  9  -.017 10    .031 11    .022 12   .058 13  -.090 14   .006
    15    .020 16  -.005 17    .017 18    .011 19  -.017 20  -.001 21  -.001
    22   -.009 23   .586
24   1    .020  2  -.008  3    .004  4   -.007  5   .010  6   .011  7   .002
     8   -.001  9  -.042 10    .048 11    .052 12  -.053 13  -.008 14   .008
    15    .046 16  -.054 17    .062 18    .013 19  -.032 20   .002 21  -.004
    22   -.013 23  -.008 24    .740
25   1   -.011  2  -.008  3   -.002  4    .006  5   .019  6  -.004  7   .006
     8    .003  9  -.026 10    .005 11   -.002 12   .102 13  -.021 14   .004
    15   -.063 16  -.040 17   -.008 18   -.034 19   .065 20   .002 21  -.008
    22   -.007 23   .030 24   -.005 25    .760
26   1    .034  2   .000  3    .020  4    .011  5  -.084  6   .306  7   .001
     8    .003  9  -.613 10    .456 11   -.066 12  -.016 13  -.006 14   .070
    15    .067 16   .164 17   -.035 18   -.031 19   .010 20   .007 21   .025
    22   -.010 23  -.007 24    .008 25    .022 26  1.474
27   1   -.016  2   .004  3   -.031  4   -.001  5   .085  6   .351  7   .005
     8   -.007  9  -.078 10   -.288 11   -.020 12  -.009 13  -.004 14   .054
    15    .066 16   .099 17   -.067 18   -.002 19  -.024 20  -.001 21  -.014
    22   -.002 23   .010 24    .003 25   -.016 26   .127 27   .916
28   1    .007  2   .001  3    .001  4    .001  5   .016  6   .043  7   .002
     8    .000  9   .028 10    .208 11    .004 12   .003 13   .001 14   .131
    15    .005 16  -.015 17   -.015 18   -.001 19  -.002 20   .001 21  -.012
    22    .002 23   .007 24    .018 25    .004 26   .097 27   .115 28   .803
29   1   -.151  2   .056  3    .060  4   -.121  5  -.017  6   .004  7   .000
     8    .001  9  -.023 10    .006 11   -.001 12  -.002 13   .000 14  -.002
    15   -.019 16   .019 17   -.019 18    .012 19  -.003 20  -.015 21   .004
    22   -.004 23  -.003 24   -.001 25    .004 26  -.013 27   .005 28  -.002
    29    .537
30   1    .228  2   .009  3    .030  4   -.254  5   .046  6   .011  7  -.006
     8   -.003  9   .020 10    .014 11    .000 12  -.011 13  -.003 14   .000
    15    .050 16  -.054 17    .014 18   -.017 19  -.003 20  -.045 21  -.007
    22    .001 23   .000 24    .009 25   -.001 26   .021 27   .001 28   .003
    29   -.013 30   .591
```

Table 6.9: (Continued): Non-redundant scaled force constants of CYSH

```
31   1  .048  2  .106  3 -.058  4 -.012  5 -.061  6 -.003  7 -.010
     8  .021  9 -.020 10  .042 11  .001 12  .007 13  .005 14 -.003
    15  .017 16  .007 17  .008 18 -.011 19 -.019 20  .089 21  .007
    22 -.006 23  .009 24 -.026 25 -.001 26  .026 27 -.018 28  .001
    29  .002 30  .003 31  .787

32   1 -.005  2  .017  3 -.044  4  .001  5 -.045  6  .008  7 -.004
     8 -.013  9  .000 10  .022 11  .002 12  .005 13  .004 14 -.001
    15 -.028 16  .009 17 -.115 18 -.003 19  .008 20 -.089 21  .002
    22  .010 23 -.007 24 -.023 25 -.006 26  .016 27 -.004 28  .003
    29 -.015 30  .018 31  .012 32  .572

33   1  .354  2 -.054  3 -.029  4  .285  5 -.071  6 -.018  7  .030
     8 -.012  9  .030 10 -.032 11 -.007 12  .034 13 -.001 14 -.001
    15  .124 16 -.018 17  .088 18  .080 19 -.016 20 -.006 21  .029
    22  .016 23  .014 24 -.005 25 -.024 26 -.006 27  .006 28 -.001
    29  .016 30  .004 31  .026 32 -.033 33 1.044

34   1  .003  2 -.002  3 -.002  4  .000  5 -.020  6  .049  7  .020
     8 -.005  9  .003 10  .001 11 -.012 12  .000 13 -.001 14  .002
    15 -.053 16  .008 17  .014 18 -.039 19 -.054 20 -.001 21  .001
    22  .004 23 -.009 24  .014 25  .000 26  .026 27  .034 28  .001
    29  .003 30 -.002 31 -.012 32 -.004 33  .010 34  .450

35   1  .014  2 -.002  3  .007  4 -.017  5  .000  6  .006  7  .000
     8  .016  9  .004 10 -.001 11 -.002 12  .005 13 -.002 14  .002
    15  .018 16  .006 17 -.027 18  .003 19 -.002 20 -.014 21  .001
    22 -.020 23  .012 24  .009 25  .004 26  .000 27  .005 28  .001
    29  .006 30  .013 31 -.049 32 -.003 33  .049 34 -.005 35  .096

36   1 -.022  2  .002  3  .000  4  .008  5 -.018  6 -.027  7  .005
     8  .001  9  .003 10 -.017 11 -.017 12 -.033 13  .006 14 -.001
    15 -.022 16 -.029 17 -.011 18  .017 19 -.011 20 -.004 21 -.011
    22 -.030 23  .003 24  .009 25  .035 26 -.027 27 -.006 28 -.004
    29 -.001 30 -.001 31  .004 32 -.008 33 -.010 34 -.005 35  .019
    36  .118

37   1  .100  2 -.017  3 -.005  4  .032  5 -.004  6  .018  7 -.008
     8  .029  9 -.007 10  .008 11 -.004 12  .011 13  .001 14  .000
    15  .059 16 -.010 17  .087 18  .000 19 -.041 20  .013 21  .005
    22 -.034 23  .027 24  .008 25  .005 26  .002 27  .005 28  .000
    29  .017 30  .008 31  .081 32 -.043 33  .057 34 -.010 35  .046
    36  .022 37  .246

38   1  .015  2 -.002  3  .006  4  .004  5  .014  6  .015  7 -.005
     8  .010  9 -.040 10  .033 11 -.024 12 -.008 13  .000 14  .003
    15  .012 16  .088 17  .031 18 -.030 19  .016 20  .004 21 -.007
    22  .008 23 -.025 24  .006 25  .001 26  .088 27 -.035 28 -.004
    29 -.001 30 -.003 31  .013 32  .002 33 -.001 34 -.001 35  .008
    36 -.008 37  .021 38  .090
```

Table 6.9: (Continued): Non-redundant scaled force constants of CYSH

```
39    1  -.001  2   .001  3   .000  4  -.001  5   .002  6  -.010  7  -.002
      8   .000  9  -.003 10   .008 11   .003 12   .003 13   .000 14   .001
     15   .004 16  -.008 17  -.006 18   .007 19   .010 20   .001 21   .000
     22   .000 23   .000 24  -.001 25  -.001 26  -.005 27  -.001 28   .003
     29  -.001 30   .000 31   .001 32   .002 33  -.002 34  -.013 35  -.003
     36   .000 37  -.004 38   .001 39   .158
```

Table 6.10: Non-redundant scaled force constants of SERH

```
 1    1   4.558
 2    1    .068  2  4.802
 3    1    .035  2   .041  3  4.891
 4    1    .382  2   .185  3   .142  4  4.986
 5    1    .210  2   .020  3  -.024  4   .004  5  4.857
 6    1    .168  2   .005  3  -.016  4  -.027  5   .172  6  5.156
 7    1    .044  2  -.014  3   .007  4   .002  5   .065  6   .052  7  4.849
 8    1   -.008  2  -.009  3  -.003  4  -.027  5   .000  6   .002  7   .000
      8   6.804
 9    1   -.047  2   .016  3  -.005  4   .064  5   .035  6   .501  7  -.003
      8   -.007  9 11.578
10    1   -.000  2   .006  3   .011  4   .007  5   .005  6   .258  7   .003
      8   -.003  9  1.159 10  7.267
11    1    .003  2  -.002  3  -.002  4   .006  5   .070  6  -.037  7  -.015
      8    .003  9  -.033 10   .002 11  5.460
12    1   -.012  2  -.000  3  -.003  4  -.006  5   .026  6  -.007  7   .009
      8    .002  9  -.004 10  -.013 11   .023 12  5.426
13    1   -.030  2   .005  3   .004  4  -.059  5   .095  6  -.018  7  -.001
      8   -.008  9   .004 10  -.012 11   .015 12   .011 13  5.252
14    1    .009  2   .001  3   .002  4  -.009  5  -.002  6  -.016  7   .004
      8    .003  9  -.088 10   .144 11   .001 12   .002 13   .002 14  6.519
15    1    .144  2   .002  3   .017  4   .015  5   .227  6   .263  7  -.098
      8    .006  9   .039 10  -.004 11  -.037 12   .012 13  -.015 14   .005
     15    .963
16    1   -.298  2  -.006  3   .012  4  -.087  5   .242  6   .361  7   .002
      8   -.006  9   .060 10   .016 11  -.042 12  -.029 13   .005 14   .006
     15    .193 16  1.313
17    1    .235  2  -.008  3   .021  4  -.010  5   .361  6  -.102  7   .015
      8    .010  9  -.076 10  -.021 11  -.029 12   .002 13  -.013 14  -.001
     15    .185 16  -.175 17  1.120
18    1    .180  2   .018  3  -.013  4  -.017  5  -.168  6  -.085  7  -.013
      8   -.000  9  -.025 10  -.002 11  -.006 12   .015 13   .004 14   .000
     15    .034 16  -.024 17   .002 18   .622
```

Table 6.10: (Continued): Non-redundant scaled force constants of SERH

```
19   1   .039   2  -.005   3   .007   4   .004   5   .311   6  -.079   7  -.014
     8   .002   9  -.060  10  -.020  11   .011  12  -.021  13  -.003  14   .003
    15  -.054  16   .020  17   .090  18  -.090  19   .702
20   1   .049   2   .008   3   .004   4   .354   5   .022   6  -.001   7   .001
     8   .075   9   .006  10   .003  11   .002  12   .002  13  -.004  14   .000
    15   .007  16  -.016  17  -.013  18  -.003  19   .002  20   .830
21   1   .007   2  -.004   3   .002   4  -.009   5  -.303   6   .002   7  -.008
     8  -.004   9  -.020  10   .008  11   .039  12   .065  13   .002  14  -.004
    15  -.016  16  -.026  17  -.016  18   .014  19  -.017  20  -.014  21   .562
22   1   .006   2  -.002   3   .002   4  -.004   5   .003   6  -.008   7   .000
     8  -.003   9  -.010  10   .006  11  -.063  12   .028  13   .018  14  -.000
    15  -.013  16  -.020  17   .006  18  -.017  19   .010  20  -.002  21  -.004
    22   .584
23   1  -.018   2  -.007   3   .002   4  -.004   5  -.024   6  -.025   7  -.000
     8  -.003   9   .047  10  -.023  11   .049  12   .103  13  -.070  14   .003
    15  -.032  16  -.015  17  -.034  18  -.011  19   .008  20   .001  21   .021
    22   .009  23   .573
24   1   .010   2   .012   3  -.002   4  -.019   5   .006   6  -.023   7   .005
     8  -.000   9   .040  10  -.049  11   .064  12  -.004  13  -.050  14   .003
    15  -.071  16  -.019  17  -.019  18  -.029  19   .060  20  -.011  21  -.011
    22  -.015  23  -.015  24   .769
25   1   .015   2   .000   3   .008   4  -.028   5  -.008   6  -.024   7  -.005
     8  -.007   9   .032  10  -.033  11   .017  12   .024  13  -.122  14   .003
    15  -.003  16  -.075  17   .045  18  -.007  19  -.007  20  -.022  21  -.001
    22   .002  23   .014  24   .006  25   .777
26   1  -.002   2   .004   3  -.023   4   .005   5   .171   6   .092   7  -.023
     8  -.003   9  -.644  10   .376  11   .002  12   .002  13   .001  14   .064
    15   .026  16   .062  17  -.021  18   .026  19   .023  20  -.002  21  -.033
    22  -.002  23   .020  24  -.003  25  -.016  26  1.176
27   1   .006   2   .006   3   .006   4   .023   5  -.059   6   .457   7   .015
     8  -.004   9   .064  10  -.274  11  -.028  12  -.022  13  -.018  14   .057
    15   .064  16   .081  17  -.032  18  -.022  19  -.037  20   .002  21   .015
    22  -.003  23  -.019  24  -.008  25  -.001  26   .057  27  1.015
28   1   .005   2   .000   3   .003   4  -.006   5   .020   6   .048   7   .003
     8   .002   9   .019  10   .246  11  -.002  12   .000  13  -.000   1   .139
    15   .018  16   .025  17   .004  18   .002  19   .001  20   .000  21  -.006
    22  -.003  23   .002  24   .001  25  -.002  26   .102  27   .116  28   .805
29   1  -.119   2   .085   3   .079   4  -.206   5  -.010   6   .006   7  -.002
     8   .005   9  -.005  10  -.000  11   .001  12   .000  13  -.004  14  -.000
    15  -.006  16   .001  17  -.022  18  -.013  19   .002  20   .008  21   .002
    22  -.000  23   .004  24  -.004  25  -.005  26   .002  27  -.000  28  -.001
    29   .564
```

Table 6.10: (Continued): Non-redundant scaled force constants of SERH

```
30   1   .226   2   .007   3   .010   4  -.416   5   .049   6  -.017   7   .007
     8   .030   9   .005  10   .017  11  -.002  12  -.000  13  -.017  14   .002
    15   .012  16  -.035  17   .064  18   .034  19  -.000  20   .008  21  -.010
    22  -.002  23  -.001  24  -.004  25   .003  26   .004  27   .007  28   .002
    29  -.008  30   .697

31   1   .079   2   .083   3  -.073   4   .059   5  -.073   6  -.021   7   .039
     8   .007   9  -.008  10   .003  11   .001  12  -.005  13  -.004  14  -.000
    15  -.058  16   .008  17   .019  18   .061  19   .026  20   .004  21   .013
    22   .020  23   .006  24   .003  25  -.011  26  -.002  27  -.003  28   .000
    29  -.007  30   .012  31   .753

32   1  -.011   2   .043   3  -.040   4  -.032   5  -.042   6  -.015   7   .012
     8  -.004   9   .015  10  -.012  11   .005  12  -.001  13   .007  14  -.001
    15  -.064  16   .048  17  -.084  18   .052  19  -.005  20  -.010  21   .001
    22  -.007  23  -.004  24   .010  25  -.014  26   .004  27  -.005  28  -.001
    29  -.002  30   .014  31  -.068  32   .735

33   1   .543   2  -.045   3  -.042   4   .611   5  -.086   6   .030   7  -.029
     8   .054   9   .056  10   .050  11  -.013  12  -.012  13  -.036  14  -.005
    15   .085  16  -.154  17   .080  18  -.059  19   .040  20   .083  21   .039
    22   .006  23  -.025  24   .027  25   .003  26  -.019  27   .048  28  -.002
    29  -.027  30   .123  31   .110  32  -.029  33  1.607

34   1  -.012   2  -.004   3  -.009   4  -.010   5  -.002   6   .000   7   .016
     8  -.001   9   .012  10   .009  11   .009  12  -.000  13  -.000  14   .001
    15  -.061  16   .031  17   .048  18  -.027  19  -.052  20  -.005  21   .004
    22  -.007  23   .003  24  -.013  25   .007  26   .001  27   .001  28  -.000
    29   .002  30  -.003  31  -.004  32  -.002  33  -.025  34   .438

35   1  -.009   2  -.002   3  -.003   4   .003   5   .010   6   .001   7  -.003
     8  -.007   9   .000  10   .004  11   .002  12  -.000  13   .002  14  -.000
    15  -.006  16   .004  17  -.013  18   .001  19  -.002  20   .016  21  -.005
    22  -.002  23   .001  24  -.003  25  -.007  26  -.001  27   .002  28  -.000
    29  -.001  30   .002  31  -.028  32   .010  33  -.002  34   .000  35   .031

36   1  -.021   2   .002   3   .003   4  -.002   5  -.042   6  -.028   7   .007
     8  -.003   9  -.016  10   .018  11  -.042  12   .010  13  -.018  14  -.001
    15  -.009  16   .001  17  -.035  18  -.008  19  -.010  20  -.001  21  -.009
    22   .064  23   .025  24   .017  25   .005  26   .002  27  -.014  28  -.004
    29  -.002  30  -.004  31   .009  32  -.004  33  -.008  34   .003  35  -.004
    36   .080

37   1  -.233   2   .018   3   .006   4  -.052   5   .020   6   .015   7  -.005
     8  -.003   9   .016  10  -.006  11   .004  12   .008  13   .004  14  -.000
    15   .014  16   .046  17  -.103  18  -.027  19  -.039  20  -.006  21  -.011
    22  -.036  23  -.013  24   .001  25  -.001  26   .016  27  -.005  28  -.001
    29   .002  30  -.034  31  -.071  32   .016  33  -.140  34   .010  35   .010
    36  -.018  37   .170
```

Table 6.10: (Continued): Non-redundant scaled force constants of SERH

38	1	-.002	2	.004	3	-.013	4	.008	5	.023	6	.007	7	.016
	8	-.002	9	-.014	10	.006	11	-.032	12	.002	13	-.014	14	.000
	15	.093	16	-.067	17	-.008	18	.042	19	-.012	20	.001	21	-.018
	22	.001	23	-.021	24	.026	25	-.022	26	.006	27	.009	28	.004
	29	-.006	30	.003	31	-.003	32	.005	33	.004	34	.014	35	-.001
	36	-.047	37	.008	38	.173								
39	1	-.003	2	.002	3	-.001	4	-.003	5	.013	6	.007	7	.003
	8	.000	9	-.001	10	-.010	11	-.001	12	.001	13	-.015	14	-.001
	15	.022	16	-.046	17	.009	18	.017	19	-.010	20	.000	21	-.008
	22	-.013	23	-.007	24	-.001	25	-.016	26	.008	27	-.000	28	.006
	29	.001	30	.000	31	-.000	32	.001	33	-.001	34	.002	35	-.000
	36	-.031	37	.002	38	.078	39	.073							

Bibliography

[1] Bare, G. H.; Alben, J. O.; Bromberg, P. A. *Biochemistry*, **1975**, 14, 1578.

[2] Moh, P. P.; Fiamingo, F. G.; Alben, J. O. *Biochemistry*, **1987**, 26, 6243.

[3] Yu, N. T.; East, E. J. *J. Biol. Chem.*, **1975**, 250, 2196.

[4] Chen, W.; Nie, S.; Kuck, J. F. R., Jr.; Yu, N. T. *Biophys. J.*, **1991**, 60, 447.

[5] Pande, J.; McDermott, M. J.; Callender, R. H.; Spector, A. *Arch. Biochim. Biophys.*, **1989**, 60, 250.

[6] Byler, D. M.; Susi, H.; Farrell, H. M., Jr. *Biopolymers*, **1983**, 22, 2507.

[7] Thomas, G. J., Jr.; Li, Y.; Fuller, M. T.; King, J. *Biochemistry*, **1982**, 21, 3866.

[8] Li, T.; Chen, Z.; Johnson, J. E.; Thomas, G. J., Jr. *Biochemistry*, **1990**, 29, 5018.

[9] Smith, D.; Delvin, J. P.; Scott, D. W. *J. Mol. Spectrosc.*, **1968**, 25, 174.

[10] Richter, W.; Schiel, D. *Chem. Phys. Lett.*, **1984**, 108, 480.

[11] Li, H., Thomas, G. J., Jr. *J Am. Chem. Soc.*, **1991**, 113, 456.

[12] Hayashi, M.; Shiro, Y.; Murata, H. *Bull. Chem. Soc. Jpn.*, **1966**, 39, 112.

[13] Scott, D. W.; El-Sabban, M. Z. *J. Mol. Spectrosc.*, **1969**, 30, 317.

[14] Inagaki, F.; Harada, I.; Shimanouchi, T. *J Mol. Spectrosc.*, **1973**, 46, 381.

[15] Manocha, A. S.; Fateley, W. G.; Shimanouchi, T. *J. Phys. Chem.*, **1973**, 77, 1977.

[16] Durig, J. R.; Bucy, W. E.; Wurrey, C. J.; Carreira, L. A. *J. Phys. Chem.*, **1975**, 79, 988.

[17] Pennington, R. E.; Scott, D.W.; Finke, H. L.; Mccullough, J. P.; Messerley, J. F.; Hossenlopp, I. A.; Waddington, G. *J. Am. Chem. Soc.*, **1956**, 78, 3266.

[18] Ozazki, Y.; Sugeta, H.; Miyazawa, T. *Chemm. Lett.*, **1975**, 713.

[19] Sugeta, H.; Go, A.; Miyazawa, T. *Chem. Lett.*, **1972**, 83.

[20] Sugeta, H.; Go, A.; Miyazawa, T. *Bull. Chem. Soc. Jpn.*, **1973**, 46, 3407.

[21] Nogami, N.; Sugeta, H.; Miyazawa, T. *Chemm. Lett.*, **1975**, 147.

[22] Sugeta, H. *Spectrochim. Acta* **1975**, 31A, 1729.

[23] Nogami, N.; Sugeta, H.; Miyazawa, T. *Bull. Chem. Soc. Jpn.*, **1975**, 48, 2417.

[24] Weiner, S. J.; Kollman, P. A.; Case, D. A.; Singh, U. C.; Ghio, C.; Alagona, G.; Profeta, S.; Weiner, P. *J. Am. Chem. Soc.*, **1984**, 106, 765.

[25] a) Tarakeshwar, P.; Manogaran, S. *J. Mol. Struct. (Theochem)*, **1994**, 305, 205. b) Tarakeshwar, P.; Manogaran, S. *Spectrochim. Acta*, **1994**, 51A, 925.

[26] Susi, H.; Byler, D. M.; Gerasimowicz, W. V. *J. Mol. Struct.*, **1983**, 102, 63.

[27] Madec, C.; Lauransan, J.; Garrigou-Lagrange, C. *Can. J. Spectrosc.*, **1980**, 25, 47.

[28] Madec, C.; Lauransan, J.; Garrigou-Lagrange, C. *Can. J. Spectrosc.*, **1978**, 23, 166.

[29] Machida, K.; Izumi, M.; Kagayama, A. *Spectrochim. Acta*, **1979**, 35A, 1333.

[30] Li, H.; Wurrey, C. J.; Thomas, G. J., Jr. *J. Am. Chem. Soc.*, **1992**, 114, 7463.

[31] Gargaro, A. R.; Barron, L. D.; Hecht, L. *J. Raman Spectrosc.*, **1993**, 24, 91.

[32] Barron, L. D.; Gargaro, A. R.; Hecht, L.; Polavarapu, P. L. *Spectrochim. Acta*, **1991**, 47A, 1001.

[33] Mikawa, Y.; Brasch, J. W.; Jakobsen, R. J. *Spectrochim. Acta*, **1971**, 27A, 529.

144

[34] Qian, W.; Krimm, S. *Biopolymers,* **1992,** 37, 1503.

[35] Von-Nagy-Felsobuki, E. I.; Kimura, K. *J. Phys. Chem.,* **1990,** 94, 8041.

[36] Kakar, R. K.; Quade, C. R. *J. Chem. Phys.,* **1980,** 72, 4300.

[37] Sasada, Y.; Takano, M.; Satoh, T. *J. Mol. Spectrosc.,* **1971,** 38, 33.

[38] a) Hadzi, H.; Jeramic, D. *Spectrochim. Acta,* **1957,** 9, 263. b) Stuart, A. V.; Sutherland, G. B. B. M. *J. Chem. Phys.,* **1956,** 24, 559. c) Krimm, S.; Liang, C. Y.; Sutherland, G. B. B. M. *J. Chem. Phys.,* **1956,** 25, 778.

[39] a)Tanaka, C. *J. Chem. Soc. Japan,* **1962,** , 792. b) Lake, R. F.; Thompson, H. W. *Proc. Roy. Soc.,* **1966,** A291, 469.

Chapter 7

Vibrational Analysis of Glycine Zwitterion

In this chapter, vibrational analysis of the smallest amino acid, glycine (Gly) is presented using Onsager reaction field approach. A complete set of scale factors is obtained for this important amino acid by using the fitting procedure described in chapter 3.

Gly, the smallest member of the amino acid family was the center of attention of many investigations [1-22]. Gly is one of the non essential amino acids and most commonly found in proteins along with leucine and serine. Gly is one of the three amino acids essential for the biosynthesis of the non-proteinic nitrogenous material, creatine, in human and animal tissues. Gly and succinyl CoA are the starting compounds in heme synthesis. Its role in the genesis of nucleotide purine ring as one of the important amino acids cannot be augmented [23].

The experimental IR and Raman spectra of Gly in solution phase is very limited [24,25]. This is because in aqueous solution, the absorption due to the water molecules, especially in the mid IR range, interferes with that of Gly. As a result most of the recent spectroscopic studies of Gly are based on α crystalline form [26-28]. Another important point is that since there is no chiral carbon atom in Gly, the more accurate solution phase VCD and ROA measurements are not available. As a result the correct interpretation of the available solution and/or solid phase experimental spectra requires a good theoretical model.

The structure of Gly is completely different in the gas and liquid phases. In gas phase it exhibits a non-ionic structure (NH_2CH_2COOH), whereas in the liquid or solid it exists

as a zwitterion ($N^+H_3CH_2COO^-$). The ab initio potential energy surface (PES) of gaseous Gly has been studied extensively [1-14]. But the theoretical studies on Gly zwitterion are relatively few [20-22]. Attempts to study the isolated Gly zwitterion using ab initio methods have not been successful so far because the calculation of isolated Gly zwitterion either goes to the gas phase structure or even when optimized restrictively generates imaginary frequency. For example, attempts to deduce the ab initio force field on the Gly zwitterion crystal geometry retains the residual linear forces because this is not a true minima in the PES [20]. Here we show that the choice of appropriate basis set can reach the right minima in the PES but suffer from the intramolecular H-bonding problem which is absent in solid or solution phase. As a result such ab initio calculation on isolated molecule cannot reproduce the true features of experimental vibrational spectra. The extra stability of amino acid zwitterion in the solution or solid phase over the gas phase, comes through the interaction with the solvent and through the intermolecular interactions. Thus the effect of the solvent environment and the intermolecular H-bonding cannot be ignored in the theoretical calculation of amino acid zwitterion. Two different theoretical approaches have emerged for the improvement of the ab initio model in this regard; the supermolecular approach and the Onsager reaction field model. As discussed in chapter 5, the supermolecular approach although produces improved results over the ab initio force field, difficult to generalize to higher systems. This is because with the increase in the number of atoms, the number of water molecules also increases and hence becomes computationally intensive. Also the PEDs get mixed up with the water modes and is difficult to separate. Using the more general Onsager reaction field approach with judicial choice of basis set and the radius of the molecular volume at a particular dielectric medium appears to give the more appropriate solution for describing the amino acid zwitterions.

Thus in this chapter our endeavour is to present a solvated Gly zwitterion calculation with an appropriate choice of basis set and the radius of the cavity (which is achieved on a trial and error basis) which will produce the equivalent of inter-molecular H-bonded environment in the condensed phase of Gly zwitterion. Different basis sets (4-21G, 6-31G*, 6-31+G, 6-31++G, 6-31++G* and 6-31++G**), are used to select 6-31++G* as the right one

for the Onsager model of the Gly zwitterion. Also a complete set of nonredundant force constants for Gly based on the solvated ab initio calculation is presented.

7.1 Calculations

The ab initio force constants and frequencies of Gly were calculated analytically at the optimized geometry. The recommended ab initio radius of solvent model is reduced by 0.5 A° for all the calculations unless otherwise mentioned. The cartesian force constant matrix was transformed to the nonredundant local coordinate. The nonredundant local coordinates of Gly are given in Table-7.1 and Figure 7.1. The fitting procedure described in detail in chapter 3 is used to get the force field of Gly by fitting four different isotopomers. The fitting produced an average deviation of 7.9 cm^{-1} from the available experimental data.

7.2 Results

7.2.1 Geometry

The optimized geometry of solvated Gly obtained by using different basis sets is shown in Table-7.2 along with the crystal structure [29], molecular dynamics (MD) simulated structure [20] and the calculated HF/6-31++G* isolated zwitterion structure. Table-7.2 clearly indicates that the ab initio calculated structure is slightly different from the experimental structure. Even if the optimization is done at its full degree of freedom, the ab initio model produces a structure closer to planar symmetric (Cs) compared to the crystal geometry irrespective of the basis set. In the crystal structure all the three N$^+$H bond lengths are quite different (1.054, 1.037 and 1.025), with the planar N$^+$H slightly longer than the other two. This may be due to different extent of H-bonding experienced by each N$^+$H bond in the crystal environment. In the ab initio calculation, both the out of plane N$^+$H bond lengths are the same in isolated as well as solvated calculations. But the only improvement introduced through the solvent model is the relative difference between the planar and nonplanar N$^+$H gets reduced significantly. In the isolated model the intramolecular H-bonding is more pronounced and hence the planar N$^+$H bond length

(1.053) is much longer than the solvated one (1.020). The CC and CN$^+$ bond lengths are overestimated and do not change much from the isolated model. Both the CO bond lengths are exactly the same in the crystal structure due to the equal extent of H-bonding with the neighbouring N$^+$H$_3$ groups and calculations for the different basis sets produce results close to this. The calculated bond angles for various basis sets are relatively of the same order but 6-31++G* produces slightly improved results over others. The low value of the C(2)-N$^+$(1)-H(3) (planar) angle (98.9°) in the isolated model is probably due to the formation of a five membered ring through intramolecular H-bonding. The 4-21G and 6-31++G** basis sets in solvated model produce structures oriented differently from the other basis sets and are closer to the isolated structure. The optimized structures in isolated and solvated models at 6-31++G* basis set along with the X-ray structure are shown in Figure 7.2.

7.2.2 Selection of the right model

The aim of the present work is to choose a suitable ab initio model for proper description of the features of the experimental vibrational spectra of amino acids, using Gly as a test case. The existing literature on the vibrational spectra of amino acids and their isotopomers infer the following general observations.

i) In most of the solution or solid state spectra N$^+$H$_3$ asymmetric bend and CO asymmetric stretch appear at around 1600 cm^{-1}, the first one appearing at a higher frequency.

ii) N$^+$H$_3$ symmetric bend appears next at around 1520 cm^{-1}, followed by CO symmetric stretch at around 1400 cm^{-1}. The 1400 cm^{-1} is confirmed to be CO stretch because of its invariance to isotopic substitution. Also, in alanine the more accurate VCD spectra show the same difference of around 200 cm^{-1} between the two CO stretches.

iii) Most of the other band positions vary depending on the structure of the amino acids.

Criterion 1: The sensitive frequencies obtained from different basis sets in solvated model are given in Table-7.3 along with their PEDs. The PEDs match with the expected order for δ_aN$^+$H$_3$, ν_aCO and δ_sN$^+$H$_3$ as discussed above only for 6-31++G* basis set.

Criterion 2: The radii used in the solvated model for different basis sets are reduced by 0.5 Åfrom the recommended value since the recommended one corresponds to a value increased by 0.5 Åfrom the actual computed value [30]. Although criterion 1 is met by 6-31++G* basis set, criterion 2 i.e. $\nu_s CO$ should appear as a major component below $\delta_s N^+ H_3$ is not fulfilled properly. So we investigated the effect of the cavity radius on the PEDs. We tried different possibilities and the best model appears to be the one corresponding to a value 3.2 Åas shown in Table-7.3 [31].

After fitting to the experimental frequencies of the four different isotopomers, the fitted force constants produced excellent description of the different normal modes as shown in Tables-7.4 and 7.5.

7.2.3   Vibrational Frequencies

Fitted frequencies of Gly-d_0 is given in Table-7.4 along with their PEDs. Table-7.5 contains the calculated frequencies of different isotopomers. The fitted frequencies are in excellent agreement with the experimental frequencies except for the lowest three, mainly torsions and skeletal deformations. Ab initio model is known to be very poor for these modes. Thus we excluded these numbers in calculating the average error. Our fitted PEDs match very well with the earlier reported PEDs obtained by using the MD simulated force field, [20] with few exceptions. In the fitting we used the experimental data from both crystal and solution spectra. The N^+H and CH frequencies were overestimated significantly in the earlier work, [20] while the present numbers are in good agreement. In this region we choose all bands from the crystal spectra except for 3011 cm^{-1} which is from the solution Gly-d_0. Both the $\delta_a N^+ H_3$ appear above νCO followed by $\delta_s N^+ H_3$ in the Gly-d_0 spectra as expected. All these four bands are calculated at 1645, 1624, 1595 and 1523 cm^{-1} and get shifted to 1174, 1167, 1588 and 1205 cm^{-1} in Gly-N^+D_3, 1643, 1622, 1592 and 1522 cm^{-1} in Gly-CD_2 and 1176, 1168, 1585 and 1208 cm^{-1} in Gly-$N^+D_3CD_2$ spectra. The δCH_2 and νCO modes give a better fit with the 1440 and 1410 cm^{-1} solution phase frequencies and so these are used for the fitting. This 1410 cm^{-1} $\nu CO + \nu CC$ mode remain invariant in different isotopomers as expected. The 1327 cm^{-1} solution band matches very well with

our fitted frequency of 1326 cm^{-1} and is assigned to tCH$_2$ + ρCH$_2$. This band gets shifted to 1316, 935, 930 cm^{-1} in Gly-N$^+$D$_3$, Gly-CD$_2$ and Gly-N$^+$D$_3$CD$_2$ respectively. The 1138 and 1119 cm^{-1} bands are both assigned as mixed modes of ρN$^+$H$_3$, tCH$_2$ and ρCH$_2$. These two bands shift in isotopic spectra to 821, 763 cm^{-1} in N$^+$D$_3$, 1215, 1178 cm^{-1} in CD$_2$ and 807 and 707 cm^{-1} in N$^+$D$_3$CD$_2$ spectra respectively. The 1037 cm^{-1} crystal band is used for νCN$^+$ mode in Gly-d$_0$ and it agrees very well with our 1039 cm^{-1} band. The δCOO + δCCN$^+$ + ρCOO mixed mode could be assigned to either 704 cm^{-1} from the crystal spectra or to 665 cm^{-1} from the solution in Gly-d$_0$. Earlier SQM assignment matches well with the solution phase value. Our fitting produces this band at 668 cm^{-1} and is in support to the earlier SQM assignment. This frequency gets shifted to 634, 646, 618 cm^{-1} respectively in the other three isotopomers, in good agreement with the expected experimental fundamentals confirming the assignment.

The non redundant fitted force constants of Gly is given in Table-7.6.

7.3 Conclusions

The Onsager reaction field approach is found to be very successful in reproducing the vibrational spectra of the smallest amino acid, Gly. The selection of basis set and the radius of the molecular volume is considered as two prime factors for mimicking the experimental spectra within this model. The fitting procedure to obtain the scale factors from the ab initio force field of Gly has shown to be very successful giving an average deviation of 7.9 cm^{-1} between the predicted and the experimental frequencies for four isotopomers. A complete set of non redundant force constants were obtained for Gly. The excellent agreement between the fitted and experimental frequencies clearly implies that the methodology could, in principle, be applied successfully to other amino acids.
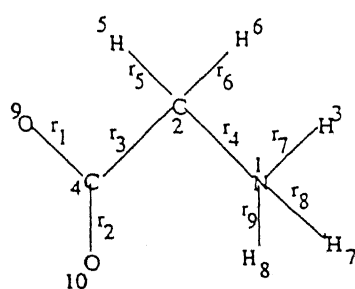
al= O(9)-C(4)-O(10), bl= C(2)-C(4)-O(10), b2= C(2)-(4)-O(10)

a2= H(5)-C(2)-H(6), a3= C(4)-C(2)-H(5), a4= C(4)-C(2)-H(6)

b3= N(1)-C(2)-H(5), b4= N(1)-C(2)-H(6), b5= N(1)-C(2)-C(4)

a5= H(3)-N(1)-H(7), a6= H(3)-N(1)-H(8), a7= H(7)-N(1)-H(8)

b6= C(2)-N(1)-H(3), b7= C(2)-N(1)-H(7), b8= C(2)-N(1)-H(8)

Figure 7.1: Internal coordinates of Gly.
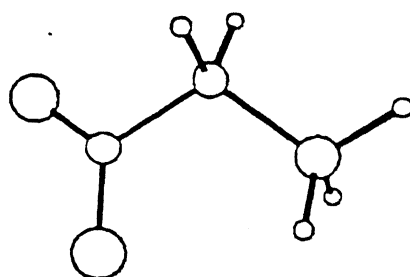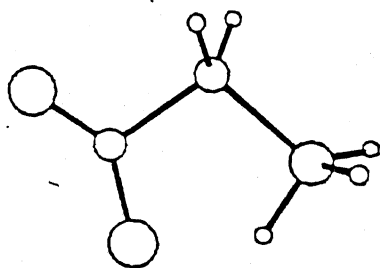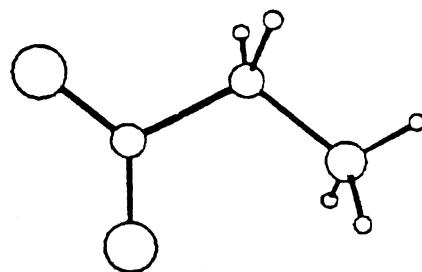
Figure 7.2: Structure of X-ray and optimized Gly using 6-31++G* basis set. a) X-ray structure b) isolated c) solvated with radius 3.2 Å

Table 7.1: Local symmetry coordinates^a of Gly

$S_{1-9}=$	r_{1-9}(all stretch)	$S_{17}=$	$a_5+a_6+a_7-b_6-b_7-b_8$ $(\delta_s N^+H_3)$
$S_{10}=$	$2a_1-b_1-b_2$ (δCOO)	$S_{18}=$	$2a_7-a_5-a_6$ $(\delta_a N^+H_3)$
$S_{11}=$	b_1-b_2 (δCOO)	$S_{19}=$	a_5-a_6 $(\delta_a N^+H_3)$
$S_{12}=$	$4a_2-a_3-a_4-b_3-b_4$ (δCH_2)	$S_{20}=$	$2b_6-b_7-b_8$ (ρN^+H_3)
$S_{13}=$	$a_3+a_4-b_3-b_4$ (ωCH_2)	$S_{21}=$	b_7-b_8 (ρN^+H_3)
$S_{14}=$	$a_3-a_4+b_3-b_4$ (ρCH_2)	$S_{22}=$	γ_{24910} (γCO)
$S_{15}=$	$a_3-a_4-b_3+b_4$ (tCH_2)	$S_{23}=$	τ_{24} (τCC)
$S_{16}=$	$5b_5-a_2-a_3-a_4-b_3-b_4$ (δCCN^+)	$S_{24}=$	τ_{21} (τCN^+)

a. Internal coordinate numberings are according to Figure 7.1.

Table-7.2: Optimized geometries of Gly at different basis sets*

Internal[a] coord.	Solvated zwitterion at different basis sets						Molecular[b] dynamics	Crystal[c]	Isolated[c] 6-31++G*
	4-21G	6-31G*	6-31++G	6-31++G* 3.1	3.2	6-31++G**			
N1-C2	1.527	1.504	1.514	1.502	1.501	1.502	1.510	1.476	1.504
N1-H3	1.041	1.024	1.032	1.020	1.018	1.014	1.064	1.054	1.053
N1-H7	1.017	1.011	1.013	1.011	1.010	1.013	1.051	1.037	1.005
N1-H8	1.017	1.011	1.013	1.011	1.010	1.010	1.033	1.025	1.005
C2-H5	1.078	1.080	1.081	1.080	1.080	1.079	1.081	1.089	1.079
C2-H6	1.078	1.080	1.081	1.080	1.080	1.081	1.080	1.090	1.079
C2-C4	1.575	1.559	1.560	1.553	1.552	1.552	1.536	1.526	1.566
C4-O9	1.259	1.226	1.252	1.228	1.229	1.231	1.245	1.250	1.245
C4-O10	1.245	1.252	1.305	1.250	1.244	1.240	1.260	1.250	1.207
C2-N1-H3	113.5	111.8	110.3	111.9	112.3	113.2	115.8	112.1	98.9
C2-N1-H7	101.2	113.5	115.2	112.9	112.0	108.6	117.0	111.7	114.0
C2-N1-H8	113.5	113.5	115.2	112.9	112.4	112.8	113.8	110.4	114.0
N1-C2-H5	109.1	106.4	106.1	106.8	107.2	108.4	105.3	109.0	109.6
N1-C2-H6	109.1	106.4	106.1	106.8	107.0	107.5	105.4	108.5	109.6
N1-C2-C4	106.6	117.0	121.0	115.0	113.5	112.1	112.2	111.8	105.4
C2-C4-O9	113.8	126.8	122.9	118.0	117.0	116.3	114.7	117.5	112.0
C2-C4-O10	116.5	118.9	115.2	114.4	114.5	114.8	113.8	117.1	115.0
H3-N1-C2-H5	119.2	56.9	56.5	57.4	62.5	93.1	48.5	55.6	-119.8
H7-N1-C2-H5	-120.9	176.2	173.9	177.3	-177.1	-145.3	169.4	177.9	123.0
H8-N1-C2-H5	-1.1	-62.3	-60.8	-62.5	-58.1	-26.8	-72.1	-63.7	-2.7
H3-N1-C2-H6	1.1	-57.0	-56.6	-57.6	-53.4	-23.5	-65.1	-62.8	119.8
H3-N1-C2-C4	-119.8	179.9	180.0	179.8	-175.2	-143.6	170.3	183.7	-0.0
N1-C2-C4-O9	-0.0	-0.0	-0.0	-0.0	2.1	7.1	21.9	18.9	-0.0
N1-C2-C4-O10	-180.0	180.0	180.0	-179.9	-178.3	-171.2	-158.0	-161.8	180.0

a. Bond lengths are in A° and angles are in rad.
b. Ref. [20]
c. Ref. [29]
* The recommended radius in Gaussian-94 is reduced by 0.5 A° in different basis set calculations. In 6-31++G*, this corresponds to 3.1 (see text).

Table-7.3: Selective unscaled vibrational frequencies of solvated Gly at different basis sets[a]

Expt.[a]	4-21G	6-31G*	6-31+G	6-31++G	6-31++G**
1634	1842 $\delta_a N^+H_3$	1848 νCO	1830 $\delta_a N^+H_3$	1838 $\delta_a N^+H_3$	1817 νCO
1618	1840 $\delta_a N^+H_3+\nu CO$	1812 $\delta_a N^+H_3$	1827 $\delta_a N^+H_3+\delta_s N^+H_3$	1836 $\delta_a N^+H_3$	1804 $\delta_a N^+H_3$
1597	1817 $\nu CO+\delta_a N^+H_3$ $\delta_s N^+H_3$	1809 $\delta_a N^+H_3$	1776 $\delta_s N^+H_3+\delta_a N^+H_3$	1774 $\delta_s N^+H_3$	1776 $\delta_a N^+H_3$
1533	1646 $\delta_s N^+H_3+\delta CH_2$ ωCH_2	1708 $\delta_s N^+H_3$	1640 $\nu CO+\delta CH_2$	1648 $\nu CO+\delta CH_2$	1645 $\delta_s N^+H_3$
1410	1467 ωCH_2	1566 $\omega CH_2+\nu CO$ νCC	1532 $\omega CH_2+\nu CO$ νCC	1541 $\omega CH_2+\nu CC$ νCO	1548 $\omega CH_2+\nu CC$ νCO
1138	1227 $\rho N^+H_3+\omega CH_2$	1197 $tCH_2+\rho CH_2$ $\rho N^+H_3+\gamma CO$	1238 $\rho N^+H_3+tCH_2$ ρCH_2	1232 $\rho N^+H_3+tCH_2$ ρCH_2	1189 $tCH_2+\rho CH_2$ $\rho N^+H_3+\gamma CO$
1119	1191 $\rho N^+H_3+tCH_2$ ρCH_2	1164 $\rho N^+H_3+\omega CH_2$	1202 ρN^+H_3	1208 $\rho N^+H_3+\omega CH_2$	1169 $\rho N^+H_3+\omega CH_2$

Expt.[a]	6-31++G*(3.1)	6-31++G*(3.6)	6-31++G*(3.35)	6-31++G*(3.2)
1634	1818 $\delta_a N^+H_3(80)$	1860 $\nu CO(84)$	1835 $\nu CO(48)+\delta_a N^+H_3(42)$	1824 $\delta_a N^+H_3(63)+\nu CO(28)$
1618	1805 $\delta_a N^+H_3(94)$	1836 $\delta_a N^+H_3(96)$	1832 $\delta_a N^+H_3(52)+\nu CO(38)$	1806 $\delta_a N^+H_3(74)$
1597	1790 $\nu CO(74)$	1813 $\delta_a N^+H_3(81)$	1804 $\delta_a N^+H_3(70)$	1799 $\nu CO(52)+\delta_a N^+H_3(32)$
1533	1699 $\delta_s N^+H_3(79)$	1642 $\delta_s N^+H_3(65)+\delta CH_2(17)$	1662 $\delta_s N^+H_3(77)$	1695 $\delta_s N^+H_3(83)$
1410	1564 $\omega CH_2(40)+\nu CC(18)$ $\nu CO(15)$	1534 $\nu CO(45)+\nu CC(20)$ $\omega CH_2(16)$	1549 $\nu CO(37)+\omega CH_2(24)$ $\nu CC(20)$	1563 $\omega CH_2(35)+\nu CO(29)$ $\nu CC(19)$
1138	1198 $\rho N^+H_3(31)+tCH_2(28)$ $\rho CH_2(25)+\gamma CO(14)$	1188 $\rho N^+H_3(28)+tCH_2(27)$ $\rho CH_2(21)+\gamma CO(14)$	1194 $\rho N^+H_3(37)+tCH_2(26)$ $\rho CH_2(22)+\gamma CO(12)$	1191 $tCH_2(30)+\rho N^+H_3(29)$ $\rho CH_2(25)+\gamma CO(14)$
1119	1170 $\rho N^+H_3(64)+\omega CH_2(13)$	1181 $\rho N^+H_3(67)+\omega CH_2(12)$	1176 $\rho N^+H_3(64)+\omega CH_2(12)$	1172 $\rho N^+H_3(62)+\omega CH_2(13)$

a. Ref. [24,25]

* The recommended radius in Gaussian-94 is reduced by 0.5 A° in different basis set calculations. In 6-31++G*, this corresponds to 3.1 (see text).

Table-7.4: Frequencies of isolated and solvated (radius=3.2 A°) Gly-d$_0$ at 6-31++G* basis set

No.	Isolated				Solvated		
	unscaled	PED	unscaled	PED	fitted	expt[a]	PED
1	3806	νN^+H	3740	νN^+H	3188	3180	νN^+H
2	3730	νN^+H	3702	νN^+H	3162	3152	νN^+H
3	3364	νCH	3590	νCH	3078	3058	νN^+H
4	3298	νCH	3347	νCH	3025	3011	νCH
5	2991	νN^+H	3289	νCH	2975	2973	νCH
6	1957	νCO	1824	$\delta_a N^+H_3(63)+\nu CO(28)$	1645	1634	$\delta_a N^+H_3(82)+\delta_s N^+H_3(12)$
7	1834	$\delta_a N^+H_3$	1806	$\delta_a N^+H_3(74)$	1624	1618	$\delta_a N^+H_3(91)$
8	1794	$\delta_a N^+H_3+\delta_s N^+H_3$	1799	$\nu CO(52)+\delta_a N^+H_3(32)$	1595	1597	$\nu CO(77)$
9	1697	δCH_2	1695	$\delta_s N^+H_3(83)$	1523	1533	$\delta_s N^+H_3(81)+\nu CO(11)$
10	1537	$\delta_s N^+H_3+\nu CO$	1614	δCH_2	1438	1440	$\delta CH_2+\omega CH_2+\nu CO$
11	1467	$\nu CO+\omega CH_2+\nu CC$	1563	$\omega CH_2(35)+\nu CO(29)+\nu CC(19)$	1415	1410	$\nu CO(29)+\delta CH_2(27)+\nu CC(21)$
12	1413	$\omega CH_2+\delta_s N^+H_3+\nu CO$	1463	$\omega CH_2+\nu CO$	1326	1327	$t CH_2+\rho N^+H_3+\rho CH_2$
13	1410	$t CH_2+\rho N^+H_3$	1454	$t CH_2+\rho N^+H_3$	1318	1315	$\omega CH_2+\nu CO$
14	1170	$\rho N^+H_3+\omega CH_2$	1194	$t CH_2(30)+\rho N^+H_3(29)+\rho CH_2(25)+\gamma CO(14)$	1135	1138	$\rho N^+H_3(49)+\omega CH_2(18)+\nu CN^+(16)$
15	1166	$t CH_2+\rho N^+H_3+\rho CH_2+\gamma CO$	1172	$\rho N^+H_3(62)+\omega CH_2(13)$	1096	1119	$t CH_2(44)+\rho CH_2(23)+\rho N^+H_3(18)+\gamma CO(14)$
16	1007	νCN^+	1057	$\nu CN^++\nu CC$	1039	1037	νCN^+
17	996	$\rho CH_2+\rho N^+H_3+\gamma CO$	970	$\rho N^+H_3+\rho CH_2+\gamma CO$	938	919	$\rho N^+H_3+\rho CH_2+\gamma CO$
18	934	$\nu CC+\delta COO$	928	$\delta COO+\nu CC+\nu CN^+$	882	896	$\nu CC+\delta COO$
19	748	$\delta COO+\delta CCN^++t CH_2$	702	$\delta COO+\nu CC+\delta CCN^+$	668	665	$\delta COO+\delta CH_2+\rho COO$
20	615	$\gamma CO+\rho CH_2+t CH_2$	643	$\gamma CO+\rho CH_2$	615	613	$\gamma CO+\rho CH_2$
21	539	$\delta COO+\nu CC+\delta CCN^++\nu CN^+$	502	$\delta COO+\nu CC+\delta COO+\nu CN^+$	498	507	$\rho COO+\delta COO+\nu CC+\nu CN^+$
22	354	$\delta COO+\delta CCN^++\nu N^+H$	240	$\delta CCN^++\rho COO$	242	—	$\delta CCN^++\rho COO$
23	299	$\tau CN^++\delta_a N^+H_3$	170	$\tau CN^++\tau CC$	169	364	$\tau CN^++\tau CC$
24	90	$\tau CN^++\tau CC$	20	$\tau CC+\tau CN^+$	22	238	$\tau CC+\tau CN^++\delta_a N^+H_3$

a. Ref. [24,25]

Table 7.6: The symbolic F matrix of Gly in non-redundant local coordinates

```
1
2   3
4   5   6
7   8   9   10
11  12  13  14  15
16  17  18  19  20  21
22  23  24  25  26  27  28
29  30  31  32  33  34  35  36
37  38  39  40  41  42  43  44  45
46  47  48  49  50  51  52  53  54  55
56  57  58  59  60  61  62  63  64  65  66
67  68  69  70  71  72  73  74  75  76  77  78
79  80  81  82  83  84  85  86  87  88  89  90  91
92  93  94  95  96  97  98  99  100 101 102 103 104 105
106 107 108 109 110 111 112 113 114 115 116 117 118 119 120
121 122 123 124 125 126 127 128 129 130 131 132 133 134 135 136
137 138 139 140 141 142 143 144 145 146 147 148 149 150 151 152 153
154 155 156 157 158 159 160 161 162 163 164 165 166 167 168 169 170 171
172 173 174 175 176 177 178 179 180 181 182 183 184 185 186 187 188 189
190
191 192 193 194 195 196 197 198 199 200 201 202 203 204 205 206 207 208
209 210
211 212 213 214 215 216 217 218 219 220 221 222 223 224 225 226 227 228
229 230 231
232 233 234 235 236 237 238 239 240 241 242 243 244 245 246 247 248 249
250 251 252 253
254 255 256 257 258 259 260 261 262 263 264 265 266 267 268 269 270 271
272 273 274 275 276
277 278 279 280 281 282 283 284 285 286 287 288 289 290 291 292 293 294
295 296 297 298 299 300
```

Fitted non-redundant force constants of Gly

```
 8.577   2.154  10.089   0.461   0.544   4.123   0.104  -0.005   0.080
 4.719   0.011   0.009   0.023   0.082   4.949   0.010   0.011   0.026
 0.085   0.038   4.948  -0.027  -0.044  -0.031   0.027   0.001   0.002
 5.312   0.009  -0.035  -0.011   0.048  -0.022   0.002   0.028   5.570
 0.012  -0.038  -0.009   0.037   0.003  -0.023   0.022   0.030   5.556
 0.325   0.299  -0.374  -0.021  -0.002  -0.004   0.050   0.015   0.016
 1.174   0.398  -0.342   0.042  -0.261   0.036   0.045  -0.010  -0.020
-0.018  -0.017   1.104  -0.017   0.007  -0.083  -0.200   0.078   0.074
 0.006  -0.003  -0.001   0.005  -0.043   0.548   0.061   0.027   0.100
```

Table 7.6: (Continued): The symbolic F matrix of Gly in local coordinates

-0.432	-0.025	-0.022	0.016	0.004	0.005	-0.032	0.057	0.068
0.632	0.002	-0.001	0.000	0.001	0.089	-0.093	0.005	0.023
-0.029	-0.001	0.001	-0.002	0.003	0.949	0.001	0.001	0.000
0.004	-0.003	0.002	-0.002	-0.011	0.009	-0.000	0.007	0.001
-0.004	-0.196	0.606	-0.058	0.072	0.144	0.076	-0.051	-0.035
-0.013	-0.049	-0.046	-0.010	-0.179	0.017	0.038	-0.003	-0.002
1.079	-0.036	0.038	0.014	-0.258	-0.011	-0.011	0.069	0.067
0.075	-0.008	0.052	0.011	0.027	-0.002	-0.002	0.031	0.565
0.020	-0.028	-0.044	-0.039	-0.001	-0.002	-0.074	0.050	0.042
0.018	-0.041	0.004	0.006	0.003	-0.003	-0.039	0.018	0.594
-0.007	0.003	0.004	0.003	-0.001	0.001	-0.006	0.067	-0.072
-0.001	0.006	-0.000	0.001	-0.041	-0.001	0.013	-0.003	0.002
0.623	-0.007	0.081	0.034	-0.002	-0.002	-0.004	-0.008	-0.006
0.004	-0.022	-0.010	0.033	0.036	-0.000	-0.003	0.100	-0.021
0.008	-0.001	0.738	0.003	-0.008	-0.006	-0.001	0.006	-0.005
-0.003	0.008	-0.000	0.002	-0.003	-0.001	-0.001	0.070	-0.071
-0.006	0.003	-0.002	0.043	0.001	0.664	0.002	0.002	-0.001
0.000	0.020	-0.021	-0.001	-0.003	0.008	0.003	0.002	0.002
-0.002	0.044	0.070	0.003	0.001	0.002	0.019	0.001	-0.009
0.532	-0.004	0.003	-0.002	0.004	0.014	-0.014	-0.000	-0.023
0.012	0.001	0.008	-0.002	-0.000	-0.111	0.009	0.004	-0.003
-0.006	-0.009	-0.003	0.023	0.074	0.105	-0.005	0.005	-0.002
-0.011	0.003	0.001	0.005	-0.008	-0.008	0.001	0.000	0.001
0.005	-0.003	-0.010	0.004	-0.002	-0.004	-0.060	-0.008	0.019
0.007	-0.028	0.024						

Bibliography

[1] a) Vijay, A.; Sathyanarayana, D. N. *J. Phys. Chem.*, **1992**, 96, 10735. b) Grenie, Y.; Lagrange, C. G. *J. Mol. Spectrosc.*, **1972**, 41, 240.

[2] Csaszar, A. G. *J. Am. Chem. Soc.*, **1992**, 114, 9568.

[3] Frey, R. F.; Coffin, J.; Newton, S. Q.; Ramek, M.; Cheng, V. K. W.; Momany, F. A.; Schafer, L. *J. Am. Chem. Soc.*, **1992**, 114, 5369.

[4] Jensen, J. H.; Gordon, M. S. *J. Am. Chem. Soc.*, **1991**, 113, 7917.

[5] a) Ramek, M. *Int. J. Quantum Chem., Quantum Biol. Symp.*, **1990**, 17, 45. b) Ramek, M.; Cheng, V. K. W.; Frey, R. F.; Newton, S. Q.; Schafer, L. *J. Mol. Struct. (Theochem)*, **1991**, 235, 1.

[6] a) Sellers, H. L.; Schafer, L. *J. Am. Chem. Soc.*, **1978**, 100, 7728. b) Schafer, L.; Sellers, H. L.; Lovas, F. J.; Suenram, R. D. *J. Am. Chem. Soc.*, **1980**, 102, 6566.

[7] a) Vishveshwara, S.; Pople, J. A. *J. Am. Chem. Soc.*, **1977**, 99, 2422. b)Tse, Y. C.; Newton, M. D.; Vishveshwara, S.; Pople, J. A. *J. Am. Chem. Soc.*, **1978**, 100, 4329.

[8] Dykstra, C. E.; Chiles, R. A.; Garrett, M. D. *J. Comput. Chem.*, **1981**, 2, 266.

[9] a) Clementi, E.; Cavallone, F.; Scordamagila, R. J. *J. Am. Chem. Soc.*, **1977**, 99, 5531. b) Carozzo, L.; Corongiu, C.; Petrongolo, C.; Clementi, E. *J. Chem. Phys.*, **1978**, 68, 787.

[10] Siam, K.; Klimkowski, V. J.; Ewbank, J. D.; Van Alsenoy, C.; L. *J. Mol. Struct. (Theochem)*, **1984**, 110, 171.

[11] a) Palla, P.; Petrongolo, C.; Tomasi, J. *J. Phys. Chem.*, **1980**, 84, 435. b) Bonaccorsi, R.; Palla, P.; Tomasi, J. *J. Am. Chem. Soc.*, **1984**, 106, 1945.

[12] Wright, L. R.; Borkman, R. F. *J. Am. Chem. Soc.*, **1980**, 102, 6207.

[13] a) Imamura, A.; Fujita, H.; Nogata, C. *Bull. Chem. Soc. Jpn.*, **1969**, 3118. b) Oegerle, W. R.; Sabin, J. R. *J. Mol. Struct.*, **1973**, 15, 131. c) Chung, K.; Hedges, R. M.; Macfarlane, R. D. *J. Am. Chem. Soc.*, **1976**, 98, 7523. d) Kier, L. B.; George, J. M. *Theor. Chim. Acta*, **1969**, 14, 258.

[14] Millefiori, S.; Millefiori, A. *J. Mol.Struct.*, **1983**, 91, 391.

[15] Sulzbatch, H. M.; Schleyer, P. V. R.; Schaefer, H. F. *J. Am. Chem. Soc.*, **1994**, 116, 3967.

[16] a) Brown, R. D.; Godfrey, P. D.; Storey, J. W. V.; Bassez, M. P. *J. Chem. Soc. Chem. Commun.*, **1978**, 547. b) Brown, R. D.; Godfrey, P. D.; Storey, J. W. V.; Bassez, M. P.; Robinson, B. J.; Batchelor, R. A.; McCulloch, M. G.; Rydbeck, O. E. H.; Hjalmarson, A. G. *Mon. Not. R. Astron. Soc.*, **1979**, 186, 5.

[17] a) Suenram, R. D.; Lovas, F. J. *J. Mol. Struct.*, **1978**, 72, 372. b) Suenram, R. D.; Lovas, F. J. *J. Am. Chwem. Soc.*, **1980**, 102, 7180.

[18] Iijima, K.; Tanaka, K.; Onuma, S. *J. Mol. Struct.*, **1991**, 246, 257.

[19] Almlof, J.; Kvick, A.; Thomas, J. O. *J. Chem. Phys*, **1973**, 59, 3901.

[20] a) Alper, J. S.; Dothe, H.; Coker, D. F. *Chem. Phys.*, **1991**, 153, 51. b) Alper, J. S.; Dothe, H.; Lowe, M. A. *Chem. Phys,*, **1992**, 161, 199.

[21] Jensen, J. H.; Gordon, M. S. *J. Am. Chem. Soc.*, **1995**, 117, 8159.

[22] Ding, Y.; Korgh-Jespersen, K. K. *Chem. Phys. Lett.*, **1992**, 199, 261.

[23] Stroev, E. A.. in Biochemistry, Mir Publishers Moscow, **1989**.

[24] Takeda, M.; Iavazzo, R. E. S.; Garfinkel, D.; Scheinberg, I. H.; Edsall, J. T. *J. Am. Chem. Soc.*, **1958**, 80, 3813.

[25] Ghazanfar, S. A. S.; Myers, D. V.; Edsall, J. T. *J. Am. Chem. Soc.*, **1964**, 86, 3439.

[26] Kakihana, M.; Akiyama, M.; Nagumo, T.; Okamoto, M. *Z. Naturforsch*, **1988**, 43A, 774.

[27] Destrade, C.; Garrigou-Lagrange, C.; Forel, M. T. *J. Mol. Struct.*, **1971**, 10, 203.

[28] Machida, K.; Kagayama, A.; Saito, Y.; Kuroda, Y.; Uno, T. *Spectrochim. Acta*, **1977**, 33A, 569.

[29] Jonsson, P. G.; Kvick, A. *Acta Cryst.*, **1972**, 28B, 1827.

[30] Frisch, M. J.; Frisch, A.; Foresman, J. B. in Gaussian 94 User's Reference, Gaussian, Inc., Pittsburgh, 1994, p 151.

[31] Between 3.21 to 3.33 Åradius the calculation of the Onsager model produces one imaginary frequency for the lowest torsional mode (τCC). The calculated frequency for this particular mode changes from radius 3.10 to 3.35 Åas follows: 42 cm^{-1} at 3.1, 20 cm^{-1} at 3.2, -4 cm^{-1} at 3.21, -25 cm^{-1} at 3.25, -42 cm^{-1} at 3.30 and 64 cm^{-1} at 3.35 Å. The optimized structures for all these radii resemble very closely and so it is difficult to explain why some values produce negative frequency. It appears that the shallow potential for this coordinate is partly responsible for this problem as mentioned by Bour et al. (Bour, p.; Tam, C. N.; Shaharuzzaman, M.; Chickos, J. S.; Keiderling, T. A. *J. Phys. Chem.*, **1996**, 100, 15041.).

Chapter 8

Theoretical Prediction of the Vibrational spectra of Cysteine and Serine Zwitterions

There have been a number of ab initio studies of the gas phase vibrational analysis of amino acids, such as glycine [1], alanine (Ala) [2], cysteine (Cys), serine (Ser) [3], and proline [4]. In the zwitterionic form a solvated model of glycine was used to obtain the vibrational frequencies and assignments as described in chapter 7. A good number studies of Ala in the solid state in both IR and Raman spectroscopy is available in the literature [5-18]. Ala being the smallest chiral amino acid, was the subject of interest for VCD and ROA spectra [2,19,20]. A complete vibrational assignment based on VCD spectra using Urey-Bradeley force field of Ala in solution was first presented by Diem et al. [20]. The ab initio calculations of isolated molecule [2] and more recently the Onsager reaction field model [19] were used to assign the experimental vibrational spectra of Ala zwitterion in the region 800 to 1600 cm^{-1}. Ab initio isolated model calculations of Cys and Ser were used to assign their experimental spectra [21]. The previous quantum mechanical calculations of Cys include studies of protonation and ionization potential [22], a comparison of PCILO and SCF results [23] and minimum energy conformations [24]. Calculations of Ser include studies of protonation [23,25,26], lattice energies [27], energy differences of enantiomers [28,29], crystal and peptide structures [30] and low energy conformations [31,32]. The thiol group in the Cys residue side chain is responsible for the stabilization of the secondary structure of proteins and hence was the subject of a number of spectroscopic studies for

163

characterizing its conformers (chapter 6). In the experimental side, solid state structures of L-Cys and L-Ser have been determined by neutron diffraction [33,34] and a large number of vibrational spectral studies of Cys and Ser zwitterions are available [35-40], the most recent one being that of Gargaro et al. based on their ROA study [40].

In this chapter, the scale factors of Ala, EtSH and EtOH are generated by fitting their ab initio force constants to their respective experimental spectra. The vibrational spectra of Cys and Ser zwitterions are theoretically predicted by transferring the scale factors of Ala for the backbone and EtSH and EtOH for the side chain respectively. A complete set of non-redundant force constants of Cys and Ser are also presented.

8.1 Calculations

The ab initio force constants and frequencies of Cys, Ser, Ala, EtSH and EtOH were calculated analytically for the optimized geometries at 6-31++G* level using the Onsager reaction field approach to include the solvent effect. The cartesian force constant matrices were then transformed to the non-redundant local coordinate space. The non-redundant local coordinates of EtSH and EtOH are same as used in chapter 6, that of Ala is given in Table-8.1 and Figure 8.1 and the corresponding Cys and Ser are given in Table-8.2 and Figure 8.2. The optimized geometry of Ala is given in Table-8.3 and those of Cys and Ser are given in Table-8.4. The ab initio force fields of Ala, EtSH and EtOH were then fitted to their corresponding experimental spectra to obtain a non-redundant set of force constants and scale factors using the methodology described in chapter 3. We used experimental frequencies from five different isotopomers namely, Ala-d_0, Ala-Cd_3, AlaN$^+d_3$, Ala-CdN^+d_3 and Ala-$Cd_3N^+d_3$ for the present study. Radius of 3.3 Åwas used for the solvated model calculation of Ala. The scale factors of EtSH and EtOH along with Ala when used to scale the ab initio force fields of Cys and Ser, good agreements were obtained with experimental frequencies. Cavity radii of 3.5 and 3.4 Åwere used for the solvated model calculations of Cys and Ser respectively.

8.2 Results

EtSH and EtOH

The most stable gauche form in the isolated EtSH calculation (chapter 6) is retained in the solvated model calculation for the present study at 6-31++G* level. The ab initio calculated frequencies are fitted to the experimental ones reported in chapter 6. In EtOH again the most staggered conformation is retained as the most stable one in the solvated model calculation, following our earlier EtOH result reported in chapter 6. In condensed phase the presence of intermolecular H-bonding causes a lowering of the νOH frequency in EtOH. In the present solvated study of EtOH the νOH frequency is lowered compared to the earlier ab initio calculation on the isolated molecule as expected. We used the same experimental frequencies (as reported in chapter 6) to fit the ab initio calculated frequencies in the present study. The fitted frequencies and their PEDs of both EtSH and EtOH are shown in Table-8.5.

8.2.1 Vibrational Frequencies of Ala

The fitted spectra of Ala and its deuterated isotopomers are shown in Tables-8.6 to 8.8. The fitted frequencies are very close to the experimentally observed frequencies for all the five isotopomers considered here with an average deviation of 7.2 cm^{-1}. The lowest two torsions and the NH$_3$ stretching frequencies are omitted from the error calculation. The torsional modes are not well described in the HF calculation [41].

The recent work of Yu et al. based on their Onsager reaction field model ab initio calculation and experimental ROA spectra gives the theoretical assignments of Ala zwitterion in the range 800 to 1600 cm^{-1}. In their study, Yu et al. assigned the 1613 cm^{-1} band as a mixed mode of νCO + δ_aN$^+$H$_3$ followed by δ_sN$^+$H$_3$ at 1503 cm^{-1}. Due to the presence of strong intermolecular H-bonding in the solution phase, the δ_aN$^+$H$_3$ mode is expected to appear above νCO. Earlier Diem et al. [20] assign based on their normal mode analysis both the δ_aN$^+$H$_3$ (1645,1625 cm^{-1}) above νCO (1607 cm^{-1}). We, in the present study consider 1645, 1625 and 1613 cm^{-1} bands as the three fundamentals in this region for Ala-d$_0$.

In the νN^+H and νCH stretching regions we used experimental frequencies of Diem et al. [20] wherever available. Our assignment matches very well with that of Diem et al. for Ala-d_0, Ala-Cd$_3$ and Ala-N$^+$d$_3$. The agreement between the calculated and experimental bands is excellent in all the modes except that of the highest two νN^+H, which were significantly overestimated in the ab initio model calculation. In the solvated model ab initio calculation the intramolecular H-bonding is avoided by putting the molecule in a dielectric continuum and hence the discrepancy in the isolated model (the H-bonded N$^+$H stretching frequency appearing below νCH) is overcome in the present case.

From the VCD spectra it was observed that the difference between the two νCO stretching bands in Ala-d_0 appear around 200 cm^{-1} [19]. We assigned the higher νCO band at 1613 cm^{1-} and the lower one as a mixed mode at 1412 cm^{-1}, in agreement with this observation. In the 1600-1400 cm^{-1} region we consider the earlier assignment of Diem et al. [20] appears to be the satisfactory ones and our fitted PEDs agree very well with that. In Ala-d_0 we assigned the 1645 and 1625 cm^{-1} bands as $\delta_a N^+H_3$ and 1503 cm^{-1} band as $\delta_s N^+H_3$. These numbers appear at 1647, 1623 and 1507 cm^{-1} in Ala-d_0, 1647, 1622 and 1506 cm^{-1} in Ala-Cd$_3$, 1176, 1141 and 1201 cm^{-1} in Ala-N$^+$d$_3$, 1175,1162 and 1207 cm^{-1} in Ala-CdN$^+$d$_3$ and 1178, 1154 and 1200 cm^{-1} in Ala-N$^+$d$_3$Cd$_3$ after scaling. Both the $\delta_a C_\beta H_3$ modes are assigned at 1457 cm^{-1} and are calculated at 1464 and 1458 cm^{-1}. The corresponding $\delta_s C_\beta H_3$ appear at 1359 cm^{-1} and is calculated at 1375 cm^{-1}. The $\rho C_\beta C_\alpha C$ mode is assigned at 1379 cm^{-1} and is calculated at 1382 cm^{-1}. These two closely spaced bands got exchange during the fitting. Both the $\delta_a C_\beta H_3$ and $\delta_s C_\beta H_3$ appeared at 1044, 1032, 1058 cm^{-1} in Ala-Cd$_3$, 1464, 1459, 1377 cm^{-1} in Ala-N$^+$d$_3$ and 1460, 1456, 1372 cm^{-1} in Ala-CdN$^+$d$_3$ and 1055, 1043, 1072 cm^{-1} in Ala-Cd$_3$N$^+$d$_3$ in our calculated spectra.

The two ρN^+H_3 modes appear as a mixed modes with $\rho C_\beta H_3$ and $\delta C_\beta C_\alpha C$ at 1241 and 1147 cm^{-1} for Ala-d_0 after scaling. These two modes are assigned to the experimental bands at 1238 and 1145 cm^{-1} of Susi et al. [5]. These bands get shifted to 1194 and 1155 cm^{-1} in Ala-Cd$_3$, 887, 842 cm^{-1} in Ala-N$^+$d$_3$, 846, 797 cm^{-1} in Ala-CdN$^+$D$_3$ and 818, 794 cm^{-1} in Ala-Cd$_3$N$^+$d$_3$. The $\nu C_\alpha N^+$ mode in Ala-d_0 is assigned to the observed band at 1113 and 922 cm^{-1} as a mixed mode with $\rho C_\beta H_3$, νCC_α and $\nu C_\alpha C_\beta$ and are calculated at 1130 and 928 cm^{-1} respectively. The γCO and δCOO appear as mixed mode in Ala-

d_0 at 781 cm^{-1} and is calculated at 796 cm^{-1}. This band is calculated at 736 cm^{-1} in Ala-Cd$_3$, 782 cm^{-1} in Ala-N$^+$d$_3$, 749 cm^{-1} in Ala-CdN$^+$d$_3$ and 732 cm^{-1} in Ala-Cd$_3$N$^+$d$_3$ spectra. The observed band at 633 cm^{-1} is assigned to a mixed mode of $\nu C_\alpha C - \delta COO + \nu C_\alpha C_\beta + \gamma CO$ and is calculated at 640 cm^{-1}. This band is more or less invariant with the isotopic substitution and appear at 611 cm^{-1} in Ala-Cd$_3$, 612 cm^{-1} in Ala-N$^+$d$_3$, 597 cm^{-1} in Ala-CdN$^+$d$_3$ and 594 cm^{-1} in Ala-Cd$_3$N$^+$d$_3$ in our fitted spectra.

8.2.2 Vibrational Frequencies of Cys

We transferred all the scale factors from Ala except for the CH$_2$SH stretching, bending and torsional modes. The side chain residue is successfully represented by using the scale factors of EtSH. The predicted frequencies of Cys are given in Table-8.9 along with their PEDs. The prediction is in good agreement with the experimental frequencies producing an average error of 9.0 cm^{-1} for Cys spectra observed bands excluding NH$_3$ stretchings. Many ambiguities regarding the assignment of vibrational modes, especially in the 1600-1400 cm^{-1} region observed in our earlier ab initio calculated results on isolated molecule with simple Durig's scaling [42] are resolved successfully in the present study.

Unlike the isolated model, in the νN^+H_3 stretching region, all the N$^-$H stretching bands appear above the C$_\beta$H$_2$ and C$_\alpha$H modes as expected. The predicted νN^+H_3 frequencies are less than the observed values and the predicted numbers are quite close to that of Ala. The predicted values of both the C$_\beta$H$_2$ and the C$_\alpha$H agree very well with the observed bands of L-Cys and D,L-Cys. The predicted band at 2947 cm^{-1} ($\nu C_\beta H_2 + \nu C_\alpha H$) agree well with the observed band at 2935 cm^{-1} in D,L-Cys compared to 2918 cm^{-1} in L-Cys. The νSH frequency predicted at 2573 cm^{-1} matches very well with the observed bands of L-Cys and D,L-Cys. The present assignment in this region matches very well with that of Li et al. [39].

In the 1600 cm^{-1} region the predicted frequencies appear at 1646 ($\delta_a N^+H_3$), 1636 νCO) and 1599 ($\delta_a N^+H_3$) cm^{-1}. This is not in agreement with the gross experimental features of amino acids, namely $\delta_a N^+H_3$ modes appear above νCO. Changing the basis set and the cavity radii would have resolved this problem. However our aim is to compare the force fields of different amino acids in the same basis set. Surprisingly our predicted

assignment matches exactly with that of Li et al. [39]. The $\delta_s N^+ H_3$ band matches well with the experimental frequencies of L-Cys and D, L-Cys and also in agreement with the earlier assignment of Li et al. [39] and Madec et al. [37]. The $\delta C_\beta H_2$ appear as a mixed mode with $\nu C_\alpha C$ at 1431 and 1409 cm^{-1} in the prediction and agrees quite well with the observed bands of L-Cys and D,L-Cys. The lower νCO appear as a mixed mode in our predicted spectra at 1431 cm^{-1} and 1316 cm^{-1}. This band was earlier assigned at 1400 cm^{-1} in L-Cys by Li et al. [39] and at 1406 cm^{-1} by Madec et al. [37] in D, L-Cys spectra. . The $\omega C_\beta H_2$ mode is predicted at 1292 cm^{-1} and are assigned to the observed band at 1296 in L-Cys and at 1308 cm^{-1} in D,L-Cys. The $t C_\beta H_2$ mode is assigned at 1206 cm^{-1} in our predicted spectra and agrees well with the earlier assignment at 1203 cm^{-1} by Madec et al. for L-Cys. Both the $\rho N^+ H_3$ modes are predicted at 1144 and 1124 cm^{-1} and agrees well with the observed bands at 1140 cm^{-1} in the Raman spectra of L-Cys by Madec et al. [37] and at 1118 cm^{-1} of L-Cys in the ROA spectra of Gargaro et al. [40]. The $\nu C_\alpha N^+$ mode appear as a mixed mode at 1085 and 934 cm^{-1} in the predicted spectra and is in agreement with the Ala assignment. These two bands are assigned at 1069 and 936 cm^{-1} in L-Cys and 1073 and 934 cm^{-1} in D, L-Cys. The γCO mode also appear as a mixed mode in the predicted spectra with δCOO at 881 and 823 cm^{-1}. This band appear at a higher frequency compared to Ala where it is assigned at 796 cm^{-1}. The $\nu C_\beta S$ frequency is predicted at 693 cm^{-1} and agrees very well with the 692 cm^{-1} band in L-Cys. This band is observed at 657 cm^{-1} in EtSH spectra. The predicted band at 610 cm^{-1} is assigned to $\nu C_\alpha C$ and matches very well with the observed band of 615 cm^{-1} in both L-Cys and D, L-Cys. The lower frequency modes below 400 cm^{-1} are not available in the experimental spectra and hence our predicted numbers cannot be compared.

8.2.3 Vibrational Frequencies of Ser

Same strategy of transferring the scale factors of Ala and EtOH, as in Cys is applied. The predicted frequencies of Ser along with the PED is given in Table-8.10. The agreement is excellent with the zwitterionic frequencies for both L and D,L-Ser with an average error of 10.1 cm^{-1}. The $\nu OH_{(alc)}$ mode appears at 3392 cm^{-1} in our prediction and the corresponding experimental frequencies are not available. Both the $\delta_a N^+ H_3$ bending

vibrations appear above νCO followed by δ_sN$^+$H$_3$ in our predicted spectra as expected. These modes are predicted at 1645, 1626, 1611 and 1493 cm^{-1} respectively and agrees very well with our Ala assignment. These bands are not observed in the L-Ser spectra but matches quite well with the D,L-Ser spectra. The δC$_\beta$H$_2$ mode appear at higher frequency compared to that of Cys. This frequency appears at 1460 and 1455 cm^{-1} in the experimental spectra deviates considerably form the predicted band at 1482 cm^{-1}. This could be due to the structural variation of C$_\beta$H$_2$ in Ser and EtOH. The fundamental predicted at 1414 cm^{-1} is assigned to a mixed mode of ωC$_\beta$H$_2$ and δC$_\beta$OH and agrees reasonably well to the observed band at 1430 cm^{-1} in EtOH spectrum. The tC$_\beta$H$_2$ mode is predicted at 1275 cm^{-1} and is in agreement with that of L-Cys predicted value. The predicted band at 1210 cm^{-1} is also assigned to a mixed mode of ωC$_\beta$H$_2$ and δC$_\beta$OH and appear at a lower frequency compared to the experimental ones at 1242 and 1247 cm^{-1} in L-Ser and D,L-Ser respectively. The corresponding band is observed at 1276 cm^{-1} in EtOH spectrum. Both the ρN$^+$H$_3$ appear at 1187 and 1154 cm^{-1} as mixed modes in the predicted spectra and matches very well with the observed bands of L-Ser and D,L-Ser. The νC$_\alpha$N$^+$ mode appear at 1093 and 868 cm^{-1} in the calculated spectra and are observed at 1090 and 851 cm^{-1} in L-Ser and 1093 and 852 cm^{-1} in D,L -Ser. The νC$_\beta$O mode is predicted spectra at 1039 cm^{-1} and agrees well with the observed band at 1040 and 1029 cm^{-1} in L-Ser and D,L-Ser respectively. This mode was earlier assigned at 978 cm^{-1} by Machida et al. [36]. The observed band at 978 cm^{-1} is predicted at 985 cm^{-1} and is assigned to a mixed mode of ρC$_\beta$H$_2$ + ρN$^+$H$_3$ + νC$_\alpha$C$_\beta$. The main discrepancy appear in the observed bands at 773 and 620 cm^{-1} in the ROA spectra of L-Ser. We do not have any frequency correspond to these in our prediction. The earlier assignment of Ser based on isolated model calculation predicted these two bands at 796 and 615 cm^{-1} respectively. In the lower frequency range 200-400 cm^{-1} our predicted frequencies match quite well with the observed D,L- Ser spectra.

The predicted non-redundant force constants of both Cys and Ser and the fitted non-redundant force constants of Ala are given in Tables-8.11 to 8.13.

8.3 Conclusions

The theoretical prediction of the vibrational spectra of Cys and Ser based on solvated ab initio calculation is found to be satisfactory. The scale factors of smallest chiral amino acid, Ala is found to be very useful in predicting the higher chiral amino acids. The present study, led us to infer that the non-redundant set of scale factors of Ala could be used to predict the vibrational spectra of other structurally related amino acids and peptides. However further studies of other amino acids are needed to verify this conclusion. This further implies that the structurally related small organic compounds can be used to mimic the force fields of amino acid side chain residues.
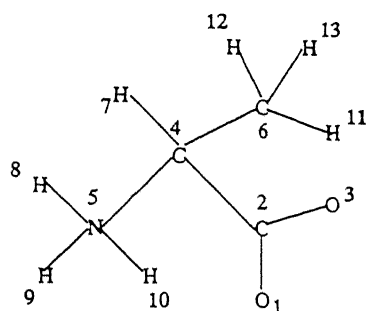
a=O(1)-C(2)-O(3) , a1=C(4)-C(2)-O(1), b1=C(4)-C(2)-O(3)

a2=C(2)-C(4)-H(7), a3=N(5)-C(4)-H(7), a4=C(6)-C(4)-H(7)

b2=N(5)-C(4)-C(6), b3=C(2)-C(4)-N(5), b4=C(2)-C(4)-C(6)

a5=H(8)-N(5)-H(9), a6=H(8)-N(5)-H(10), a7=H(9)-N(5)-H(10)

b5=C(4)-N(5)-H(8), b6=C(4)-N(5)-H(9), b7=C(4)-N(5)-H(10)

a8=H(11)-C(6)-H(12), a9=H(11)-C(6)-H(12), a10=H(12)-C(6)-H(13)

b8=C(4)-C(6)-H(11), b9= C(4)-C(6)-H(12), b(10)=C(4)-C(6)-H(13)

Figure 8.1: Internal coordinates of Ala
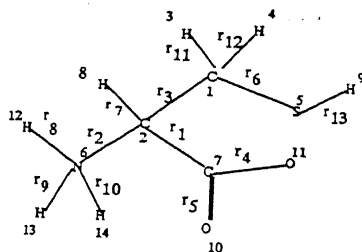
a=O(10)-C(7)-O(11), a1=C(2)-C(7)-O(10), b1=C(2)-C(7)-O(11), a2=C(7)-C(2)-H(8)
a3=N(6)-C(2)-H(8), a4= C(1)-C(2)-H(8), b2= C(1)-C(2)-N(6), b3=C(1)-C(2)-C(7)
b4=N(6)-C(2)-C(7), a5= H(12)-N(6)-H(13), a6= H(12)-N(6)-H(14), a7=H(13)-N(6)-H(14)
b5= C(2)-N(6)-H(12), b6= C(2)-N(6)-H(13), b7= C(2)-N(6)-H(14), a8= H(3)-C(1)-H(4)
a9= H(3)-C(1)-S(5), a10= H(4)-C(1)-S(5), b8=C(2)-C(1)-S(5), b9= C(2)-C(1)-H(3)
b10=C(2)-C(1)-H(4), b= C(1)-S(5)-H(9)
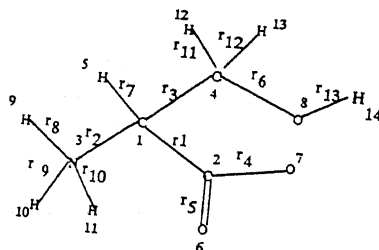
a=O(6)-C(2)-O(7), a1= C(1)-C(2)-O(6), b1= C(1)-C(2)-O(7), a2= C(2)-C(1)-H(5)
a3= N(3)-C(1)-H(5), a4= C(4)-C(1)-H(5), b2= C(4)-C(1)-N(3), b3= C(4)-C(1)-C(2)
b4= N(3)-C(1)-C(2), a5= H(9)-N(3)-H(10), a6= H(9)-N(3)-H(11), a7=H(10)-N(3)-H(11)
b5= C(1)-N(3)-H(9), b6= C(1)-N(3)-H(10), b7= C(1)-N(3)-H(11), a8= H(12)-C(4)-H(13)
a9= H(12)-C(4)-O(8), a10= H(13)-C(4)-O(8), b(8)= C(1)-C(4)-O(8), b9= C(1)-C(4)-H(12)
b10=C(1)-C(4)-H(13), b= C(4)-O(8)-H(14)

Figure 8.2: Internal coordinates of Cys and Ser.
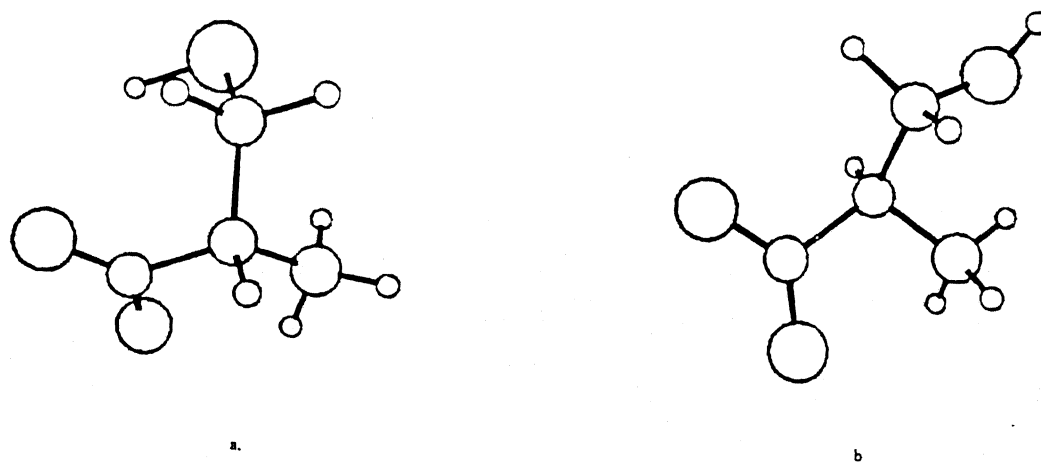
Figure 8.3: Optimized structure of a) Cys and b) Ser at HF/6-31++G* level.

Table 8.1: Local symmetry coordinates of Ala *

$S_{1-12}=$	r_{1-12}(all stretch)	$S_{23}=$	$2a_7-a_5-a_6(\delta_a N^+H_3)$
$S_{13}=$	$2a-a_1-b_1$ (δCOO)	$S_{24}=$	a_5-a_6 $(\delta_a N^+{}_3)$
$S_{14}=$	$a_1-b_1(\rho$COO)	$S_{25}=$	$a_8+a_9+a_{10}-b_8-b_9-b_{10}(\delta_s C_{beta}H_3)$
$S_{15}=$	$a_2+a_3+a_4-b_2-b_3-b_4$ ($\delta N^+C_\alpha C$)	$S_{26}=$	$2a_{10}-a_8-a_9(\delta_a C_\beta H_3)$
$S_{16}=$	$2a_2-a_3-a_4$ ($\delta C_\beta C_\alpha C$)	$S_{27}=$	a_8-a_9 $(\delta_a C_\beta H_3)$
$S_{17}=$	a_3-a_4 $(\rho C_\beta C_\alpha C)$	$S_{28}=$	$2b_8-b_9-b_{10}$ $(\rho C_\beta H_3)$
$S_{18}=$	$2b_2-b_3-b_4$ ($\delta C_\beta C_\alpha H$)	$S_{29}=$	b_9-b_{10} $(\rho C_\beta H_3)$
$S_{19}=$	b_3-b_4 $(\rho C_\beta C_\alpha H)$	$S_{30}=$	γ_{4213} $(\gamma$CO)
$S_{20}=$	$a_5+a_6+a_7-b_5-b_6-b_7$ ($\delta_s N^+H_3$)	$S_{31}=$	τ_{24} $(\tau C_\alpha C)$
$S_{21}=$	$2b_5-b_6-b_7$ (ρN^+H_3)	$S_{32}=$	τ_{45} $(\tau N^+ C_\alpha)$
$S_{22}=$	b_6-b_7 (ρN^+H_3)	$S_{33}=$	τ_{46} $(\tau C_\alpha C_\beta)$

*. Internal coordinate numberings are according to Figure 8.1.

Table 8.2: Local symmetry coordinates of Cys and Ser *

$S_{1-13}=$	r_{1-13}(all stretch)	$S_{25}=$	$a_5-a_6(\delta_a N^+H_3)$
$S_{14}=$	$2a-a_1-b_1$ (δCOO)	$S_{26}=$	$4a_8-a_9-a_{10}-b_9-b_{10}$ $(\delta_s C_\beta H_2)$
$S_{15}=$	$a_1-b_1(\rho$COO)	$S_{27}=$	$a_9+a_{10}-b_9-b_{10}(\omega C_{beta}H_2)$
$S_{16}=$	$a_2+a_3+a_4-b_2-b_3-b_4$ ($\delta N^+C_\alpha C$)	$S_{28}=$	$a_9-a_{10}+b_9-b_{10}$ $(\rho C_\beta H_2)$
$S_{17}=$	$2a_2-a_3-a_4$ ($\delta C_\beta C_\alpha C$)	$S_{29}=$	$a_9-a_{10}-b_9+b_{10}$ $(tC_\beta H_2)$
$S_{18}=$	a_3-a_4 $(\rho C_\beta C_\alpha C)$	$S_{30}=$	$5b_8-a_8-a_9-a_{10}-b_9-b_{10}$ $(\delta C_\alpha C_\beta S/\delta C_\alpha C_\beta O)$
$S_{19}=$	$2b_2-b_3-b_4$ ($\delta C_\beta C_\alpha H$)	$S_{31}=$	b (δCSH/δCOH)
$S_{20}=$	b_3-b_4 $(\rho C_\beta C_\alpha H)$	$S_{32}=$	$\gamma_{271011}/\gamma_{1267}$ $(\gamma$CO)
$S_{21}=$	$a_5+a_6+a_7-b_5-b_6-b_7$ ($\delta_s N^+H_3$)	$S_{33}=$	τ_{12}/τ_{14} $(\tau C_\alpha C_\beta)$
$S_{22}=$	$2b_5-b_6-b_7$ (ρN^+H_3)	$S_{34}=$	τ_{15}/τ_{48} $(\tau C_\beta S/\tau C_\beta O)$
$S_{23}=$	b_6-b_7 (ρN^+H_3)	$S_{35}=$	τ_{27}/τ_{12} (τCC_α)
$S_{24}=$	$2a_7-a_5-a_6$ $(\delta_a N^+H_3)$	$S_{36}=$	τ_{26}/τ_{13} $(\tau C_\alpha N^+)$

*. Internal coordinate numberings are according to Figure 8.2.

Table 8.3: Optimized geometrical parameters of Ala

param*	Ala	param	Ala	param	Ala
r_{1-2}	1.233	a_{245}	110.0	a_{11612}	108.4
r_{3-2}	1.239	a_{246}	115.0	a_{11613}	108.3
r_{4-2}	1.558	a_{546}	108.9	a_{12613}	108.4
r_{5-4}	1.512	a_{547}	105.1	τ_{3218}	-168.2
r_{6-4}	1.524	a_{247}	107.6	τ_{1245}	5.2
r_{7-4}	1.082	a_{458}	110.4	τ_{1246}	128.5
r_{8-5}	1.010	a_{459}	112.1	τ_{1247}	-108.8
r_{9-5}	1.011	a_{4510}	112.6	τ_{2458}	-36.7
r_{10-5}	1.015	a_{859}	106.1	τ_{24611}	-59.9
r_{6-11}	1.086	a_{8510}	109.1	τ_{2459}	81.4
r_{6-12}	1.081	a_{9510}	106.2	τ_{24612}	-158.9
r_{6-13}	1.084	a_{4611}	111.2	τ_{12647}	-62.0
a_{123}	128.4	a_{4612}	108.8	τ_{11647}	178.6
a_{124}	116.3	a_{4613}	111.6	τ_{8547}	78.9
τ_{9547}	-163.0				

* Internal coordinates are according to Figure 8.1.

Table 8.4: Optimized geometrical parameters of Cys and Ser

param*	Cys	Ser	param	Cys	Ser	param	Cys	Ser
r_1	1.563	1.552	a_3	107.7	108.3	b_9	111.2	110.7
r_2	1.504	1.504	a_4	105.9	105.2	b_{10}	108.0	108.8
r_3	1.525	1.526	b_1	108.7	107.6	τ_{6213}/τ_{31412}	-55.5	-66.9
r_4	1.232	1.237	b_2	110.9	106.4	τ_{6215}/τ_{3148}	64.1	53.4
r_5	1.232	1.237	b_3	114.8	117.5	τ_{7213}/τ_{21412}	-178.9	58.3
r_6	1.823	1.392	b_4	108.5	111.1	τ_{7215}/τ_{2148}	59.3	178.6
r_7	1.083	1.082	a_5	106.7	106.1	τ_{8213}/τ_{51412}	60.5	-179.2
r_8	1.014	1.016	a_6	107.5	107.4	τ_{8215}/τ_{5148}	-179.9	-58.9
r_9	1.012	1.007	a_7	110.0	109.9	τ_{12710}/τ_{4126}	-42.7	-129.2
r_{10}	1.012	1.009	b_5	107.6	109.8	τ_{82710}/τ_{5126}	78.4	108.7
r_{11}	1.084	1.088	b_6	111.1	111.6	τ_{62710}/τ_{3126}	-167.4	-6.3
r_{12}	1.078	1.082	b_7	113.7	111.9	τ_{12627}/τ_{2139}	-29.7	-62.9
r_{13}	1.328	0.952	a_8	108.0	108.6	τ_{12621}/τ_{4139}	-156.6	66.1
a	129.9	129.0	a_9	105.8	104.1	$\tau_{13627}/\tau_{10312}$	86.9	55.8
a_1	115.0	115.8	a_{10}	109.6	112.6	$\tau_{13621}/\tau_{10314}$	-40.0	-175.1
b_1	115.0	115.2	b_8	114.0	111.8	τ_{2159}/τ_{14814}	62.2	-170.3

* Internal coordinates are according to Figure 8.2

Table 8.5: Fitted frequencies of EtSH and EtOH

no.	EtSH			EtOH			EtOD		
	expt	calc	PED	expt	calc	PED	expt	calc	PED
1	2988	2988	$\nu C(H_2)+\nu C(H_3)$	3336	3437	νOH	—	2503	νOD
2	2967	2967	$\nu C(H_3)+\nu C(H_2)$	2975	2975	$\nu C(H_3)$	—	2975	$\nu C(H_3)$
3	2932	2932	$\nu C(H_3)$	2940	2943	$\nu C(H_3)$	—	2940	$\nu C(H_3)$
4	2902	2902	$\nu C(H_2)$	2920	2920	$\nu C(H_2)$	—	2920	$\nu C(H_2)$
5	2875	2875	$\nu C(H_3)$	2890	2890	$\nu C(H_3)$	—	2890	$\nu C(H_3)$
6	2571	2571	νSH	2877	2877	$\nu C(H_2)$	—	2877	$\nu C(H_2)$
7	1460	1460	$\delta_a CH_3$	1498	1492	δCH_2	1490	1490	$\delta CH_2+\delta_a CH_3$
8	1450	1450	$\delta_a CH_3$	1480	1478	$\delta_a CH_3$	1474	1475	$\delta_a CH_3+\delta CH_2$
9	1434	1434	δCH_2	1450	1449	$\delta_a CH_3+\rho CH_3$	1447	1449	$\delta_a CH_3+\rho CH_3$
10	1376	1376	$\delta_s CH_3$	1430	1446	$\delta COH+\omega CH_2+\delta CH_2+\delta_a CH_3$	1401	1401	$\delta_s CH_3+\omega CH_2+\nu CC$
11	1273	1273	ωCH_2	1381	1385	$\delta_s CH_3$	1365	1357	$\omega CH_2+\delta_s CH_3$
12	1251	1251	$tCH_2+\rho CH_3$	1328	1318	$tCH_2+\rho CH_3$	1309	1318	$tCH_2+\rho CH_3$
13	1091	1094	$\rho CH_3+\delta CSH+tCH_2+\rho CH_2$	1273	1277	$\omega CH_2+\delta COH$	1170	1169	$\rho CH_3+\delta COD+\delta CCO+\nu CC$
14	1052	1052	$\nu CC+\rho CH_3+tCH_2$	1149	1153	$\rho CH_2+\rho CH_3+tCH_2$	1158	1154	$\rho CH_2+\rho CH_3+tCH_2$
15	970	970	$\nu CC+\rho CH_3$	1089	1091	ρCH_3	1055	1053	$\nu CO+\nu CC$
16	869	869	$\delta CSH+tCH_2+\rho CH_3$	1050	1052	$\nu CC+\nu CO$	954	946	$\delta COD+\rho CH_3+\omega CH_2$
17	737	737	$\rho CH_2+\rho CH_3+\delta CSH$	880	887	$\nu CO+\nu CC+\rho CH_3$	877	870	$\nu CO+\nu CC+\rho CH_3$
18	657	657	νCS	802	800	$\rho CH_3+\rho CH_2+tCH_2$	797	799	$\rho CH_3+\rho CH_2+tCH_2$
19	319	319	δCCS	433	439	$\delta CCO+\rho CH_3$	435	429	$\delta CCO+\rho CH_3$
20	247	247	τCC	260	264	$\tau CO+\tau CC$	—	236	τCC
21	191	191	τCS	217	219	$\tau CC+\tau CO$	—	180	$\tau CO+\tau CC$

Table 8.6: Fitted frequencies and PEDs of Ala-d$_0$

		Ala-d$_0$		
no.	unscaled	scaled	expt[a]	PED
1	3734	3124	3080	νN^+H_3
2	3707	3100	3060	νN^+H_3
3	3614	3028	3020	νN^+H_3
4	3324	3015	3003	$\nu C_\beta H_3$
5	3288	3005	2993	$\nu C_\beta H_3$
6	3271	2961	2962	$\nu C_\alpha H$
7	3213	2945	2949	$\nu C_\beta H_3$
8	1829	1647	1645	$\delta_a N^+H_3$
9	1808	1623	1625	$\delta_a N^+H_3$
10	1791	1613	1613	$\nu CO + \delta_s N^+H_3$
11	1672	1507	1503	$\delta_s N^+H_3$
12	1636	1464	1457	$\delta_a C_\beta H_3$
13	1630	1458	1457	$\delta_a C_\beta H_3$
14	1577	1420	1412	$\delta_a C_\beta H_3 + \nu CO + \nu CC_\alpha + \delta_s C_\beta H_3$
15	1540	1382	1379[b]	$\rho C_\beta C_\alpha C$
16	1497	1375	1359[b]	$\delta_s C_\beta H_3$
17	1449	1306	1302	$\delta C_\beta C_\alpha C + \nu CO$
18	1314	1241	1238[b]	$\rho N^+H_3 + \rho C_\beta H_3$
19	1221	1147	1145	$\rho N^+H_3 + \delta C_\beta C_\alpha C$
20	1187	1130	1113	$\nu C_\alpha N^+ + \rho C_\beta H_3 + \nu C_\alpha C_\beta$
21	1050	1023	1003	$\rho C_\beta H_3 + \rho N^+H_3 + \rho C_\beta C_\alpha C$
22	1037	1001	995	$\nu C_\alpha C_\beta + \rho N^+H_3 + \rho C_\beta H_3$
23	973	928	922	$\nu C_\alpha N^+ + \rho C_\beta H_3 + \nu CC_\alpha$
24	891	856	848	$\delta COO + \nu C_\alpha N^+ + \nu C_\alpha C_\beta + \gamma CO$
25	844	796	781	$\gamma CO + \delta COO$
26	642	633	640	$\nu C_\alpha C + \delta COO + \nu C_\alpha C_\beta + \gamma CO$
27	532	525	527	$\rho COO + \nu C_\alpha N^+$
28	422	402	399	$\delta C_\beta C_\alpha H + \delta N^+C_\alpha C$
29	324	318	296	$\delta C_\beta C_\alpha H + \delta N^+C_\alpha C$
30	266	266	283	$\rho C_\beta C_\alpha H + \rho COO$
31	249	247	219	$\tau C_\alpha C_\beta$
32	126	135	184	τN^+C_α
33	58	72	—	$\tau C_\alpha C + \tau N^+C_\alpha$

a. Ref [19,20] b. Ref. 5.

Table 8.7: Fitted frequencies and PEDs of Ala-Cd$_3$ and Ala-N$^+$d$_3$

Ala-Cd$_3$			Ala-N$^+$d$_3$		
scaled	expt[a]	PED	scaled	expt[a]	PED
3124	3080	νN$^+$H	3015	3003	νC$_\beta$H$_3$
3100	3060	νN$^+$H	3005	2993	νC$_\beta$H$_3$
3028	3020	νN$^+$H	2962	2962	νC$_\alpha$H
2962	2962	νC$_\alpha$H	2945	2949	νC$_\beta$H$_3$
2239	2251	νC$_\beta$D$_3$	2306	2290	νN$^+$D$_3$
2229	2236	νC$_\beta$D$_3$	2288	—	νN$^+$D$_3$
2116	2126	νC$_\beta$D$_3$	2176	2160	νN$^+$D$_3$
1647	1645	δ_aN$^+$H$_3$	1605	1608	νCO
1622	1625	δ_aN$^+$H$_3$	1464	1459	δ_aC$_\beta$H$_3$+ρC$_\beta$H$_3$
1612	1615	νCO+δ_sN$^+$H$_3$	1459	1459	δ_aC$_\beta$H$_3$
1506	1511	δ_sN$^+$H$_3$	1416	1409	δ_aC$_\beta$H$_3$+νCO+νCC+δ_sC$_\beta$H$_3$
1421	1414	νCC+νCO+δC$_\beta$C$_\alpha$O+δCOO	1377	1376	δ_sC$_\beta$H$_3$
1378	1360	ρC$_\beta$C$_\alpha$C	1365	1355[b]	ρC$_\beta$C$_\alpha$C
1304	1305	δC$_\beta$C$_\alpha$C+νCO	1298	1299[b]	δC$_\beta$C$_\alpha$C+νCO
1199	1194	ρN$^+$H$_3$+ρC$_\beta$C$_\alpha$C+νC$_\alpha$C$_\beta$	1201	1193	δ_sN$^+$D$_3$+νC$_\alpha$N$^+$
1145	1155	ρN$^+$H$_3$+δC$_\beta$C$_\alpha$C	1187	—	ρC$_\beta$H$_3$+νC$_\alpha$C$_\beta$+ρN$^+$D$_3$
1120	1128	δ_sCD$_3$+νC$_\alpha$C$_\beta$+νC$_\alpha$N$^+$	1176	—	δ_aN$^+$D$_3$
1058	1066	δ_sCD$_3$+δ_aCD$_3$+νC$_\alpha$N$^-$	1149	1161	δ_aN$^+$D$_3$
1044	1051	δ_aCD$_3$	1114	1100	ρC$_\beta$H$_3$+δ_sN$^+$D$_3$+δC$_\beta$C$_\alpha$C
1032	—	δ_aCD$_3$$\nu$C$_\alpha$N$^+$	1070	1058	νC$_\alpha$C$_\beta$+ρC$_\beta$H$_3$+δ_sN$^+$D$_3$
950	954	νC$_\alpha$C+ρN$^+$H$_3$+δ_sC$_\beta$D$_3$+νC$_\alpha$C$_\beta$	919	922	ρC$_\beta$H$_3$+νCC$_\alpha$+νC$_\alpha$N$^+$
930	931	ρC$_\beta$D$_3$+γCO+ρN$^-$H$_3$-δN$^+$C$_\alpha$C	887	878	ρN$^+$D$_3$+ρC$_\beta$H$_3$+νC$_\alpha$N$^+$
839	832	δCOO+ρC$_\beta$D$_3$	842	849	ρN$^+$D$_3$+δCOO
777	804	ρC$_\beta$D$_3$+νC$_\alpha$N$^+$	812	815	ρN$^+$D$_3$+νC$_\alpha$C$_\beta$+δCOO+νC$_\alpha$N
736	758	γCO+ρC$_\beta$D$_3$	782	776	γCO+ρN$^+$D$_3$
611	610	νC$_\alpha$C+δCOO+νC$_\alpha$C$_\beta$	612	613	νC$_\alpha$C+δCOO
514	509	ρCOO+νC$_\alpha$C	507	513	ρCOO+νC$_\alpha$N$^+$
371	374	δC$_\beta$C$_\alpha$H+δN$^+$C$_\alpha$C	376	377	δN$^+$C$_\alpha$C+δC$_\beta$C$_\alpha$H
304	297	δN$^+$C$_\alpha$C+δC$_\beta$C$_\alpha$H+δCOO	304	335	δC$_\beta$C$_\alpha$H+ δN$^+$C$_\alpha$C
246	220	ρC$_\beta$C$_\alpha$H+ρCOO	255	273	ρC$_\beta$C$_\alpha$H+ρCOO
180	191	τC$_\alpha$C$_\beta$	247	258	τC$_\alpha$C$_\beta$+ρC$_\beta$C$_\alpha$H
134	184	τC$_\alpha$N$^+$	105	211	τC$_\alpha$N$^+$+τC$_\alpha$C
70	—	τC$_\alpha$C+τC$_\alpha$N$^+$	65	184	τC$_\alpha$C+ τC$_\alpha$N$^+$

a. Ref. [19,20] b. Ref. 5.

Table 8.8: Fitted frequencies and PEDs of Ala-CdN$^+$d$_3$ and Ala-Cd$_3$N$^+$d$_3$

	Ala-CdN$^+$d$_3$			Ala-Cd$_3$N$^+$d$_3$	
scaled	expt[a]	PED	scaled	expt[a]	PED
3015	—	$\nu C_\beta H_3$	2962	—	$\nu C_\alpha H$
3004	—	$\nu C_\beta H_3$	2306	—	$\nu N^+ D_3$
2945	—	$\nu C_\beta H_3$	2288	—	$\nu N^+ D_3$
2305	—	$\nu N^+ D_3$	2239	—	$\nu C_\beta D_3$
2288	—	$\nu N^+ D_3$	2229	—	$\nu C_\beta D_3$
2186	—	$\nu C_\alpha D$	2176	—	$\nu N^+ D_3$
2176	—	$\nu N^+ D_3$	2116	—	$\nu C_\beta D_3$
1605	1605	νCO	1605	1608	νCO
1460	1460	$\delta_a C_\beta H_3 + \rho C_\beta H_3$	1415	1412	$\nu CC + \nu CO + \delta COO + \delta C_\beta C_\alpha C$
1456	1460	$\delta_a C_\beta H_3 + \rho C_\beta H_3$	1360	1343	$\rho C_\beta C_\alpha C$
1406	1414	$\delta_s C_\beta H_3 + \nu CO + \nu C_\alpha C + \delta COO$	1295	1291	$\delta C_\beta C_\alpha C + \nu CO$
1372	1380	$\delta_s C_\beta H_3 + \nu CO$	1200	1206	$\delta_s N^+ D_3 + \nu C_\alpha N^-$
1235	—	$\nu C_\alpha C_\beta + \rho N^+ D_3$	1178	1175	$\delta_a N^+ D_3$
1207	1212	$\delta_s N^+ D_3 + \nu C_\alpha N^+$	1154	1147	$\delta_a N^+ D_3$
1175	—	$\delta_a N^+ D_3$	1148	—	$\nu C_\alpha C_\beta + \delta_s C_\beta D_3 + \delta_a N^+ D_3$
1162	1159	$\delta_a N^+ D_3 + \rho C_\beta H_3$	1072	1080	$\delta_s C_\beta D_3 + \rho C_\beta D_3 + \nu C_\alpha N^+$
1148	—	$\rho C_\beta H_3 + \delta_a N^+ D_3 + \nu C_\alpha C_\beta$	1055	1057	$\delta_a C_\beta D_3 + \rho C_\beta D_3$
1140	1134	$\delta_s N^+ D_3 + \delta_a N^+ D_3$	1043	—	$\delta_a C_\beta D_3$
1011	1009	$\rho C_\beta C_\alpha C + \rho C_\beta H_3 + \rho N^+ D_3 + \delta C_\beta C_\alpha C$	1027	1026	$\delta_a C_\beta D_3 + \delta N^+ C_\alpha C$
941	944	$\delta C_\beta C_\alpha C + \gamma CO + \nu C_\alpha N^+$	1007	—	$\delta_s C_\beta D_3 + \nu C_\alpha N^+$
901	894	$\nu CC_\alpha + \delta COO + \rho C_\beta H_3 + \nu C_\alpha N^+$	859	857	$\delta COO + \nu C_\alpha C + \rho N^+ D_3$
846	845	$\rho N^+ D_3 + \nu C_\alpha C_\beta + \delta COO$	818	821	$\rho N^+ D_3 + \gamma CO$
826	825	$\rho C_\beta C_\alpha C + \nu C_\alpha C_\beta + \rho C_\beta H_3 + \delta COO$	794	796	$\rho N^+ D_3 + \nu C_\alpha C_\beta + \delta COO$
797	—	$\rho N^+ D_3 + \rho C_\beta C_\alpha C + \nu C_\alpha N^+ + \delta COO$	756	754	$\rho C_\beta D_3 + \nu C_\alpha N^+$
749	—	$\gamma CO + \delta C_\beta C_\alpha C + \rho N^+ D_3$	732	—	$\gamma CO + \rho C_\beta D_3$
597	—	$\nu C_\alpha C + \delta COO + \rho COO$	594	—	$\nu C_\alpha C + \delta COO + \nu C_\alpha C_\beta$
501	—	$\rho COO + \nu C_\alpha N^+$	500	—	$\rho COO + \nu C_\alpha N^+$
374	—	$\delta C_\beta C_\alpha D + \delta N^+ C_\alpha C$	347	—	$\delta N^+ C_\alpha C + \delta C_\beta C_\alpha H$
302	—	$\delta C_\beta C_\alpha D + \delta N^+ C_\alpha C$	284	—	$\delta C_\beta C_\alpha H + \delta N^+ C_\alpha C$
255	—	$\rho C_\beta C_\alpha D + \rho COO$	241	—	$\rho C_\beta C_\alpha H + \rho COO$
247	—	$\tau C_\alpha C_\beta + \rho C_\beta C_\alpha D$	180	—	$\tau C_\alpha C_\beta$
105	—	$\tau C_\alpha N^+ + \tau C_\alpha C$	183	—	$\tau C_\alpha N^+ + \tau C_\alpha C$
65	—	$\tau C_\alpha C + \tau C_\alpha N^+$	64	—	$\tau C_\alpha C + \tau C_\alpha N^+$

a. Ref. [19]

Table 8.9: Predicted frequencies and PEDs of Cys

no.	calc	expt		PED
		L-Cys[a]	D,L-Cys[b]	
1	3108	3167	—	νN^+H_3
2	3099	3167	—	νN^+H_3
3	3034	3055	—	νN^+H_3
4	3003	2998	2989	$\nu C_\beta H_2$
5	2960	2960	2976	$\nu C_\alpha H + \nu C_\beta H_2$
6	2947	2918	2935	$\nu C_\beta H_2 + \nu C_\alpha H$
7	2573	2582	2570	νSH
8	1646	—	1663	$\delta_a N^+H_3$
9	1636	1616	1628	νCO
10	1599	1576	1585	$\delta_a N^+H_3$
11	1491	1510	1500	$\delta_s N^+H_3$
12	1431	1427	1426	$\delta C_\beta H_2 + \nu C_\alpha C + \nu CO$
13	1409	1400	1406	$\delta C_\beta H_2 + \nu C_\alpha C$
14	1393	1376	1366	$\rho C_\beta C_\alpha C$
15	1316	1320	1342	$\delta C_\beta C_\alpha C + \nu CO + \delta COO$
16	1292	1296	1308	$\omega C_\beta H_2 + \nu C_\alpha C_\beta$
17	1206	1203	1265	$tC_\beta H_2 + \nu C_\alpha N^+$
18	1144	1140	1163	$\rho N^+H_3 + \delta C_\beta C_\alpha C$
19	1124	1118	1128	$\rho N^+H_3 + \omega C_\beta H_2 + \rho C_\beta C_\alpha C$
20	1085	1069	1073	$\nu C_\alpha N^+ + \delta C_\beta SH + \rho C_\beta H_2 + tC_\beta H_2$
21	992	990	1000	$\rho N^+H_3 + \delta C_\beta SH + \nu C_\alpha C_\beta$
22	934	936	934	$\nu C_\alpha N^+ + \delta C_\beta SH + \nu C_\alpha C + \nu C_\alpha C_\beta$
23	881	875	892	$\gamma CO + \delta COO + \delta N^+ C_\alpha C$
24	823	823	826	$\delta COO + \gamma CO + \delta C_\beta SH$
25	792	779	775	$\rho C_\beta H_2 + \delta C_\beta SH + \nu C_\alpha N^+$
26	693	692	—	$\nu C_\beta S + \gamma CO$
27	610	615	615	$\nu C_\alpha C + \nu C_\alpha N^+ + \delta COO$
28	543	538	540	$\rho COO + \rho C_\beta C_\alpha H$
29	495	—	464	$\delta N^+ C_\alpha C + \delta C_\alpha C_\beta S + \delta C_\beta C_\alpha H$
30	341	—	—	$\delta C_\beta C_\alpha H + \tau C_\beta S + \tau C_\alpha C_\beta$
31	327	—	—	$\tau C_\beta S + \tau C_\alpha N^+$
32	273	—	—	$\tau C_\alpha N^+ + \rho C_\beta C_\alpha H + \tau C_\beta S$
33	268	—	—	$\tau C_\alpha N^+$
34	187	—	—	$\delta C_\beta C_\alpha S + \tau C_\alpha C + \delta N^+ C_\alpha C + \tau C_\alpha C_\beta$
35	107	—	—	$\tau C_\alpha C_\beta + \tau C_\alpha C + \nu CO$
36	91	—	—	$\tau C_\alpha C + \tau C_\alpha C_\beta$

a. Ref. [39,21] b. Ref [37]

Table 8.10: Predicted frequencies and PEDs of Ser

no.	calc	expt		PED
		L-Ser[a]	D,L-Ser[a]	
1	3392	—	—	νOH
2	3160	—	—	νN$^+$H$_3$
3	3115	—	—	νN$^+$H$_3$
4	3018	—	—	νN$^+$H$_3$
5	2971	—	—	νC$_\alpha$H+νC$_\beta$H$_2$
6	2958	—	—	νC$_\beta$H$_2$+ νC$_\alpha$H
7	2886	—	—	νC$_\beta$H$_2$
8	1645	—	1637	δ_aN$^+$H$_3$
9	1626	—	1626	δ_aN$^+$H$_3$
10	1611	—	1587	νCO
11	1493	—	1523	δ_sN$^+$H$_3$
12	1482	1460	1455	δC$_\beta$H$_2$
13	1438	—	1436	νC$_\alpha$C+ρC$_\beta$C$_\alpha$ +νCO
14	1414	1412	—	ωC$_\beta$H$_2$+δC$_\beta$OH+νC$_\alpha$C$_\beta$+νCC$_\alpha$
15	1381	1390	1377	ρC$_\beta$C$_\alpha$C+δC$_\beta$O
16	1318	1323	1309	δC$_\beta$C$_\alpha$C+νCO
17	1275	—	—	tC$_\beta$H$_2$+ρN$^+$H$_3$
18	1210	1242	1247	ωC$_\beta$H$_2$+δC$_\beta$OH
19	1187	—	1182	tC$_\beta$H$_2$+ρC$_\beta$H$_2$+ρN$^-$H$_3$+ρC$_\beta$C$_\alpha$C
20	1154	1150	1156	ρN$^+$H$_3$+δC$_\beta$C$_\alpha$C+νC$_\alpha$N$^+$
21	1093	1090	1093	νC$_\alpha$N$^+$+νC$_\alpha$C$_\beta$
22	1039	1040	1029	νC$_\beta$O
23	985	978	982	ρC$_\beta$H$_2$+ρN$^+$H$_3$+νC$_\alpha$C$_\beta$
24	957	919	—	νC$_\alpha$C+ρC$_\beta$H$_2$
25	868	851	852	νC$_\alpha$N$^+$+ρC$_\beta$H$_2$
26	805	809	815	δCOO+γCO
27	687	—	—	γCO+δC$_\alpha$C$_\beta$O+ δCOO
28	535	525	528	ρCOO+ρC$_\beta$C$_\alpha$H
29	433	—	—	δC$_\beta$C$_\alpha$H+δC$_\alpha$C$_\beta$O+νC$_\alpha$C+δ_sN$^+$H$_3$
30	375	—	383	δC$_\alpha$C$_\beta$O+δN$^+$C$_\alpha$C+δN$^+$C$_\alpha$H
31	322	—	324	τC$_\beta$O
32	291	—	288	τC$_\beta$O+δC$_\beta$C$_\alpha$H+δN$^+$C$_\alpha$C+ρCOO
33	207	—	222	ρC$_\beta$C$_\alpha$H+δC$_\beta$C$_\alpha$H+ρCOO
34	170	—	—	τC$_\alpha$N$^-$
35	114	—	—	τC$_\alpha$C$_\beta$+τC$_\beta$O
36	52	—	—	τC$_\alpha$C+τC$_\alpha$N$^+$

a. Ref. [21]

Table 8.11: Ala symbolic F matrix in non-redundant local coordinates

```
1
2   3
4   5   6
7   8   9   10
11  12  13  14  15
16  17  18  19  20  21
22  23  24  25  26  27  28
29  30  31  32  33  34  35  36
37  38  39  40  41  42  43  44  45
46  47  48  49  50  51  52  53  54  55
56  57  58  59  60  61  62  63  64  65  66
67  68  69  70  71  72  73  74  75  76  77  78
79  80  81  82  83  84  85  86  87  88  89  90  91
92  93  94  95  96  97  98  99  100 101 102 103 104 105
106 107 108 109 110 111 112 113 114 115 116 117 118 119 120
121 122 123 124 125 126 127 128 129 130 131 132 133 134 135 136
137 138 139 140 141 142 143 144 145 146 147 148 149 150 151 152
153
154 155 156 157 158 159 160 161 162 163 164 165 166 167 168 169
170 171
172 173 174 175 176 177 178 179 180 181 182 183 184 185 186 187
188 189 190
191 192 193 194 195 196 197 198 199 200 201 202 203 204 205 206
207 208 209 210
211 212 213 214 215 216 217 218 219 220 221 222 223 224 225 226
227 228 229 230 231
232 233 234 235 236 237 238 239 240 241 242 243 244 245 246 247
248 249 250 251 252 253
254 255 256 257 258 259 260 261 262 263 264 265 266 267 268 269
270 271 272 273 274 275 276
277 278 279 280 281 282 283 284 285 286 287 288 289 290 291 292
293 294 295 296 297 298 299 300
301 302 303 304 305 306 307 308 309 310 311 312 313 314 315 316
317 318 319 320 321 322 323 324 325
326 327 328 329 330 331 332 333 334 335 336 337 338 339 340 341
342 343 344 345 346 347 348 349 350 351
352 353 354 355 356 357 358 359 360 361 362 363 364 365 366 367
368 369 370 371 372 373 374 375 376 377 378
379 380 381 382 383 384 385 386 387 388 389 390 391 392 393 394
395 396 397 398 399 400 401 402 403 404 405 406
407 408 409 410 411 412 413 414 415 416 417 418 419 420 421 422
423 424 425 426 427 428 429 430 431 432 433 434 435
```

Table 8.11: (Continued): Ala symbolic F matrix in local
coordinates

```
436 437 438 439 440 441 442 443 444 445 446 447 448 449 450 451
452 453 454 455 456 457 458 459 460 461 462 463 464 465
466 467 468 469 470 471 472 473 474 475 476 477 478 479 480 481
482 483 484 485 486 487 488 489 490 491 492 493 494 495 496
497 498 499 500 501 502 503 504 505 506 507 508 509 510 511 512
513 514 515 516 517 518 519 520 521 522 523 524 525 526 527 528
529 530 531 532 533 534 535 536 537 538 539 540 541 542 543 544
545 546 547 548 549 550 551 552 553 554 555 556 557 558 559 560
561
```

Non-redundant fitted force constants

```
 9.755   1.495   7.882   0.466   0.359   4.139   0.098  -0.003   0.112
 4.384  -0.003  -0.004   0.108   0.208   4.358   0.016   0.011   0.053
 0.069   0.060   4.818  -0.019  -0.014  -0.033   0.122  -0.002   0.001
 5.351   0.009  -0.036  -0.010   0.054   0.009  -0.016   0.022   5.332
-0.011  -0.037  -0.026   0.033   0.003   0.006   0.022   0.027   5.168
 0.013   0.016   0.002   0.021   0.066  -0.011  -0.001  -0.001  -0.002
 4.913   0.004   0.016  -0.035  -0.007   0.034   0.006  -0.005  -0.007
-0.004   0.049   4.913   0.010   0.001  -0.010   0.015   0.044   0.006
 0.003   0.002   0.005   0.048   0.043   4.942   0.226   0.327  -0.450
-0.015  -0.002  -0.009   0.028   0.015   0.032  -0.011   0.013  -0.005
 1.497   0.433  -0.351   0.130  -0.242   0.026   0.038  -0.027  -0.012
-0.006  -0.001   0.031  -0.002  -0.078   1.246  -0.001  -0.019  -0.129
-0.148  -0.100   0.095   0.007   0.054  -0.016   0.016  -0.020  -0.012
 0.028   0.005   0.968   0.047   0.016   0.143  -0.183  -0.110   0.004
 0.013  -0.002   0.014  -0.016  -0.004   0.007  -0.026   0.037  -0.066
 0.616  -0.008  -0.007   0.017   0.372  -0.183   0.012  -0.008   0.014
-0.024  -0.027   0.009   0.000   0.006   0.031   0.053  -0.065   0.786
-0.051  -0.017  -0.285   0.277   0.213   0.006   0.052  -0.009  -0.009
-0.001   0.068  -0.014   0.085   0.014  -0.062  -0.046   0.016   1.268
-0.022   0.037   0.149   0.297  -0.181   0.012  -0.052  -0.037  -0.015
-0.008   0.044  -0.021  -0.031  -0.008  -0.206  -0.041   0.046  -0.122
 1.277  -0.059   0.040   0.020  -0.245  -0.012  -0.013   0.040   0.077
 0.071  -0.009   0.002  -0.004  -0.013   0.058  -0.005   0.026  -0.029
-0.050   0.019   0.565   0.025  -0.052  -0.035   0.000   0.023   0.001
 0.082  -0.009  -0.008  -0.004   0.015  -0.007   0.027  -0.006  -0.034
 0.007  -0.019   0.089  -0.044   0.015   0.735   0.007  -0.055  -0.012
 0.005  -0.003   0.007   0.011  -0.002   0.008   0.016  -0.005  -0.004
 0.012   0.017   0.057  -0.029   0.052   0.019  -0.050   0.007  -0.011
 0.721   0.004   0.004  -0.004   0.002   0.005   0.000  -0.069   0.051
 0.051   0.001  -0.004   0.004  -0.004  -0.001  -0.011  -0.013  -0.002
```

Table 8.11: (Continued): Ala Symbolic F matrix in local
coordinates

```
 0.017  -0.025   0.003  -0.029   0.013   0.605   0.031  -0.028  -0.029
-0.044   0.007  -0.002   0.042   0.066  -0.056  -0.004   0.001   0.000
 0.013  -0.029   0.007   0.004  -0.019   0.036  -0.045   0.034  -0.033
-0.001   0.005   0.591  -0.007  -0.023   0.018  -0.034  -0.328  -0.007
-0.002   0.001   0.002   0.073   0.061   0.069   0.005  -0.020   0.017
 0.010   0.018  -0.059   0.003   0.010   0.002  -0.001  -0.005  -0.001
 0.554   0.020  -0.015   0.009   0.005  -0.010  -0.004  -0.001  -0.003
 0.000  -0.111   0.047   0.036  -0.004  -0.005   0.007   0.003  -0.006
-0.019  -0.011   0.000   0.003   0.004  -0.007  -0.001  -0.003   0.534
-0.001  -0.008   0.004   0.005  -0.017   0.000  -0.001   0.002  -0.002
-0.008   0.072  -0.070   0.000  -0.006   0.020   0.004  -0.003  -0.019
-0.017   0.002   0.003  -0.006  -0.003   0.003   0.013   0.010   0.530
-0.011  -0.014  -0.029  -0.055   0.019   0.028  -0.004   0.011   0.001
 0.076  -0.054  -0.024   0.006  -0.014   0.084  -0.037  -0.071  -0.061
 0.037   0.004  -0.013   0.010  -0.001  -0.001  -0.005  -0.006  -0.014
 0.739  -0.034  -0.011  -0.004   0.091  -0.025   0.003   0.000  -0.010
-0.004   0.002   0.101  -0.063   0.014  -0.027  -0.033   0.001  -0.002
 0.150   0.061  -0.005   0.030   0.001  -0.002   0.001   0.025   0.020
 0.009   0.009   0.673   0.012   0.011  -0.008   0.003   0.033  -0.023
 0.009   0.008  -0.003   0.000   0.011   0.001   0.010   0.018  -0.043
-0.060   0.010  -0.023  -0.022   0.004  -0.012   0.003  -0.016   0.002
-0.014  -0.001   0.005  -0.002  -0.012   0.537  -0.012   0.021  -0.029
 0.030   0.007  -0.011  -0.044   0.000   0.001   0.004   0.024  -0.003
 0.010   0.042   0.061   0.009   0.047  -0.010   0.063  -0.020   0.038
-0.001   0.014  -0.021   0.001  -0.011   0.006   0.003  -0.002   0.043
 0.119  -0.026   0.012  -0.016  -0.034  -0.001   0.005  -0.043  -0.018
 0.017  -0.001  -0.001  -0.002   0.007  -0.004   0.006   0.010  -0.020
-0.014   0.003  -0.013   0.043   0.002   0.035   0.001  -0.003  -0.001
 0.001   0.003  -0.006   0.003  -0.012   0.033   0.004  -0.003   0.022
-0.006  -0.003   0.000   0.001  -0.005   0.002   0.004   0.001  -0.006
-0.005  -0.010  -0.018   0.007  -0.010  -0.015  -0.017   0.000  -0.004
-0.001  -0.002   0.001   0.006   0.017   0.010   0.009  -0.007  -0.009
-0.001  -0.005   0.121
```

* Non-redundant local coordinates are according to Table-8.1.

Table 8.12: Non-redundant scaled force constants of Cys

```
1    1  4.363
2    1   .083  2  4.828
3    1   .048  2   .031  3  4.837
4    1   .269  2   .072  3   .041  4  3.086
5    1   .230  2  -.020  3  -.065  4  -.044  5  4.677
6    1   .103  2   .011  3  -.007  4   .054  5   .060  6  4.142
7    1   .060  2   .009  3   .008  4  -.002  5   .065  6   .028  7  4.792
8    1  -.028  2  -.016  3   .006  4  -.038  5  -.016  6   .035  7   .001
     8  3.801
9    1  -.056  2  -.023  3   .000  4   .125  5  -.132  6   .450  7   .011
     8   .001  9  9.710
10   1  -.072  2   .036  3   .031  4   .206  5  -.061  6   .466  7   .008
     8   .014  9  1.424 10  8.331
11   1  -.046  2   .007  3  -.016  4  -.082  5   .229  6   .068  7  -.001
     8  -.005  9   .081 10  -.135 11  4.921
12   1   .010  2   .000  3  -.005  4  -.049  5   .102  6   .014  7  -.011
     8  -.001  9  -.041 10   .009 11   .031 12  5.229
13   1   .000  2   .012  3  -.001  4  -.098  5   .093  6   .022  7   .008
     8  -.006  9   .007 10  -.009 11   .018 12   .031 13  5.147
14   1  -.008  2  -.012  3   .003  4  -.016  5  -.013  6  -.579  7   .000
     8  -.007  9   .240 10  -.051 11   .001 12   .007 13   .006 14  1.488
15   1  -.002  2   .094  3   .068  4  -.010  5   .160  6  -.241  7  -.041
     8  -.004  9   .261 10 -1.052 11  -.264 12   .016 13  -.104 14   .175
    15  1.458
16   1  -.255  2   .006  3   .011  4   .025  5  -.342  6  -.144  7   .079
     8   .084  9  -.040 10   .362 11  -.137 12  -.059 13  -.302 14   .064
    15  -.053 16  1.161
17   1  -.089  2   .102  3   .106  4   .009  5  -.233  6   .147  7  -.108
     8   .037  9  -.038 10   .056 11   .146 12   .084 13   .199 14  -.038
    15  -.030 16  -.085 17   .667
18   1  -.153  2  -.048  3  -.047  4  -.059  5   .389  6  -.005  7   .055
     8  -.020  9  -.160 10  -.307 11   .088 12   .020 13   .064 14  -.026
    15  -.020 16   .012 17  -.081 18   .767
19   1   .171  2  -.126  3  -.056  4   .022  5   .172  6  -.350  7   .030
     8   .064  9  -.188 10  -.091 11  -.687 12   .152 13  -.299 14   .102
    15   .027 16  -.008 17  -.041 18   .000 19  1.461
20   1   .316  2   .205  3   .128  4   .008  5  -.488  6  -.328  7  -.044
     8  -.044  9  -.090 10  -.580 11  -.545 12   .115 13  -.186 14   .085
    15   .126 16   .212 17   .005 18  -.057 19   .214 20  1.673
```

Table 8.12: (Continued): Non-redundant scaled force constants of Cys

```
21   1  -.007   2  -.003   3   .005   4  -.002   5  -.312   6   .039   7  -.011
     8   .002   9   .058  10  -.034  11  -.306  12  -.033  13   .235  14  -.018
    15  -.049  16   .020  17   .040  18  -.031  19  -.003  20   .017  21   .659
22   1   .021   2  -.005   3   .011   4  -.025   5   .107   6  -.037   7   .004
     8   .001   9  -.079  10   .029  11  1.087  12  -.228  13   .477  14   .033
    15  -.021  16  -.138  17   .042  18  -.002  19   .008  20  -.031  21  -.050
    22  1.009
23   1   .004   2   .004   3   .002   4   .003   5   .049   6  -.004   7   .003
     8   .001   9  -.018  10   .026  11   .143  12   .149  13   .219  14   .009
    15  -.034  16   .020  17  -.019  18   .055  19   .021  20   .039  21  -.032
    22   .046  23   .789
24   1   .018   2   .003   3  -.005   4  -.005   5   .000   6  -.023   7  -.001
     8  -.002   9  -.004  10   .007  11  -.089  12   .121  13  -.197  14   .001
    15   .021  16  -.041  17   .000  18  -.007  19   .105  20   .070  21  -.050
    22  -.104  23   .037  24   .604
25   1   .002   2   .002   3   .005   4  -.002   5  -.042   6  -.009   7  -.002
     8   .001   9  -.013  10   .037  11   .348  12   .026  13  -.181  14   .003
    15   .026  16   .062  17   .022  18   .000  19  -.002  20   .039  21   .004
    22   .009  23  -.069  24   .017  25   .606
26   1  -.114   2   .198   3  -.127   4  -.140   5  -.011   6   .014   7  -.001
     8  -.007   9  -.030  10   .010  11   .001  12  -.001  13   .000  14  -.003
    15   .018  16   .019  17  -.005  18  -.012  19  -.037  20   .009  21   .005
    22   .002  23   .002  24  -.006  25  -.001  26   .554
27   1  -.231   2   .004   3  -.009   4   .277   5  -.052   6   .004   7   .008
     8   .014   9  -.031  10  -.035  11   .008  12   .010  13   .009  14   .012
    15   .021  16   .043  17  -.004  18  -.016  19  -.024  20  -.040  21   .008
    22  -.006  23   .005  24   .001  25  -.001  26  -.007  27   .590
28   1   .027   2  -.165   3  -.277   4   .029   5  -.047   6   .018   7   .034
     8   .159   9  -.195  10   .041  11  -.168  12   .018  13  -.094  14  -.034
    15  -.050  16   .043  17  -.009  18   .000  19  -.002  20  -.025  21   .007
    22  -.045  23   .001  24   .017  25  -.036  26  -.040  27   .016  28   .796
29   1   .014   2   .093   3   .118   4   .009   5   .052   6   .002   7   .012
     8   .031   9  -.070  10  -.041  11  -.047  12  -.002  13  -.024  14   .002
    15   .020  16  -.044  17   .005  18   .001  19   .087  20  -.040  21  -.003
    22   .022  23   .001  24  -.002  25  -.006  26   .019  27   .017  28  -.009
    29   .567
30   1   .291   2  -.089   3   .021   4   .276   5  -.029   6  -.044   7   .052
     8  -.115   9  -.232  10  -.404  11   .050  12   .112  13   .129  14  -.030
    15   .042  16  -.143  17  -.054  18  -.047  19   .028  20   .003  21   .023
    22   .027  23   .013  24   .041  25  -.010  26   .000  27   .009  28  -.002
    29   .018  30  1.042
```

Table 8.12: (Continued): Non-redundant scaled force constants of Cys

```
31   1   .004  2   .017  3  -.002  4   .198  5  -.010  6   .008  7  -.005
     8  -.205  9   .039 10  -.003 11  -.006 12  -.004 13  -.002 14  -.008
    15  -.002 16  -.033 17   .008 18   .008 19  -.019 20   .030 21   .001
    22   .004 23   .000 24  -.001 25   .001 26  -.020 27   .054 28   .071
    29   .105 30  -.014 31   .871

32   1  -.004  2  -.030  3  -.036  4  -.018  5   .006  6   .015  7   .034
     8  -.034  9   .202 10  -.269 11  -.020 12  -.024 13  -.016 14   .001
    15   .051 16   .040 17   .048 18   .008 19   .020 20  -.015 21  -.007
    22   .006 23  -.003 24   .006 25  -.023 26   .003 27   .000 28   .001
    29   .010 30   .017 31  -.003 32   .460

33   1   .037  2   .383  3   .452  4   .170  5   .033  6   .058  7   .052
     8   .171  9  -.418 10  -.035 11  -.185 12   .022 13  -.095 14  -.061
    15   .003 16   .027 17   .038 18  -.025 19   .072 20  -.030 21   .001
    22  -.019 23  -.001 24   .010 25  -.038 26   .015 27   .041 28   .054
    29   .036 30  -.037 31   .031 32  -.004 33   .379

34   1   .007  2  -.003  3  -.002  4   .033  5   .015  6   .007  7  -.002
     8  -.086  9  -.024 10  -.028 11   .007 12   .009 13   .009 14  -.002
    15   .007 16  -.022 17   .001 18  -.001 19  -.024 20   .009 21  -.002
    22   .011 23   .001 24  -.010 25   .007 26   .006 27   .005 28  -.039
    29   .012 30   .020 31   .039 32  -.008 33   .020 34   .099

35   1   .010  2   .034  3   .061  4   .036  5  -.002  6  -.066  7  -.029
     8   .036  9  -.753 10  -.787 11  -.104 12  -.044 13  -.094 14  -.082
    15  -.002 16   .030 17   .007 18   .095 19   .029 20  -.045 21  -.016
    22  -.004 23  -.014 24  -.002 25  -.040 26  -.003 27   .019 28   .029
    29   .017 30   .049 31   .014 32   .003 33   .057 34  -.008 35   .363

36   1  -.009  2  -.002  3   .002  4   .027  5  -.059  6  -.036  7   .007
     8   .006  9   .010 10  -.014 11  -.731 12  -.227 13  -.570 14   .008
    15   .057 16   .045 17  -.038 18  -.048 19   .080 20   .061 21  -.039
    22  -.110 23  -.068 24   .007 25  -.137 26   .000 27  -.004 28   .044
    29   .009 30  -.032 31  -.001 32   .013 33   .056 34   .009 35   .054
    36   .357
```

* Non-redundat local coordinates are according to Table-8.2.

Table 8.13: Non-redundant scaled force constants of Ser

```
 1    1  4.419
 2    1   .091  2  4.615
 3    1   .039  2   .055  3  4.814
 4    1   .419  2   .196  3   .190  4  5.136
 5    1   .233  2   .025  3  -.016  4   .018  5  4.581
 6    1   .078  2   .003  3  -.040  4   .025  5   .102  6  4.196
 7    1   .050  2  -.011  3   .008  4   .002  5   .073  6   .043  7  4.829
 8    1  -.016  2  -.006  3  -.007  4  -.032  5   .006  6  -.021  7  -.002
      8  6.430
 9    1  -.038  2   .008  3   .002  4   .117  5   .092  6   .480  7   .012
      8  -.043  9  9.739
10    1  -.011  2   .009  3   .014  4   .054  5   .010  6   .407  7   .010
      8  -.010  9  1.465 10  8.106
11    1   .008  2  -.001  3  -.005  4   .003  5   .071  6  -.021  7  -.017
      8   .002  9   .009 10  -.029 11  5.394
12    1  -.005  2  -.001  3  -.005  4  -.006  5   .053  6  -.022  7   .004
      8   .009  9   .003 10  -.030 11   .019 12  5.495
13    1  -.030  2   .003  3   .000  4  -.035  5   .104  6  -.030  7   .000
      8  -.012  9  -.012 10  -.035 11   .025 12   .021 13  5.109
14    1   .007  2  -.006  3   .012  4  -.071  5  -.019  6  -.440  7  -.007
      8   .027  9   .217 10   .302 11   .021 12   .018 13   .032 14  1.476
15    1   .016  2  -.002  3   .037  4   .006  5  -.231  6   .129  7   .035
      8   .006  9   .444 10  -.373 11  -.023 12  -.022 13  -.012 14  -.069
     15  1.183
16    1  -.087  2   .008  3  -.021  4  -.032  5  -.176  6  -.097  7   .099
      8   .008  9   .013 10  -.031 11   .046 12  -.004 13   .016 14   .017
     15   .005 16   .972
17    1  -.152  2  -.008  3  -.001  4   .011  5  -.223  6   .128  7  -.017
      8  -.003  9   .040 10   .016 11  -.001 12   .011 13   .009 14  -.022
     15   .031 16  -.055 17   .601
18    1  -.169  2  -.019  3   .014  4   .014  5   .366  6   .024  7   .009
      8   .002  9  -.012 10  -.003 11   .010 12  -.021 13  -.028 14   .004
     15   .030 16   .049 17  -.068 18   .820
19    1   .503  2  -.007  3   .037  4  -.016  5   .346  6  -.203  7   .009
      8   .056  9  -.042 10  -.017 11   .007 12   .051 13  -.017 14   .047
     15   .022 16  -.154 17  -.073 18   .035 19  1.529
20    1   .102  2   .016  3  -.043  4   .099  5  -.296  6  -.156  7  -.010
      8  -.026  9   .035 10  -.069 11   .052 12   .068 13   .014 14   .033
     15   .056 16   .211 17   .039 18  -.040 19   .109 20  1.134
```

Table 8.13: (Continued): Non-redundant scaled force constants of Ser

```
21   1   .007  2  -.006  3   .005  4  -.016  5  -.255  6   .012  7  -.013
     8  -.005  9  -.049 10   .032 11   .076 12   .060 13   .023 14  -.009
    15   .046 16   .005 17   .013 18  -.027 19  -.022 20  -.006 21   .569
22   1  -.001  2   .015  3  -.006  4  -.011  5   .004  6  -.014  7   .008
     8   .001  9   .006 10  -.024 11   .023 12  -.010 13  -.033 14   .012
    15   .007 16   .110 17  -.036 18   .056 19  -.014 20   .031 21  -.003
    22   .754
23   1   .014  2   .002  3   .011  4  -.028  5  -.005  6  -.025  7   .000
     8  -.016  9   .011 10  -.074 11   .000 12   .027 13  -.062 14   .020
    15   .007 16   .006 17  -.001 18  -.001 19   .093 20   .057 21   .019
    22   .007 23   .735
24   1   .004  2   .003  3   .002  4  -.018  5   .026  6   .024  7   .002
     8  -.005  9  -.030 10   .016 11  -.087 12   .019 13  -.001 14  -.007
    15   .025 16   .003 17   .004 18   .025 19   .001 20  -.031 21  -.035
    22  -.026 23   .009 24   .592
25   1  -.020  2  -.007  3   .003  4  -.002  5  -.025  6  -.022  7  -.001
     8  -.009  9   .019 10  -.023 11   .002 12   .077 13  -.064 14   .013
    15  -.023 16   .025 17   .010 18   .007 19   .004 20   .028 21   .018
    22  -.020 23  -.009 24   .020 25   .580
26   1  -.136  2   .090  3   .086  4  -.212  5  -.010  6   .007  7  -.004
     8   .005  9   .000 10  -.006 11   .001 12  -.001 13  -.003 14  -.001
    15  -.006 16   .011 17   .005 18   .011 19  -.027 20   .013 21   .003
    22  -.005 23  -.005 24  -.001 25   .004 26   .563
27   1  -.245  2  -.004  3  -.012  4   .386  5  -.043  6   .016  7  -.015
     8  -.027  9  -.004 10  -.025 11   .001 12   .000 13   .013 14   .009
    15  -.002 16  -.001 17   .015 18   .031 19  -.074 20   .015 21   .008
    22   .004 23  -.006 24   .004 25   .001 26   .005 27   .675
28   1   .086  2   .099  3  -.084  4   .007  5  -.077  6  -.020  7   .040
     8   .006  9  -.015 10   .019 11   .005 12  -.004 13  -.017 14   .003
    15   .008 16   .058 17  -.052 18  -.041 19   .012 20  -.025 21   .011
    22   .005 23  -.016 24   .016 25   .005 26  -.010 27  -.008 28   .856
29   1   .000  2  -.033  3   .044  4   .000  5   .046  6   .006  7  -.012
     8  -.011  9  -.008 10   .003 11  -.008 12   .001 13  -.010 14   .002
    15   .006 16  -.069 17   .021 18   .051 19   .095 20  -.004 21   .000
    22  -.015 23   .014 24   .005 25   .005 26   .005 27   .018 28   .074
    29   .707
30   1   .486  2  -.055  3  -.047  4   .603  5  -.068  6   .039  7  -.047
     8   .111  9   .102 10   .082 11  -.009 12  -.013 13  -.039 14  -.063
    15   .056 16  -.071 17  -.005 18   .072 19   .118 20   .082 21   .031
    22   .028 23   .008 24   .009 25  -.014 26  -.031 27  -.128 28   .104
    29   .013 30  1.661
```

Table 8.13: (Continued): Non-redundant scaled force constants of Ser

```
31   1   .026   2   .001   3   .008   4   .354   5   .018   6  -.012   7   .003
     8   .021   9   .000  10  -.019  11   .002  12   .001  13  -.004  14   .014
    15   .002  16  -.004  17  -.003  18   .006  19  -.006  20   .026  21  -.007
    22  -.008  23  -.017  24   .001  25  -.002  26   .007  27  -.005  28  -.003
    29  -.001  30   .067  31   .805
32   1  -.020   2  -.002   3  -.009   4  -.005   5  -.009   6  -.004   7   .022
     8  -.010   9  -.016  10  -.016  11  -.005  12   .000  13  -.001  14  -.010
    15  -.001  16   .044  17   .059  18  -.006  19   .031  20  -.029  21   .000
    22  -.009  23   .006  24  -.009  25  -.009  26   .000  27   .004  28  -.003
    29   .000  30  -.015  31  -.001  32   .514
33   1  -.111   2   .007   3   .004   4  -.011   5   .024   6   .024   7  -.011
     8  -.005   9   .000  10  -.002  11   .003  12   .007  13   .019  14  -.003
    15  -.016  16  -.045  17   .045  18   .005  19  -.118  20   .023  21  -.011
    22   .004  23   .002  24  -.032  25  -.016  26   .002  27   .011  28  -.097
    29  -.021  30  -.082  31  -.016  32   .013  33   .230
34   1  -.037   2   .006   3   .002   4  -.024   5   .005   6   .000   7  -.003
     8  -.007   9   .027  10  -.029  11  -.004  12  -.001  13   .008  14   .001
    15  -.006  16   .021  17   .012  18  -.008  19  -.027  20   .010  21   .001
    22  -.003  23  -.003  24   .000  25   .005  26   .002  27   .006  28  -.071
    29  -.022  30  -.046  31   .007  32  -.003  33   .051  34   .044
35   1  -.009   2  -.002   3  -.017   4   .020   5  -.006   6   .002   7   .012
     8  -.005   9   .020  10  -.027  11  -.007  12   .018  13   .002  14  -.003
    15  -.034  16  -.058  17  -.010  18  -.042  19   .008  20   .030  21   .006
    22   .022  23  -.015  24   .008  25   .020  26  -.008  27   .001  28  -.003
    29   .000  30  -.004  31   .000  32   .032  33   .003  34  -.002  35   .090
36   1  -.035   2   .003   3   .004   4  -.014   5   .002   6   .004   7   .003
     8  -.005   9   .010  10  -.004  11   .007  12   .016  13  -.040  14  -.003
    15   .002  16  -.006  17  -.001  18   .007  19  -.019  20   .011  21  -.006
    22   .001  23  -.050  24   .056  25   .065  26  -.002  27   .004  28  -.004
    29   .004  30  -.022  31   .000  32   .006  33  -.001  34   .001  35  -.028
    36   .058
```

* Non-redundant local coordinates are according to Table-8.2.

Bibliography

[1] Vijay, A.; Sathyanarayana, D. N. *J. Phys. Chem.*, **1992**, 96, 10735.

[2] Barron, L. D.; Gargaro, A. R.; Hecht, L.; Polavarapu, P. L. *Spectrochim. Acta*, **1991**, 47A, 1001.

[3] Tarakeshwar, P.; Manogaran, S. *J. Mol. Struct. (Theochem)*, **1994**, 305, 205.

[4] Tarakeshwar, P.; Manogaran, S. *J. Mol. Struct. (Theochem)*, **1996**, 365, 167.

[5] Susi, H.; Byler, M. *J. Mol. Struct.*, **1980**, 63, 1.

[6] Takeda, M.; Iavazzo, R. E. S.; Garfinkel, D.; Scheinberg, J. H.; Edsall, J. T. *J. Am. Chem. Soc.*, **1958**, 80, 3813.

[7] Fukushima, K.; Onishi, T.; Shimanouchi, T.; Mizushima, S. *Spectrochim. Acta*, **1959**, 15, 236.

[8] Suzuki, S.; Oshima, T.; Tamiya, N.; Fukushima, K.; Shimanouchi, T.; Mizushima, S. *Spectrochim. Acta*, **1961**, 17, 969.

[9] Oshima, T.; Tamiya, N. *Spectrochim. Acta*, **1961**, 17, 384.

[10] Tsuboi, T.; Takenishi, T.; Nakamura, A. *Spectrochim. Acta*, **1961**, 17, 634.

[11] Wang, C. H.; Storms, R. D. *J. Chem. Phys.*, **1971**, 55, 3291.

[12] Srivastava, R. B.; Gupta, V. D. *Indian J. Pure Appl. Phys.*, **1972**, 10, 596.

[13] Fross, S.; Stenman, R. *Phys. Fenn.*, **1973**, 8, 365.

[14] Adamowicz, R. F.; Sage, M. L. *Spectrochim. Acta*, **1974**, 30, 1007.

[15] Machida, K.; Kagayama, A.; Saito, Y.; Uno, T. *Spectrochim. Acta*, **1978**, 34A, 909.

[16] Machida, K.; Kagayama, A.; Saito, Y. *J. Raman Spectrosc.*, **1978**, 7, 188.

[17] Byler, D. M.; Susi, H. *Spectrochim. Acta*, **1979**, 35A, 1365.

[18] Percy, G. C.; Stenton, H. S. *J. Chem. Soc., Dalton Trans.*, **1976**, 2429.

[19] Yu, G.; Freedman, T. B.; Nafie, L. A.; Deng, Z.; Polavarapu, P. L. *J. Phys. Chem.*, **1995**, 99, 835.

[20] Diem, M.; Polavarapu, P. L.; Oboodi, M.; Nafie, L. A. *J. Am. Chem. Soc.*, **1982**, 104, 3329.

[21] Tarakeshwar, P.; Manogaran, S. *Spectrochim. Acta*, **1995**, 51A, 925.

[22] Sellers, H. L.; Schafer, L. *J. Am. Chem. Soc.*, **1978**, 100, 7728.

[23] Lawrence, P. R.; Thomson, C. *Theor. Chim. Acta*, **1981**, 58, 121.

[24] Schafer, L.; Siam, K.; Klimkowski, V. J.; Ewbank, J. D.; Alsenoy, C. V. *J. Mol. Struct.*, **1990**, 204, 361.

[25] Maezey, P. G.; Ladik, J. J.; Suhai, S. *Theor. Chim. Acta*, **1979**, 51, 323.

[26] Wright, L. R.; Borkman, R. F. *J. Am. Chem. Soc.*, **1980**, 102, 6207.

[27] Voogd, J.; Derssen, J. L.; Duijenveldt, F. B. *J. Am. Chem. Soc.*, **1981**, 103, 7701.

[28] Tranter, G. E. *Mol. Phys.*, **1985**, 4, 825.

[29] Tranter, G. E. *J. Theor. Biol.*, **1986**, 119, 467.

[30] Smolyar, A. E.; Abramov, A. R.; Narimanbekov, O. A.; Shakhtakhtinski, T. N. *Azerb. Khim. Zhu.*, **1984**, 42.

[31] Alsenoy, C. V.; Scarsdale, J. N.; Sellers, H. L.; Schafer, L. *Chem. Phys. Lett.*, **1981**, 80, 124.

[32] Alsenoy, C. V.; Kulp, S.; Siam, K.; Klimkowski, V. J.; Ewbank, J. D.; Schafer, L. *Chem. Phys. Lett.*, **1981**, 80, 124.

[33] Kerr, K. A.; Ashmore, J. P.; Koetzle, T. F. *Acta Crystallogr.*, **1975**, 31B, 2022.

[34] Frey, M. N.; Lehmann, M. S.; Koetzle, T. F. *Acta Crystallogr.*, **1973**, 29B, 876.

[35] Susi, H.; Byler, D. M.; Gerasimowicz, W. V. *J. Mol. Struct.* , **1983**, 102, 63.

[36] Machida, K.; Izumi, M.; Kagayama, A. *Spectrochim. Acta*, **1979**, 35A, 1333.

[37] Madec, C.; Lauransan, J.; Garrigou-Lagrange, C. *Can. J. Spectrosc.*, **1980**, 25, 47.

[38] Madec, C.; Lauransan, J.; Garrigou-Lagrange, C. *Can. J. Spectrosc.*, **1978**, 23, 166.

[39] Li, H.; Wurrey, C. J.; Thomas, G. J., Jr. *J. Am. Chem. Soc.* **1992**, 114, 7463.

[40] Gargaro, A. R.; Barron, L. D.; Hecht, L. *J. Raman Spectrosc.*, **1993**, 24, 91.

[41] Bour, p.; Tam, C. N.; Shaharuzzaman, M.; Chickos, J. S.; Keiderling, T. A. *J. Phys. Chem.*, **1996**, 100, 15041.

[42] Durig, J. R.; Wang, A. Y.; Little, J. S.; Breltic, P. A. *J. Chem. Phys.*, **1990**, 93, 905.

Chapter 9

Conclusions and Future Scope

The availability of a number of empirical force fields and their popularity in getting useful chemical and biochemical insights clearly demonstrate the necessity of having a dependable force field for the molecules of interest. It has been shown that adjusting the empirical parameters to reproduce the experimental vibrational frequencies have significant improvement on the inferences made from the simulations. Ab initio force fields having a firm theoretical basis is expected to provide more reliable parameters than the empirical ones. To this end, in this thesis we proposed an alternative methodology for scaling the ab initio force constants. The resulting scaled quantum mechanical force field in terms of a complete set of non-redundant force constants is utilized for interpretation and prediction of the vibrational spectra of few organic molecules and amino acids. The results show that the methodology works as good as other known scaling procedures and better in few favourable cases.

In the case of organic molecules many well studied systems are available in the literature. We used some of them like acrolein, benzene, naphthalene etc. to interpret their vibrational spectra. By transferring the scale factors from structurally related molecular systems the predictive ability of the present methodology has been tested for few molecules like pyridine, benzaldehyde and anthracene. The final results suggest the general applicability of the scaling methodology. A set of reliable non-redundant scaled force constants have been obtained for all the organic molecules studied. However incorporating these parameters, into simulation of molecular mechanics and dynamics is deferred for future work.

The use of ab initio methods to describe the vibrational characteristics of amino acids is still in its infancy. The nature of intermolecular H-bonding present in the condensed phase poses serious problems in mimicking the experimental features of vibrational spectra using ab initio calculations on isolated molecules. Different ways of incorporating this environmental effect into calculations involving single molecule are explored. Single molecular calculation on hydrochlorides of amino acids and Onsager reaction field approach of immersing the molecule in a dielectric continuum on amino acid zwitterions are found to give reasonably good results. A complete set of non-redundant force constants were obtained for the amino acids and their hydrochlorides investigated in this thesis. To incorporate these results into molecular mechanics simulations require the data for other amino acids, work in this direction is in progress in our laboratory.

List of Publications :

1.Theoretical study of the ground state vibrations of methoxydifluorophosphine-d_0 and d_3

D.Chakraborty and S.Manogaran, *J.Mol.Struct.(THEOCHEM)*, **1993**, *284*, 163.

2.Ground state vibrations of N-glycylglycine hydrochloride - An ab initio study

D.Chakraborty, A.Yash and S.Manogaran, *J.Mol.Struct.(THEOCHEM)*, **1994**, *303*, 265.

3.Ground state vibrations of guanidinium and methylguanidinium ions - An ab initio study

D.Chakraborty, and S.Manogaran, *Indian J. Chem.*, **1994**, *33A*, 969.

4.Force field and assignment of vibrational spectrum of anthracene - Theoretical prediction.

D.Chakraborty, R.Ambashta and S.Manogaran, *J.Phys.Chem.*, **1996** *100*, 13693

5.Accurate prediction and interpretation of vibrational spectra - a modified ab initio scaled quantum mechanical approach

S.Manogaran and D.Chakraborty, *J.Phys.Chem.*, manuscript under revision.

6. Theoretical prediction of vibrational spectra of N-glycylglycine hydrochloride - An ab initio study

D.Chakraborty and S.Manogaran *J.Phys.Chem.*, manuscript under revision.

7. Vibrational analysis of glycine zwitterion - An ab initio study

D.Chakraborty and S.Manogaran, *J.Phys.Chem.*, manuscript under revision.

8.Groud state vibrational spectra of cystien and serine hydrochloride - A Theoretical

prediction

D.Chakraborty and S.Manogaran, *J. Mol. Struct.(THEOCHEM)* submitted.

9.An accurate prediction and interpretation of vibrational spectrum of L-cystiene and L-serine - An ab initio study

D.Chakraborty and S.Manogaran, Manuscript under preparation.

CHM-1996- D—CHA-GRO